

**COMPUTATIONAL AND BIOCHEMICAL APPROACHES FOR THE
PREDICTION AND CHARACTERIZATION OF DNA REPAIR SYNERGY
IN CANCERS**

by

Jonathon M. Gast

A Dissertation

Submitted to the Faculty of Purdue University

In Partial Fulfillment of the Requirements for the degree of

Doctor of Philosophy



Department of Medicinal Chemistry and Molecular Pharmacology

West Lafayette, Indiana

May 2021

THE PURDUE UNIVERSITY GRADUATE SCHOOL
STATEMENT OF COMMITTEE APPROVAL

Dr. Vincent Jo Davission, Chair

Department of Medicinal Chemistry and Molecular Pharmacology

Dr. Tony Hazbun

Department of Medicinal Chemistry and Molecular Pharmacology

Dr. Cheng-Deng Hu

Department of Medicinal Chemistry and Molecular Pharmacology

Dr. Daisuke Kihara

Department of Medicinal Chemistry and Molecular Pharmacology

Dr. Michael Wendt

Department of Medicinal Chemistry and Molecular Pharmacology

Approved by:

Dr. Andy Hudmon

To my parents, Tony and Dawn, and my siblings who nurtured my curiosity and tempered it with contemplation and to my wife, Elaine, who strengthened and walked with me through this

ACKNOWLEDGMENTS

The last several years have been the greatest challenge I have engaged in my life. Without the encouragement, support, and instruction of numerous undergraduate and graduate students, post-doctoral researchers, technicians, and professors, I would not have been able to meet this challenge. Beyond this, they have enriched my personal and professional development for the better.

I would firstly like to thank my advisor and mentor Dr. Davisson for not just years of advice, but the patience and thoughtfulness to help see me through the last several years. Dr. Davisson provided both many resources and opportunities that has led to any success I have achieved here at Purdue. The environment of discovery and focus on the progression of patient care in the near and long term allowed for the varied projects I engaged in. Further, the allowance of my pursuit into informatics and systems biology sparked a passion I had only noticed briefly before and will likely enjoy for the rest of my career. I would also like to acknowledge and thank my graduate committee of Dr. Tony Hazbun, Dr. Cheng-Deng Hu, Dr. Daisuke Kihara, and Dr. Michael Wendt for their guidance and tutelage throughout the course of this project. Their encouragement and sound advice only improved my experience and has helped me greatly. I would also like to thank Dr. Wanqing Liu for his instruction and guidance while he was present at Purdue.

I would also like to thank the numerous graduate and undergraduate students that contributed to my education. Dr. Tony Pedley, Dr. Matt Bartolowits, Dr. Dino Petrov, and Dr. Aaron Lindstrom all provided me with great advice as to how to engage my project. I would like to especially thank Dr. Dino Petrov and Dr. Aaron Lindstrom for the excellent and enjoyable work environment they provided. I would also like to thank Dr. Naoaki Fujii, for his expertise in DNA damage repair, your insights and experience helped me greatly. Kyle Harvey remains in his own category as I have been helped by him regardless of his position, whether in pharmacy school or graduate school. His help initially with cell culture or later with microscopy has been instrumental in my progress. I was especially helped by three undergraduate students including Moa Shao, Lauren Orr, Renee Oles, and Avni Bhalgat. Your assistance with my work was valuable and I anticipate your graduate school success in the near future. I would also like to acknowledge the other undergraduate students who also worked with me in the Davisson lab during my time and

wish them the best in their careers: Madison McAteer, Rani Bendersky, Drew Thieme, and Anthony Cirrincione.

I would like to thank my many other friends, both in and outside the department. Their support throughout graduate school has allowed me to counter the stress and weariness with amusement and relief. I would also like to again specifically mention my family whose love, support, and visits were bright spots throughout my time at Purdue. Finally, I must thank my wife Elaine for always being there and supporting me regardless of obstacles that arose.

Financial support for this work was provided by the Purdue Research Foundation, Purdue University Graduate School, and the Pharmaceutical Research and Manufacturers of America.

“Scientific discovery consists in the interpretation for our own convenience of a system of existence which has been made with no eye to our convenience at all”

-Norbert Weiner

TABLE OF CONTENTS

LIST OF TABLES.....	11
LIST OF FIGURES	12
LIST OF EQUATIONS.....	17
LIST OF ABBREVIATIONS.....	18
ABSTRACT.....	20
CHAPTER 1. INTRODUCTION	22
1.1 Rapid Proliferation Negatively Impacts Genome Stability	26
1.1.1 Cell Cycle Progression and Genome Stability is Uncoupled from Apoptosis in Tumors	27
1.1.2 Cell Cycle Progression and DNA Damage Repair are Mutually Regulated.....	29
1.1.3 DNA Replication and Cell Cycle Drive DNA Damage Repair Outcomes	30
1.2 Identifying Disease Markers through Informatic Approaches and Pathway Analysis.....	31
1.2.1 Somatic Mutations	32
1.2.2 Differential Gene Expression.....	33
1.2.3 Protein-Protein Interactions	34
1.3 Enhancing Current Therapeutic Options in Cancer	35
1.3.1 Utilizing Drugs in Ideal Contexts by Identifying Relevant Biomarkers	39
1.3.2 Inducing Synthetic Lethality through Drug Combinations.....	40
1.3.3 Essential Genes and Synthetic Lethality	42
1.4 Scope.....	43
CHAPTER 2. CLASSES OF SMALL MOLECULE PCNA INHIBITORS DEFINED BY MECHANISM OF ACTION	44
2.1 Introduction	44
2.1.1 Double-Strand Break Repair.....	45
2.1.2 DNA Replication	48
2.1.3 Translesion Synthesis	49
2.1.4 PCNA Ligands and Inhibitors.....	49
2.2 Rationale.....	56

2.3	Methodology.....	57
2.3.1	Cell Culture	57
2.3.2	Drug Combinations and Synergism.....	59
2.3.3	Cell Proliferation.....	60
2.3.4	Cell Survival	61
2.3.5	DNA Double-Strand Breaks	61
2.3.6	Homologous Recombination Assessment through Rad51 Foci	62
2.3.7	DNA Replication and Translesion Synthesis.....	63
2.3.8	Inhibitor Feature Profile Assessment	63
2.4	Results.....	65
2.4.1	Cell Proliferation and Survival	65
2.4.2	DNA Double-Strand Breaks	71
2.4.3	RAD51/ γ H2AX Foci	74
2.4.4	DNA Replication	79
2.4.5	Translesion Synthesis	81
2.4.6	PCNA Inhibitor Profile	83
2.5	Discussion.....	85
2.5.1	AOH Compound PCNA Antagonism Description	85
2.5.2	T2AA and Tripeptoid PCNA Antagonism Description	88
2.5.3	Overcoming Olaparib Resistance through Induced Synthetic Lethality	89
2.5.4	Leveraging High-Content Assays through Drug Combinations and Differentiated Biology.....	89
2.6	Conclusions and Impact.....	89
CHAPTER 3. A NETWORK APPROACH TO PREDICT SYNERGISTIC DNA REPAIR ANTAGONIST COMBINATIONS IN CANCER		91
3.1	Introduction	91
3.1.1	Gene Expression Network.....	92
3.1.2	Disease Networks	95
3.1.3	Synergy Networks	96
3.2	Rationale.....	97
3.2.1	Method Design and Application	98

3.3	Methods	99
3.3.1	Data Sources	101
3.3.2	Network Creation.....	101
3.3.3	Base Total Network Analysis	103
3.3.4	Eigenvector Centrality.....	103
3.3.5	Impact Matrix.....	103
3.3.6	GO Term Based Analysis and Parent Group Hierarchy.....	104
3.3.6.1	GO Impact	105
3.3.6.2	GO Cohesion.....	105
3.3.6.3	GO Adhesion.....	105
3.3.7	Process Network Creation.....	106
3.3.8	Somatic Mutations.....	106
3.3.9	Network Disruption	107
3.3.10	Combinatorial Drug Treatment	109
3.3.11	Cell Culture.....	110
3.3.12	Cell Proliferation	111
3.4	Results.....	112
3.4.1	Initial Differential Gene Expression Networks.....	113
3.4.2	Graphical Representations of Gene Influence	114
3.4.2.1	Gene Expression	116
3.4.2.2	Degree Centrality	116
3.4.2.3	Eigenvector Centrality	116
3.4.2.4	Source-Weighted Eigenvector Centrality.....	117
3.4.2.5	Enrichment through Gene Expression Compared to Centrality.....	119
3.4.2.6	Gene Expression Analysis of Base Networks.....	119
3.4.2.7	Eigenvector Centrality Analysis of Base Networks	120
3.4.2.8	Source-Weighted Eigenvector Centrality Analysis of Base Networks	121
3.4.3	Cell Line-Specific Process Networks	122
3.4.3.1	Summary on Process Network Analysis	128
3.4.4	Predictions through Node Removal.....	129
3.4.4.1	TCGA Gene Expression Network Analysis of BRCA1 +/+ and -/- Contexts	129

3.4.4.2	TNBC Process Network Analysis of BRCA1 -/- versus BRCA1 Simulated Deletion	132
3.4.4.3	TNBC Process Network Analysis of BRCA1 and PARP1 Synergy through Simulated Deletion.....	134
3.4.5	Synergism Predictions and Measured Outcomes	136
3.4.6	Method Results Summary	143
3.5	Discussion.....	143
3.5.1	Eigenvectors as a Biomarker Metric	144
3.5.2	Integrated Pathway Analysis through Inter- and Intra-connectivity	145
3.5.3	Gene Removal as a Model of Inhibition	145
3.5.4	Network Disruption Measured through Pathway Dynamics	146
3.6	Conclusions and Impact.....	146
CHAPTER 4. FUTURE DIRECTIONS.....		148
4.1	Further Evaluation of Specific DNA Damage Repair Inhibition through PCNA.....	148
4.1.1	Understanding Differential Inhibition of Homologous Recombination.....	150
4.1.2	Evaluating Any PCNA Inhibition of Nucleotide Excision and Base Excision Repair ..	152
4.2	Improving Process Network Mapping and Resolution.....	154
4.2.1	Defining Node and Edge Activity as Discrete Groups through Known Complexes and Somatic Mutations	154
4.2.2	Introducing Transcription Factor and miRNA Networks to Create New Edges	156
APPENDIX A. ADDITIONAL DATA CHARACTERIZING PCNA INHIBIT OR CLASSES' MECHANISMS OF ACTION.....		158
APPENDIX B: ADDITIONAL GRAPHS AND MATRICES DESCRIBING PROCESS NETWORKS		161
REFERENCES		193

LIST OF TABLES

Table 1.1: Essential genes within cancer contexts. Of the over 2,000 essential genes many of them are more associated with certain tumor types. Much of this has to do with the tissue of origin, but many are so tied to basic cancer pathophysiology that they are important to all types.	23
Table 1.2: Traditional chemotherapies that target conserved phenotypes in all tumors. The primary process they are associated with and their basic function are listed.....	36
Table 1.3: Drug combinations approved by the FDA. Combinations that did not include a targeted therapy were excluded and combinations that utilized the same strategy as another were excluded with the first combination filed being kept.	38
Table 1.4: Targeted inhibitors in DNA damage repair, cell cycle, and DNA replication. The primary process they are associated with and their basic function are listed as well. Their FDA status is reported if they have been submitted at some point, otherwise, they are labeled as preclinical.....	41
Table 2.1: PCNA inhibitors and binders discovered and developed. *Molecules used in this study. †Lactam bridge between K145 and E149	55
Table 2.2: Cell Line Properties; Doubling times were determined after culturing cells for 2-3 passages as this was more accurate to cell growth speed during assays.	58
Table 2.3: Small Molecules Utilized to Examine Effects of PCNA Antagonism	59
Table 2.4: PCNA Inhibitor Feature Classification; LD50 is the concentration measured in the clonogenic assay that results in half the cells' death. GI50 is the concentration measured in the proliferation assay that results in half the cell growth.....	64
Table 3.1: Descriptors of Network and Experimental Evaluation of Synergism and Disruption	108
Table 3.2: Small molecule PCNA inhibitors to be evaluated in this study.....	109
Table 3.3: Cell Line Properties; Doubling times were determined after culturing cells for 2-3 passages as this was more accurate to cell growth speed during assays.	111
Table 3.4: Cell Line Network Summary Statistics. Density is the proportion of edges that could possibly exist compared to the amount that do. Clustering compares how connected a node's neighbors are to how connected they could possibly be. Centralization of a network is a measurement of how the average node is compared to the most central node. Heterogeneity is a measurement of the variance in the number of neighbors each node possesses throughout the whole network.....	114

LIST OF FIGURES

Figure 1.1: Essential genes and tumor genes influence. There are 26,047 nodes and 569,182 edges, with 1,151 genes being considered essential genes by the Database of Essential Genes, last updated December 2017. Oncogenes were qualified through the loss-of-deletion approach outlined in (Pertesi, 2019). The entire proteome with protein-protein interactions from BioGrid. Interactions that involve essential genes are yellow, interactions including tumor suppressors are magenta, and those that include oncogenes are cyan, and those without any of those are gray. Figure was visualized with Cytoscape version 3.8.124

Figure 1.2: Blue objects are proteins, green objects are histone acetyltransferase, orange objects are histone deacetylases, purple objects are acetylation PTMs, yellow objects are ubiquitin PTMs, and red objects are anti-tumor pathways.....25

Figure 1.3: Cell Cycle and DNA damage repair in a tumor context. Due to tumors possessing an increased proliferation rate, this makes them more predisposed to utilizing the homologous recombination (HR) over the non-homologous end-joining (NHEJ), the two main double-strand break repair pathways. Due to the increased proliferation rate, that is undue stress on DNA in replication that is mitigated by translesion synthesis (TLS) to tolerate the damage sustained by the stress. Green objects facilitate increased growth, red objects suppress tumors, blue objects progress the cell cycle, and orange objects slow cell cycle.28

Figure 1.4: PCNA structure and PTM impact on pathways. PCNA is a highly modulated scaffold protein that impacts the numerous interactors and pathways it is involved in. The crystal structure is marked at the residues by the modification type with the functional change listed.30

Figure 2.1: DNA Double-Strand Break Repair via Homologous Recombination46

Figure 2.2: DNA Double-Strand Break Repair via Classical Non-Homologous End Joining47

Figure 2.3: DNA Double-Strand Break Repair via Alternative Non-Homologous End Joining ..47

Figure 2.4: Translesion Synthesis DNA Damage Tolerance Pathway49

Figure 2.5: MTT Plate Configuration; A) Control plate; B) Test plate; Red: No cells, negative control; Green: Cells, no treatment, positive control; Blue: Cells, treatment60

Figure 2.6: Cell proliferation effects of PCNA inhibitors. Cells were exposed to 10 step dilution set using a dilution factor of 3 starting at 200 μ M, except for doxorubicin which started at 50 μ M. These were done in the cell lines shown and with the dilution set of an inhibitor at the title as well as 1/10 GI50 of the PCNA antagonist denoted. A) HCC1937; B) MDA-MB-231; C) MDA-MB-436; D) MDA-MB-46867

Figure 2.7: Cell proliferation effects of PCNA antagonists. Cells were exposed to a 5 step dilution set using a dilution factor of 3 starting at a concentration relative to their GI50. These were done in the cell lines shown and with the dilution set of an inhibitor at the title as well as 1/10 GI50 of the PCNA antagonist denoted. A) HCC1937; B) MDA-MB-231; C) MDA-MB-436; D) MDA-MB-46869

Figure 2.8: DNA damage in HCC1937 measured by a neutral comet assay. A. Exposed to no DNA damage agent; B. Exposed to 10 μ M Doxorubicin over 1 hour 71

Figure 2.9: DNA damage effects of PCNA inhibitors. Cells were exposed to 10 μ M doxorubicin for 1 hour and then allowed 8 hours to repair. These were done in the cell lines shown and with the listed concentration of an inhibitor at the title as well as 1/10 GI₅₀ of the PCNA antagonist denoted. The % DNA tail was averaged over cells with damage and the cells without damage tallied. A) HCC1937; B) MDA-MB-231; C) MDA-MB-436; D) MDA-MB-468..... 73

Figure 2.10: RAD51 and γ H2AX Foci Formation in MDA-MB 231 Cells. MDA-MB 231 were either exposed to 10 μ M doxorubicin as a DNA damage agent. Cells were then exposed to T2AA over either 8 or 24 hours. 76

Figure 2.11: PCNA Antagonist Effects on Homologous Recombination in Combination with DNA Damage Agents and Repair Antagonists in MDA-MB-231 Cells. A) Cells were exposed to PCNA inhibitors at 1/3 GI₅₀ over 8 hours. B-C) Cells were exposed to PCNA inhibitors at 1/3 GI₅₀ as well as an amount of DNA damage repair antagonists over 8 hours 25. D-E) Cells were exposed to doxorubicin for 1 hour and then washed of PCNA inhibitors. 77

Figure 2.12: PCNA Antagonist Effects on Homologous Recombination in Combination with DNA Damage Agents and Repair Antagonists in MDA-MB-436 Cells. A) Cells were exposed to PCNA inhibitors at 1/3 GI₅₀ over 8 hours. B-C) Cells were exposed to PCNA inhibitors at 1/3 GI₅₀ as well as an amount of DNA damage repair antagonists over 8 hours 25. D-E) Cells were exposed to doxorubicin for 1 hour and then washed followed by 8 or 24 hours of PCNA inhibitors. 78

Figure 2.13: Measuring Replication through Quantifying DNA. A. No treatment; B. 30 μ M T2AA 79

Figure 2.14: DNA Replication Effects of PCNA inhibitors. Three different cell lines were exposed to five doses of PCNA inhibitors as monotherapies. These therapies start at 1/3 GI₅₀ and utilize a dilution factor of 3 to measure the effect. A) MDA-MB-231; B) MDA-MB-436; C) MDA-MB-468 80

Figure 2.15: Translesion synthesis effects of PCNA inhibitors. Three different cell lines were exposed to five doses of PCNA inhibitors as monotherapies as well as UV. These therapies start at 1/3 GI₅₀ and utilize a dilution factor of 3 to measure the effect. A) MDA-MB 231; B) MDA-MB 436; C) MDA-MB468..... 82

Figure 2.16: PCNA Antagonist Profile by Pathway Specific Features. All PCNA inhibitors had each major feature specificity calculated as reported in the methods. The goal was to utilize multiple assays to determine the isolated effects on each pathway or function listed. *Toxicity* – based on the LD₅₀ of the antagonist alone; *DNA Damage* – % DNA Tail of the antagonist at GI₅₀/3; *HR:NHEJ* – The overall effects of PCNA antagonists in HR specific vs. NHEJ-specific contexts; *Rad51 Foci* – the amount of Rad51 foci maintained after 24h while treated by the PCNA antagonist; *Replication* – the amount of cells in S phase after dosing with GI₅₀/3; *TLS* – the amount of cells in S phase after dosing with GI₅₀/3 83

Figure 2.17: Drug Interaction in Double-Strand Break Repair Pathways and PCNA Inhibitor Impact; This is the validate mechanisms of our small molecule DNA repair antagonists in the

context of homologous recombination (HR), classical non-homologous end joining (cNHEJ), and alternative non-homologous end joining (aNHEJ). These compounds are outlined with black. The PCNA inhibitors assessed in this study are outlined in green. AOH compounds have been shown previously to inhibit HR, but neither in that study, or this one, was a specific target identified. However, DNA damage was detected with the AOH compounds as a monotherapy. Due to the Rad51 foci persistence, the effects of T2AA, TEP, LPB, and LPT can be narrowed down to an effect that includes Rad54 or Polymerase association. Synergistic relationships require effects that include at least HR and either NHEJ pathway. A) HR; B) cNHEJ; C) aNHEJ 87

Figure 3.1: Gene Networks; Gene networks represent the possible interactions of gene products often with expression or network topography measurements determining the color of nodes. They provide an intuitive presentation to represent pathway regulation. Arrows and wedges can be used to show activating and deactivating relationships. Further, modifications can be used to show functional changes created by interactions. A) Simple metabolic pathway; B) Complex signaling pathway 93

Figure 3.2: Co-Expression Network; Gene networks are representations of physical interactions of their products. Co-expression is also used to determine clustering of gene product that are effective simultaneously. 94

Figure 3.3: Disease Networks; Disease networks can be used to analyze how diseases are similar or connections between disease pathophysiology to biomolecular features. A) This disease similarity network creates edges between diseases that have more than 5 associated genes in common; B) Disease regulation network utilizes genomic, proteomic, and treatment data along with disease data to identify biological features at the gene, pathway, and tissue levels. 96

Figure 3.4: Synthetic Lethal Network; Synthetic lethal relationships are a result of targets prominence in a context and the ability of a drug to shift that prominence. This often includes genomic conditions specific to a disease to ensure selectivity. Understanding genes through their relationship using this perspective can involve interactions that would appear distant or close in other network approaches. 97

Figure 3.5: Overall Project Workflow: The initial gene network involves a limited dataset of gene product interactions and gene expressions. What follows is a set of network analyses that compound the effects of network connectivity on overall genomic dynamics that simulate treatment. *APOP* – apoptosis; excision repair; *CC* – cell cycle; *DDR* – DNA damage repair; MAPK – MAPK pathway 100

Figure 3.6: Cell Line GO Term-Specific Network Formation Process; A) After hub selection, a hub network is formed through selecting all of the interactors within two steps of the hub protein. B) Expression data for a specific to a subtype is then applied to the nodes. C) All nodes that are either over- or underexpressed above or below the threshold is then selected (yellow outline), but those that are in common between both subtypes are excluded (blue outline). D) All neighbors between the selected nodes are then used to form the new subtype specific network (green outline). E) GO terms are used to describe nodes within subtype-specific networks F) Subnetworks are analyzed for aberrant connections related to known disease phenotypes to observe functional subunits within the subtype-specific network. 102

Figure 3.7: GO Term Tier; GO terms are organized in hierarchal tree structure based on the relationship between terms. Maximizing the distance a term has from the source term provides optimal overview. 104

Figure 3.8: Results Section Summary 112

Figure 3.9: Initial Cell Line Networks; These networks were created through a $\pm 6X$ differential expression threshold. Each cell line network was then focused further on MAPK, DNA damage repair, cell cycle, and apoptosis pathway related genes. A. HCC1937; B. MCF7; C. MDA-MB-231; D. MDA-MB-436; E. MDA-MB-468; F. SKBR3; 115

Figure 3.10: Node Attribute Analysis; The HCC1937 network was overlaid with either differential gene expression, node degree, eigenvector, or source-weighted eigenvector values. A) Differential Expression, B) Node Degree, C) Eigenvector Values, D) Weighted Eigenvector Values..... 118

Figure 3.11: Pathway Analysis by Treatment Type; Utilizing the pathway analysis method described previously using eigenvector analysis, we assessed didn't tumor subtypes for overall modifications. A) HCC1937; B) MCF7; C) MDA-MB-231; D) MDA-MB-436; E) MDA-MB-468; F) SKBR3; *APOP* – apoptosis; *BER* – base excision repair; *CC* – cell cycle; *HR* – homologous recombination; *ICL* – interstrand cross-linking repair; *MMR* – mismatch repair; *NER* – nucleotide excision repair; *NHEJ* – non-homologous end joining 124

Figure 3.12: BRCA1 Loss-of-Function Mutation Effect on Homologous Recombination. Homologous recombination associated genes in TNBC tumor samples from TCGA were used to create networks. Networks were analyzed for weighted eigen centrality which corresponds to node size and with gene expression representing the color of nodes. A. BRCA1 +/- TNBC tumor samples; B. BRCA1 -/- TNBC tumor samples 130

Figure 3.13: Network Disruption by Loss-of-Function Compared to Removal of Gene; Networks were created from TCGA TNBC tumor sample expression data according to the same method as the cell lines. Similar pathway analysis and centrality measurements were taken with sample groups with and without BRCA1 loss-of-function mutations. Networks were then created without BRCA1 entirely and the loss of edges and BRCA1 itself was measured. A. TCGA TNBC; B. TCGA TNBC BRCA1 -/-; C. TCGA TNBC BRCA1 removed; *APOP* – apoptosis; *BER* – base excision repair; *CC* – cell cycle; *HR* – homologous recombination; *ICL* – interstrand cross-linking repair; *MMR* – mismatch repair; *NER* – nucleotide excision repair; *NHEJ* – non-homologous end joining; 131

Figure 3.14: Disruption from Homologous Recombination and Non-Homologous End Joining Components in TNBC tumors; Networks were created from TNBC expression data and analyzed similarly to the base networks, but without the nodes specified. Network features were then measured as before and the relative difference in each process and their connectivity was measured. A) BRCA1; B) PARP1; C) BRCA1/PARP1; *APOP* – apoptosis; *BER* – base excision repair; *CC* – cell cycle; *HR* – homologous recombination; *ICL* – interstrand cross-linking repair; *MMR* – mismatch repair; *NER* – nucleotide excision repair; *NHEJ* – non-homologous end joining;..... 133

Figure 3.15: Disruption from Homologous Recombination and Non-Homologous End Joining Components in TNBC tumors; Networks were created from TNBC expression data and analyzed similarly to the base networks, but without the nodes specified. Network features were then

measured as before and the relative difference in each process and their connectivity was measured. A) PCNA; B) PARP1; C) PCNA/PARP1; *APOP* – apoptosis; *BER* – base excision repair; *CC* – cell cycle; *HR* – homologous recombination; *ICL* – interstrand cross-linking repair; *MMR* – mismatch repair; *NER* – nucleotide excision repair; *NHEJ* – non-homologous end joining;.....135

Figure 3.16: Disruption Indices for Combinatorial Gene Removal in Breast Cancer Cell Line Networks; Cell line networks were analyzed for their differential process centrality through the deletion of two genes corresponding to drug targets. Disruption indices were calculated according to our reported formula in the method section. Values above 1 indicate significant disruption to the network through the connectivity within and between processes analyzed. A. HCC1937; B. MCF7; C. MDA-MB-231; D. MDA-MB-436; E. MDA-MB-468; F. SKBR3137

Figure 3.17: Combination Indices for Drug Combinations in Breast Cancer Cell Lines; Cells were tested in combination using a MTT assay and their combination indices (CI) determined through Chou-Talalay. The maximal 1/CI value for a concentration was used that was above the minimal drug concentrations and below the GI_{50} concentration of a single chemotherapy. Values above 1.1 have a confidence greater than 95% to be synergistic. A. HCC1937; B. MCF7; C. MDA-MB-231; D. MDA-MB-436; E. MDA-MB-468; F. SKBR3138

Figure 3.18: Simple Statistical Assessment of Disruption Index (DI) and Combination Index (CI). A) The ability of the DI to predict combinations that will be synergistic as seen through experimental results for CI. B) A simple correlation of DI to CI showing the ability to predict the magnitude of synergism143

Figure 4.1: PCNA Post-Translational Modification and DNA Damage Repair Pathway Influence. PCNA is involved as a scaffold protein to form protein-DNA complexes in the four repair pathways represented: mismatch repair (MMR), nucleotide excision repair (NER), homologous recombination (HR), base excision repair (BER). Proteins that are involved in complexes with PCNA are represented by rhombuses and modifiers of PCNA are represented by rectangles. The different arrows represent different modifications with EGFR phosphorylating PCNA, RAD18 ubiquinating PCNA, and SETD sumoylating PCNA.149

Figure 4.2: DNA Double-Strand Break Repair via Homologous Recombination with Inhibitor Targets. Black squares outline targets with selective inhibitors.151

Figure 4.3: DNA Single-Strand Break Repair through Base Excision Repair153

Figure 4.4: DNA Single-Strand Break Repair through Nucleotide Excision Repair153

Figure 4.5: Additional Network Descriptor Model. A) Node complex model; nodes that can comprise a similar complex with interchangeable components can be modeled as a complex node. Complex nodes may possess different functions depending on the members of the complex. Overexpressed genes, designated in yellow, will be more favored over complexes including underexpressed genes, designated in blue. B) Node GO commonality can be used to describe groups of nodes. Their uncommon GO terms can be used to describe the influence of nodes on other processes.156

Figure 4.6: Representation of a Transcription Factor Network157

LIST OF EQUATIONS

Equation 3.1: Eigenvector Centrality	103
Equation 3.2: Impact Matrix	104
Equation 3.3: GO Impact.	105
Equation 3.4: GO Cohesion.	105
Equation 3.5: GO Adhesion.	106
Equation 3.6: Disruption Index.	107

LIST OF ABBREVIATIONS

APIM-	AlkB Homolog 2 PCNA Interacting Motif
APOP-	Apoptosis
ATCC-	American Type Culture Collection
ATM-	Ataxia-Telangiectasia Mutated Serine-Threonine Kinase
BER-	Base Excision Repair
BLM-	Bloom Helicase
BSA-	Bovine Serum Albumin
CB-	Betweenness Centrality
CC-	Cell Cycle
CCLE-	Cancer Cell Line Encyclopedia
CD-	Degree Centrality
CDK-	Cyclin Dependent Kinase
CE-	Eigenvector Centrality
CI-	Combination Index
DDR-	DNA Damage Repair
DGE-	Differential Gene Expression
DI-	Disruption Index
DNA-	PK- DNA Protein Kinase
DSB-	Double-Strand Break
EGFR-	Epidermal Growth Factor Receptor
FEN1-	Flap Endonuclease 1
FLIP-	FADD-Like Apoptosis Regulator
GO-	Gene Ontology
GOF-	Gain-of-Function
GWAS-	Genome-Wide Association Study
HDAC-	Histone Deacetylase
HIPPIE-	Human Integrated Protein-Protein Interaction rEference
HR-	Homologous Recombination

ICL-	Interstrand Cross-Linking
IDCL-	Interdomain Connecting Loop
LOF-	Loss-of-Function
MAPK-	Mitogen Activated Protein Kinase
MMR-	Mismatch Repair
NER-	Nucleotide Excision Repair
NGS-	Next-Gen Sequencing
NHEJ-	Non-Homologous End Joining
PARP1-	Poly-Adenosine Ribosylating Polymerase 1
PBS-	Potassium Buffered Saline
PCNA-	Proliferating Cell Nuclear Antigen
PIPM-	PCNA Interacting Protein Motif
PL-	Pogo Ligase
PPI-	Protein-Protein Interaction
PTM-	Post-Translational Modification
SM-	Somatic Mutation
SNP-	Single Nucleotide Polymorphism
SSB-	Single-Strand Break
T3-	Triiodothyronine
TCGA-	The Cancer Genome Atlas
TDF-	Tumor Dependent Function
TLS-	Translesion Synthesis
TNBC-	Triple-Negative Breast Cancer
UV-	Ultraviolet
WT1-	Wilm's Tumor Protein 1

ABSTRACT

This thesis Cancer is the second leading cause of death in the modern world, only trailing congestive heart disease. Many factors contribute to the mortality rate, including the diversity of tumors, development of chemoresistance, and recurrence of metastatic tumors. Conventional chemotherapeutic approaches focus on universal features of cancer derived from its rapid proliferation. Rapid proliferation inherently produces stress on metabolic systems, but also on the limiting macromolecule to cell proliferation: DNA. DNA replication and overall genomic stability are negatively impacted by rapid cell proliferation and is mitigated by dysregulation of DNA damage repair (DDR) and apoptosis pathways. Somatic mutations and aberrant gene expression provide both avenues of therapy and resistance. Understanding tumor sensitivity to optimize care expeditiously can be furthered by investigating additional targeted molecular and integrated bioinformatic approaches.

Proliferating cell nuclear antigen (PCNA) is an essential gene to numerous tumor-dysregulated processes including DNA replication and repair. Conventional wisdom would prohibit targeting PCNA due to its status as an essential gene, as directly antagonizing it would cause toxic effects in healthy cells. However, multiple groups have created small molecule antagonists capable of targeting PCNA without affecting normal cells. Some of these antagonists have been qualified biochemically providing insights into their mechanisms of action. I sought out to define the different classes of PCNA antagonists to describe possible clinical utility. This work resulted in three defined classes that are separated by their effects on general DNA damage induction, selective inhibition of DDR pathways, and DNA replication processivity.

Network theory has been utilized to integrate disparate informatic approaches to extract multilevel data with greater explanatory power than the original source data. Network approaches utilizing differential gene expression and drug response profiles have led to the discovery of novel targets and disease subtypes. I sought to use a network approach to leverage differential gene expression (DGE), gene ontology (GO) terms, and protein-protein interactions (PPI) data to determine synergistic drug combinations in cancer cell lines with disparate DDR backgrounds. I limited the scope of this work to DDR, cell cycle, DNA replication, apoptosis, and MAPK associated genes. To power this approach, I created three novel metrics of PPI network

connectivity through GO term and DGE: GO Impact, GO Cohesion, and GO Adhesion. From these novel metrics, I created a visualization technique dubbed a Process Network that recharacterizes a PPI network into a set of pathway interactions. Using gene removal as a model of inhibition, I measured resulting network disruption to determine synergistic relationships. I produced a method with 90.2% specificity and 88.7% sensitivity.

CHAPTER 1. INTRODUCTION

Cancer is the second leading cause of death in the modern world, only trailing congestive heart disease.¹ Many factors contribute to the mortality rate, including the diversity of tumors, development of chemoresistance, and recurrence of metastatic tumors.² Conventional chemotherapeutic approaches focus on universal features of cancer from which it derives its rapid proliferation. These approaches include DNA damage, mitogenic therapy, and metabolic toxins, all of which cause general toxic effects that exacerbate treatment and limit the use of these therapies.^{3,4} Further, the diversity of tumors goes beyond tissues of origin and progression but includes driver mutations, cell survival plasticity, and re-engineered proliferation loops that provide chemoresistance.⁵⁻⁷ Within these unique cancer features, genes that possess a heightened importance in cancer biology has provided fodder for effective targeted therapeutics. These insights have spurred the development of personalized specific therapies for pre-selected patient populations to achieve higher success rates.⁸⁻¹⁰ However, further stratifying diverse diseases slows treatment progress.¹¹⁻¹⁴ Clinical trials seeking to apply molecular therapies that target features common within different tumor types continue to increase the number of successful new^{15,16} treatments through drug repositioning. However, these targeted features must be distinct from healthy tissue pathways to offer advantages over traditional chemotherapies. Further data analysis and chemical tools are needed to accelerate the discovery process for understanding these distinctions.

At the heart of the issue is that as different as cancerous systems are from healthy ones, they are both utilizing, for the most part, the same components. For example, in both “normal” biology and cancer biology, there are shared “essential genes”.^{17,18} Essential genes if deleted, or sufficiently mutated to more extended function, result in embryonic lethal phenotypes. All these genes have roles in fundamental processes of cell growth and function, such as DNA replication, cell cycle, or cell survival.^{19,20} Many of these essential genes products are considered “untargetable” due to their importance in healthy cells (Table 1.1). The exceptions are proteins that are key to rapid proliferation, especially those involved in DNA replication and cytokinesis as tumors rely on them more heavily than most normal cells do. Still, these possess strong side effects due to their cytotoxicity which limits their utility.

Table 1.1: Essential genes within cancer contexts. Of the over 2,000 essential genes many of them are more associated with certain tumor types. Much of this has to do with the tissue of origin, but many are so tied to basic cancer pathophysiology that they are important to all types.

Essential Gene Class	Tumor Types	Example Genes
Neuronal Development	Glioma, Breast, Ovarian	DCX, SIX3, ZIC2
Gonad Development	Prostate, Testicular, Ovarian, Cervical, Breast	DHH, PROK2, FSHR
Endothelial Tissue Development	All	GATA3, ECE1, HSPG2
Differentiation	All	DNMT3B, TBX5, CREBBP
Sugar Metabolism	All	MAN2B1, DLD, FH
Fatty Acid Metabolism	Liver, Colorectal, Pancreatic	ACOX1, VLCAD, PLA2G6
DNA Maintenance/Replication	All	PCNA, FANCG, ATM
Mitochondrial Function	Lung, Breast, Ovarian, Cervical, Glioma, Urothelial	HADHA, SLC25A19, POLG, PCCA
Tumor Suppressors	All	GPR54, TP53, RB1
Cell Adhesion	Colorectal, Pancreatic	ITG, CADH
Cytoskeleton	Colorectal, Renal, Pancreas, Glioma	SALL1, BBS2, MKKS
Hormone Synthesis	Prostate, Testicular, Ovarian, Cervical, Breast	AR, CRH, CTSD
Proteolysis Overturn	Colon	UBR1, PSMA1
Cell Stress Regulators	Lung, Prostate, Stomach, Colorectal	NAG, HSP90A, HSP1

Figure 1.1 shows the extent that essential genes make up the human protein interactome. Essential genes frequently are found as hubs of activity and intersections between multiple molecular signaling pathways. Further, interactions with essential genes have considerable overlap with oncogenes in their areas of influence. It follows that they are highly connected in cellular networks to currently drugged systems and provide the context for much of cancer therapy mechanisms.^{21,22} With this in mind, understanding how these genes can be manipulated to reduce cancer systems' plasticity can lead to a reduction in chemoresistance. As essential genes, targeting them directly, remains risky unless disease contexts and aberrant stressors are identified that separate them from their essential functions. These stressors can be introduced or enhanced through well-defined mechanisms of current chemotherapeutics and next-generation options.

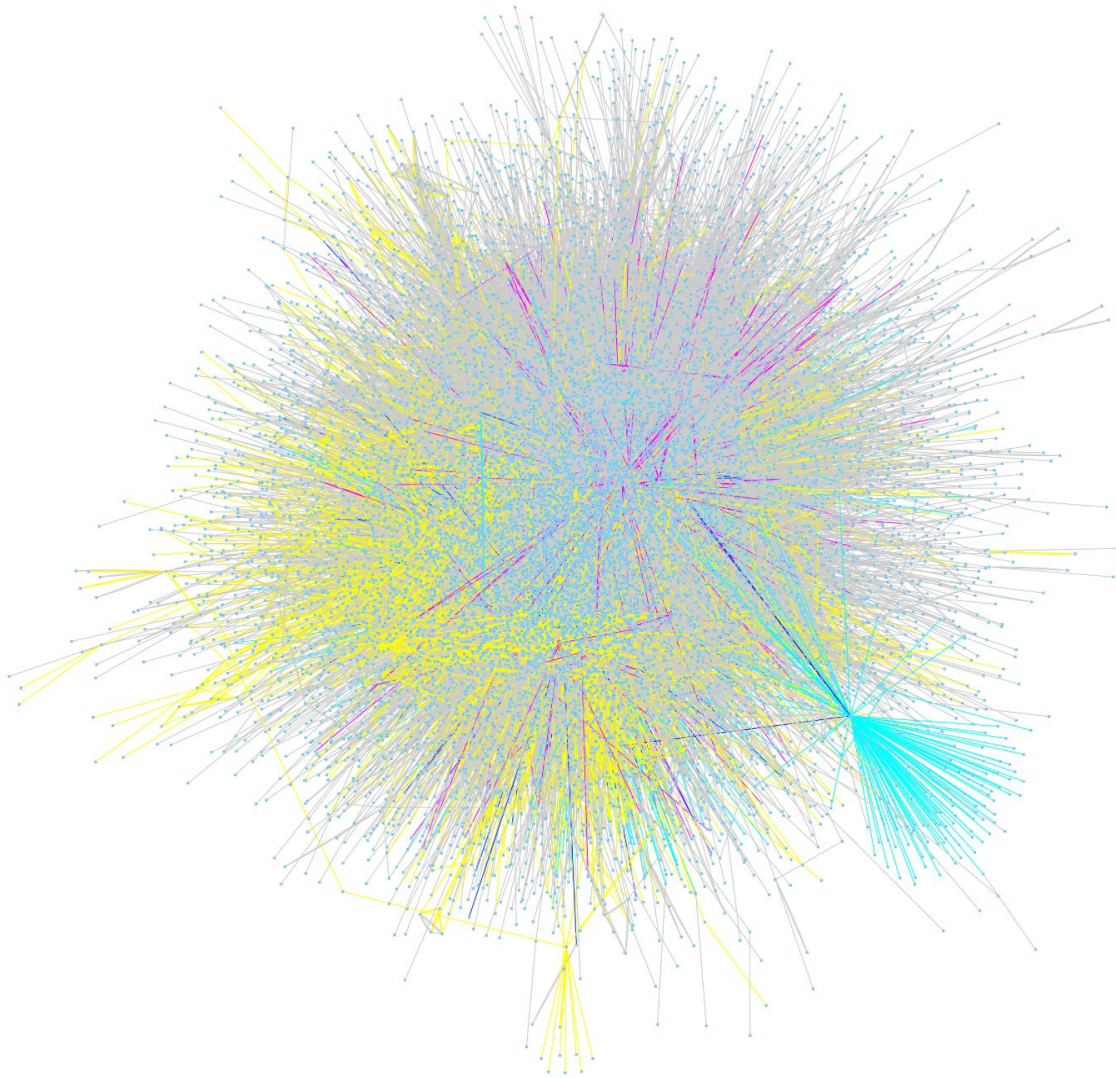
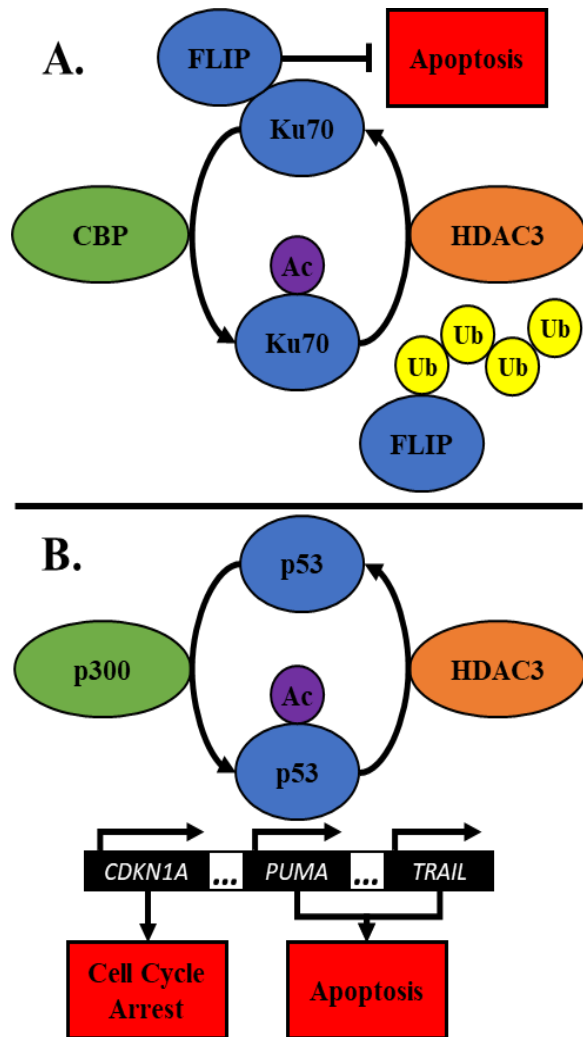


Figure 1.1: Essential genes and tumor genes influence. There are 26,047 nodes and 569,182 edges, with 1,151 genes being considered essential genes by the Database of Essential Genes, last updated December 2017. Oncogenes were qualified through the loss-of-deletion approach outlined in (Pertesi, 2019). The entire proteome with protein-protein interactions from BioGrid. Interactions that involve essential genes are yellow, interactions including tumor suppressors are magenta, and those that include oncogenes are cyan, and those without any of those are gray. Figure was visualized with Cytoscape version 3.8.1

Stressors could take the form of high-stress genomic changes, small molecules, or engineered macromolecules.

An example is the FDA-approved HDAC3 inhibitor, vorinostat.²³ HDAC3 is a Class I histone deacetylase known for its vital role in histone remodeling surrounding DNA damage repair and DNA replication.²⁴ While there is some redundancy in this function with HDAC1 and HDAC2, the complete loss of HDAC3 in healthy cells remains lethal.²⁵ Class I HDACs are also involved in



deacetylating non histone proteins. In this way, they modulate numerous key pathways with HDAC3 being responsible for apoptosis suppression through numerous mechanisms, two of which are shown in Figure 1.2.²⁶ In gastric cancers, FADD-like apoptosis regulator (FLIP) is responsible for inhibiting caspase 8 activation through the extrinsic apoptosis pathway via the FADD receptor.²⁷ HDAC3 ensures FLIP's stability through deacetylating Ku70, allowing it to complex with flip and prevent FLIP's degradation.²⁸ The loss of HDAC3 activity reduces the amount of FLIP expressed and sensitizes patients to the extrinsic apoptosis pathway activators.²⁹ In some types of lung and colon cancer, overexpressed HDAC3 deacetylates p53 reduces its transcriptional activity, which reduces the expression of numerous cell cycle arrest and pro-apoptotic genes.^{30,31} HDAC3 inhibition allows p53 to be highly transcriptionally active and sensitize cells to cisplatin and other traditional chemotherapeutics. Through overexpression of HDAC3 and different modulations to the tumor's genome, certain functions of HDAC3 become emphasized and essential to tumor biology. We

Figure 1.2: Blue objects are proteins, green objects are histone acetyltransferase, orange objects are histone deacetylases, purple objects are acetylation PTMs, yellow objects are ubiquitin PTMs, and red objects are anti-tumor pathways.

consider these to be the tumor-dependent functions (TDF) of HDAC3 and these TDFs allow HDAC3 to be targeted in these systems and leverage the activity of other therapeutics such as orlistat. Thus, the key to targeting essential genes in tumors is to assess TDF's context and discover new drugs and/or appropriate combinations of existing drugs to take advantage of the tumor's novel dependencies.

The hypothesis tested in this work is that drug combinations that include essential genes can leverage sufficiently compromised contexts to treat tumors safely with current therapeutic options specifically.^{14,32} Essential genes, due to their roles in biological systems, cannot be circumvented by the typical chemoresistance mechanisms that tumors utilize without consequences on survival. As such, our focus is on systems that are highly flexible and dependent on essential genes but show significant modulation in disease contexts to be target candidates for pharmacological agents. Inhibition of essential genes can exacerbate reductions in redundant and compensatory processes that tumors make to maximize proliferation and minimize apoptosis. The use of targeted secondary therapy can ensure the stress induced by such a system results in cell death by inducing a context that relies on the essential gene or vice versa. This approach multiplies efforts in targeted therapy by enhancing efficacy.

1.1 Rapid Proliferation Negatively Impacts Genome Stability

Cancer is a genetic disease often brought on by incorrect processing or repair of the host's DNA. These errors progress to a gain-of- or loss-of-function mutation in oncogenes or tumor suppressors respectively, to create a state of tumorigenesis.³³ Genes that commonly cause this transformation surround cell survival and cell proliferation (Fig. 1.3).³⁴⁻³⁶ Many subsequent mutations throughout tumor development occur in genes for DNA replication, repair, and maintenance, all of which are requisite for successful cell growth and survival. Scaffold proteins, including proliferating cell nuclear antigen (PCNA), facilitate these processes by creating platforms for enzymes to act on DNA.^{37,38} As a nexus of necessary operations, PCNA function is essential, and tumor cells enhance the protein status through its central roles in proliferation. Further, PCNA and several other scaffold proteins act as hubs to numerous disease-modulated pathways. DNA damage repair (DDR), DNA replication, and cell cycle signaling show extensive mutations and differential expression in a disease state.³⁹⁻⁴¹ Between tumor types, different suites

of changes provide unique contexts for how these three processes interconnect and dysregulate cells with novel mechanisms to the same overall outcome, increased cell proliferation. Further, many changes brought on by the stress of rapid proliferation cause changes in related processes, making the origin of dysregulation often cryptic.

1.1.1 Cell Cycle Progression and Genome Stability is Uncoupled from Apoptosis in Tumors

Many checkpoint proteins prevent the progression of cell cycle depending upon the cell's status. Some check point factors monitor the available energy and resources the cell possesses to ensure that the required DNA replication and mitosis components are available.^{42,43} Other checkpoint factors monitor the expression of enzymes required for each step to ensure uninterrupted progression during cell division. Finally, numerous proteins exist that monitor during genome replication the DNA status in the cell to ensure that it is an accurate copy to be passed on to the daughter cells. These checkpoint proteins are most active during S phase, when DNA replication occurs, and at the G2/M checkpoint, just before the cell divides.⁴⁴⁻⁴⁸

DNA damage is a constant stress point during cell proliferation and intensifies the metabolic pathways upregulated in tumors.⁴⁹⁻⁵¹ To overcome this stress, cancers must greatly enhance its ability to repair damaged DNA and/or increase tolerance of damaged DNA. DNA damage stress in tumors is mitigated directly through modulating DDR or indirectly by reducing the effectiveness of DNA damage to induce apoptosis signaling.^{3,52-59} Many DDR proteins are overexpressed in tumors to expedite repair, and TP53 is commonly mutated in tumors severing the primary connection between DNA damage and apoptosis. However, TP53 is not the only route to cell death from DNA damage. DNA damage often delays cell cycle progression, even halting it in S phase, causing a cascade of signaling resulting in cell death through several intrinsic apoptosis signal proteins in the mitochondria. This pathway allows DNA damage to faithfully cause cell death in the absence of several apoptotic markers.

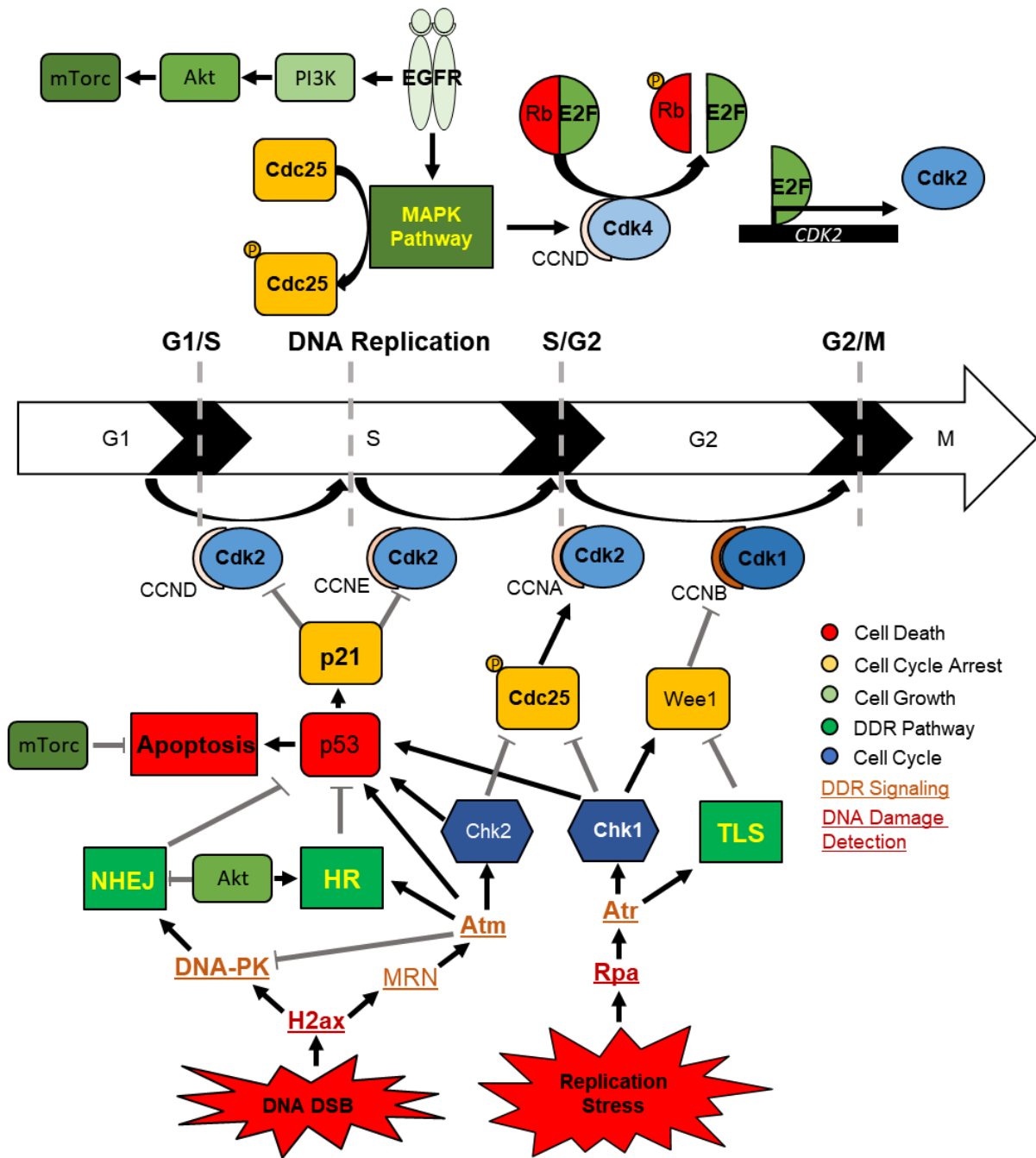


Figure 1.3: Cell Cycle and DNA damage repair in a tumor context. Due to tumors possessing an increased proliferation rate, this makes them more predisposed to utilizing the homologous recombination (HR) over the non-homologous end-joining (NHEJ), the two main double-strand break repair pathways. Due to the increased proliferation rate, that is undue stress on DNA in replication that is mitigated by translesion synthesis (TLS) to tolerate the damage sustained by the stress. Green objects facilitate increased growth, red objects suppress tumors, blue objects progress the cell cycle, and orange objects slow cell cycle.

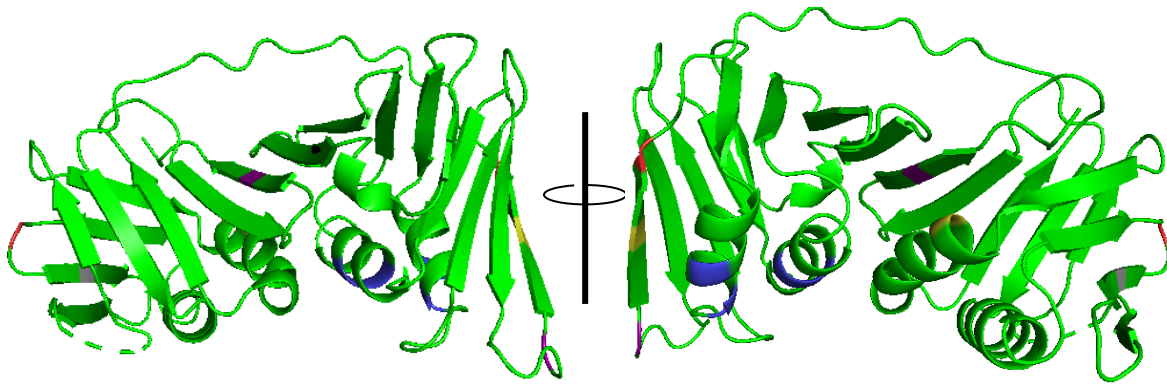
1.1.2 Cell Cycle Progression and DNA Damage Repair are Mutually Regulated

Tumors often modulate cell cycle proteins to prevent the delay of any phase regardless of DNA damage status.^{65,66} This condition often occurs through loss-of-function mutations to checkpoint proteins and constitutive upregulation of DNA repair proteins. These defects generally appear together since DNA damage sensors and checkpoint proteins are required to activate and increase DDR proteins' expression. By increasing overall DDR levels, DNA damage sensors that link to apoptosis are circumvented without losing overall genomic integrity. However, this scenario causes a dependence upon specific DDR pathways. In many cases, when S phase proteins are overexpressed, homologous recombination (HR), becomes preferred in other phases. Alternatively, a reduction mismatch repair function occurs to increase DNA damage tolerance pathways. Both strategies enable rapid proliferation despite genome instability. These processes still allow for increases in gene translocations, point mutations, and other means of tumor development.

DDR processes also include numerous mitogenic factors, and their successful repair suppresses cell cycle arrest. In this way, DDR can complete a positive feedback loop that ensures that checkpoint proteins cannot halt cell cycle and lead to apoptosis. Further, both cell cycle progression and DDR processes can enhance cell survival pathways to ensure rapid proliferation. Unsurprisingly, efforts to counter DDR and cell cycle affect one another and leads to lowered cell survival and the onset of apoptosis. Many means of regulating cell cycle that balances the influence of DDR on cell cycle are removed early on in tumor development. This mutual modulation services key junctions in cell cycle and DDR, but often are non-specific and affect all dividing cells.

1.1.3 DNA Replication and Cell Cycle Drive DNA Damage Repair Outcomes

DNA is most commonly packaged as chromatin, a protein-DNA complex that protects DNA from stress and tangling. In order for DNA replication to occur, the entire genome must sequentially dissociate from this complex and be exposed to multiple sources of DNA damage. DNA unraveling using helicases can cause high stress levels that result in single-strand breaks (SSB) or even double-strand breaks (DSB), leading to cell death. During this phase, different DDR mechanisms activate to prevent loss of DNA and to maintain an accurate replication. G_0 and G_1



Residue	Modification	Key	Writer	Function
K13	Acetylation	Blue	CPB/p300	PCNA Degradation
K14	Acetylation	Blue	CPB/p300	PCNA Degradation
K77	Acetylation	Blue	CPB/p300	PCNA Degradation
K80	Acetylation	Blue	CPB/p300	PCNA Degradation
K168	ISGylation	Gray	EFP	Terminate TLS
K110	Methylation	Purple	EZH2	Promotes longer Okazaki Fragments
K248	Methylation	Purple	SETD8	Polymerase switch to POLD
Y114	Phosphorylation	Yellow	NA	Adipogenesis
Y211	Phosphorylation	Yellow	EGFR	Prevents degradation, inhibits MMR
K254	Sumoylation	Teal	UBC9	DSB foci formation
K117	Ubiquitin	Red	NA	UV damage response
K164	Ubiquitin	Red	Rad5, Rad18, RNF8	Promotes DNA synthesis at damaged site

Figure 1.4: PCNA structure and PTM impact on pathways. PCNA is a highly modulated scaffold protein that impacts the numerous interactors and pathways it is involved in. The crystal structure is marked at the residues by the modification type with the functional change listed.

phase DDR mechanisms rely on limiting the DNA's exposure and the speed of the repair, whereas S and G₂ phase DDR mechanisms prioritize accuracy of repair. DNA replication is then coordinated by numerous protein complexes and signaling cascades.

At the center of both DNA replication and repair is proliferating cell nuclear antigen (PCNA), which acts as a platform for assembly of protein-DNA complexes called the replisome. The entire replisome forms around PCNA. Higher order regulation of the replisome occurs through post-translational modifications (PTM) of PCNA to coordinate DDR and DNA damage tolerance.⁶⁰⁻⁶⁶ Figure 3 summarizes the sites of PTMs on PCNA and the known biological regulatory roles. These changes determine only if DDR occurs, but which pathways are active. Examples like phosphorylation of Y211 are known to stabilize PCNA homotrimers, and prevents mismatch repair activation.^{67,68} The ubiquitination of K164 is required for polymerase switching in translesion synthesis. The regulation of many PTMs is through the MAPK pathway's effectors and replisome regulators such as BRCA1. Other scaffold proteins are recruited and modified by DNA damage sensors, such as XRCC1/4 by PARP1 or the MRN complex.⁶⁹⁻⁷⁵ Overall, these processes are not monolithic pathways following a direct sequence of events but highly interconnected processes modified through upstream signal proteins and the final complexes' enzymes. Numerous other PTMs of PCNA allow it to be a modular scaffold for DNA processes through its 200+ interactors that rely on multiple binding modes. Changes in the PTMs of PCNA bias DDR outcomes as well as modifications to the surrounding pathways.

1.2 Identifying Disease Markers through Informatic Approaches and Pathway Analysis

With the exponential growth in available genome data, more specific patient information are accessible to understand disease prognosis and progression.⁷⁶ To utilize genomic information, libraries that organize these data into useful formats and data tools become rate-limiting. The progress in ontology and informatics has mirrored the rise in genomic data availability as a result. In the past ten years, genome-wide association studies (GWAS), pathway analysis tools, and simple gene enrichment studies are available for almost every tumor type.⁷⁷ Patient-derived tumor genome sequencing, coupled with pathway analyses, are now used to identify key driver mutations that include mitogenic factors as guides to predict treatment effectiveness.^{78,79}

While correlation studies have virtually found oncogenes and tumor suppressors, they require discrete genomic changes, such as somatic mutations.^{80,81} Often, the gene changes impact multiple pathways that can thwart treatments due to these genomic changes. Both researchers and clinicians require more detailed descriptions of these changes' impacts on pathway regulation to guide decision-making. In biological networks, the vertices are often genes, gene products, or biological processes, while the edges denote some link between the two vertices. In pathway analysis, many network theory algorithms find great utility in determining changes in cell process dynamics.⁷⁷ The questions that remain are how to construct networks with the most critical content to represent the diseases under consideration.

1.2.1 Somatic Mutations

Somatic mutations were the earliest biomarkers used in determining tumor progression and the likelihood of tumors developing in one's lifetime. Genes that, when mutated, caused tumor development through enabling rapid proliferation were named oncogenes. These were often genes that signaled cell proliferation, and the mutations often removed safeguards that allowed them to be regulated.⁸² Tumor suppressors act to prevent rapid proliferation or to initiate apoptosis once it occurs.⁸³ The loss of tumor suppressor functions, often through a nonsense mutation or a loss of enzyme activity, allows tumors to develop. By comparing tumor genomes to normal tissue genomes, additional oncogenes, and tumor suppressors, gene discovery has occurred. Sets of somatic mutations remain the primary biomarker used in determining treatment due to their transparency and well-defined impact.

Primary networks are formed based on concurrent somatic mutations creating links between genes.⁸⁴⁻⁸⁶ Those trends can then be used to see if there are links between the patient or clinical data from those samples. Response to treatment, tumor subtype, and development stage are all often used and provide a means to predict drug response or aid in prognosis.⁸⁷ Further, these data used in conjunction with biological pathway models can discern what cell functions are most affected by the set of mutations. Somatic mutation sets show redundancy, but they allow clinicians to narrow down treatment options in many tumor types.

1.2.2 Differential Gene Expression

Differential gene expression (DGE) quantifies the differences in expression between two or more sets of tissues. The resultant patterns are useful to differentiate tissues and to understand how different organs and cells function.^{88,89} In oncology, normal tissue is compared to tumors to distinguish what changes in gene expression associate with tumor growth and progression. Since many identified genes that cause cancers are signaling proteins, there remains ample dysregulation downstream of the expressed gene to explain differences in tumor types and subtypes. DGE has been instrumental in stratifying tumor subtypes beyond morphology and surface antigens. Outside of the clinic, differential gene expression has been key in determining drug targets and mechanisms of action and therapy resistance.^{90,91}

DGE provides an alternative dataset for clinicians to stratify tumors into subtypes that can describe prognosis and drug responsiveness.⁹²⁻⁹⁴ This approach takes into consideration somatic mutations in key oncogenes or tumor suppressors to more fully describe the disease context. While useful when they are apparent, morphological and cell surface markers only capably describe cells that are defined by those features. In the case of triple negative breast cancer (TNBC), there are no surface markers or somatic mutation to distinguish this diverse group of tumors. Other tumor types are described by unsuccessful treatments that the patient has undergone, such as castration-resistant prostate cancer which suffers the same ontological issues as TNBC. These ill-defined tumor subtypes often lack targeted therapies and resistance to traditional chemotherapy along with recurrence is common.^{95,96} The few targeted therapies available in these contexts can be effective, but features to select by are sometimes transient and stable biomarkers are rare, limiting the usage of such therapies.^{13,97} It is essential to describe mechanisms by which therapies can be effective and translate this to effective biomarkers. This can take the form of somatic mutations and differential gene expression contexts that possess favorable phenotypes to expand these therapy types. Of course, doing so in the current model requires robust tools that do not yet exist.

Due to the aberrant biology of tumors, DGE has also been used to assess novel biology that is actionable for treatment options. Network approaches that integrate DGE data and novel pathway linkages offer perspective in specific disease contexts. Often DGE data is derived through treated samples and cell lines to discern changes related to either sensitivity or chemoresistance. When paired with siRNA and CRISPR, a considerable amount of pathway analysis can be achieved.^{98,99} Even without these additional experimental techniques, network theory approaches

that examine concurrent DGE across different contexts can identify gene sets related to tumor biology. This goes past gene enrichment studies to discern novel interactions between pathways, but still rely upon well-understood gene sets preventing discovery past what are already defined cancer targets.

1.2.3 Protein-Protein Interactions

Proteomics offers considerable insight into pathophysiology and drug discovery in cancers. Crystal structures of many oncoproteins contribute to the determination of targeting mechanisms, which lead to numerous therapeutic options. Examples are the increased understanding of protein complexes and interactions for the crucial changes in ubiquitination-based protein degradation, including mdm2-p53 or transcription factor activity.^{100,101} Further, strategies that target post-translational modifications allow for entirely novel strategies in addressing tumors, adding another degree of complexity.

Network approaches are particularly useful in understanding protein-protein interaction (PPI) dynamics.^{102,103} In tumor contexts, both an increase and decrease in protein interaction can mirror gain-of- or loss-of-function somatic mutations. Disease networks described by protein-protein interactions are among the most commonly used for drug repurposing as a result.^{104,105} Predicting common features resulting from general changes without the constraint of gene sets and concurrent changes provides a less biased discovery context. However, the risk of using broader datasets remains evident since more possible explanations must be investigated using the appropriate experiments or ruled out by previously published works.

Structural biology, as a subtopic of proteomics contributes considerable insights to the role of mutations in protein-protein interactions. The acceleration in recent years due to the development of Cryo-EM technologies allows for the visualization of more complex protein assemblies for the first time.^{106,107} These protein complexes are key in tumor contexts due to the novel complexes that occurring when individual protein expression change from either mutant and wild-type genes. Shifts in the complexes functional states can alter the roles of individual gene functions in disease. An example is the Wilm's Tumor protein 1, which normally acts as a tumor suppressor through activating p53, but becomes an oncoprotein when overexpressed through sequestration of p53.^{108,109} Shifts in the functional states of protein complexes can be theorized

through predictive techniques. However, an understanding at the molecular level is required to elucidate new targeting strategies unique to cancer disease.

As changes in PPIs are sufficient to induce or progress a disease state they represent an emerging class of drug targets.¹¹⁰ Instead of an enzyme where you can target the active site, PPI inhibitors often go after conserved binding regions of one or more proteins in the complex. To achieve this, PPI inhibitors must target one or more pockets or subpockets along the interface of one of the target interaction proteins.¹¹¹ The advantage of a PPI inhibitor is that instead of abrogating all functions of a protein, only functions dependent on that interaction which contribute to the disease state are impacted. This is especially advantageous in the case of essential genes that possess many necessary interactions, but only a subset is contributing to the disease state. In the case of p53 and WT1, a reduction in the WT1 interaction would reverse the sequestration effect and allow the cell to properly activate apoptosis.¹¹²

In the case of PCNA, which is necessary for several processes, inhibiting a specific or subset PPIs would also effectively target surrounding disease effects without losing its essential functions. The numerous post-translational modifications and binding modes of PCNA creating many scenarios provides multiple avenues for this approach. A single-nucleotide polymorphism (SNP) in PCNA, S228I, provides the basis for an autosomal recessive neurodegenerative disorder that results from a deficiency of the nucleotide excision repair (NER) pathway to achieve proper DNA repair.¹¹³ This mutation functionally restricts a flexible region of PCNA, the inter-domain connecting loop, which conforms to proteins that bind to PCNA, stabilizing the interaction.¹¹⁴ DNA replication and other processes still occur in cells with this mutation showing that modulation of one binding site of PCNA can produce specific functional outcomes.

1.3 Enhancing Current Therapeutic Options in Cancer

The difficulties in general chemotherapy approaches, such as microtubule inhibitors, metabolic toxins, or DNA damage agents, is that drug-induced toxicity is not unique to tumors. These on-target toxicities severely limit their utility long term and often leads to chemoresistance in tumors, exacerbating the issue.^{115,116} These chemotherapeutic approaches rely on inhibitors of oncogenic pathways, cell survival, cell cycle, DNA maintenance, and apoptosis. A conundrum emerges from these observations since these pathways from a molecular perspective show high

tumor specificity. However, these same processes show the highest levels of plasticity for survival.^{117,118} Traditional chemotherapies work by leveraging the increased stress on tumor systems that over-rely on these processes for survival relative to normal cells. Table 1.2 shows a cross-section of traditional chemotherapies that are components of standard-of-care in oncology for decades. Molecularly-targeted therapies that inhibit the tumors' ability to cope with the increased stress have now made significant progress. Many of these newer therapies depend upon appropriate biomarkers to identify patients whose tumors will be sensitive to these treatments.^{119–121} However, the utilities for most of these new targeted therapies are limited by the diversity of tumors and the remaining redundancy between biological systems within tumors.^{122–124} Unfortunately, identifying individual targets in each tumor context takes considerable time and effort to discover and reduce to practice.

Table 1.2: Traditional chemotherapies that target conserved phenotypes in all tumors. The primary process they are associated with and their basic function are listed.

Drug	Target	Process
Anthracyclines	TOP2A	DNA tangle, supercoil relief
Irinotecan	TOP1A	DNA stress
Cisplatin	DNA cross-linker	DNA damage
Ifosfamide	Alkylating agents	DNA damage
5-FU	Thymidylate synthase	Nucleotide metabolism
Gemcitabine	Anti-metabolite	DNA synthesis
Taxanes	TUBB1B	Cytokinesis
Letrozole	Aromatases	Hormone metabolism
Leuprolide	Luteinizing Hormone Releasing Hormone	Hormone metabolism
Fulvestrant/ Nilutamide	Hormone receptors	Tyrosine receptor kinase activate pathways

Two strategies to expedite and enhance the application of novel and current therapies for cancer patients include drug repositioning and unique drug combinations. Drug repositioning involves using a drug in a novel disease context, often discovering that it possesses an alternative target

relevant in that disease state. It can also occur through the discovery of increased importance of the drug target in particular disease contexts. The development of drug combinations currently focuses on expanding the utility of two monotherapies through empirical clinical trials (Table 1.3). An extensive understanding of the genomic and proteomic context in the patient tumors is needed to maximize the appropriate application. However, with sufficiently advanced informatics tools, singular discrete features, such as a somatic mutation, would not be required. Instead, a tool that predicts phenocopy events through diverse features, including multiple data types, could be used as a druggable context. Current approaches exist to identify novel disease markers that are consistent with pathophysiology by determining overall mechanisms and finding phenocopy events.¹²⁵⁻¹²⁷ However, this needs to be extended to druggable contexts to combat the heterogeneity of tumors and expand the use of targeted therapies.

Table 1.3: Drug combinations approved by the FDA. Combinations that did not include a targeted therapy were excluded and combinations that utilized the same strategy as another were excluded with the first combination filed being kept. Drug list and targets were collected from the accessdata.fda.gov.

Drug A	Drug Class A	Drug B	Drug Class B
Flutamide	Antiandrogen	Leuprolide	Luteinising hormone-releasing hormone
Idarubicin hydrochloride	Anthracycline	Cytarabine	Pyrimidine analog
Vinorelbine tartrate	Tubulin antagonist	Cisplatin	DNA cross-linker
Trastuzumab	Anti-HER2 Antibody	Paclitaxel	Tubulin stabilizer
Cetuximab	Anti-EGFR Antibody	Irinotecan	Topoisomerase inhibitor
Bevacizumab	Anti-VEGF Antibody	5-Fluorouracil	Pyrimidine analog
Lapatinib	EGFR kinase inhibitor	Capecitabine	Pyrimidine analog
Ixabepilone	Beta-tubulin inhibitor	Capecitabine	Pyrimidine analog
Pertuzumab	Anti-HER2 Antibody	Trastuzumab, Docetaxel	Anti-HER2 Antibody, Tubulin stabilizer
Ziv-aflibercept	Angiogenic inhibitor	5-Fluorouracil, Leucovorin, Irinotecan	Pyrimidine analog
Obinutuzumab	Anti-CD20 antibody	Chlorambucil	Alkylating agent
Idelalisib	PI3K kinase inhibitor	Rituximab	Anti-CD20 antibody
Nivolumab	Anti-PD-1 antibody	Ipilimumab	Anti-PD-L1 antibody
Palbociclib	CDK4/6 kinase inhibitor	Letrozole	Aromatase inhibitor
Necitumumab	Anti-EGFR Antibody	Gemcitabine, Cisplatin	Pyrimidine analog, DNA cross-linker
Ribociclib	CDK4/6 kinase inhibitor	Letrozole	Aromatase inhibitor
Midostaurin	FLT3 inhibitor	Cytarabine, Daunorubicin	DNA Polymerase inhibitor,
Abemaciclib	CDK4/6 kinase inhibitor	Fulvestrant	ESR1 dimerization inhibitor
Glasdegib	SMO receptor inhibitor	Cytarabine	DNA Polymerase inhibitor
Alpelisib	PI3K kinase inhibitor	Fulvestrant	ESR1 dimerization inhibitor

1.3.1 Utilizing Drugs in Ideal Contexts by Identifying Relevant Biomarkers

Clinicians have several criteria that they use to categorize patients to determine a prognosis and therapeutic regimen. Tumor morphology and surface antigens have been the primary means of making these decisions for decades, but genomic information using next generation sequencing (NGS) technologies are rapidly emerging as a first choice.^{84,93,128,129} The rapid identification of biomarkers that provide sensitive contexts for existing therapies is one means of expanding the use of current therapies. Multiple genotype tests have been FDA approved to determine treatments in breast cancer.^{130–132} Somatic mutations have been the favored biomarker to be used, but in clinical trials and drug discovery, tumor gene expression are also useful to determine if treatments will be effective.

Multiple approaches can determine whether a biomarker is likely to be relevant for a particular drug or disease context. GWAS are used to broadly examine disease states for genomic variants that are universal across many sample types.^{133,134} While broad in its scope, GWAS alone cannot convey the direct functional impact of detected gene loci on phenotypic outcomes. Gene enrichment is a similar differential analysis that relies on gene expression instead of somatic mutations, as is the case with GWAS.^{135,136} Both approaches are aided by pathway analyses that provide additional biological contexts to these genetic sequences' differences and their impact on a disease phenotype.

Pathway analysis methods, such as KEGG pathway analysis or IPA analysis, utilize a priori knowledge of biological processes and PPI's that facilitate their function.^{137,138} These curated pathways represent current understanding including any biochemical or regulatory process from kinase signaling to anabolic or catabolic metabolism. Within these pathways, existing pathway analysis methods can identify the impact of the loss of a gene product either through a loss-of-function mutation or down-regulated expression within the pathway.¹³⁹ However, the impact is only understood in individual pathways and not the possible downstream effects on other pathways. Further, these tools do not consider the compounding effects within the aberrant tumor biology with novel connections between pathways. The ability to evaluate patients with criteria based on system functionality rather than discrete pathway markers that only imply function is an unmet need.

1.3.2 Inducing Synthetic Lethality through Drug Combinations

Synthetic lethality is when the loss of two genes produces a much more significant loss in viability than the loss of either gene alone. Often this is done by targeting two compensatory or parallel processes, or vertical inhibition in key pathways^{140,141} but due to cancer's disruption of biological processes, more distant pairings are possible.¹⁴² Synthetic lethal opportunities have only been utilized in the clinic where one gene product is lost to mutation giving leverage to a targeted monotherapy.¹⁴³⁻¹⁴⁵ Drug combinations have consistently been used to decrease the individual toxicities of chemotherapy agents. These combinations generate additional stress to tumor cells that do not allow for the same plasticity as a monotherapy. However, these combinations are rarely designed to induce leverageable contexts that impact overall tumor biology. If deployed, this approach provides a means to produce a highly leverageable context instead of merely anticipating one. However, the interaction of two drugs in a system is orders of magnitude more difficult to evaluate, which has limited this approach.

As with all cancer treatment types, both informatic and experimental approaches to identify suitable disease contexts for synthetic lethal opportunities are the subject of many research tools. The discovery of CRISPR-Cas9 created a rapid means of specifically reducing proteins' content in a high-throughput screen format.^{146,147} This technology allows researchers to remove combinations of proteins and artificially create networks that describe synthetic lethal events. Multiple driver mutations common to many tumor subtypes (such as KRAS, BRAF, etc.) have been identified which enables discovery of specific weak points in proliferative pathways that were theoretically non-redundant.^{148,149} This approach is leading the development of most current therapies which rely on direct targeting of an upstream signal protein that drives an oncogenic system such as EGFR inhibitors and the MAPK pathway.^{150,151} Synthetic lethality is being used in special context of somatic mutations in the BRCA1/2 genes that reveal a sensitivity to PARP1 inhibitors.^{8,144} Tools that rapidly identify contexts for the combined uses of targeted therapeutics through identifying non-canonical phenocopy, either drug combinations or sensitization through genomic features, events is an unmet need that could greatly expand the use of these therapeutics.

What has yet to emerge are *de novo* synthetic lethal therapies that rely on general features of tumors. As shown in Table 4, current combination therapies either include a quality-of-life drug, such as an antiemetic, to tolerate a highly cytotoxic therapeutic or are a previously approved targeted therapeutic with an approved traditional chemotherapeutic. Synthetic lethal informatics approaches have created exhaustive lists of likely synthetic lethal pairings across numerous contexts.^{152–154} Many focus on concurrent somatic mutations within drug sensitive tumor populations while analyzing the disease context’s pathway significance.¹⁵⁵ Others analyze DGE patterns across drug sensitive and resistant populations while using experimental synthetic lethal data to identify genetic profiles.¹⁵⁶ However, both of these approaches focus on total loss of gene function, which prevents them from considering other modes of inhibition.

Table 1.4: Targeted inhibitors in DNA damage repair, cell cycle, and DNA replication. The primary process they are associated with and their basic function are listed as well. Their FDA status is reported if they have been submitted at some point, otherwise, they are labeled as preclinical

Drug	Target	Process	Function	FDA Status
Alpelisib	PI3K	PI3K-AKT Pathway	Kinase	Phase III
Gefitinib	EGFR	RTK, MAPK pathway	Kinase	Phase III
Olaparib	PARP1	a-NHEJ	PAR polym erase	Phase III
NU7026	DNA-PK	c-NHEJ	Kinase	Preclinical
KU55933	ATM	HR, DNA lesion detection	Kinase	Preclinical
PFM01	MRE11	End-resectioning, DSB repair	Endonuclease	Preclinical
ML216	BLM	End-resectioning, DSB repair	Helicase	Preclinical
NSC617145	WRN	End-resectioning, DSB repair	Helicase	Preclinical
PF477736	CHEK1	Cell cycle halting	Kinase	Preclinical
RS-1	RAD51	Strand recombining	Recombinase	Preclinical
D-I03	RAD52	Strand annealing, HR	DNA binder	Preclinical
Streptonigrin	RAD54	Loop resolution	Helicase	Preclinical
Palbociclib	CDK4/6	G1/S checkpoint	Kinase	Phase III
Roscovitine	CDK1/2	S checkpoint	Kinase	Phase II
Alisertib	AURKA	Cell cycle progression	Kinase	Phase II
AZD1775	WEE1	Cell cycle progression	Phosphatase	Phase I

1.3.3 Essential Genes and Synthetic Lethality

The selective inhibition of an essential gene, a gene whose loss results in an embryonic lethal phenotype, through functional antagonism of the encoded protein can be leveraged in disease contexts. Total inhibition essential genes cause toxicities as seen observed with traditional chemotherapeutics. Functional selective antagonism of essential genes as a target requires a disease context for synthetic lethal pairs of agents or genetic defects that lead to drug sensitivity. Thus, disease contexts must be assessed for their dependence on functions and not individual gene expression to select appropriate therapeutic strategies. However, the challenge remains that pathway signaling changes to allow for cancer phenotypes create gaps in understanding the disease context.^{157–159} Essential genes can provide insight into these systems since they are rarely changed outside of their expression and their change in function can be assessed through their interactions.¹⁶⁰ While their biological roles may not alter, their context and regulation are often thoroughly changed to enable the pathologies associated with those systems. Utilizing targets with low flexibility within the networks can provide long term solutions as long as combinations can produce unique conditions. Through drug combinations surrounding these essential gene targets, novel contexts that enhance conventional treatment effects can be achieved.

My approach will investigate the potential to identify synthetic lethal combinations and contexts within currently recognized targets surrounding the interregulated DNA replication, repair, and cell cycle systems.^{53,54,56–58,161–163} This focus provides numerous existing inhibitors as starting points allowing any discoveries made to be more rapidly applicable to a clinical setting. Table 5 represents a survey of targets with a potent and specific inhibitor that has at least been demonstrated utility in pre-clinical animal studies. These biological systems possess several proteins with well-understood functionally dependent interactions. The system's flexibility also provides a considerable compensatory activity that would allow healthy cells to overcome drug combinations based on tumor biases. The addition of PCNA functional antagonism offers an opportunity to stress the system in a manner that gene expression and somatic mutation models are unable to duplicate.

1.4 Scope

As developed in the sections above, a clear unmet need in cancer research is the predictable molecular links of tumor diversity and adaptability. The current approaches utilizing discrete biomarkers to indicate sensitivity and then seeking out either general therapeutic approaches before developing targeted therapies for each one will take decades if not longer. Drug combinations of successful treatments limited by disease context could provide solutions that can be produced at a much higher rate. Further, inducing synthetic sickness would allow for far lower toxicity than conventional approaches. Yet, their utilization would require new tools to evaluate complex biomarkers involving multiple data types.

This work aims to create data analysis tools capable of integrating somatic mutation, gene expression, and PPI data to identify complex biomarkers to evaluate drug combinations. Single discrete biomarkers are useful since there is confidence in their identification, even if they are limited in their utility. Complex biomarkers can indicate cell biology changes through data combinations of protein function changes, expression, and dynamics. Systematic approaches capable of evaluating each of these often require a great deal of expertise to process and interpret. Therefore, our secondary objective is to create useful graphing options that do not sacrifice rigor of analysis but enhances ease of use.

A second goal is to define and reduce to practice an example of an essential gene as a drug target due to TDFs in breast cancers. This will work similarly to the HDAC3 inhibitor development by assessing what functions can be targeted and developing strategies to make the effect specific to the tumor type. I evaluate the utility of inhibiting an essential gene, PCNA. Understanding how to leverage the centrality of essential genes in chemoresistant contexts will allow for rapid expansion of both current and future therapeutic options. However, it is important to monitor the multiple pathways that are influenced by PCNA to determine if specificity can be achieved through direct inhibition. Modulation of DNA replication, DDR, DNA damage tolerance, or cell cycle all influence multiple chemoresistant strategies and being able to reduce the functionality of any of them could lead to synthetic sickness. With few redundancies in these processes, it is unlikely that further resistant phenotypes could arise making this strategy very rewarding in several contexts.

CHAPTER 2. CLASSES OF SMALL MOLECULE PCNA INHIBITORS DEFINED BY MECHANISM OF ACTION

2.1 Introduction

Proliferating cell nuclear antigen (PCNA) represents a hub in cell processes required for cancer development, including DNA replication, histone modification, DNA damage repair (DDR), and telomere maintenance.^{164–166} Many of these roles are also necessary for all proliferating cells, not merely cancerous cells. Simultaneous targeting of all PCNA functions would be disastrous due to its status as an essential gene. All the processes that PCNA controls through organizing DNA-protein complexes have been targeted indirectly through traditional DNA damaging chemotherapeutics or directly through targeted therapies.^{25,44,167} If a pharmacological agent could modulate only a select subset of PCNA functions, there could be a biological context for numerous other approaches that target novel unstable biological states. PCNA would then join an emerging group of drug targets whose regulation through post-translational modifications and protein-protein interactions (PPI), provide numerous therapeutic applications.^{168–171}

One of the few known PCNA genetic mutations occurs at S228I, which resides in the interdomain connecting loop (IDCL) used to stabilize protein-protein interactions. The mutation reduces IDCL flexibility, stabilizing PPI with PCNA after initial binding at the PCNA interacting protein motif (PIPM) site.¹⁷² This loss of flexibility reduces a subset of PCNA interactions required for the nucleotide-excision repair (NER) pathway, which repairs single-strand breaks and adducts. However, this mutation does not prevent DNA replication functions of PCNA, allowing patients to reach adulthood before developing neurodegenerative effects. The selective impact of another mutation at Y211F shows that phosphorylation at this site is necessary for prolonged polymerase loading, integral to a successful S phase of cell cycle.^{67,173,174} Yet, cells possessing this mutation were able to repair DNA damage caused by cisplatin. Another example of a selective effector of PCNA function emerges from the small molecule inhibitors T2AA and PCNA-I1 that reduce the amount of ubiquitination of K164, contributing to a loss of the translesion synthesis (TLS) DNA damage tolerance pathway.^{175–177} These examples highlight the potential of direct effectors to

modulate PCNA related functions selectively. Identifying the disease contexts for a PCNA inhibitor's utility remains a challenge that this study seeks to address.

2.1.1 Double-Strand Break Repair

Double-strand breaks (DSB) are the deadliest form of DNA damage, and cells possess multiple strategies to overcome their effects. Homologous recombination (HR) is a pathway for the repair of DSB (Fig. 2.1). HR is only active during and immediately after S phase through its regulation by cell cycle checkpoint proteins and other proliferation pathways including MAPK.^{178–182} PCNA is required for new strand elongation and ligation following the Rad51 nucleoprotein complex sister chromatid invasion.^{183–185} Without PCNA to help resolve this pathway's component, the interstrand complex may collapse, causing considerable damage to both chromatids. Further, these roles occur at a stage already committed to the HR pathway. Therefore, a lack of functional PCNA would have little effect on the upstream signal proteins that begin the HR process.

The compensatory pathway for HR is non-homologous end joining (NHEJ), which is most active during G0 and G1 phases of the cell cycle but remains active in other phases.^{186–188} NHEJ, in both its forms, involves only four steps that include a low number of proteins: site recognition, end processing, gap filling, and ligation (Fig. 2.2). Since this repair method is not template-directed, it is error-prone and includes a deletion of nucleotides as the DNA ends are rejoined.^{189,190} This pathway remains the primary DSB repair pathway through its rapid response and relatively fewer proteins required despite its error-prone nature. The two NHEJ pathways are the classical NHEJ pathway (Fig. 2.2), controlled by DNA-PK and Ku70/80, and the alternative NHEJ pathway, which PARP1 controls. (Fig. 2.3)

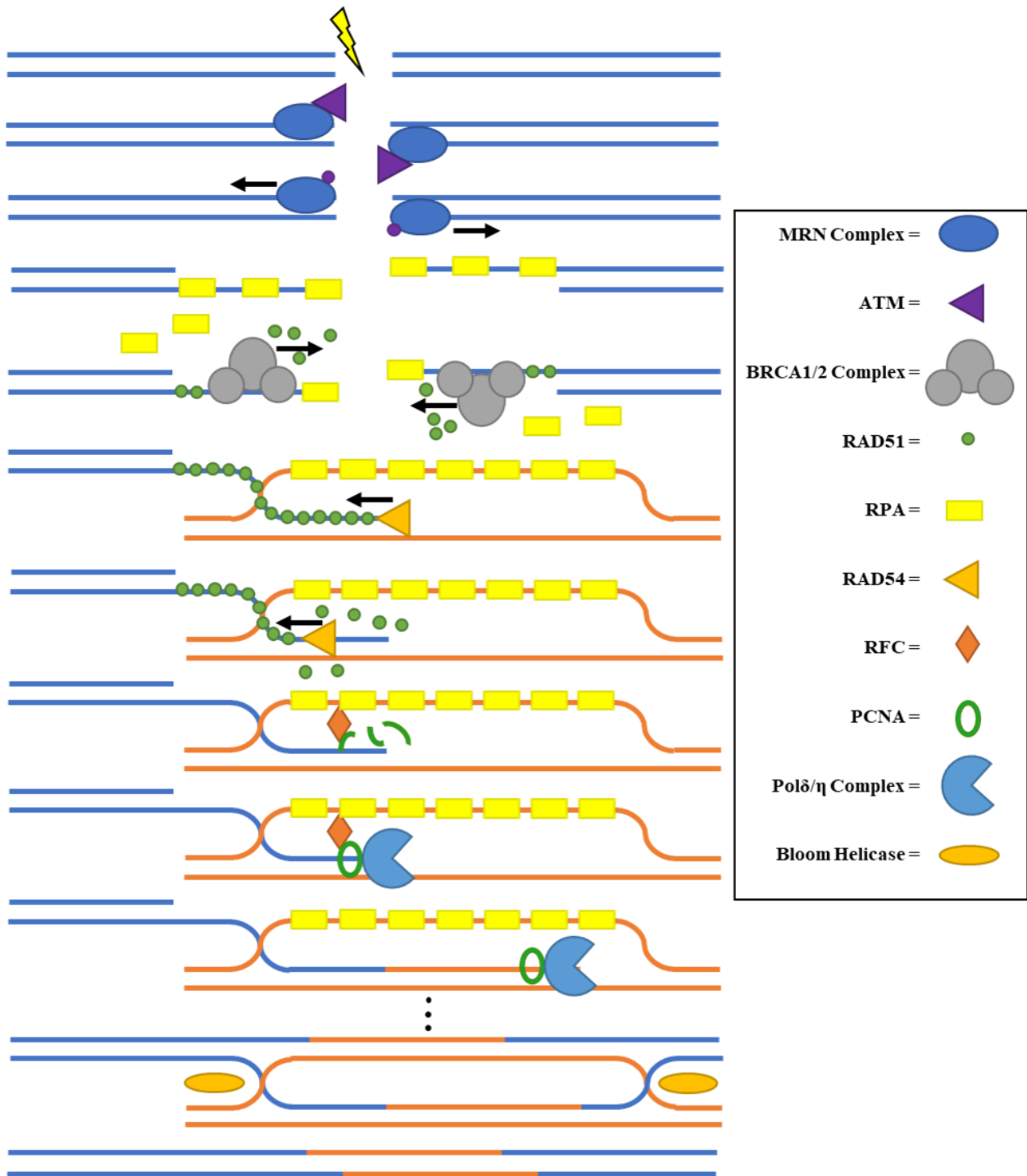


Figure 2.1: DNA Double-Strand Break Repair via Homologous Recombination

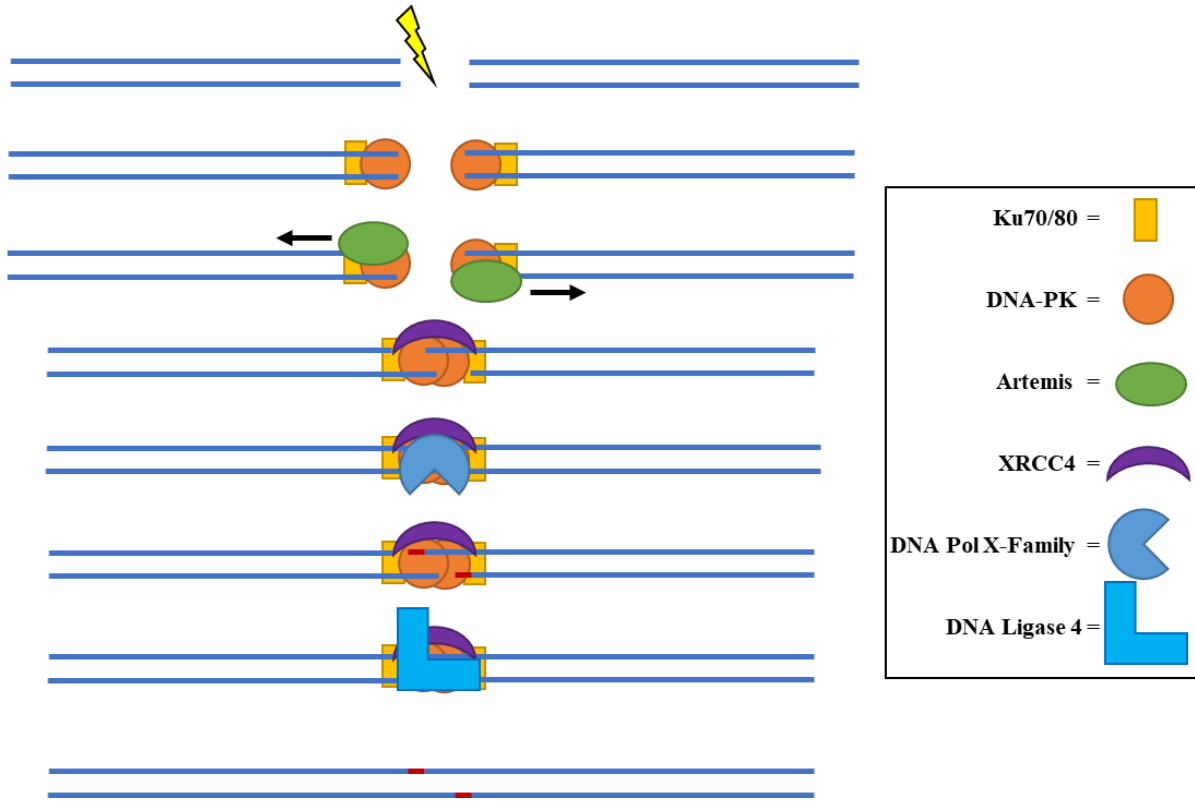


Figure 2.2: DNA Double-Strand Break Repair via Classical Non-Homologous End Joining

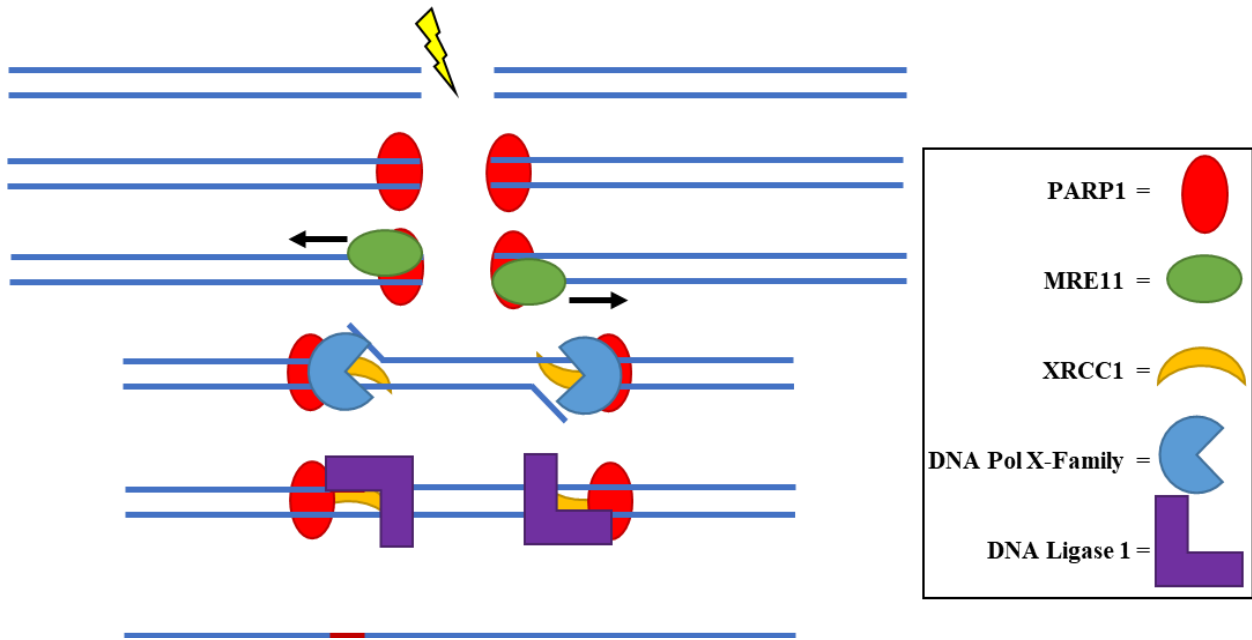


Figure 2.3: DNA Double-Strand Break Repair via Alternative Non-Homologous End Joining

PARP1 antagonists have emerged as a viable molecularly-targeted therapy in ovarian, breast, and lung cancer.^{8,132,191} They rely upon a BRCA1 mutation for utility since it reduces the HR pathway's functionality. Olaparib traps PARP1 at damaged sites preventing Ku70/80 foci formation, effectively inhibiting both classical and alternative NHEJ.^{192,193} Combined with a loss of HR, cancer cells are unable to overcome DSBs that occur. Numerous other mutations reduce the HR pathway's functionality at various stages of the process, including BRCA2, ATM, and RAD52. Genes whose loss-of-function mimics BRCA1's deficiency by losing an effective HR pathway impose "BRCAness". In the context of olaparib drug resistance, inhibitors of gene products that induce "BRCAness" traits show restoration of drug sensitivity when used in combinations.^{143,194,195} However, multiple olaparib-resistant contexts capably counter these combinations as "BRCAness" genes affect upstream signal proteins that regulate the activity of HR triggering feedback loops that overcome an upstream block of HR. Since the functional roles of PCNA occur after commitment to the HR pathway, an inhibitor may provide a unique opportunity to reduce HR effectiveness without modulating the signaling pathways that activate HR. This scenario would create a new context for inducing tumor cell sensitivity to olaparib.

2.1.2 DNA Replication

DNA replication provides one of the most stressed states of the human genome. During replication, much of the DNA is decondensed from the nucleosome, increasing overall exposure. The unwinding of DNA also induces physical and mechanical stresses through coiling and supercoiling.^{196,197} Even with topoisomerases present to mitigate this stress, DNA damage and subsequent breaks still occur. A lack of DDR before or during strand synthesis causes stalls at the replication fork. This temporal effect can then lead to a state of fork collapse, which triggers cell cycle arrest and the apoptotic pathway's induction.¹⁹⁸ PCNA is the central component of the replisome responsible for DNA polymerase activity. The coordination of helicase and DNA polymerase activities depends on PCNA to allow longer strands to be replicated for S phase of cell cycle progression. Inhibitors of PCNA that bind at the PIPM site cause S phase delays by reducing DNA polymerase affinity for the replisome and ultimately slowing replication.^{199,200}

DNA replication through the PIPM interaction site.²¹⁰ Nuclear localization and binding affinity of different protein interfaces regulate strand elongation through initially lower affinity interactions supported by other complexing factors.²¹¹ Ligases seal the ends of each strand and displace earlier complexes to finish strand elongation. The p21 protein is the negative regulator of DNA replication and S phase progression. The protein is an inhibitor of cyclin and cyclin-dependent kinases (CDK) while also possessing a high affinity for PCNA binding at the PIPM site to block association with other factors, including DNA polymerases.²¹²

The previous work with PCNA from the Davison laboratory evaluated the potential of PCNA as a flexible platform for multi-modal complex formation.²¹⁰ The IDCL forms part of the PIPM binding site undergoing a disordered-to-ordered transition, and can contribute multiple conformational states of the receptor. The cooperativity of binding at the homotrimer's multiple PCNA binding sites is likely due, in part, to the IDCL's flexibility. By evaluating various PIPM sequences in the human proteome and their ability to interact with PCNA, a reverse-PIPIM sequence was shown to possess high affinity. The notable reverse-PIPIM characteristic was established in the AKT kinase, a key cytoplasmic and nuclear regulator of DDR and cell survival. This interaction was known abstractly, but this work capably demonstrates the direct interaction between these proteins. While several PIPM-peptides consistently utilized key residues within the IDCL, the PCNA conformations differed among binding states. However, at the base of the IDCL, there are three regions that create subpockets for the PIPM motif to bind: I128-Y133, D232-L234, and Y250-K254. The interactions at these sites are conserved across PIPM presenting peptides and provide the foundation for both engineered peptides and small molecules. All this only heightens the interest in producing functionally selective small molecule inhibitors to manipulate this platform.

Multiple studies have sought to rationally optimize peptide ligands for PCNA using insights from the natural sequences such as p21. ACR2 is an example of an engineered peptide that displaces proteins essential to DNA replication.²¹³ ACR2 contains an intramolecular cyclic substructure or "staple" that stabilizes a 3₁₀ α -helix in a PIPM sequence motif. This secondary structure element allows for enhanced binding affinity by mimicking the local structure present when larger peptides bind at the PIPM binding site in PCNA. A related but distinct design approach relies on enhancing the peptide binding avidity of multiple PIPM binding sites and providing a novel tool compound. The homotrimer defines structural topology for three PIPM binding sites.

Using p21 20mer peptide sequence as a starting point, allowed for small protein constructs produced through recombinant DNA methods. The trivalent constructs show a 100-fold increase in affinity for PCNA PIPM binding sites based upon a direct displacement of the monovalent p21 peptide. In this case, the increases in affinities are far from a conservative additive prediction of 20-fold, but further highlights the presence of multiple functional PIPM binding sites in the PCNA homotrimer.

Another method of PCNA binding that has been explored for inhibition is utilizing the interior of PCNA. PCNA binds to chromatin and dsDNA through the negative backbone of nucleic acids. An aptamer, α -PCNA, was created to explore this alternative binding site of PCNA. α -PCNA was shown to reduce the capability of DNA polymerase δ and ϵ . However, this only occurred in the presence of PCNA showing that the aptamer reduces the processivity granted by PCNA. The aptamer was developed using a recombinant PCNA bound to streptavidin as bait. A PCNA pull-down revealed the high-affinity aptamers, which were then optimized for affinity through nucleotide deletions at the 3' and 5' ends. Targeting the interior of PCNA using nucleic acids offers a binding site at nanomolar affinity for selecting the functional role in DNA replication processes. This distinguishes the aptamer from both peptides and small molecules, which target multiple processes. While this aptamer has a known direct effect on DNA replication, the only effect related to DDR is synergism with doxorubicin.²¹⁴

An alternative but overlapping peptide-ligand binding site on PCNA has shown that functions can be differentially affected by the ligand bind site. The AlkB homolog 2 PCNA interacting motif (APIM) was first implicated in the nucleotide excision repair (NER) pathway by preventing XPA association.²¹⁵ APIM peptides have been optimized similarly to PIPM peptides, however instead of producing engineered peptides optimizing binding affinity, nuclear localization and stability were the focus to produce ATX-101.²¹⁶ Overall, APIM peptides possess a reduced effect on DNA replication and enhanced effects on DDR of single-strand breaks (SSBs).²¹⁷ Further, PCNA modified at K164 by ubiquitination showed selective binding for APIM peptides over PIPM peptides.¹¹³ The ATX-101 peptide has been registered for a Phase I clinical trial.²¹⁸ While the details of the mechanisms remain less clear, there is ample evidence supporting the premise that PTMs are capable of modulating which protein interactors engage PCNA.^{64-66,114,219}

Approaches using peptides have shown great utility, but peptides have not shown differential effects outside of the APIM binding sites. All PIPM peptides possess similar

biochemical features but do show some structural differences in PCNA-peptide complexes. The effects of these peptides are expected to impact many functions of PCNA and preclude other targets within the same pathway. PIPM peptides are also tolerable to most normal cells as monotherapies but show general toxic effects when used in combination with DNA damage agents *in vitro*. Still, only APIM peptides show any selective antagonism towards DDR pathways associated with PCNA.

In addition to utilizing these peptides to determine PCNA protein interactions, they also provide insights for structure-based drug design. Several PCNA inhibitors are known using different discovery strategies. A high throughput biochemical screening campaign for PCNA ligands capable of displacing the high-affinity PL peptide for the PIPM site enabled the discovery of the natural hormone triiodothyronine (T3). A simple modification of T3 to T2AA provides the first example of a small molecule inhibitor selective for PCNA.^{113,177} T3 and T2AA induce an unprecedented binding pocket contiguous with the PIPM binding site near the base of the IDCL.¹⁷⁷ The cellular effects of T2AA include enhancing DNA damage agents and inhibition of TLS.²²⁰ These effects are similar to the PIPM-containing peptides; however, T2AA does not block S phase progression directly or directly modulate kinase activity.²²¹ Therefore, T2AA is the first small molecule able to show selectivity in downstream events by binding to PCNA. T2AA block prevents ubiquitination at K164 by Rad18, which is necessary for translesion synthesis (TLS). The mechanism for this is unclear but is not dependent on or correlated to Y211 phosphorylation status. These distinct cellular effects of T2AA establishes the proof of concept that a small molecule inhibitor of PCNA function and the PTMs can be modulated more precisely than with a peptide-based inhibitor.

Using an *in silico* approach to target the PCNA-dimer interface led to discovery of an inhibitor class represented by PCNA-I1 (Table 2.1).²²² PCNA can form homotrimers that are not suitable for loading into DNA without pathway-specific loading factors, including RFC, that utilize ATP hydrolysis to promote “clamping” of PCNA.²²³ This trimeric sliding-clamp on DNA is the scaffold providing important docking sites for protein complexes. The stabilization of the trimeric PCNA in the absence of DNA is a strategy for inhibiting a broad range of PCNA functions.²²⁴ Since PCNA-I1 prevents the recruitment of PCNA clamps, it is expected to abolish PCNA’s DNA related functions and thus serves as an example of a pan-PCNA inhibitor distinct from the functionally selective effects demonstrated by T2AA.

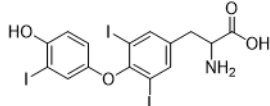
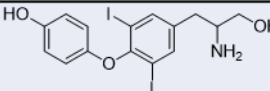
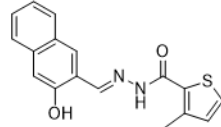
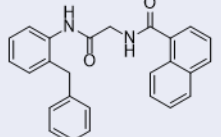
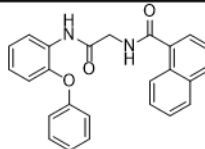
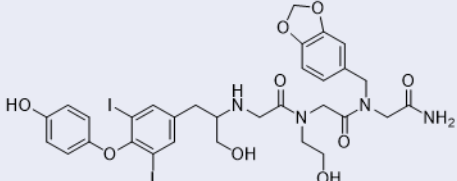
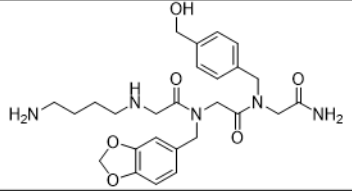
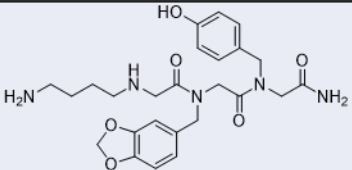
A concept of a cancer-specific PCNA has been advanced for many years by the Malkas laboratory.²²⁵ Evidence of this is the development of a peptide-specific to the cancer-specific region, L126-Y133.²²⁶ To create a more specific PCNA inhibitor that impacts cancer cells, this same group assessed a putative cancer-associated PCNA isoform region.²²⁵ This region occurs near the PIPM binding site as well as the T2AA binding site. The results of a virtual screening campaign provide a series of molecules that claim to leverage cancer-associated differences.²²⁷ Information for only the PCNA inhibitors AOH39 and AOH1160 have recently been disclosed. The observations include specific effects in cancer cell cultures with some enhancement of DNA damage through HR.²²⁷ Additional claims include some impact on DNA replication. The affinity and binding site(s) by which AOH039 and AOH1160 engage PCNA remains ambiguous at this time. The authors could not displace the PL peptide through a fluorescence polarization assay. Using NMR spectroscopy for detection and T2AA as a control ligand, AOH1160 induces resonance changes attributed to a similar set of amino acids consistent with the binding of PCNA but not definitive for a specific site. Since AOH1160 represents the second class of small molecule PCNA inhibitors with a different functional selectivity inhibition profile, inclusion in this study is warranted.

Our laboratory has utilized a novel fragment-based ligand design approach to leverage multiple receptor features of PCNA that enhance binding with potential inhibition profiles distinct from T2AA or AOH1160.²⁰⁸ To expand the functional selectivity of PCNA inhibitors, binding in multiple protein subpockets was hypothesized to leverage the flexible interface of the PIPM binding sites. Based on Pedley et al. observations²¹⁰, accommodation for the receptor flexibility relies on the inclusion of apo-PCNA and multiple ligand co-crystal structures during the *in silico* screening phase.^{220,228,229} Using the FEN1, p21, Pol ϵ , and T3 binding modes produce a consensus of receptor features that define binding subpockets induced upon ligand-binding in this flexible region of PCNA. Compound libraries were based upon N-alkyl glycines that simultaneously display three subpocket ligands linked by a relatively flexible peptoid backbone. This backbone has enhancements in drug-like physicochemical properties, including superior metabolic stability over traditional peptides.^{230–233}

The results of the virtual screens yielded multiple PCNA ligands with representatives in Table 2.1. All candidate ligands were initially screened for direct competitive binding with the PL peptide to establish affinity at the PIPM binding site in PCNA. Binding in this critical region

confirms the virtual, flexible docking screen. Additionally, *in silico* analyses using molecular dynamics simulations also highlights the screening approach's capacity to discover ligands that bind distinct receptor PCNA conformations. Furthermore, using principal component analyses of the ligand-bound conformations of PCNA provide comparisons to the known peptide ligands, including PL, Abl, Akt. In all cases, the higher affinity tripeptoids show stabilization of distinct PCNA conformations from those for the PIPM-containing peptides and T2AA. Initial *in vitro* cellular activity assessment of these tripeptoids shows synergism with DSB and SSB damage agents in drug-resistant cell lines. Further evaluation of how the binding of these agents in the PCNA PIPM site enable selective inhibition of PCNA's function is the focus of this study.

Table 2.1: PCNA inhibitors and binders discovered and developed. *Molecules used in this study. †Lactam bridge between K145 and E149

Compound	Structure	IC ₅₀ (μM)	K _i (μM)
P21-Peptide	RRQTSMTDFYHS	1.8 ± 0.5	0.477
PL- Peptide	SAVLQKKITDYFHPRK	0.145 ± 0.013	0.136
APIM Peptide	MDRWLVKW	11 ± 0.5	NA
ATX-101	AcMDRWLVKWKKKRRKIRRRRRRRRRRR	11 ± 0.5	NA
ACR2	GRKRRQK ₁₄₅ SMTE ₁₄₉ FYH [†]	1.61 ± 0.076	NA
T3		19.0 ± 0.42	7.8
T2AA*		1.34 ± 0.33	0.128 ± 0.0318
PCNA-I1		1.60 ± 0.36	0.41 ± 0.17
AOH39*		NA	NA
AOH1160*		NA	NA
T2AA-NEal-NPip (TEP)*		1.82 ± 0.37	0.175 ± 0.0356
NLys-NPip-NBal (LPB)*		0.482 ± 0.328	0.0464 ± 0.0316
NLys-NPip-NTyr (LPT)*		1.29 ± 0.31	0.118 ± 0.0265

2.2 Rationale

Current PCNA peptide and small molecule inhibitors have shown some ability to downregulate specific functions of PCNA. Further, these effects have implications either on or through PTMs of PCNA that regulate PPIs of PCNA. These effects require increased stress through DNA damage to emerge as potential therapeutic options. However, due to the numerous possible PCNA functions associated with cells' sensitization to general genomic stress, especially DNA damage, this approach offers little insight if any functional selectivity. The overall objective of this section is to show the ability to create functionally selective inhibitors of PCNA. To understand the nature of the small molecules that bind to the PIPM binding region and the extent of selectivity, I performed a series of assays alone and in combination with other DDR inhibitors while utilizing DNA damage agents as controls. The objective of this is to understand what possible synthetic lethal or synergistic relationships exist between PCNA inhibitors and related DDR pathways.

While some of these inhibitors have already reported functionally selective inhibition, the studies here seek to provide rigorous criteria for the profiling of PCNA inhibitor target engagement and pharmacological effects. While not exhaustive, these assays will differentiate between three major PCNA functions already observed as important in cancer diseases including: DSB repair through HR, DNA replication, and TLS. To examine PCNA's role in DNA damage and cell viability, I will be assessing the effect of PCNA inhibitors in combination with DSB repair pathway inhibitors (Table 2.2). Since NHEJ and HR pathways are compensatory, PCNA inhibitors' ability to synergize NHEJ inhibitors selectively can further validate HR-specific inhibition.

The design of experiments for selective cell PCNA inhibitor effects relies on varied genetic contexts to test PCNA function in different biological states. Cells lacking the HR pathway should show limited PCNA inhibitor effects if they are selective for PCNA's functional state in HR. DNA damage-resistant tumor cell lines carry TP53 or PTEN mutations that directly affect apoptosis and DDR responses. These mutations reduce a single agent's effect but provide a background for efficient evaluation of two agent combinations. MAPK pathway gain-of-function mutations, such as KRAS or BRAF, and loss-of-function mutations to cell cycle regulators, such as RB1 and CDKN2A, prevent S phase delays through signaling, but not through direct manipulation of the replisome. The combination of cell line diversity and DNA repair antagonist combinations enables separation of DNA damage effects on cell cycle from replisome effects specific to PCNA inhibition.

PCNA inhibitors that do not target a specific functional role could be considered general chemotherapeutics. Functionally selective PCNA inhibitors would provide a new class of antagonists that enhance other targeted inhibitors' utility by leveraging genomic stress contexts. The combinations studied here reflect PCNA inhibitors' selective capabilities and whose synergies can be interpreted with tumor cell genomic contexts.

2.3 Methodology

2.3.1 Cell Culture

The human TNBC cell lines HCC1937, MDA-MB-231, MDA-MB-436, and MDA-MB-468 were purchased from the American Type Culture Collection (ATCC). MDA-MB-231 was cultured in DMEM supplemented with 10% FBS. HCC1937 and MDA-MB-468 were cultured in DMEM supplemented with 5% FBS. MDA-MB-436 was cultured in L-15 supplemented with 10% FBS, 10 µg/ml insulin, and 16 µg/ml glutathione. Incubation of HCC1937, MDA-MB-231, and MDA-MB-468 cell cultures were conducted at 37° C and 5% CO₂ in a humidified incubator. Incubation of MDA-MB-436 was also at 37° C but with no gas exchange. All cells were harvested as cells reached 70-80% confluency utilizing Trypsin-EDTA (0.25%) and were split 1:10 for cells with a doubling time close to 24 h or 1:5 for cells with doubling times greater than 24 h. Cells with doubling times below 24 h had media replaced every 2-3 days or 3-5 days for cells with doubling times greater than 24 h (Table 2.2).

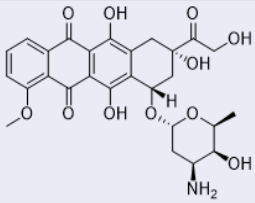
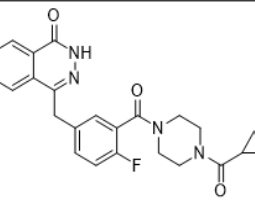
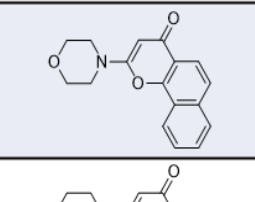
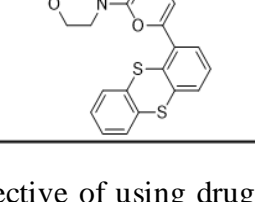
Table 2.2: Cell Line Properties; Doubling times were determined after culturing cells for 2-3 passages as this was more accurate to cell growth speed during assays.

Cell Line	Type/Subtype	Mutations	HR Status	Growth Conditions	Doubling Time (h)
MDA-MB-231	Mesenchymal-like	BRAF, CDKN2A, KRAS, NF2, TP53	+	10% FBS, DMEM, 5% CO ₂	~21
MDA-MB-436	Basal-1	BRCA1, RB1, TP53	-	10% FBS, L-15, 10 µg/ml insulin, 16 µg/ml glutathione	~36
MDA-MB-468	Basal-1	PTEN, RB1, SMAD4, TP53	+	5% FBS, DMEM, 5% CO ₂	~22
HCC1937	Basal-1	BRCA1, PTEN, RB1, TP53	+	5% FBS, DMEM, 5% CO ₂	~54
HEK293	Embryonic Kidney	-	+	10% FBS, DMEM, 5% CO ₂	~22

2.3.2 Drug Combinations and Synergism

PCNA inhibitors were evaluated in combination with the ATM antagonist KU-55933, the DNA-PK antagonist NU7026, the PARP1 antagonist olaparib, and the DNA damage agent doxorubicin.

Table 2.3: Small Molecules Utilized to Examine Effects of PCNA Antagonism

Compound	Structure	Process
Doxorubicin		Damaging Agent, Double-Strand Break
Olaparib		Alternative Non-Homologous End Joining
NU7026		Classical Non-Homologous End Joining
KU-55933		Homologous Recombination

Doxorubicin is a topoisomerase II antagonist that preferentially causes DSBs. ATM is an early signaling protein in the HR pathway and an intersection between DNA damage and cell cycle. DNA-PK is responsible for much of the signaling and coordination of the classical NHEJ pathway. PARP1 maintains a similar role in alternative NHEJ, but also has the potential to prevent Ku70/80 foci formation. These combinations will allow this study to survey HR selectivity as well as compare PCNA antagonism to general chemotherapeutic effects. (Table 2.3)

The objective of using drug combinations in pathways surrounding PCNA is to discern whether an inhibitor affects PCNA functions associated with those pathways. NHEJ is a compensatory pathway to the PCNA-dependent HR pathway; inhibiting both the DNA repair pathways would produce a synergistic response. This condition would constitute a “chemical synthetic lethality” in analogy to PARP-1 inhibitor's clinical utility when tumor genomes bear BRCA1 loss-of-function mutations.

Synergism is a pharmacological effect that is not explained as the sum of two independent outcomes. Identification of synergism occurs when the two agents used in combination have greater effect together than either used alone. The quantification of synergism between any two inhibitors makes use of the equation offered by Chou and Talalay.²³⁴ By quantifying the pharmacological effects as synergistic, additive, or subadditive, we can define PCNA inhibitors'

impacts in multiple tumor genome contexts through drug combinations. Quantification of the effect of a drug combination makes use of a combination index (CI) where values > 1 are considered synergistic, 1 is additive, and < 1 are subadditive.

2.3.3 Cell Proliferation

Tumor cell proliferation was measured using the MTT (3-(4, 5-dimethylthiazol-2-yl)-2,5-diphenyltetrazolium bromide) cell proliferation reagent. Cells were plated on flat-bottom 96-well plates at a density of 1×10^4 cells per 100 μL per well, following patterns dependent on plate type (Fig. 2.5). Cells attached over 4 hours at 37°C in an incubator. Control plates were then exposed

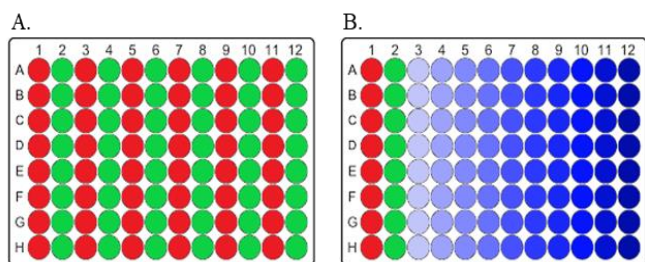


Figure 2.5: MTT Plate Configuration; A) Control plate; B) Test plate; Red: No cells, negative control; Green: Cells, no treatment, positive control; Blue: Cells, treatment

to 10 μL of MTT (5 mg/mL in growth media) was added to each well at a final concentration of (0.5 mg/mL) to metabolize for 4 hours at 37°C . After the incubation period, 50 μL of solubilization solution (10% Triton-X 100, acidic isopropanol (0.1N HCl)) was added, and the plate was stored without light overnight on an agitator to improve solubilization.

Experimental plates were treated with either a monotherapy or drug combination. For monotherapies, each compound started at 200 μM and used a dilution factor of 3 to produce the series of 10 concentrations. An exception was a 50 μM starting value for doxorubicin due to its potency. All the drug molecules were tested as monotherapies, including the PCNA inhibitors. Drug combination studies were designed to include PCNA inhibitors at $\text{GI}_{50}/3$ (max. 30 μM), $\text{GI}_{50}/10$ (max. 10 μM), and $\text{GI}_{50}/30$ (max. 3 μM). These PCNA inhibitors' dosages were applied in combination with a DNA damage agent or repair antagonist following the monotherapy dosage protocol. These concentrations provide enough data to determine synergism while minimizing the PCNA inhibitor used.²³⁴ The drug combination experiments duration were approximately three cell doubling times for each cell line.

To measure the cell proliferation, light absorbance readings were collected at 570 nm to assess reduced MTT, and 650 nm to eliminate background. Absorbance values were normalized

to the 570 nm readings to calculate the percent cell growth by comparing to an appropriate control plate for each cell line. The control plates were used to standardize base cell counts and normalize the experimental plates' positive and negative controls.

2.3.4 Cell Survival

Cell survival studies were conducted using a clonogenic assay.²³⁵ Cells were plated on flat bottom 6-well plates at a density of 1×10^3 cells with 1 mL per well. After allowing cells to attach over 4 h, the cultures were treated with single-drugs using with five concentrations of DNA-damaging agent, DDR inhibitor, or PCNA inhibitor followed by incubation for 24 h. The MTT results were examined for drug concentrations that elicited a reduction in total cell numbers from Day 0 to ensure cell death. The dosage range of the best 5 doses within the 10-step 3-fold dilution curve used in the MTT assay. Combinations utilized the same 5 concentrations of DNA-damaging agent or DDR inhibitor used in the single-drug treatments. The PCNA inhibitor dosages were $GI_{50}/3$ (max. 30 μ M), $GI_{50}/10$ (max. 10 μ M), and $GI_{50}/30$ (max. 3 μ M). Cells were washed with 1 mL of PBS to remove the drug treatment and incubated in 1 mL of the appropriate buffer at 37 °C under the specific atmospheric conditions stated above. After 6-7 cell doubling periods when the control colonies were visible, the cells were fixed in 4% *p*-formaldehyde and stained with DAPI solution (1 μ g/mL DAPI, 0.1% Triton-X 100, PBS) for counting using a Cytation 3 in image cytometer mode. Normalization was calculated from the drug-treatment cell colony data to colony counts and control cells in drug-free medium.

2.3.5 DNA Double-Strand Breaks

DSBs were analyzed using a neutral comet assay.²³⁶ Cells were plated on flat-bottom 96-well plates at a density of 2×10^4 cells per 100 μ L per well and incubated for 4 h in an appropriate medium at 37 °C under the specific atmospheric conditions. Cells were treated with 1 μ M doxorubicin for 1 h to induce DNA damage. Media was exchanged with fresh media before treatment with 5 concentrations of each compound for 8 h to allow for repair. In combination studies, cells were also exposed to a single dosage of PCNA inhibitor at $GI_{50}/3$ (max. 30 μ M). After the proper exposure time, cell cultures were treated with Trypsin-EDTA (0.25%) to suspend in 100 μ L of 0.5% low melting agarose in PBS at 45°C. Fifty microliters of diluted cells were

immobilized onto microscope slides which had been pretreated by dipping in 1% Agarose in nanopure water and allowed to dry overnight. Glass coverslips were placed on top of the cell deposition, and the slides were incubated at 4°C for 10 min to solidify the low melting agarose. Slides were moved to room temperature for 5 min, the coverslips removed, and immobilized cells were lysed in 4°C neutral lysis buffer (25 mM Tris HCl pH 8.0, 100 mM EDTA, 2.5 M NaCl, 0.1% Triton X-100) overnight at 4°C. After removal from the lysis buffer, the slides were equilibrated in neutral comet electrophoresis buffer (90 mM Tris HCl pH 8.0, 90 mM Boric Acid, 2 mM EDTA) for 20 min and electrophoresis at 14V, 21mA for 40 min. After electrophoresis, slides were equilibrated in 0.4 M Tris-HCl pH 7.4 for 5 min at room temperature, the buffer was replaced twice for a total of three wash steps. Sixty microliters of 4,6-diamidino-2-phenylindole (DAPI, 1 µg/mL in H₂O) was applied dropwise to the agarose pad and incubated at 4°C for 15 minutes. Comets were then imaged using a BioTek Cytation 3 Cell Imaging Multi-Mode Reader with a 4x objective and analyzed using BioTek Gen 5 software. To quantify the “% tail DNA”, a protocol published by BioTek was utilized on a minimum of 100 cells identified with an area appropriate for each cell assessed through the negative control of non-drug treated cells.²³⁷

2.3.6 Homologous Recombination Assessment through Rad51 Foci

HR activity was evaluated through Rad51 foci.²³⁸ Cells were plated on µ-Slide 8 Well Chamber Slides at a density of 2×10^4 cells per 150 µL per well and allowed to attach over 4 h at 37°C. Cells were then pretreated with 10 µM of doxorubicin for 1 h at 37°C followed by replacing the media and then treatment at 2 concentrations of DDR antagonists for 8 h or 24 h. Cells were treated using the same drug concentrations used in the comet assay, GI₅₀/2 for DDR antagonists and GI₅₀/3 for PCNA inhibitors. Cells were then fixed with 4% *p*-formaldehyde in PBS at room temperature for 10 minutes. To assess PCNA inhibitors' potential impact on HR competence, we examined RAD51 foci formation. As a control, γ-H2AX foci were analyzed as a general DNA damage marker. After fixation, cells were permeabilized with 0.1% Triton X-100 in PBS at room temperature for 5 m. A 1% bovine serum albumin (BSA) solution in PBS was used to block nonspecific binding to the permeable cells. Primary antibody stains were diluted in 1% BSA blocking solution in PBS were added followed by DAPI (2 µg/mL). Finally, the permeable cells were exposed to the appropriate secondary antibodies diluted in 1% BSA blocking solution in PBS.

The primary antibodies used were (1:100). Secondary antibody was anti-mouse-FITC (1:100). A Nikon TE2000 inverted fluorescence microscope (Nikon Instruments Melville, NY, USA) enabled imaging of the stained cells under oil immersion with a 40X objective. The number of foci were estimated utilizing DAPI to determine the nucleus for each cell followed by inclusion points of interest in those regions. A minimum of 50 cells were analyzed for each biological replicate. The arrays of foci count for each biological replicate were subjected to further analysis to determine the average number of foci per cell, and the percentage of cells with zero foci.

2.3.7 DNA Replication and Translesion Synthesis

DNA replication efficiency was analyzed by DNA quantification over a sub-doubling time period.²³⁹ Cells were plated on flat-bottom 96-well plates at a density of 1×10^4 cells per 100 μ L per well, allowed to attach over 4 h. For studies using synchronized cell populations, the media was replaced with an FBS-free media followed by incubation for 24 h. For the studies of the effects TLS, cells were exposed to 300 uJ/cm^2 UV radiation utilizing a Spectronics XL-3000 UV Crosslinker. When evaluating just the effects on DNA replication delays, this UV-irradiation step was omitted. Cells were then treated with 6 concentrations of each compound for approximately 85% of each cell line's doubling time. At the end of the appropriate time periods, cells were fixed with 4% *p*-formaldehyde in PBS and stained with DAPI in PBS (2 $\mu\text{g}/\text{ml}$). Data for DNA quantification were acquired using with a Cytation 3 (4x objective) and compared to no drug addition controls, but FBS addition, and cells that did not receive any FBS after the synchronization period. These control cells provided the standards to assess whether DNA replication was complete and proceeded past the G1/S checkpoint.

2.3.8 Inhibitor Feature Profile Assessment

A set of descriptors were developed to profile the different effects of PCNA inhibitors quantitatively. The phenotypic effects under investigation are a general response to DNA damage, DDR through HR, DNA replication, and TLS summarized in Table 2.4. Discrete values that quantify all the measured drug effects were used to profile PCNA inhibitors quantitatively.

Toxicity was derived using LD₅₀ values for each PCNA inhibitor as a monotherapy

Table 2.4: PCNA Inhibitor Feature Classification; LD₅₀ is the concentration measured in the clonogenic assay that results in half the cells' death. GI₅₀ is the concentration measured in the proliferation assay that results in half the cell growth.

Feature	Assessment Protocol
Toxicity	$-\log_{10}(\text{LD}_{50}) - 3$
DNA Damage	% DNA Tail at GI ₅₀ /3
HR Selectivity	$\frac{\text{GI}_{50, \text{HR}}}{\text{GI}_{50, \text{NHEJ}}}$
Persistent Rad51 Foci	$\frac{\text{Rad51 foci ct.}}{\gamma\text{H2AX foci ct.}}$ at GI ₅₀ /3; 24 h
Replication	% S Phase at GI ₅₀ /3
Translesion Synthesis	% S Phase at GI ₅₀ /3

adjusted using the equation in Table 2.4. The general toxicity of a PCNA inhibitor is critical to determine if any dose range window exists for functionally selective effects. This information is also essential to understand the necessity of combinations to affect tumor cells without side effects on normal cells.

DNA damage was determined by the amount of damage caused by a PCNA inhibitor at a concentration equal to 1/3 GI₅₀ using a comet assay without an initial doxorubicin exposure. This information assesses if the PCNA

inhibitor has any intrinsic DNA damage causing capabilities. The ability to enhance DNA damage through inhibiting repair is an effect that can be leveraged in multiple disease contexts, but general DNA damage effects need to be utilized differently.

HR selectivity (HR:NHEJ) was determined using a ratio of the average enhancement effect of a PCNA inhibitor, in combination with NHEJ antagonists in HR competent contexts, divided by the average enhancement effect of PCNA inhibitors, in combination with an HR antagonist or HR incompetent cells. This ratio evaluates how much the PCNA inhibitor can synergize with DDR antagonists in a PCNA-dependent DDR.

Rad51 foci form as HR progresses in response to DNA damage. These foci displace the general DNA damage marker γH2AX . Rad54 inhibition shows a reduction in γH2AX foci as any Rad51 foci that form are unable to resolve.^{240,241} As PCNA antagonism occurs near the same step, Rad51 foci persistence indicates a failure of HR to progress to completion. If Rad51 foci levels remain high after 24 h, and γH2AX foci levels are less than the 8 h measurements, it is consistent that the HR pathway is being affected by the PCNA inhibitor.

DNA Replication and TLS effects are established responses to PCNA inhibitors that can serve as a baseline effect. Since these effects are understood mechanisms, observing inhibitory effects on these pathways with a new PCNA inhibitor when used alone is sufficient to explain the impact on tumor cell growth.

2.4 Results

2.4.1 Cell Proliferation and Survival

PCNA inhibitors have shown several direct effects on cell proliferation. This property is considered a result of delays in DNA replication through replisome inhibition. Inhibiting PCNA also decreases DDR potential, which would lead to cell cycle checkpoint activation. Sufficient destabilization of the cell cycle through these pathways will result in the activation of apoptosis and cell death. Evaluating potential cancer therapeutics' ability to reduce tumor cell growth and induce tumor cell death is standard practice.

As detailed above, selecting drug combinations and cell lines with varied genomic profiles is an approach to parse the degree of PCNA inhibition due to select functions. Loss of NHEJ and HR simultaneously is a clinically validated form of synthetic lethality.^{149,242} NHEJ inhibitors should be synergistic in the presence of a PCNA inhibitor that directly impacts HR's role. Likewise, utilizing an NHEJ antagonist, either olaparib or NU7026 should be highly effective in an HR compromised cell line. However, in HR deficient cells, either through a BRCA1 mutation or ATM inhibition by KU55933, PCNA inhibitors that selectively inhibit HR should be non-synergistic.

Their effects as single agents immediately separated the PCNA inhibitors we evaluated in these studies. In all four cancer cell lines, the average GI₅₀ for AOH39 was 2 μ M, and 180 nM for AOH1160. In contrast, T2AA and TEP, LPB, and LPT (tripeptoids) all show GI₅₀ values > 100 μ M. (Fig. 2.6) These results are consistent with previously reported values for these inhibitors.^{208,220,227} What they all share in common is the ability to synergize with doxorubicin. Utilizing the Chou-Talalay method to determine synergism in drug combinations, a CI above 2 is observed for all the PCNA inhibitor combinations with doxorubicin in the HR competent cell lines. However, the tripeptoids and T2AA routinely show a greater CI than the AOH compounds, with a CI above 3 in HR competent cell lines often nearing 4 or 5 (Table A.1). AOH compounds are the only inhibitors to reach a CI of 2 in the HR-deficient cell line MDA-MB 436. These differences

imply that AOH synergism is not HR-dependent, but T2AA and the tripeptoids have a greater dependency on HR competence to be effective in combination with a DNA damage agent.

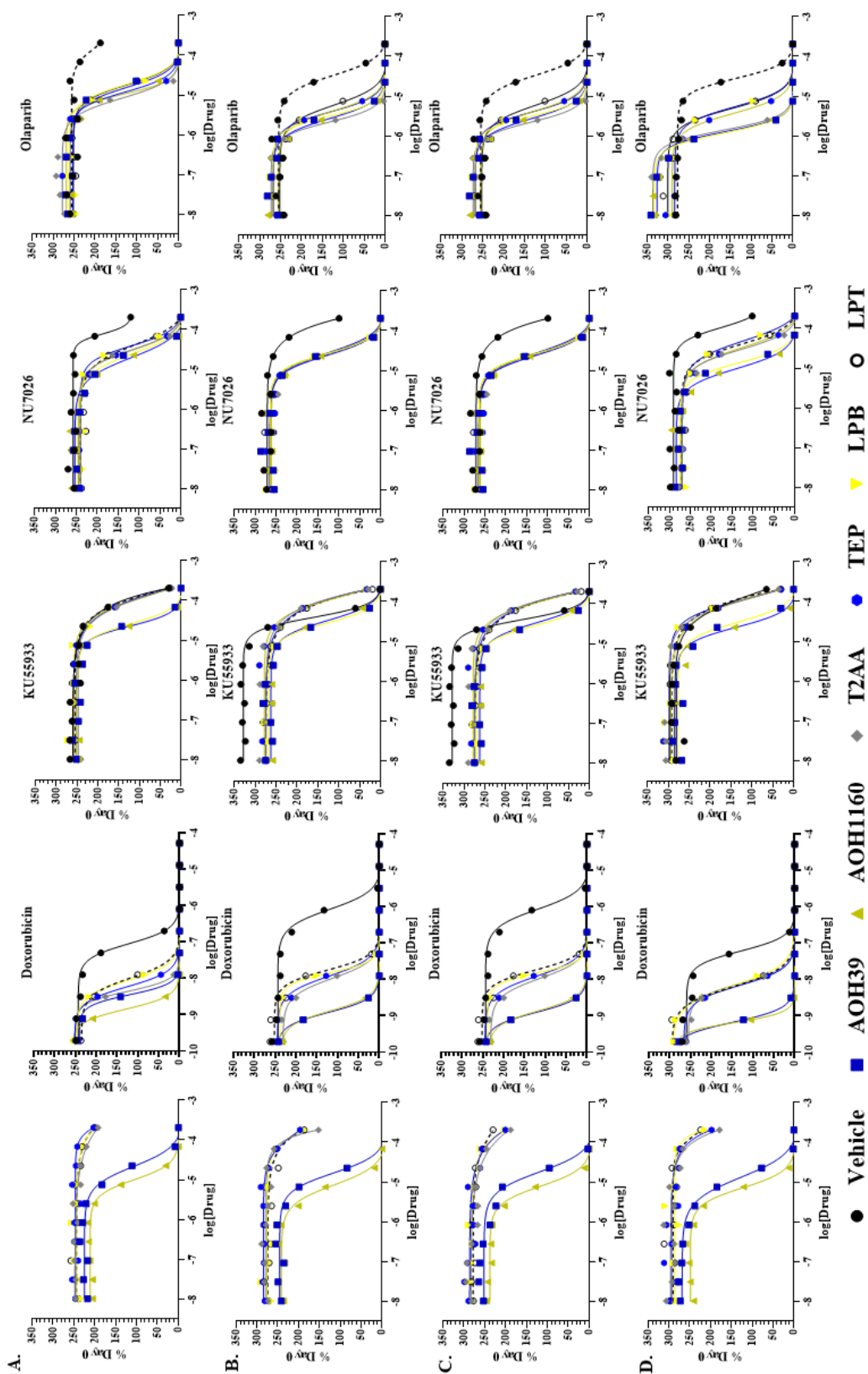


Figure 2.6: Cell proliferation effects of PCNA inhibitors. Cells were exposed to 10 step dilution set using a dilution factor of 3 starting at 200 μM , except for doxorubicin which started at 50 μM . These were done in the cell lines shown and with the dilution set of an inhibitor at the title as well as 1/10 GI50 of the PCNA antagonist denoted. A) HCC1937; B) MDA-MB-231; C) MDA-MB-436; D) MDA-MB-468

The combinations with NU7026 and KU55933 further evaluate pathway specificity of the PCNA inhibitors. NU7026 targets DNA-PKcs, an enzyme responsible for regulating the early stages of NHEJ necessary for function (Fig. 2.2). KU55933 inhibits ATM activity, which governs the MRN activity required for HR activation and processing (Fig. 2.1). Synergism with NU7026 would imply the PCNA inhibitor possesses a strong HR effect that results in loss of function of both DSB repair pathways. This dual blockade is analogous to loss-of-function mutations that reduce HR competence and sensitize cells to NHEJ inhibitors. Synergism with ATM suggests other effects that are not PCNA and HR dependent since they would inhibit sequential steps in the same pathway. Synergism with NU7026 in HR incompetent cell lines, MDA-MB-436, also provide evidence of non-HR specific inhibition of PCNA.

The AOH antagonists showed synergism with NU7026 in all cell lines, including MDA-MB-436. However, the CI values were above 2.3 in HR competent cell lines and only 1.6 in MDA-MB-436. While these results show that the AOH molecules might have an HR effect, they also elicit other effects independent HR. The synergism observed with KU55933 in all cell lines except MDA-MB-436 where it was only additive, also supports the AOH compounds' HR-independent effects. The greatest CI was observed in HR-competent cell lines at 1.8 suggesting some synergism. However, T2AA and the tripeptoids showed a different synergism profile. These molecules showed no synergism with KU55933 in any context, at times suggesting borderline antagonism, or in MDA-MB-436 with either NU7026 or KU55933. T2AA and the tripeptoids showed synergism with NU7026 in all HR competent cell lines with CI above 3 in all of them.

Olaparib is another NHEJ antagonist utilized to test the specificity of the HR effect of the selected PCNA inhibitors. Olaparib differs from NU7026 in that it traps PARP1 at damaged sites while NU7026 prevents DNA-PK foci formation. This mechanistic distinction enables olaparib to inhibit the formation of other NHEJ DDR complexes increasing its overall efficacy. Similar to the combinations with NU7026, the AOH compounds were synergistic with olaparib in all cell contexts, including the HR incompetent MDA-MB-436. However, T2AA and the tripeptoids showed a similar profile with olaparib as they did in combinations with NU7026. T2AA and the tripeptoids were able to synergize with olaparib in all HR competent cell lines with CI values above 2, and in the olaparib-insensitive HCC1937, robust CI values close to 5.

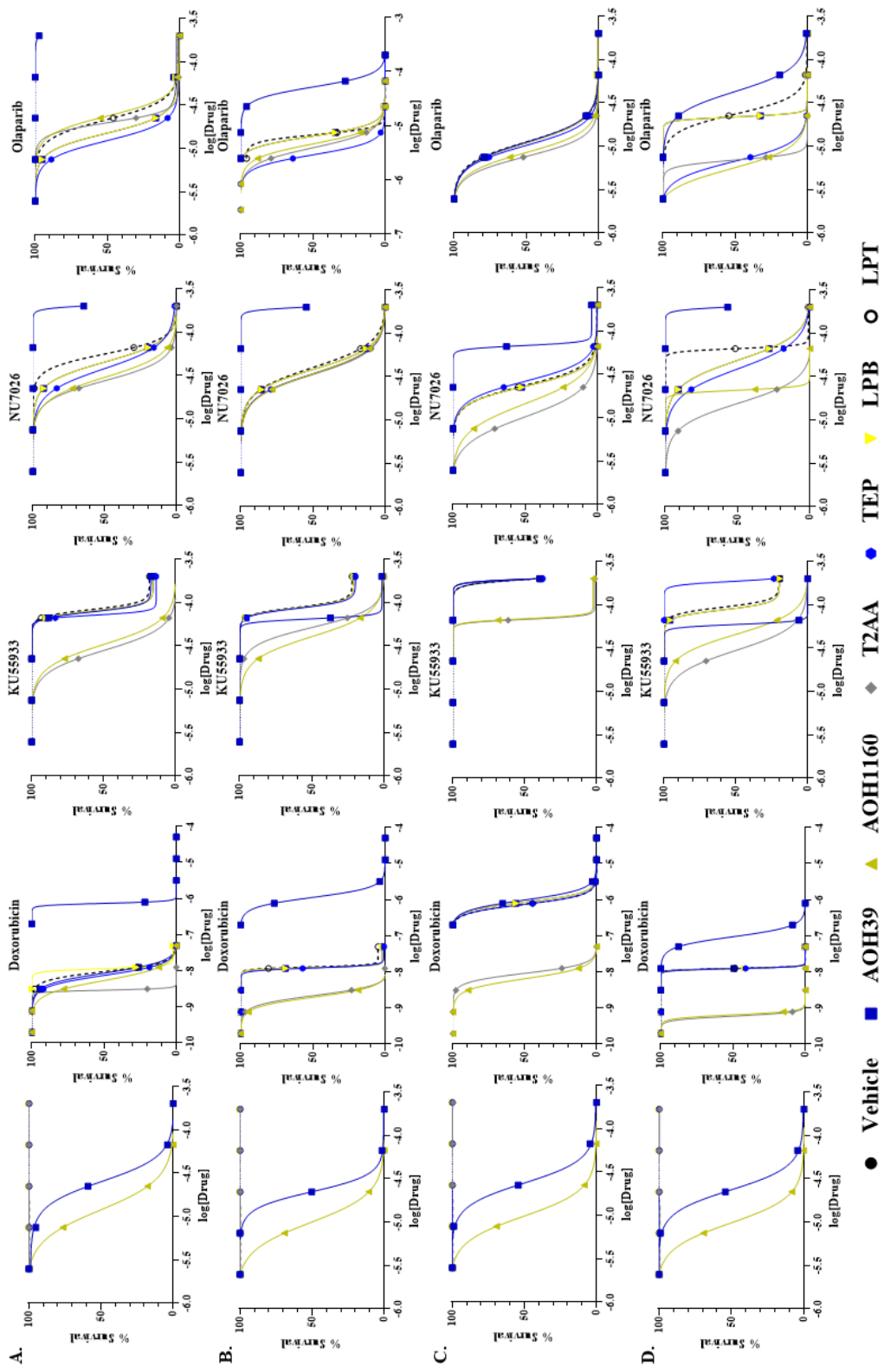


Figure 2.7: Cell proliferation effects of PCNA antagonists. Cells were exposed to a 5 step dilution set using a dilution factor of 3 starting at a concentration relative to their GI50. These were done in the cell lines shown and with the dilution set of an inhibitor at the title as well as 1/10 GI50 of the PCNA antagonist denoted. A) HCC1937; B) MDA-MB-231; C) MDA-MB-436; D) MDA-MB-468

Overall, these observations are consistent with HR specific effects for T2AA and the tripeptoids PCNA inhibitors. These results also further substantiate that the AOH compound possesses additional cellular effects not dependent on HR.

The clonogenic assays were designed based on the MTT proliferation assay's observations to establish the LD₅₀ values for each of the PCNA inhibitors. The dosage ranges were selected to create the most statistically robust curve based upon the GI₅₀ values of each single agent to ensure a data point with 100% cell survival. Doxorubicin being more toxic, showed the greatest cell killing effect with the PCNA inhibitors. LD₅₀ values were higher than estimated through MTT, as is typical with this assay due to the dosing regimen's difference (Fig. 2.7). However, synergism and sensitivity remained consistent between all combinations.

The AOH compounds were the only PCNA inhibitors to be effective as single agents with significant effects on GI₅₀ and LD₅₀. Further, the AOH compounds showed greater enhancement of DDR antagonists in general at their GI₅₀/3 than other PCNA inhibitors. AOH compounds showed the same ability to synergize with KU55933 implying a separate mechanism from the previous HR effect reported. This result further confirmed in the HR-incompetent cell line MDA-MB-436. AOH compounds also were capable of sensitizing the resistant cell line, HCC1937, to olaparib.

T2AA and the tripeptoids possess similar profiles in the clonogenic assays as they did in the MTT assay. These compounds showed exceptional ability to enhance doxorubicin potency in all HR-competent cell lines. They also capably synergized with olaparib in HR-competent cell lines, including HCC1937. Most importantly, these inhibitors show no toxic effects as single agents up to 200 μ M in this assay as well. These compounds require destabilization of the cellular genomes to increase stress upon multiple processes adjacent to PCNA functions.

The differentiation of the AOH and other PCNA inhibitors is further distinguished when examining the clonogenic results. These results indicate that the AOH of inhibitors has additional effects beyond HR due to their ability to synergize with ATM inhibitors and cells that do not possess a competent HR pathway. The other PCNA inhibitors show some specificity as HR antagonists due to synergizing with NHEJ antagonists only in HR-competent cell lines.

2.4.2 DNA Double-Strand Breaks

PCNA's direct ties to DDR and consistent enhancement of DNA damage agents makes direct evaluation of DNA damage necessary to understand the impact of inhibition. Comet assays are a standard of the field in observing gross amounts of DNA damage. I assessed DSBs specifically through a neutral comet assay to measure the amount of DNA no longer tightly packaged in the nucleus due to DNA damage using the "% DNA tail" metric. Evaluating DNA damage within the drug concentrations observed in both proliferation and viability assays allows us to understand the impact of observed DNA damage. Also, we must evaluate the amount of damage after approximately 8 hours to allow time for DNA damage repair with HR or NHEJ. Shorter periods would only allow NHEJ a chance to repair damage as it is utilized in any phase and requires less time to become activated.

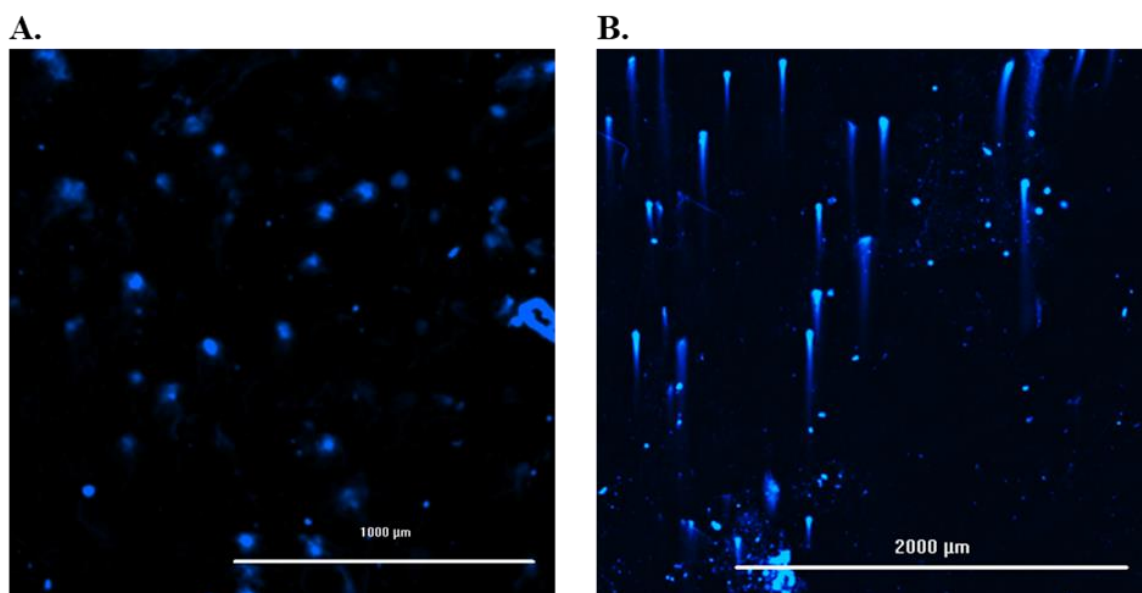


Figure 2.8: DNA damage in HCC1937 measured by a neutral comet assay. A. Exposed to no DNA damage agent; B. Exposed to 10 μ M Doxorubicin over 1 hour

First, PCNA inhibitors were evaluated as single agents. The AOH molecules were observed to induce DNA damage well below their GI_{50} value, consistent with earlier reported effects. This result further differentiates these molecules from T2AA and the tripeptoids as they cannot induce damage alone. Still, all of the PCNA inhibitors were able enhance the amount of

doxorubicin-induced damage at 1-hour exposures. Whether this enhancement is due to increasing the amount of damage sites or reducing DDR capabilities is not defined in this assay. Still, it remains that AOH molecules can induce damage as single agents while T2AA and the tripeptoids require initial damage to produce an effect.

Synergism with targeted molecules will further inform us as to the method of DNA damage enhancement. With cells exposure to a DDR antagonist targeting either NHEJ or HR, I evaluated the increase in DNA damage after 8-hours. The AOH molecules showed an ability to enhance the amount of damage present when used in combination with NHEJ antagonists regardless of the cell line's genetic background. I observed greater than 10% DNA Tail increases at or just below 2-fold increases of damage. These effects were observed in the HR-incompetent cell line MDA-MB-436 showing that these inhibitors do not require the HR pathway to be active to increase the amount of DSBs. The AOH molecules were also able to enhance DSBs in combination with the HR antagonist KU55933 in all HR competent cell lines showing a shift of close to 12% in the DNA tail and close to 20% more cells showing significant damage. All of these results are logical when compared to proliferation and survival data.

T2AA and the tripeptoids showed profiles across all cell lines and drug combinations similar to the survival and proliferation data presented above. These small molecules showed significant enhancement of DNA damage with NHEJ antagonists in HR-competent cell lines. When NU7026 was used in combination with T2AA and the tripeptoids there was an increase of ~10% in the DNA Tail across HR-competent cell lines. Olaparib showed a significantly greater synergism showing an increase of ~20% in the same cells. As before, I saw little change in the combinations of these molecules with ATM inhibitor KU55933 in MDA-MB-436, the HR-incompetent cell line. Overall, this shows selectivity towards HR inhibition by T2AA and the tripeptoids.

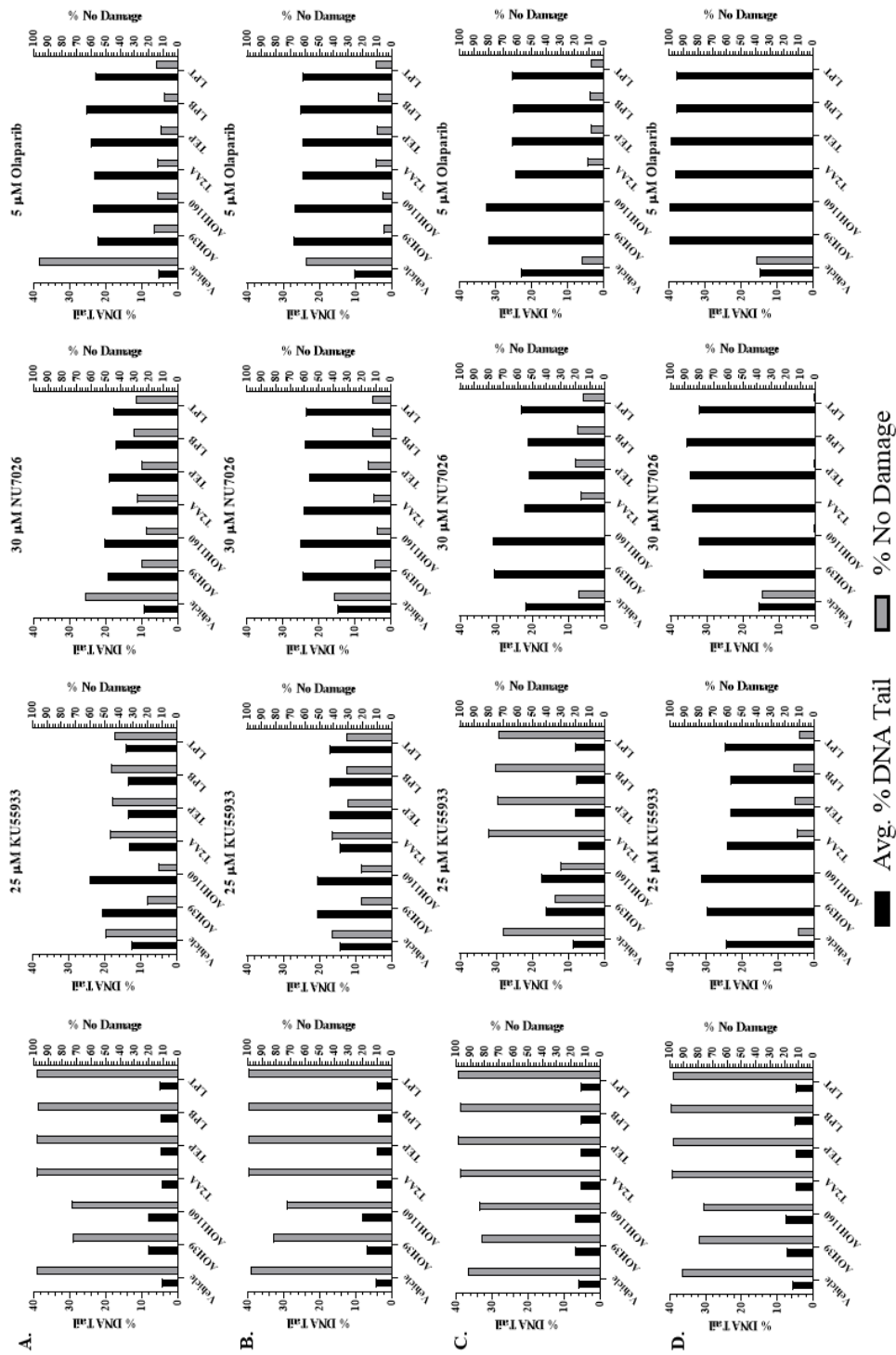


Figure 2.9: DNA damage effects of PCNA inhibitors. Cells were exposed to 10 μ M doxorubicin for 1 hour and then allowed 8 hours to repair. These were done in the cell lines shown and with the listed concentration of an inhibitor at the title as well as 1/10 GI50 of the PCNA antagonist denoted. The % DNA tail was averaged over cells with damage and the cells without damage tallied. A) HCC1937; B) MDA-MB-231; C) MDA-MB-436; D) MDA-MB-468

2.4.3 RAD51/ γ H2AX Foci

The role of PCNA inhibitors in HR-specific effects is implicated by the data obtained from the comet assay. More direct measurement of these effects requires examining the HR pathway through Rad51 foci (Fig. 2.1 & 2.10). As noted, PCNA is vital to the latter stages of HR through strand elongation. Numerous studies have shown Rad51, Rad52, BRCA1, and BRCA2 require PCNA to assemble at sites during HR.^{56,184,243–245} These proteins are all vital to HR and suggest another possible mechanism. It is important to distinguish if the impact is on early steps or late HR steps, which can be tested by the ATM inhibitor KU55933 that inhibits initial HR activation. Olaparib, an NHEJ antagonist, is used here to validate synergistic effects with PCNA inhibitors that were observed previously and to determine whether they are directly related to HR.

The overall experimental setup closely followed the comet assay to allow comparative analysis. At the 8-hour time point, Rad51 foci appear in cells with no secondary treatment after the doxorubicin exposure (Fig 2.11). PCNA inhibitors were assessed with and without doxorubicin and in combinations with DDR antagonists. The AOH inhibitors showed a significant increase in γ H2AX and Rad51 foci as single agents compared to the vehicle in HR-competent cells. Notably, the AOH molecules had the lowest ratio of Rad51: γ H2AX foci. These results are consistent with previous observations with AOH compounds ability to inhibit HR functionality. In an HR-incompetent cell line, the AOH compounds induced a larger number of γ H2AX foci and no Rad51 foci. All the other PCNA inhibitors were unable to induce either γ H2AX or Rad51 foci as single agents in either HR-competent or -incompetent cell lines. These observations are consistent with the results observed in the comet assay.

All PCNA inhibitors enhanced the DNA damage response in combination with doxorubicin in HR-competent cells. When cells are exposed to doxorubicin and then dosed with AOH molecules, γ H2AX foci count and Rad51 foci are increased >40%. These results indicate a significant increase in damage with a relatively low increase in Rad51 foci formation over 8 hours. This is consistent with the reports of the AOH molecules inhibiting HR function, but also our evidence of their capability of inducing damage as a single agent. T2AA and the tripeptoids saw a similar Rad51 foci response but a lesser γ H2AX foci effect with 2 fewer foci on average, when dosed with doxorubicin initially and given 8 hours to repair DNA damage. In the 24-hour assay, vehicle treated cells resolve the majority of their Rad51 foci and γ H2AX foci. However, the AOH compounds maintain the damage response, albeit at a lower level than at 8 hours. After exposure,

cells treated with T2AA and the tripeptoids see a drastic decrease in γ H2AX foci with a marginal reduction in Rad51 foci. The differences in this response can be attributed to AOH compounds' ability to induce DNA damage while the other PCNA inhibitors stall HR progression.

To further validate the HR specific effect, the combination of PCNA inhibitors with the targeted DDR antagonists were evaluated in the MDA-MB 436 cell line (Fig. 12). KU55933, an ATM inhibitor, was unable to induce damage as a single agent and prevented HR activation in the presence of AOH compounds. This observation is very similar to the effect of AOH compounds in the HR-incompetent MDA-MB-436. There was no additional effect in combination with other PCNA inhibitors, as expected from the previous assays.

Olaparib was utilized to understand what occurs in a reduced NHEJ function cell line. Olaparib saw a greater Rad51: γ H2AX foci ratio than doxorubicin, likely due to a reduction in NHEJ function, allowing HR to compensate. In combination with AOH compounds, there was a significant enhancement of both Rad51 and γ H2AX foci counts and cells with any foci in HR-competent cells and no Rad51 foci, but a greater amount of γ H2AX foci in HR-incompetent cells. T2AA and tripeptoids possess a larger Rad51: γ H2AX foci ratio. This could be due to both greater HR activation due to the reduced capacity of NHEJ and the persistence of Rad51 foci observed in the 24-hour doxorubicin experiment. Overall, the results confirm the features observed previously and cements the implication that T2AA and the tripeptoids exhibit both different and more specific HR functional inhibition than the AOH compounds.

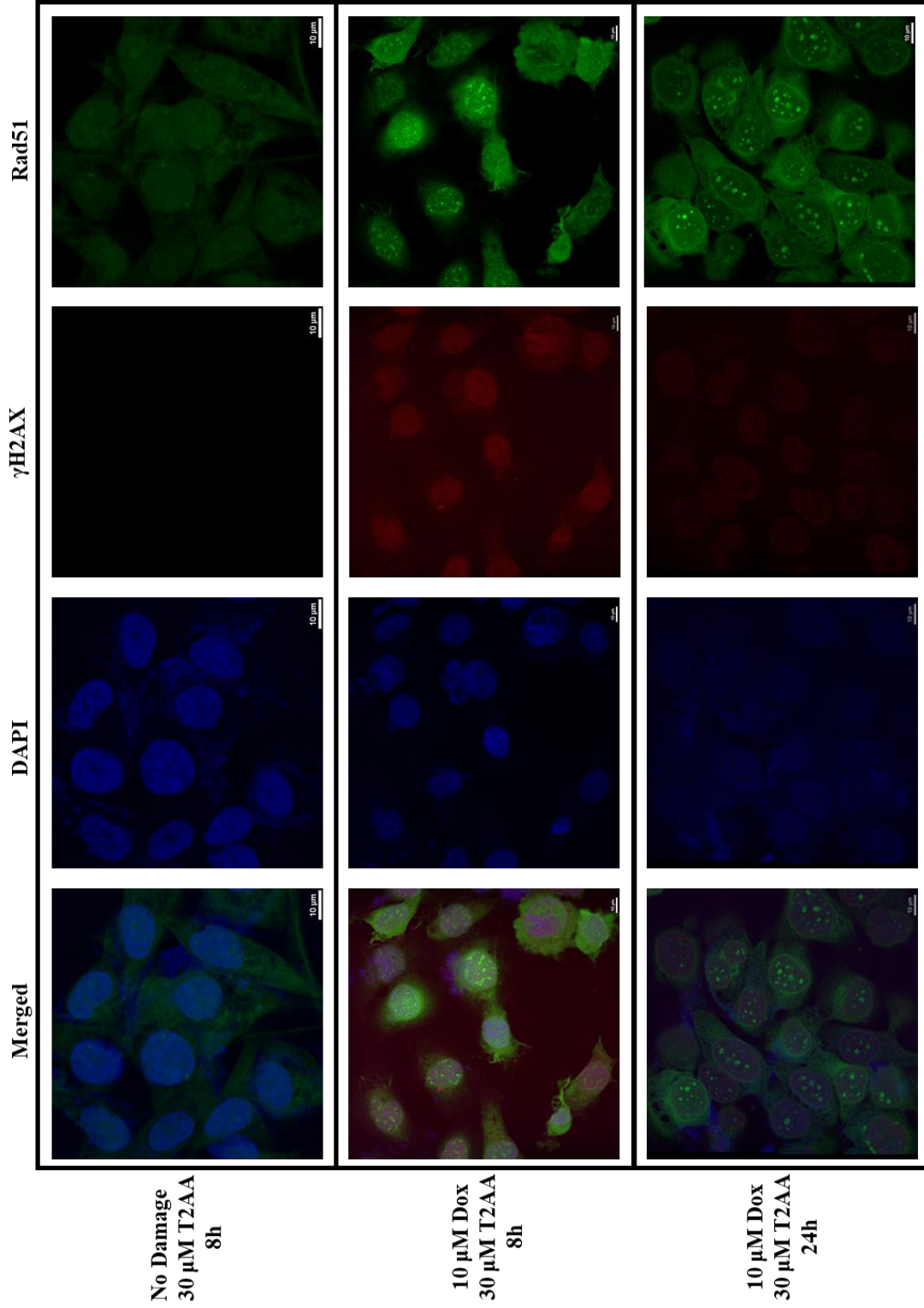


Figure 2.10: RAD51 and γ H2AX Foci Formation in MDA-MB 231 Cells. MDA-MB 231 were either exposed to 10 μ M doxorubicin as a DNA damage agent. Cells were then exposed to T2AA over either 8 or 24 hours.

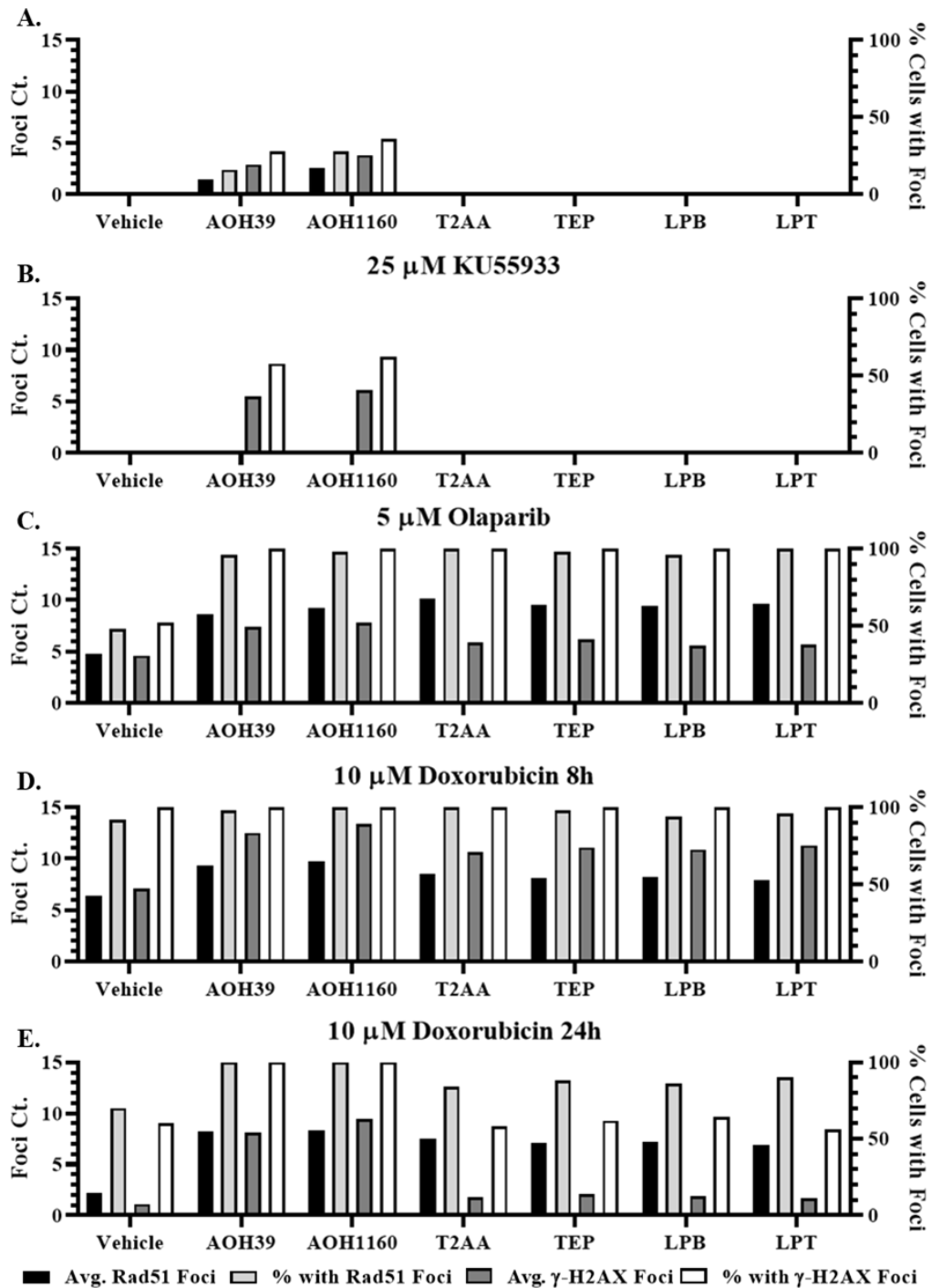


Figure 2.11: PCNA Antagonist Effects on Homologous Recombination in Combination with DNA Damage Agents and Repair Antagonists in MDA-MB-231 Cells. A) Cells were exposed to PCNA inhibitors at 1/3 GI_{50} over 8 hours. B-C) Cells were exposed to PCNA inhibitors at 1/3 GI_{50} as well as an amount of DNA damage repair antagonists over 8 hours 25. D-E) Cells were exposed to doxorubicin for 1 hour and then washed of PCNA inhibitors.

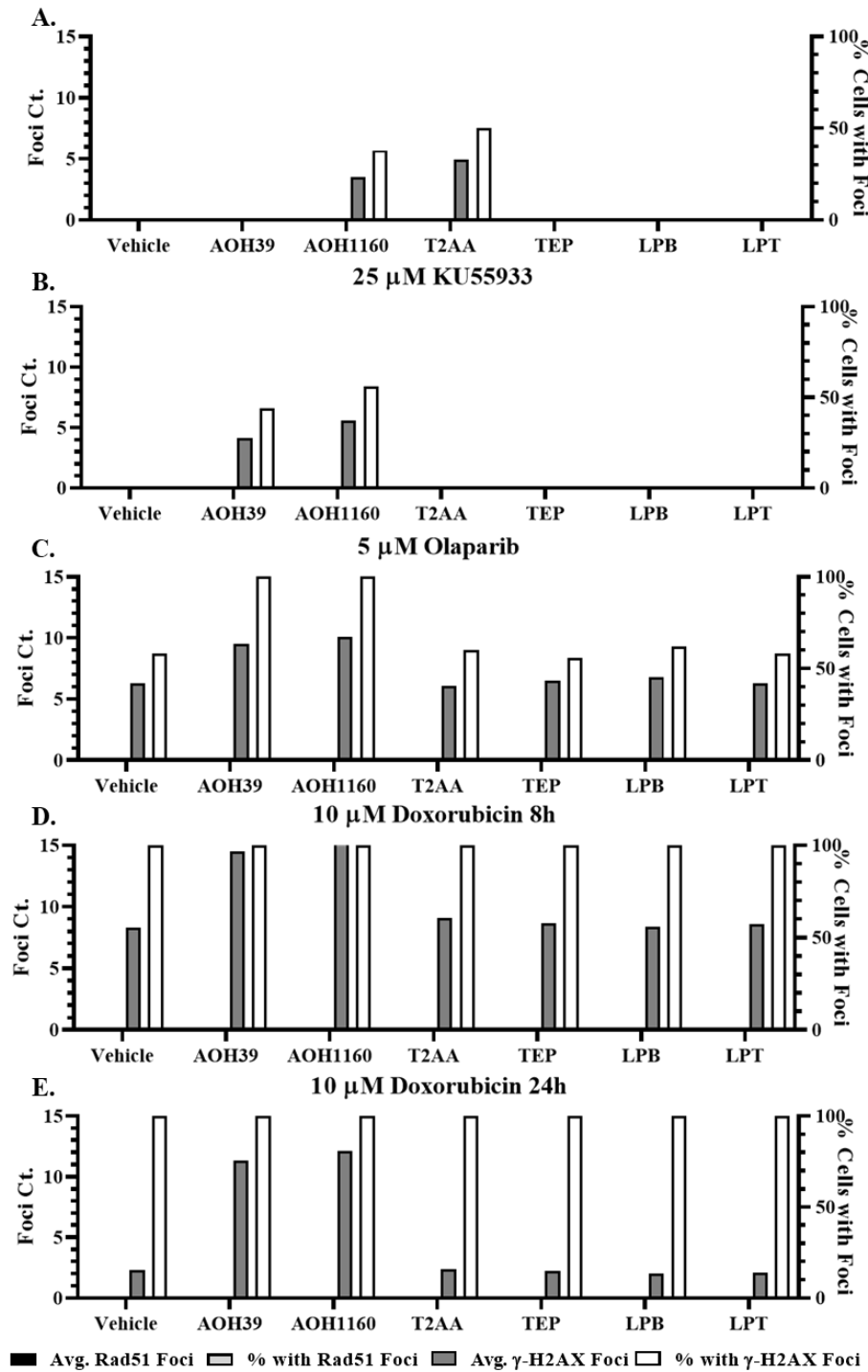


Figure 2.12: PCNA Antagonist Effects on Homologous Recombination in Combination with DNA Damage Agents and Repair Antagonists in MDA-MB-436 Cells. A) Cells were exposed to PCNA inhibitors at 1/3 GI_{50} over 8 hours. B-C) Cells were exposed to PCNA inhibitors at 1/3 GI_{50} as well as an amount of DNA damage repair antagonists over 8 hours 25. D-E) Cells were exposed to doxorubicin for 1 hour and then washed followed by 8 or 24 hours of PCNA inhibitors.

2.4.4 DNA Replication

Another PCNA process that has been impacted by previous pan-inhibitors is DNA replication (Fig. 2.13).^{66,246,247} This effect is primarily through the inhibition of PCNA-DNA polymerase interactions producing replication stress by exposed ssDNA resulting in DNA damage that causes stalls in replication and fork collapse. DNA damage independent of DNA replication can halt cells at the G1/S checkpoint, but most PCNA-centric effects require S phase to upregulate HR and begin DNA replication. T2AA has been reported to have significant effects on DNA replication processivity. This is consistent with our results. T2AA at a concentration equal to $GI_{50}/3$ saw more than a ~25% increase in cells remaining in S phase with only an average ~8% increase in cells remaining in the G1 phase (Fig. 2.14). In contrast, AOH compounds, at a concentration equal to $GI_{50}/3$, saw an average of ~5% increase in cells remaining in S-phase, but an average of ~9% increase in cells remaining in G1 phase. Referencing back to earlier experiments, this is at a concentration where DNA damage is induced by these compounds. This is all similar to doxorubicin's effects on cell cycle where there was an average of ~6% increase in S phase cells and ~12% increase in G1 phase cells across all cell lines. The tripeptoids all behaved very similarly to one another. There was only an average increase in G1 phase cells of ~2-3% and an average ~14% increase in S phase cells at a concentration equal to $GI_{50}/3$, well below any effects on growth or damage.

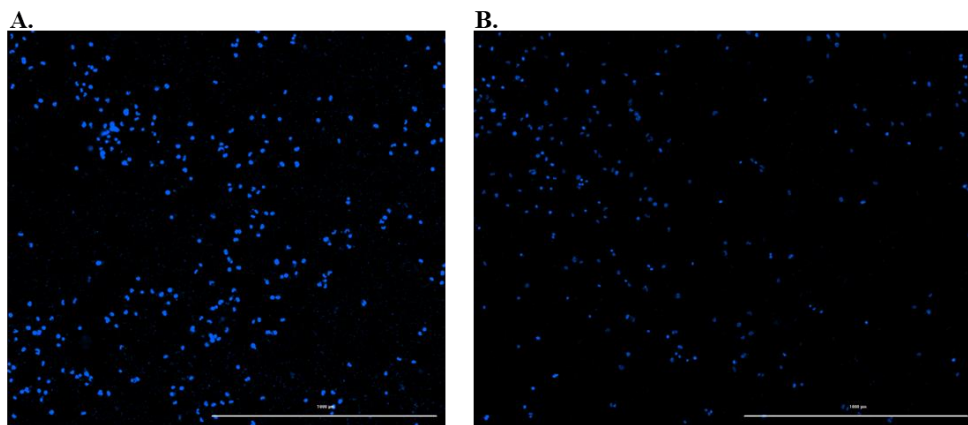


Figure 2.13: Measuring Replication through Quantifying DNA. A. No treatment; B. 30 μ M T2AA

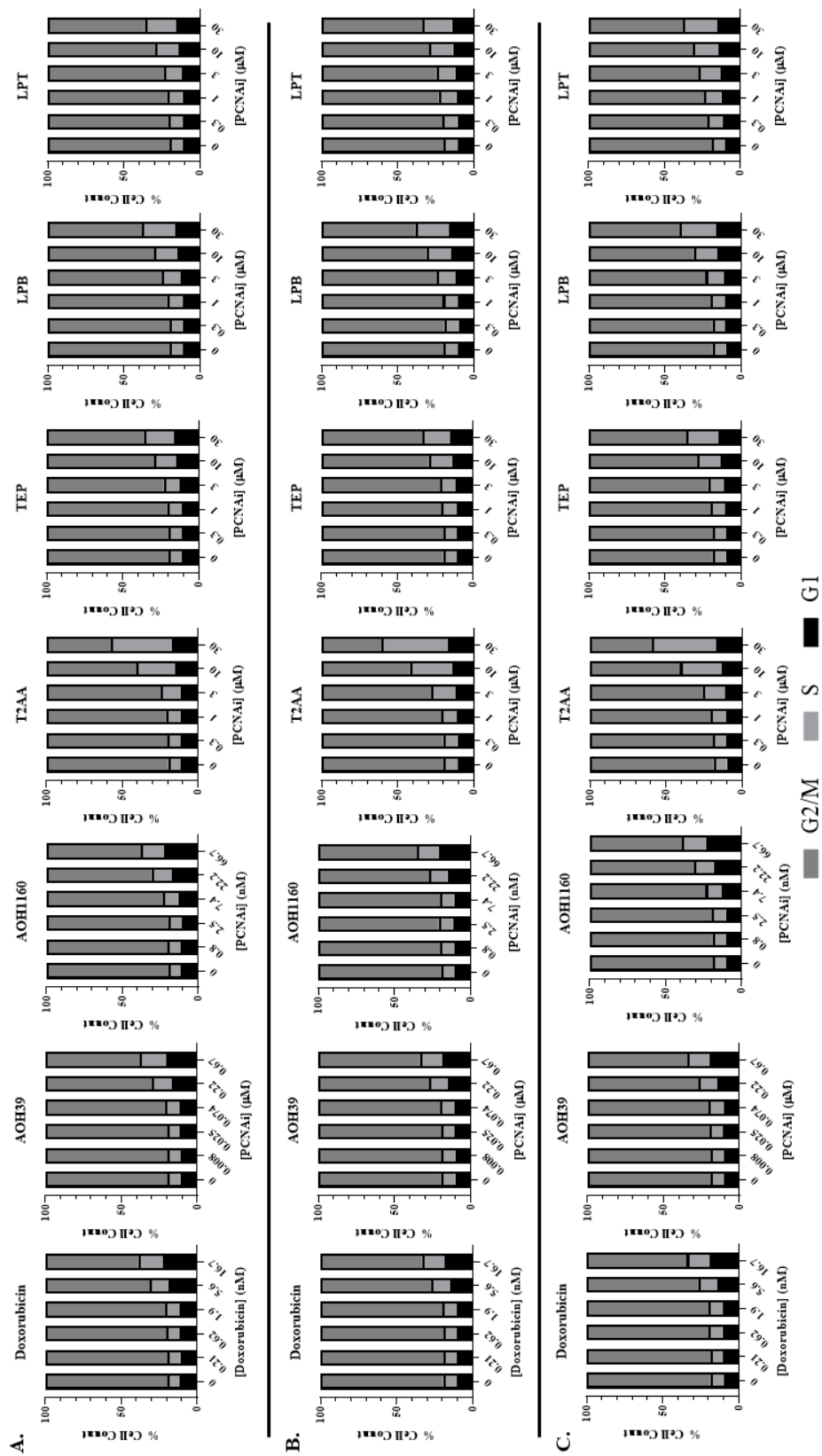


Figure 2.14: DNA Replication Effects of PCNA inhibitors. Three different cell lines were exposed to five doses of PCNA inhibitors as monotherapies. These therapies start at 1/3 GI50 and utilize a dilution factor of 3 to measure the effect. A) MDA-MB-231; B) MDA-MB-436; C) MDA-MB-468

This experiment begins to differentiate the effects of T2AA from the tripeptoids and thoroughly separates them from the AOH compounds. T2AA shows the greatest effect on DNA replication while the tripeptoids show a measurable effect at concentrations below those for growth inhibition. AOH compounds show no effects on DNA replication at dosages below concentrations that induce DNA damage. Further, AOH compounds show a similar profile to doxorubicin, increasing cell cycle arrest in G1 phase. Doxorubicin causes a strong synergism in S phase delays for T2AA, and the tripeptoids further emphasize the HR-specific effects.

2.4.5 Translesion Synthesis

TLS requires a monoubiquitination of PCNA at K164. Prior studies establish that the PCNA inhibitor T2AA directly inhibits this PTM by an unknown mechanism.²²⁰ This reduction in monoubiquitination of PCNA reduces the activity of TLS, and in turn, sensitizing cells to intra-strand crosslinks and adducts.^{248,249} UV light exposure causes thymidine dimers that require TLS and base-excision repair to overcome.²⁵⁰ Exposing cells to UV damage and then assessing cells' capability to bypass the damage and go through S phase shows a competent TLS pathway. Under these experimental conditions, it is possible to detect if the PCNA inhibitors' effects on HR and replication involve the step of TLS. The AOH compounds showed no synergism with the UV damage, all delays in cell cycle progression occurred in the G1 phase and which is indicative of DNA damage and not replication delays (Fig. 2.15). T2AA displays significant capacity to induce delays in S phase in the presence of UV radiation, an average increase of 40% of cells in S phase across all cell lines, including HR-incompetent cells. TEP, LPB, and LPT did not show significant synergism with UV radiation in slowing S phase progression. These observations suggest that while TEP, LPB, and LPT share similar HR effects as T2AA, they differ significantly in their ability to directly inhibit TLS. T2AA is the only small molecule to show significant reduction in Rad18 mediated monoubiquitination of K164. T2AA also has a proposed secondary binding site closer to K164 in addition to its PIPM binding site.¹¹³ Tripeptoids could be acting as exclusive PIPM site binders enhancing their functional selectivity on PCNA.

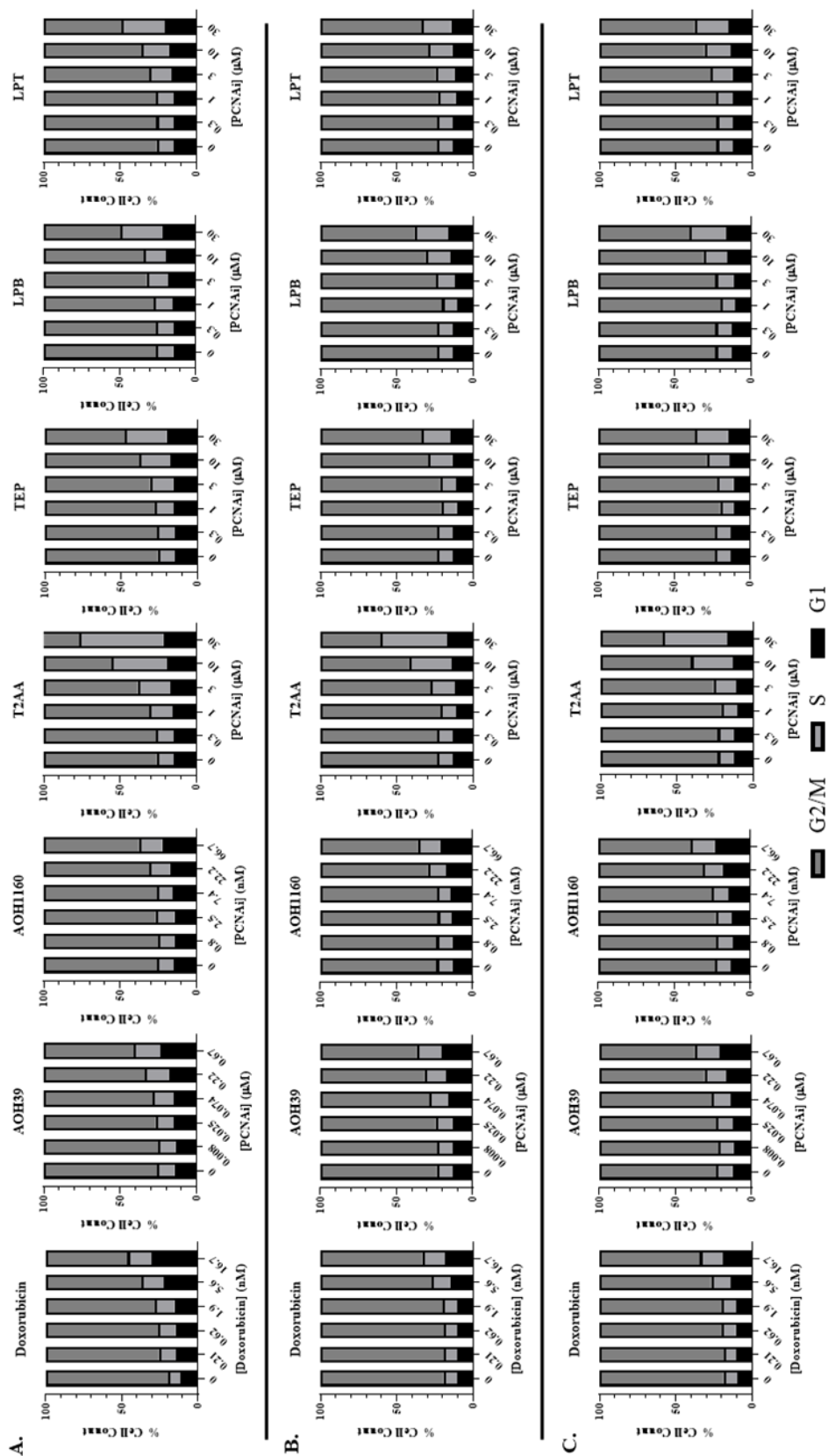


Figure 2.15: Translesion synthesis effects of PCNA inhibitors. Three different cell lines were exposed to five doses of PCNA inhibitors as monotherapies as well as UV. These therapies start at 1/3 GI50 and utilize a dilution factor of 3 to measure the effect.
 A) MDA-MB 231; B) MDA-MB 436; C) MDA-MB468

2.4.6 PCNA Inhibitor Profile

PCNA inhibitor activity can be classified by the distinguishing factors shown in each of these assays. These factors are determined by the experimental context, including effects observed through drug combinations and varying genetic backgrounds (Fig. 2.16). As such, I will define PCNA inhibitors by their effects on cell proliferation, viability, and gross DNA damage, and then by three specific effects related to the functions of PCNA evaluated here: DNA replication, TLS, and HR. As a control, doxorubicin will be used to show general DNA stress in these same contexts.

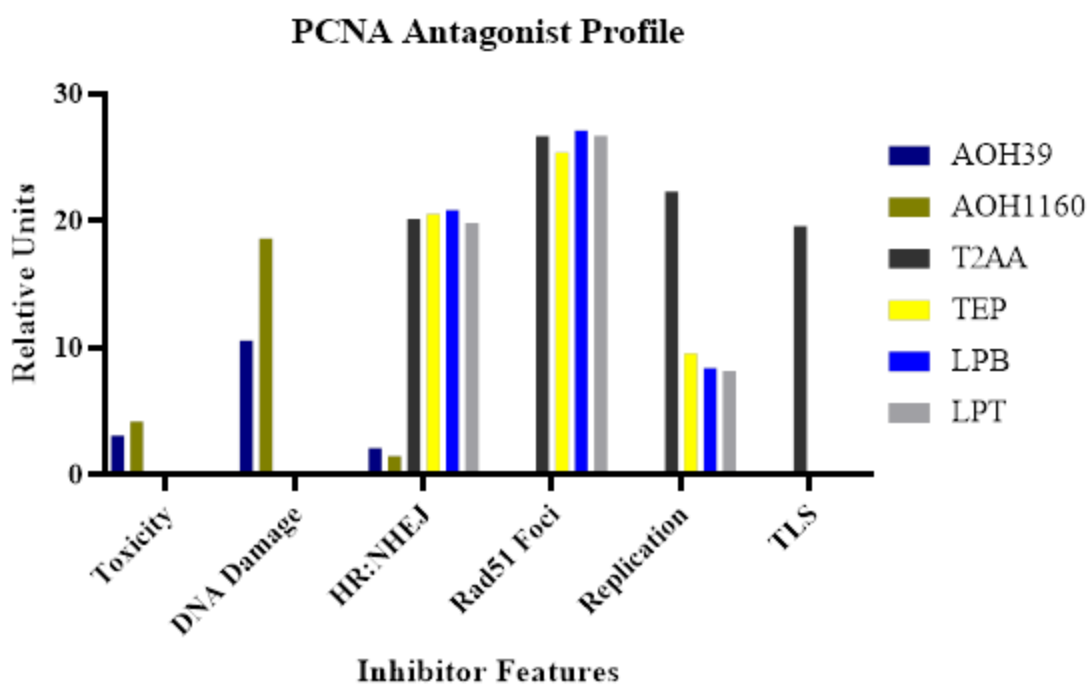


Figure 2.16: PCNA Antagonist Profile by Pathway Specific Features. All PCNA inhibitors had each major feature specificity calculated as reported in the methods. The goal was to utilize multiple assays to determine the isolated effects on each pathway or function listed. *Toxicity* – based on the LD₅₀ of the antagonist alone; *DNA Damage* – % DNA Tail of the antagonist at GI₅₀/3; *HR:NHEJ* – The overall effects of PCNA antagonists in HR specific vs. NHEJ-specific contexts; *Rad51 Foci* – the amount of Rad51 foci maintained after 24h while treated by the PCNA antagonist; *Replication* – the amount of cells in S phase after dosing with GI₅₀/3; *TLS* – the amount of cells in S phase after dosing with GI₅₀/3

T2AA is the most thoroughly analyzed PCNA small molecule inhibitor in our study. The lack of toxic effects as a single agent, including induction of DNA damage, is significant and differentiates T2AA from peptides studied to date. Since its discovery, T2AA has maintained its uniqueness as

a selective small molecule inhibitor of PCNA. T2AA's effects on DNA replication have also been thoroughly documented and understood as the ability to inhibit DNA polymerase association with PCNA. Furthermore, T2AA's ability to inhibit K164 monoubiquitination has allowed the study and evaluate the role in TLS. The enhancement of various DNA damage agents and DDR antagonists by T2AA has been investigated previously, but not in the same way as in this study. The work here establishes the capability of T2AA to sensitize resistant cell lines to NHEJ antagonists and the inability of T2AA to synergize with ATM inhibitors. The results further cement T2AA as an inhibitor of HR antagonist. The maintenance of Rad51 foci over time is a novel effect and confirms observations of PCNA peptide-based inhibitors as preventing proper Rad54 function. Overall, T2AA shows the ability to inhibit several PCNA functions, but requires additional genome stress in the system to reveal significant effects.

The AOH compounds uniquely showed significant cell toxicity and induction of DNA damage as single agents. However, they were much more effective in the presence of doxorubicin and targeted DDR antagonists. While they were more effective in synergizing with NHEJ antagonists, they also enhance the HR antagonism. Further, they synergize with both general and targeted chemotherapies in the absence of a functional HR pathway. AOH compounds do not significantly affect cell cycle progression in the DNA replication model or through TLS that could not be explained by just drug-induced DNA damage. Overall, AOH compounds show significant activity with HR, as reported, but also general effects and lack the qualities of functionally specific PCNA inhibition. AOH compounds could be understood as general stressors of PCNA related processes likely through direct and indirect effects on PCNA.

The tripeptoids possess similar traits to T2AA but show no significant toxic effects as single agents on cell growth and genome integrity. However, these compounds show strong synergistic effects with general DNA damage agents and NHEJ antagonists. These molecules require a functional HR pathway to function, supporting a specific mechanism of action. These agents show similar effect on Rad51 foci persistence which likely contributes to the specificity of pharmacological action. However, these compounds are different from T2AA in their lack of effects on DNA replication and TLS. The tripeptoids have a notably lower effect on DNA replication delays in these experiments despite having comparable, if not greater, binding affinity to PCNA than T2AA. They lack a significant enhancement on S phase delays in the presence of

UV radiation suggesting they have little effect on TLS. All these results implicate highly specific inhibition of PCNA function in the HR pathway.

2.5 Discussion

This study establishes three groups, whose features are outlined in later subsections, of PCNA inhibitors and reveals possible clinical utility for each group: AOH Compounds, T2AA, and Tripeptoids (Fig. 2.17). While different groups have assessed their own PCNA inhibitors, this is the first study that examines their mechanistic roles in determining specific inhibitory mechanisms. As a result, this study also further establishes that it is possible for PCNA inhibitors to have a context specific effect that leverages disease biased functions. More generally, this also validates the use of PPI antagonists as a strategy to affect flexible regions of proteins, such as PCNA. More clinically speaking, this provides an example of targeted therapies being capable of sensitizing resistant cells through an essential gene, further establishing their targetability in combinations. This is in contrast to more general approaches utilized with PCNA, such as PCNA peptide antagonists or the pan-PCNA inhibitor PCNA-I1. PCNA-I1 targets the site of homodimerization allowing PCNA to be loaded onto DNA and form a homotrimer capable of facilitating interaction with DNA for several proteins. This prevents all interactors that require a homotrimer complexed with DNA.

2.5.1 AOH Compound PCNA Antagonism Description

With the establishment of differential PCNA antagonism, it is necessary to evaluate what disease contexts PCNA antagonism is relevant to and which functions are targetable. Subclass A contains AOH39 and AOH1160 and possesses some HR specificity when compared to doxorubicin, but also possesses its own DNA damaging capabilities.²²⁷ This was observed in the initial publication with these molecules, but the lack of a notable Rad51 foci persistence, DNA replication, or TLS effects clearly distinguish them from the other subclasses. As a DNA damage agent that preferentially targets tumors over normal cells and with the slight HR focus subclass A could have a broad range of cell types to effect. The lack of more specific PCNA functional inhibition would likely leave it more sensitive to general resistance methods of tumor cells, however. Induction of DNA damage is the primary feature that is discernable and any effects on

DNA replication or cell cycle can be explained through this effect. A reduction in general toxicity overall should be sufficient utility to make subclass A one to pursue to reduce the use of more toxic traditional chemotherapeutics. However, our objective has been to pursue functional selectivity that leverages specific cancer biology contexts and not generalized strategies.

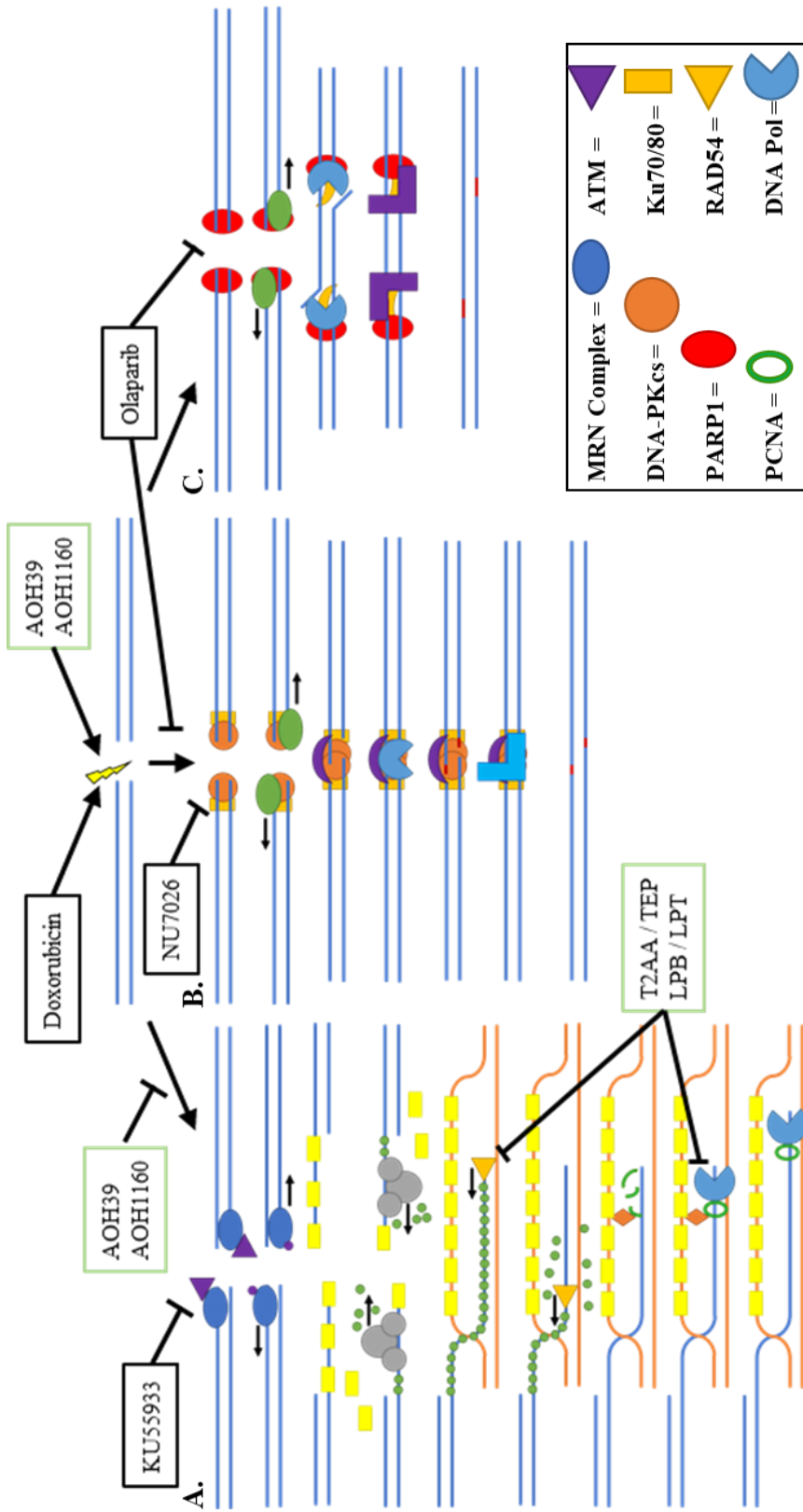


Figure 2.17: Drug Interaction in Double-Strand Break Repair Pathways and PCNA Inhibitor Impact; This is the validate mechanisms of our small molecule DNA repair antagonists in the context of homologous recombination (HR), classical non-homologous end joining (cNHEJ), and alternative non-homologous end joining (aNHEJ). These compounds are outlined with black. The PCNA inhibitors assessed in this study are outlined in green. AOH compounds have been shown previously to inhibit HR, but neither in that study, or this one, was a specific target identified. However, DNA damage was detected with the AOH compounds as a monotherapy. Due to the Rad51 foci persistence, the targets of T2AA, TEP, LPB, and LPT can be narrowed down to an effect that includes Rad54 or Polymerase association. Synergistic relationships require effects that include at least HR and either NHEJ pathway. A) HR; B) cNHEJ; C) aNHEJ

2.5.2 T2AA and Tripeptoid PCNA Antagonism Description

Subclass B and C show remarkable overlap in functional selectivity. Subclass B contains T2AA, and subclass C contains the tripeptoids developed by the Davisson group. Both show low toxicity as monotherapies in all cell types despite moderate affinity and high specificity of binding to PCNA. The greatest area of overlap between these subclasses lie in their ability to target HR and synergize with NHEJ antagonists as well as DNA damage. Their ability to antagonize HR appears to be similar in preventing the resolution of the strand invasion and therefore also preventing strand elongation and loop resolution. The persistence of Rad51 foci with the resolution of γ -H2AX is a telling feature and further confirms PCNA's role in Rad51 dissociation.^{183,251} As described earlier, this form of inhibition prevents feedback to reduce upstream signaling and allows the HR pathway to function up until PCNA is necessary. Interestingly, these antagonists do not present this feature unless the cell is stressed either through exposure to a DNA damage agent or through inhibition of the compensatory pathway NHEJ. This feature alone bears much more investigation and will provide fodder for other groups working in this area.

In addition, both subclasses also show slowing of DNA replication, likely through preventing prolonged polymerase loading at the replication fork. This has been a hallmark of PIPM protein-protein interaction inhibitors and has also been induced with p21 peptides. It is notable that T2AA was more than twice as effective in reducing the progression through S-phase than the tripeptoids developed by our group. Where these classes truly differentiate is in their effects on TLS. T2AA has been verified to inhibit K164 ubiquitination via Rad18 to induce TLS. The Rad18 binding site and K164 is distant from the PIPM binding site and the T2AA binding site.²⁵² The tripeptoids show no effect on TLS suggesting that they do not prevent this interaction as T2AA does. The increased specificity of the tripeptoids could explain the lower effect on DNA replication overall. T2AA, while more general in its effects, would still be applied to enhance DNA damage effects in multiple contexts as well as the tripeptoids. However, the narrower effects of the tripeptoids may reduce the amount of "off-target" functional effects and make them safer in few contexts than T2AA. Regardless, this demonstrates the functional selectivity of PCNA inhibitors as not merely theoretical based on past mutational studies but a fact to be leveraged and developed further.

2.5.3 Overcoming Olaparib Resistance through Induced Synthetic Lethality

The most impactful discovery for cancer therapeutics generally is the ability to inhibit the HR pathway through PCNA. This exceeds “BRCAness” features as there are no redundancies in PCNA function that are possible. The enhancement of DNA damage through this mode of inhibition will also ensure a rapid activation of apoptosis. Without a means to signal to the beginning of the process, a loss of PCNA function can quickly multiply the damage as HR is consistently activated despite its failure. This would enable oncologists to artificially create systems of lowered HR competence to sensitize tumors to PARP inhibitors. The enhancement of damage through this mechanism would also allow these inhibitors to sensitize tumors to damage that upregulate HR as a means to blunt the impact of DNA damage agents, such as doxorubicin. Further, as has been observed previously, mutations to PCNA can be even more disastrous than our inhibitors reducing the development of chemoresistance.

2.5.4 Leveraging High-Content Assays through Drug Combinations and Differentiated Biology

Overall, classifying three groups of PCNA inhibitors provides a blueprint for defining future PCNA antagonism. Understanding PCNA functional effects through a quorum of assays to determine the impact of non-mutually exclusive features that are interregulated is essential. Attempting to evaluate any of these features individually would not satisfyingly discern which feature is the primary one, as in the case of subclass A where the DNA damage effects caused delays in cell cycle. Showing the utility of functionally specific antagonists of an essential gene in combination with other targeted antagonists provides a novel approach to therapeutic strategies. These therapeutics require combinations to leverage specific stressed conditions that are inducible by the concurrent administration of targeted therapies contextualized by a specific disease state.

2.6 Conclusions and Impact

In this work, I provide clear differentiation of three classes of PCNA antagonists through toxicity, DNA damage, drug combinations involving HR and NHEJ antagonists, DNA replication, TLS effects measured through UV exposure, and Rad51 foci effects. While not an exhaustive set of characteristics, this establishes antagonists as either having general effects through PCNA or

specific effects through DNA damage repair in HR, DNA replication effects, or TLS polymerase switching. The assays selected and approaches included prioritize throughput as well as being high-content. Further, my novel examination at lower concentrations in combination with DNA damage repair antagonists for synergism provides insight into the mechanistic context as well. In the case of targeting essential genes or specific protein functions, understanding the mechanism of action through relevant combinations is key to show likely utility. Standardizing this approach through direct and indirect measurements provides definitions of functional inhibition of PCNA antagonists that will allow for the expansion of ligand types and roles through these definitions. Providing novel metrics to define specific features of functional inhibition to produce this profile also allows for additional classes to be discovered with various permutations of these features using this approach.

CHAPTER 3. A NETWORK APPROACH TO PREDICT SYNERGISTIC DNA REPAIR ANTAGONIST COMBINATIONS IN CANCER

3.1 Introduction

In the United States, cancer has surpassed cardiovascular disease as the number one cause of death in wealthy nations.^{253,254} Cancer treatments continue to be improved by increasing the personalization of therapy using molecularly targeted, and immunotherapies. The diversity and heterogeneity of tumors still present challenges for these approaches, and radiation and general chemotherapy options remain the standard of care for many indications.^{255–257} However, these therapies carry additional toxicity issues and ultimate chemoresistance developed by tumors have steadily reduced the efficacy of these treatment strategies.^{258,259} Currently, biomarkers that can effectively identify a course of treatment are limited to common cancer subtypes. As such, precision in defining biological features that are most predictive for meaningful clinical responses to new or traditional therapies has not been generally realized and leaves many gaps in the effective use of pharmacotherapies.

Agents that damage DNA remain a prominent component of the tumor chemotherapeutic strategies. The increased rates of proliferation in tumor cells affect stress and dependence on dysregulated cell cycle checkpoints.²⁶⁰ When most effective, increased DNA damage by these agents exceeds the capacity that the DNA damage repair (DDR) pathways can manage. An excess of DNA damage results in cell cycle arrest and the activation of the intrinsic apoptotic pathway, leading to the execution phase of apoptosis and cell death.^{261,262} However, due to the inherent genomic instability, cell survival is also commonly dysregulated to allow the tumor to proliferate rapidly even in a state of high stress. As such, many tumors have developed resistance to DNA damage by dysregulation of the DDR and/or reducing the responsiveness of cell cycle and apoptotic pathways to DNA damage.^{263,264} In contrast, tumor cells must maintain or enhance the means of detecting and repairing DNA to prevent overwhelming genomic instability. DDR pathways and cell cycle dysregulation have made these molecular components a focus of novel targeted therapies.

The DNA repair targeted therapies are limited in their application as they are dependent on the exact form of dysregulation. They rely upon somatic mutations and other biomarkers to

indicate the possible use of these therapies.²⁶⁵ The identification of these markers has allowed the advancement of personalized treatments. Gene expression profiles and single biomarkers are not exhaustive means of discerning the potency of personalized therapy. In many cases, the modulation of an unmodified gene can drive tumor biology, so there are multiple paths to this change.²⁶⁶ Developing a method to discern systems that are changed allows the broader use of therapies that target the system rather than just a target. Examples of biomarker-dependent application of the drugs olaparib and palbociclib are evidence for this shift in oncology.

3.1.1 Gene Expression Network

The field of pathway analysis is well established and has been used to identify disease pathology trends.^{267,268} Pathway analysis is simply assessing defined molecular signaling involved in the completion of a biological task. Scale-free network graphs representing pathways with nodes containing individual genes or proteins and edges defining modifications or actions performed by a source protein upon a target protein.²⁶⁹ These network graphs can order a simple set of linear nodes whose product is modified by subsequent nodes, such as in a metabolic pathway (Fig. 3.1A).²⁷⁰ However, most pathways include branches and regulatory loops that define a system beyond linear process (Fig. 3.1B).²⁷¹ Many pathways have well-defined early and late regulator proteins that recruit other proteins within the process or increase the expression of the genes needed. There is often more than one way to activate a pathway and multiple regulators to ensure control over the pathway. These networks' construction can represent the biological feature that only a few genes must be overexpressed for a pathway to be considered active.²⁷² These genes are known as indicator genes and can provide a condensed gene set to evaluate pathway activity. Gene and pathway enrichment have been used to create profiles for drug responsiveness and predicting similarity between diseases.^{273,274}

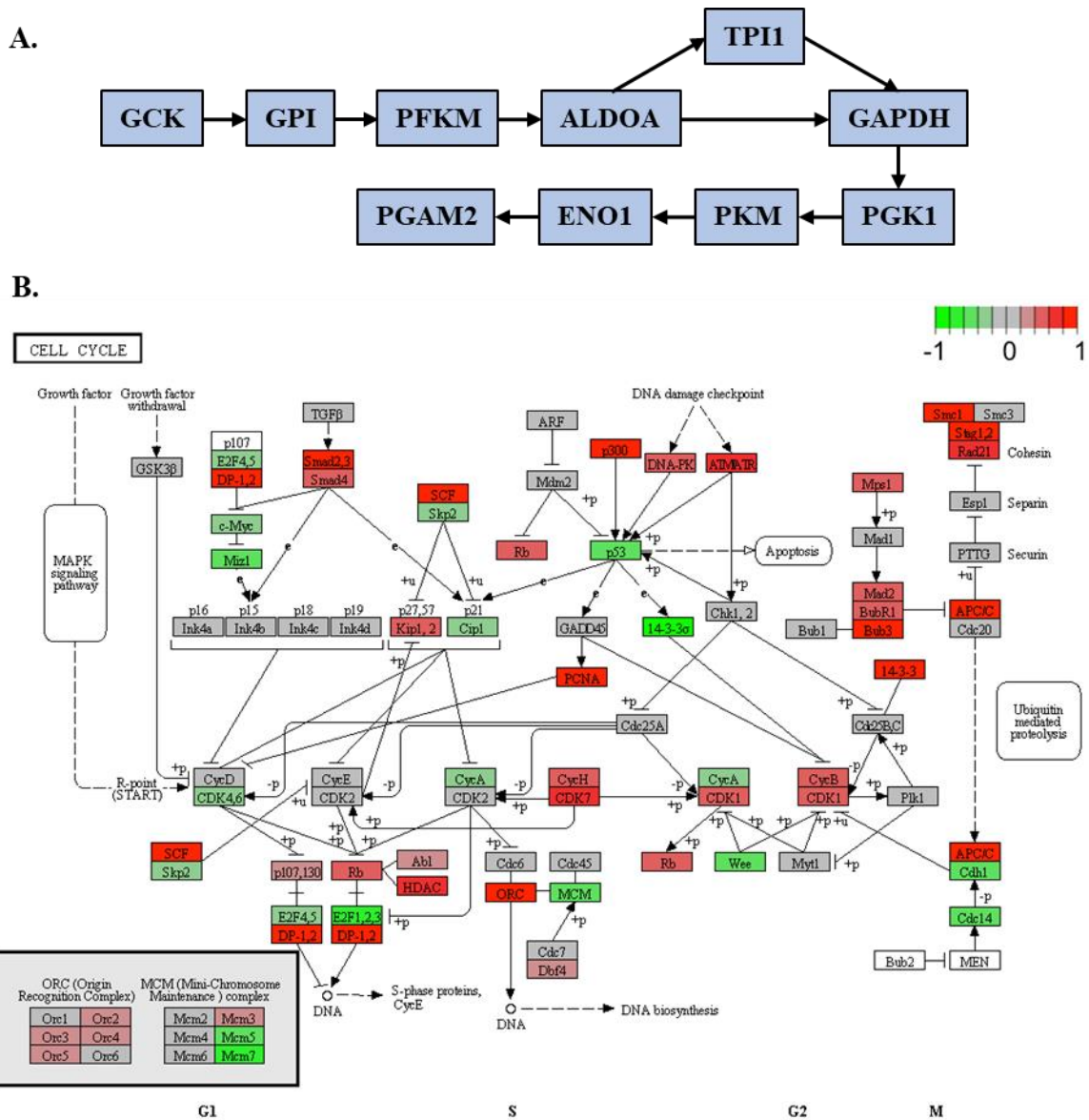


Figure 3.1: Gene Networks; Gene networks represent the possible interactions of gene products often with expression or network topography measurements determining the color of nodes. They provide an intuitive presentation to represent pathway regulation. Arrows and wedges can be used to show activating and deactivating relationships. Further, modifications can be used to show functional changes created by interactions. A) Simple metabolic pathway; B) Complex signaling pathway

Pathway networks have been created to represent connections between gene expression related to a specific context, such as drug treatment. Co-expression is then used to determine edge strength creating a network of relationships that, while less direct, define a biological capability (Fig. 3.2).²⁷⁵ A comparison of differential co-expression can provide insights into novel network dynamics that would be impossible to discern through protein-protein interactions. The layering of information with additional genomic data, including epigenetic regulators, miRNA, and lncRNA can develop a more resolved image of aberrant regulation.^{276,277} The systems focus on the mechanics of dysregulation and not merely the dysregulation itself. Gene expression remains a commonly used indicator and means to construct an understanding of disease pathology. Further investigation to understand the neighboring pathways and interactors is required to discern a meaningful potential of a drug target.

The limit of gene expression as a metric is that many genes whose activities are not solely regulated by their expression. The underexpression of one gene does not register as the overexpression of an associated gene. Many molecular complexes exist in biology whose structure change because of what genes are or are not present. Furthermore, somatic mutations can make the interaction profile entirely different, rendering differential gene expression moot. Any method that relies entirely on gene expression will possess gaps related to the functional features of proteins.

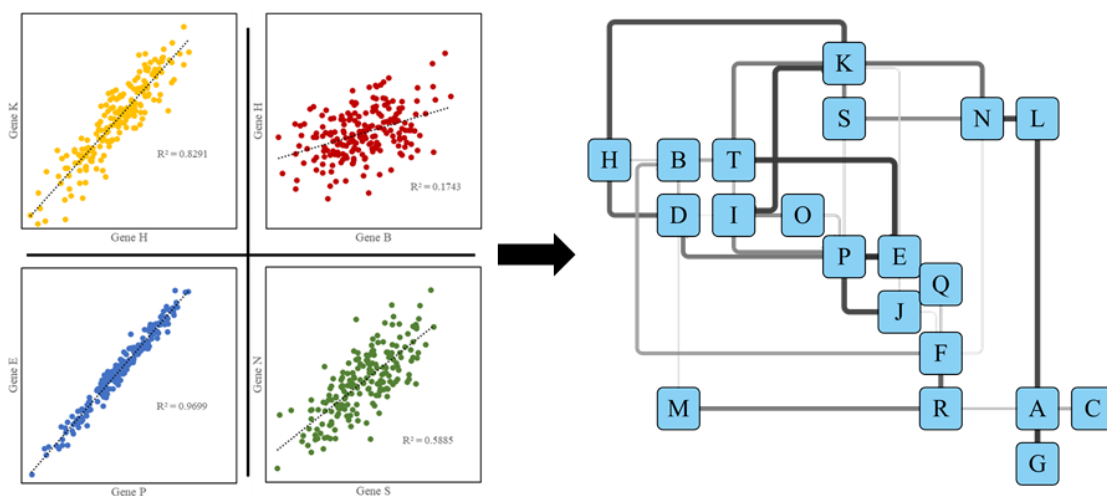


Figure 3.2: Co-Expression Network; Gene networks are representations of physical interactions of their products. Co-expression is also used to determine clustering of gene product that are effective simultaneously.

3.1.2 Disease Networks

Disease networks have been created for the same reason as pathway networks, to examine both global and local changes to discern novel connections. Disease networks are created through two general methods. The first uses the comparison of two disease networks directly to determine what relationships may exist (Fig. 3.3A).²⁷⁸ This approach aims to determine what similarities can leverage one disease's understanding through another. Connections between disease conditions have been able to offer opportunities for drug repositioning.²⁷⁹ Observations that detail similar genomic changes and network modifications can predict how a drug could behave similarly in two diseases. The approach is frequently useful with cancer diseases that possess similar somatic mutations.²⁸⁰ Examples are the broader use of gefitinib in EGFR dependent contexts or DNA damage agents where stress markers indicate enhanced sensitivities.^{281–283} Drug repositioning is also possible in infections that require similar host functions to allow disease progression.²⁸⁴ Connections between diseases can act as an effective shorthand to reduce redundancy of effort.

The second type of disease networks focus on individual disease or comparative sets of conditions seeking models of the pathophysiology's emerging biomolecular features (Fig. 3.3B).²⁸⁵ This approach can be considered an extended gene network that prioritizes processes over individual gene relationships. The sources of information emerge from examining changes at the genetic, cellular, and tissue levels. When considering such large sample sets, narrowing data to focus on features considered to be sources of changes necessary for the disease is requisite.^{286,287} To do so, information is examined at each level to analyze their connections to pathophysiology. This approach can involve the sum of pathways that influence action within and between cells.²⁸⁸ What emerges are not root causes but more information about novel connections between processes. The exact means of regulating those processes often have varied effects that depend on pathway relationships. Eventually, the resolution can be at individual genes, but a global context must be present before correctly ascertaining an outcome. Focusing on subnetworks related to disease dynamics can provide insight into cellular features that give rise to more significant issues that evade detection by examining cellular components alone.

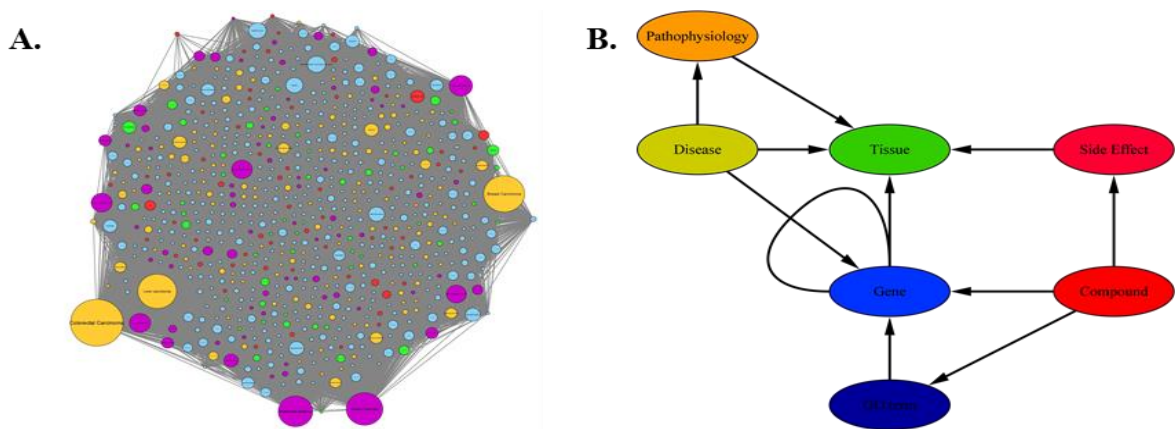


Figure 3.3: Disease Networks; Disease networks can be used to analyze how diseases are similar or connections between disease pathophysiology to biomolecular features. A) This disease similarity network creates edges between diseases that have more than 5 associated genes in common; B) Disease regulation network utilizes genomic, proteomic, and treatment data along with disease data to identify biological features at the gene, pathway, and tissue levels.

3.1.3 Synergy Networks

Synthetic lethality and synergy describe when the loss of two genes or biomolecular functions is nonadditive in their combined effect with respect to the loss of either independently.²⁸⁹ Synergism can emerge in a disease treatment scenario from either a genomic change that is co-dependent upon a monotherapy or a combination of therapies. Drug combinations have been used consistently in cancer therapy to reduce side effects from treatments or enhance the drug effects in resistant contexts.²⁹⁰ More recently, targeted therapies dependent on genomic contexts, such as olaparib and BRCA1, have shown the potency of this approach.^{291,292} As such, predicting what combination of gene function loss will most adversely affect a particular disease context can broaden the use of targeted therapies.

Synthetic lethality depends on the loss of two features that are either compensatory or contribute independently to some necessary outcome. Most frequently, these predictions arise from experimental data that remove the presence of a combination of genes and their product through genomic modification or direct inhibition.^{293–295} Network approaches can derive predictions of likely contexts for drug combinations (Fig. 3.4).²⁹⁶ Where these networks differ is they do not require the same information scope if based on experimental data. The patterns developed through these results allow molecular contexts to be identified and translated to other disease states. Often

these combinations are focused on currently drugged targets or those that are at least considered druggable to ensure that any discoveries are rapidly applicable to a disease state. Using understood therapies also ensures that the mechanism of action of these combinations are most accessible to an understanding.

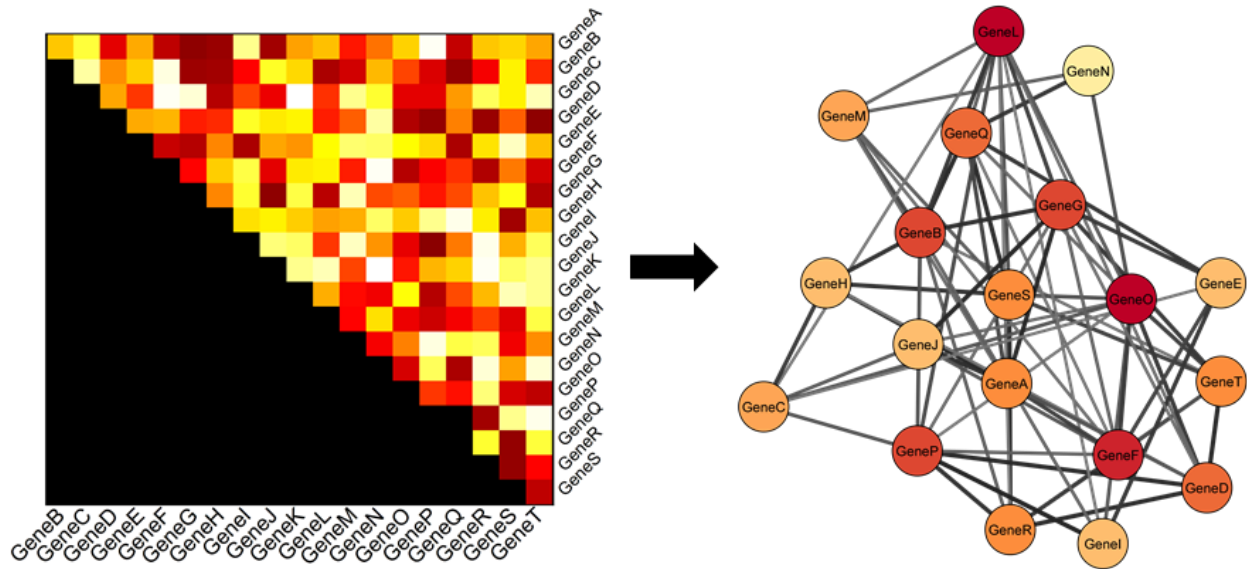


Figure 3.4: Synthetic Lethal Network; Synthetic lethal relationships are a result of targets prominence in a context and the ability of a drug to shift that prominence. This often includes genomic conditions specific to a disease to ensure selectivity. Understanding genes through their relationship using this perspective can involve interactions that would appear distant or close in other network approaches.

3.2 Rationale

The complexity of the cellular components involved in the responses to genomic stress challenges conventional means of defining the disease states' functional markers. Protein-protein interaction (PPI) networks have utility to identify pathway stress points and functional hubs within biological processes. Aberrant expression patterns and mutations have been integrated into PPI networks to show alternative network hubs indicative of disease phenotypes.^{297,298} These differentiating features from non-disease have been used to verify prognostic indicators' mechanism of action, suggest novel impacts of mutations, and identify possible drug targets.²⁹⁹⁻³⁰¹

The extensive integration of DDR, cell cycle, and DNA replication is enabled through numerous signaling proteins that compensate for each other.^{302,303} The consideration of these pathways as discrete modules within the cell does not accurately explain these systems. Importantly, many gain and loss of function mutations in these pathways are observed in patient

tumors.³⁰⁴ To identify actionable markers in these tumors, I have developed an approach that emphasizes the cell's ability to reroute and prioritize functions within these networks. These networks focus on enzymatic processes and their protein-DNA complexes as opposed to the signaling network that drives them. To understand the pathogenic modulation of these pathways, I integrate differential gene expression and topological measurements of genes to analyze multiple pathways' influences to affect the disease state.

3.2.1 Method Design and Application

The objective of this effort is to identify patterns of bias in DDR evident in different tumor genomes. As a start, gene expression data for a subset of genes within DDR, DNA replication, cell cycle, the MAPK pathway, and apoptosis are used to differentiate the tumor from other cellular contexts. Creating a PPI network from these data constructs a cell function model that is better able to assess both pathway and inter-pathway dysregulation. By considering how pathways are interconnected within a PPI network, estimates of external dependencies and redundancies influencing the overall tumor's biology can be derived. Exposing these pathways' dysregulation informs when dependencies or loss of redundancies in DDR occur and identify which forms of DNA damage will most stress a tumor subtype.

Accomplishing this through a network approach informed by differential gene expression can allow rapid individual assessment from a patient's clinical biopsy. The strategy here focuses on conserved regions that link DDR to cell cycle and apoptosis, reducing novel mechanisms' likelihood from confounding the model. A metric for evaluating these models' performance in distinguishing patient tumors resistance or responsiveness to general chemotherapy and radiation. In addition, the analysis' capacity to identify which components of a system could be targeted in the event of DNA damage stress, or resulting in cell cycle arrest, to effectively treat tumors is experimentally tested in cell models. Breast cancer cell lines were utilized as a model due to their breadth of reported features, translating to oncology practice. The connections between pathology and subtypes of breast cancers are well defined both genetically and biologically to create robust classifications of diseases emerging from the breast tissue.

3.3 Methods

This section can be divided into five themes: qualifying source data, base gene network creation and analysis, integrated metrics utilizing GO terms, gene expression, and network features, process network visualization and disruption, and model validation through *in vitro* experiments. Source data qualification and references provide reviewers with the opportunity to assess whether there are any root issues in this approach (Fig. 3.5A). Base gene network creation and analysis provides the PPI data sets to be used. Further, base gene network analysis provides fodder for the development of the more sophisticated process network (Fig. 3.5B). Integrating the GO term, PPI, and gene expression data into values describing the leverageable insights each offers in conjunction with the others creates novel pathway analysis metrics (Fig. 3.5C). These values will be visualized through the process network that seeks to describe the cell line regulation through entire pathways rather than individual genes. Synergism is itself a description of enhanced disruption within a system by targeting key genes to the overall regulation. In this section, my definition of disruption within the cell line networks is described to provide a model to examine potential synergistic relationships (Fig. 3.5D). Finally, experimental parameters are outlined for the *in vitro* validation of this model (Fig. 3.5E).

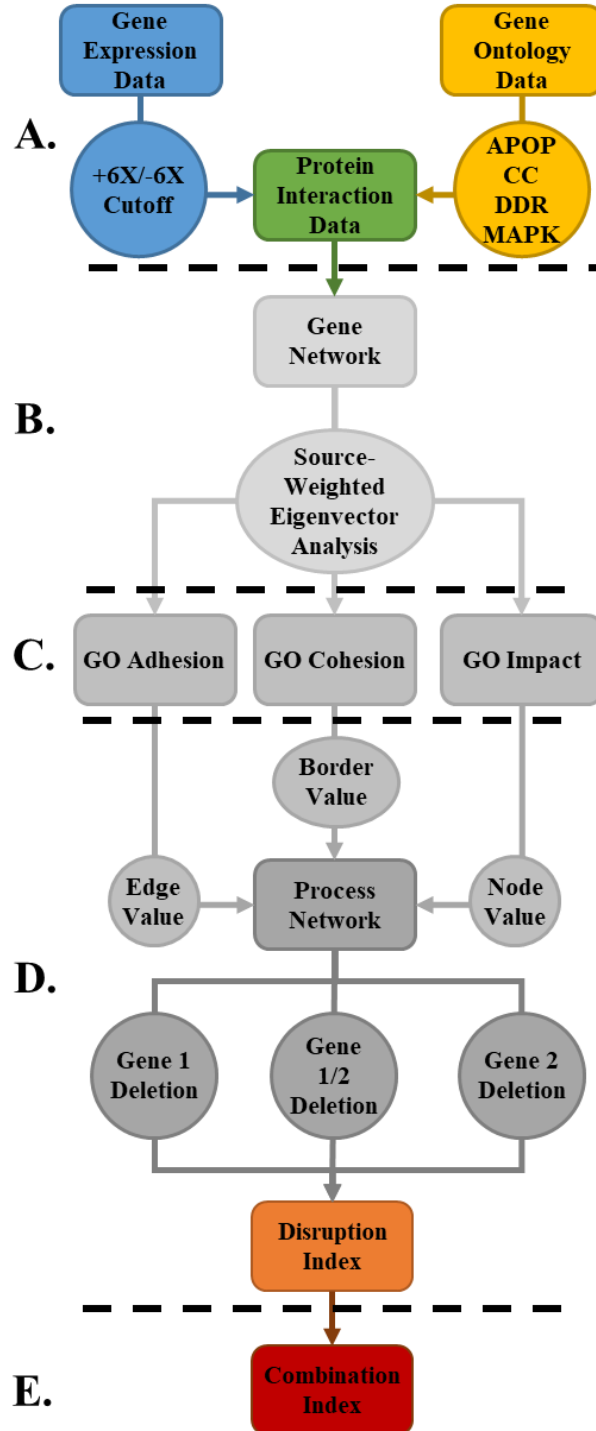


Figure 3.5: Overall Project Workflow: The initial gene network involves a limited dataset of gene product interactions and gene expressions. What follows is a set of network analyses that compound the effects of network connectivity on overall genomic dynamics that simulate treatment. *APOP* – apoptosis; excision repair; *CC* – cell cycle; *DDR* – DNA damage repair; *MAPK* – MAPK pathway

3.3.1 Data Sources

I collected data from four sources: The Cancer Genome Atlas (TCGA), Human Integrated Protein-Protein Interaction rEference (HIPPIE), the BioGRID databases, and the Broad Institute Cancer Cell Line Encyclopedia (CCLE).^{305–308} I utilized tumor genome data from TCGA, for disease networks, and the CCLE, for cell line networks, to annotate and describe PPI data collected from HIPPIE and BioGRID in breast cancer patients and cell lines. RPMI normalized breast cancer tumor gene expression data followed the “unc.edu” protocol standard of TCGA.³⁰⁹ Separations of tumor genome data into disease subtype and further by treatment outcomes were conducted before comparison to corresponding adjacent-normal tissue samples to examine fold-change expression. Cell line expression data were acquired through CCLE. PPI data were curated based on 2-step interaction networks related to a central hub protein, or protein sets, and include only interactions verified in humans and those that are considered “low-throughput” according to BioGRID. The initial filtering of the data and formation of the 2-step network and all other analyses were conducted using scripts written in RStudio. All images of networks were constructed using Cytoscape.

3.3.2 Network Creation

Both cell line and TCGA networks were created using an initial gene expression filter to identify significantly dysregulated gene sets. The next step was inclusions of all genes that are interacting with any gene from this set. Finally, all genes involving apoptosis, cell cycle, DDR, or MAPK pathways were included within this network (Fig. 3.6). Gene expression cutoffs for cell lines are defined as any gene possessing an absolute Z-score value greater than 2. In TCGA data sets, differential gene expressions were derived using fully processed, normalized, and aggregated RNA-seq data³¹⁰ and adjacent normal tissue corresponding to the same subtype. Any gene with an absolute log₂ differential gene expression value greater than 10 was included in the gene set.

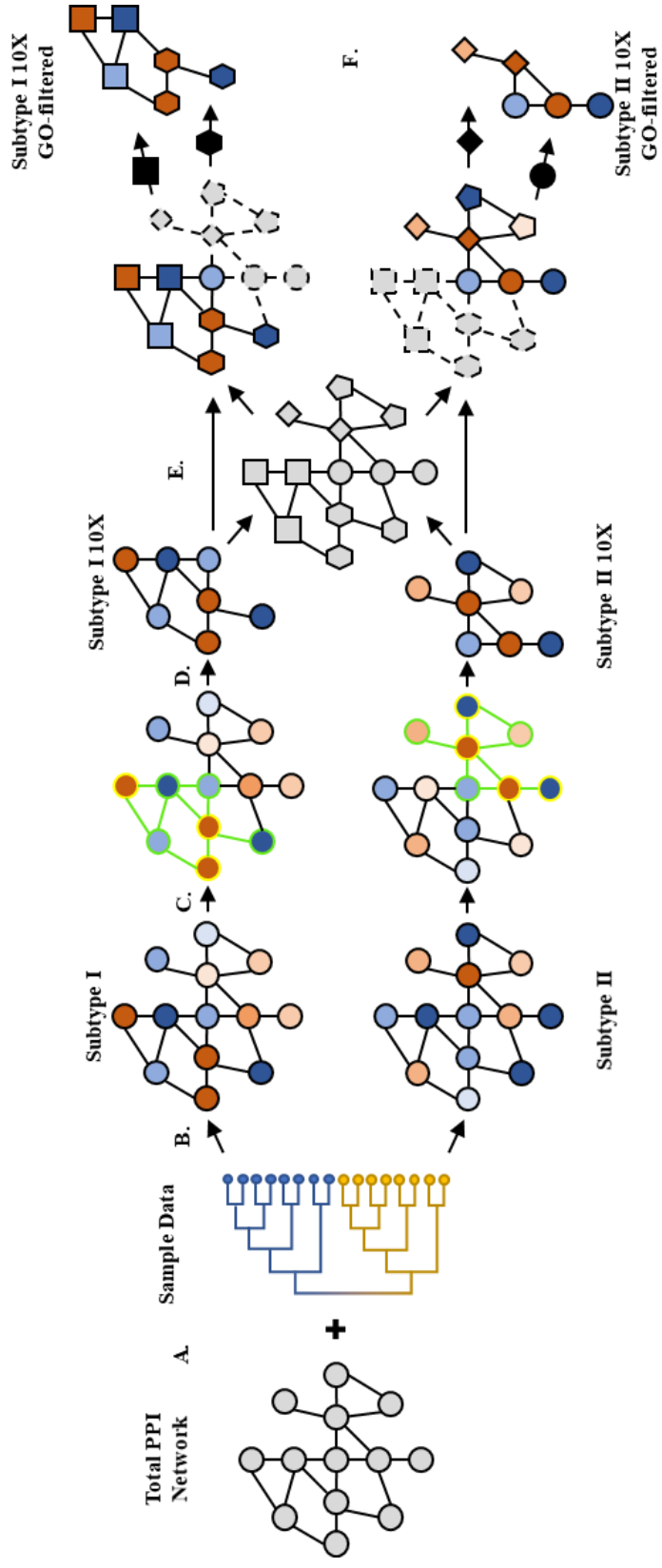


Figure 3.6: Cell Line GO Term-Specific Network Formation Process; A) After hub selection, a hub network is formed through selecting all of the interactors within two steps of the hub protein. B) Expression data for a subtype is then applied to the nodes. C) All nodes that are either over- or underexpressed above or below the threshold is then selected (yellow outline), but those that are in common between both subtypes are excluded (blue outline). D) All neighbors between the selected nodes are then used to form the new subtype specific network (green outline). E) GO terms are used to describe nodes within subtype-specific networks F) Subnetworks are analyzed for aberrant connections related to known disease phenotypes to observe functional subunits within the subtype-specific network.

3.3.3 Base Total Network Analysis

To understand differences in overall base networks, I employed several simple network metrics provided by Cytoscape.³¹¹ Comparing networks directly to one another can be difficult due to qualitative differences, however, it is necessary to understand the effect of the overall method. Each of these measurements assesses the overall connectivity and size of networks. Density is the proportion of edges that could exist compared to the amount that does exist. Clustering compares how connected a node's neighbors are to how connected they could be. Centralization of a network is a measurement of how the average node is compared to the most central node. Heterogeneity is a measurement of the variance in the number of neighbors each node possesses throughout the whole network.

3.3.4 Eigenvector Centrality

Eigenvector centrality (CE) is a measurement of the influence a node has on a network and its stress. Unlike other forms of measurements, CE focuses on the influence possessed by adjacent nodes. In this way, nodes need not have the most connections, but influential connections to achieve a high centrality value. A contrasting analysis is betweenness (CB) and degree of centrality (CD) focusing on the number of shortest paths and general connections that a node possesses. In addition, CE analysis is easily weighted by an independent value to determine the value of individual edges to the connectivity of the network. With this additional feature, gene expression can be used to determine the likelihood of an interaction to exist in a disease or cell line context.

$$CE_v = \frac{1}{\lambda} \sum_{t \in G} a_{v,t} * x_t \quad (3.1)$$

Where x_t is the centrality score of vertex t , CE_v is the centrality score of node v , λ is a constant or Weighted value, $a_{v,t}$ is the adjacency matrix, and G is the graph.

3.3.5 Impact Matrix

Not all genes possess single functions or even the same role within the same pathway. For example, WT1 shows different activity within apoptosis depending on what associations are available. EGFR generally upregulates both NHEJ and HR as a transcription factor and through direct modifications of DNA-PK and ATM. However, ATM and DNA-PK directly antagonize the other's function through phosphorylation. Being able to define a protein's role within several

pathways as either activating, facilitating, or deactivating is critical to determining the value its influence may have in each context. In each parent group of apoptosis, cell cycle, or DDR process each gene is registered as regulatory or non-regulatory and if regulatory, it is assigned either a positive or negative value. This gene assignment extends to all edges of a gene within each of these processes assessed individually during GO term analysis. To convey this information, simple matrix multiplication can be applied to each GO term calculated for.

$$H * F * R = M \tag{3.2}$$

Where H is the gene-GO term identity matrix, F is the gene-GO term influence matrix, and R is the gene-GO term regulatory matrix and M is the impact matrix (Scheme B.1).

3.3.6 GO Term Based Analysis and Parent Group Hierarchy

Gene Ontology (GO) terms were used to characterize networks by the biological processes.

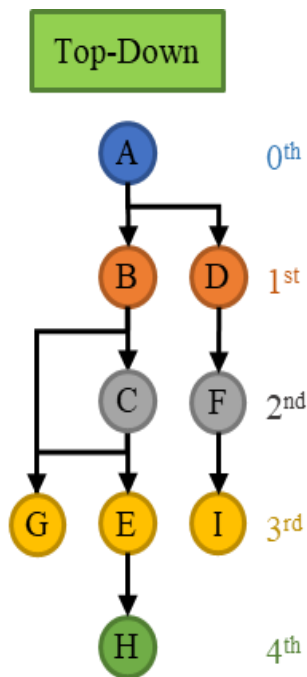


Figure 3.7: GO Term Tier; GO terms are organized in hierarchal tree structure based on the relationship between terms. Maximizing the distance a term has from the source term provides optimal overview.

These terms also provide insight to the interconnectedness of these processes in each disease subtype. GO terms were used for their high-level specificity of molecular function and biological process designation. While GO terms can be highly specific, the terms are organized in a hierarchy that forms a tree-like structure from the subsets of subsets. I have annotated this structure with a “Tier” metric that describes the distance a term has from one of the three most general terms: Biological Process, Cell Compartmentalization, and Molecular Function (Fig. 3.7). This structure allows ranking of terms by relative specificity and evaluation of their relative position in the tree. A Tier system ensures that when comparing GO terms directly to one another they are of equitable specificity (Fig. 3.6). Further, I use three GO term analyses to characterize cell line-specific networks to create subnetworks from: GO Impact, GO Cohesion, and GO Adhesion. Each of these GO analysis techniques utilizes an interaction matrix (Scheme B.2). An interaction matrix has all of the nodes as rows and columns and at intersections where there is an edge, a value of 1 is entered. This value can also be a calculated value, such as CE or gene expression.

3.3.6.1 GO Impact

GO Impact is defined by the number of times that a protein-protein interaction involved the GO terms listed. This term allows rapid characterization of which pathways and functions are most common within a network to understand the emphasized and deemphasized functional interactions. The GO Impact of GO term g can be defined as:

$$\sum_j M * I_{i_g j} = GI_g \quad (3.3)$$

Where M is an impact matrix, I is an interaction matrix (Scheme B.2) and i is an interactor which possesses the GO term g and j are all other interactors. The sum is then taken of all values in the interaction matrix that have all genes that possess GO term g . This analysis differs from GO enrichment by weighting the GO terms that have more interactions based upon aberrant gene expression.

3.3.6.2 GO Cohesion

GO Cohesion measures the amount gene products possessing the same GO term interact. This term allows for understanding how much the GO Impact value is dependent purely on interactions of gene products that share the same GO term. Independently, this measurement capably ranks the dysregulation within a pathway and how much this affects the network overall. The GO Cohesion of GO term g can be defined as:

$$\sum_{j_g} M * I_{i_g j_g} = GC_g \quad (3.4)$$

Where M is an impact matrix, I is an interaction matrix (Scheme B.2) and i is an interactor which possesses the GO term g and j is any interactor of i that also possess GO term g . The sum of the values within I that fit this description are then considered the GO Cohesion (GC_g) for that term.

3.3.6.3 GO Adhesion

GO Adhesion is a measurement of how much the gene products of two different GO terms interact. This abbreviates the amount that the dysregulation of one pathway is linked through protein-protein interactions and Weighted the gene products that possess more interactions with the gene products of different GO terms. The GO Adhesion of GO term g and h can be defined as:

$$\sum_{j_h} M * I_{i_g j_h} = GA_{g,h} \quad (3.5)$$

Where M is an impact matrix, I is an interaction matrix (Scheme B.2) and i is an interactor which possesses the GO term g and j is any interactor of i that possess GO term h . The sum of the values within I that fit this description are then considered the GO Adhesion ($GA_{g,h}$) for that term.

3.3.7 Process Network Creation

I analyzed the effects of the disease on DNA damage repair pathways as well as intrinsic apoptotic signaling and cell cycle signaling due to the integrated nature and disease/therapeutic implications therein. GO terms were used to assign genes to pathways as well as distinct steps in signaling. Gene products involved in the negative regulation of any of these pathways were analyzed separately to distinguish their effect. Both gene expression enrichment as well as weighted CE measurements were used to determine changes in pathway regulation. Further, gene products indicated as hubs via centrality were assessed for their connections to other pathways to determine interpathway influence. The GI_g measurements utilizing weighted CE measurements in the interaction matrix were used to create sets of genes. To further distinguish whether GI_g values were caused by gene sets that were in common between two GO terms or focused on a single GO term, GI_g analysis uses gene sets that contained all possible genes related to a GO term that was not shared between two GO terms. Comparing the GI_g values from these two approaches formed the values used for the individual nodes.

The $GA_{g,h}$ analysis provided values to assess the connectivity of processes to one another which were used as edges of a Process Network. The GC_g analysis was utilized to determine which edges were self-regulatory and were measured separately from external regulation by other processes. This disease network provides an estimate of how much a process may contribute to the system's dysregulation. It also provides perspective on the influence of a single process are from internal or external dysregulation.

3.3.8 Somatic Mutations

Utilizing somatic mutations (SM) data to further stratify my data allows for *in silico* modeling of some understood loss-of-function genotypes that have been identified in the disease. A key set of mutations that significantly affect DDR pathways are mutations in BRCA1 and

BRCA2 genes. Loss-of-function mutations in these genes lead to a loss of the HR pathway, disrupting a key player in DSB repair. Categorizing tumor data by SM presence in subtype specific networks can show changes in both disease subtype networks and their subnetworks. This approach can reveal the identity of other network sections affected by the SM pathway by separating samples within a subtype based on mutation status in the relevant gene. These mutations must not be silent modifications with verification as a loss-of-function mutation. Once their mutation status separates samples, the gene expression analysis is completed as it was for the subtype originally. Comparison of expression is then conducted between the wildtype samples and those that bear a loss-of-function mutation to adjacent-normal tissue gene expression.

3.3.9 Network Disruption

The network disruption caused by the loss of a gene was measured through eliminating a gene product from the initial dataset before rebuilding the network. Gene removal provides insight into the importance of a node to total network connectivity as well as to individual pathways. Further, new nodes could emerge as hubs of influence and would determine new connectivity to the system. Disruption was scored by assessing the loss of influence of related systems and weighted by the impact on the cell line's ability to prevent apoptosis progression. Proper DNA damage repair or progression successfully through cell cycle without significant delays are the two primary means of preventing apoptosis. Therefore, disruption is a measure of the changes of key pathways' influence and the amount a compensatory factor is possible. A drug combination's success is observed through the simultaneous elimination of a gene product from the initial dataset and observing the overall disruption. Disruption was measured through the relative change in the centrality of nodes surrounding the deleted gene and their effect on the overall process.

$$\sum_{j \in \mathcal{N}_i} \frac{\Delta c_{ij}^g}{c_{ij}^{g*}} = DI \quad (3.6)$$

Where Δc_{ij} is the change in centrality of neighbor j or deleted node i and c_{ij}^* is the original centrality measurement of neighbor j of deleted node i .

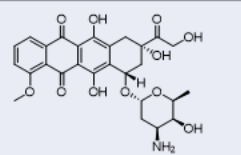
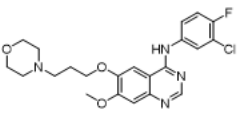
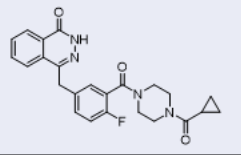
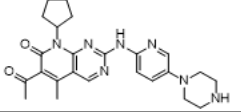
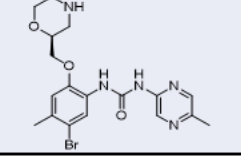
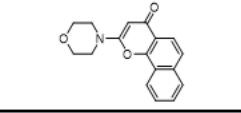
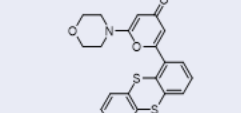
Table 3.1: Descriptors of Network and Experimental Evaluation of Synergism and Disruption

Quantitative Metrics and Terms	Abbreviation	Description
Degree Centrality	CD	the number of edges connected to this node
Betweenness Centrality	CB	the extent to which a node lies on paths between other nodes
Eigenvector Centrality	CE	the influence of a node derived by the influence of the nodes that it shares an edge with
Impact Matrix	M	matrix that transforms node values by their presumed effect on cell survival
GO Impact	GI_g	measurement of the overall influence of GO term g in the network
GO Cohesion	GC_g	measurement of the connectivity between genes possessing the GO term g
GO Adhesion	$GA_{g,h}$	measurement of the connectivity between genes possessing the GO term g and genes possessing the GO term h
Combination Index	CI	synergism derived from drug combination experiments
Disruption Index	DI	predicted synergism derived from process networks
Processivity	-	network values that represent intraregulation of a pathway
Influence	-	network values that represent interregulation of two pathways

3.3.10 Combinatorial Drug Treatment

To evaluate predicted synergism in breast cancer, drug combinations of well-understood inhibitors of ATM, DNA-PK, PARP1, PCNA, EGFR, CDK4/6, and CHK1 were all utilized. These inhibitors are used to target the MAPK, HR, NHEJ, and G1/S checkpoint pathways (Table 3.2). Different levels of dysregulation in these pathways occur in breast cancer diseases, including the

Table 3.2: Small molecule PCNA inhibitors to be evaluated in this study.

Compound	Structure	Target	Process
Doxorubicin		TOP2A	Damaging Agent, Double-Strand Break
Gefitinib		EGFR	Proliferation, DNA Damage Response
Olaparib		PARP1	Alternative Non-Homologous End Joining
Palbociclib		CDK4/6	G1/S Checkpoint
Rabusertib		CHK1	Homologous Recombination
NU7026		DNA-PK	Classical Non-Homologous End Joining
KU-55933		ATM	Homologous Recombination

cell lines selected in the Cell Culture section below. ATM is an early HR deactivator and DNA damage detection activator, and I used the KU55933 inhibitor for ATM's selectivity over ATR and PI3K inhibitors.³¹² DNA-PK is central to cNHEJ and the NU7026 inhibitor is specific for DNA-PK over numerous nuclear kinases, including AKT.³¹³ EGFR is one receptor tyrosine kinase responsible for the activation of the MAPK pathway. EGFR also has nuclear functions necessary for HR and NHEJ activation, which are not kinase dependent. PCNA, as outlined in earlier sections, has substantial implications in DNA replication and cell cycle processivity.³¹⁴ I am utilizing T2AA as it is the most studied selective PCNA inhibitor to date.²²⁰ The PARP1 inhibitor olaparib, an FDA-approved treatment of breast cancer, is used due to its specificity for

PARP1 and aNHEJ over other PARP-related functions directly tied to apoptosis.³¹⁵ CDK4/6 is a G1/S checkpoint protein vital to cell cycle progression, and the inhibitor palbociclib is another FDA-approved treatment of breast cancer.³¹⁶ CHEK1 is required for connecting DNA damage repair processes to cell cycle and apoptosis progression and was inhibited with rabusertib, which has been used in several phase II studies.³¹⁷ Combinations of these inhibitors will allow the survey

of several pathways implicated in multiple breast cancer subtypes and their interconnectedness. Combinations are all analyzed utilizing the Chou-Talalay method as before to indicate their combination index (CI).

3.3.11 Cell Culture

The human breast cancer cell lines HCC1937, MCF7, MDA-MB-231, MDA-MB-436, MDA-MB-468, and SKBR3 were purchased from the American Type Culture Collection (ATCC). MDA-MB-231 and SKBR3 were cultured in DMEM supplemented with 10% FBS. HCC1937 and MDA-MB-468 were cultured in DMEM supplemented with 5% FBS. MDA-MB-436 was cultured in L-15 supplemented with 10% FBS, 10 $\mu\text{g/ml}$ insulin, and 16 $\mu\text{g/ml}$ glutathione. MCF7 were cultured in DMEM with 10% FBS and 10 $\mu\text{g/ml}$ insulin. Incubation of HCC1937, MCF7, MDA-MB-231, MDA-MB-468, and SKBR3 cell cultures were conducted at 37° C and 5% CO₂ in a humidified incubator. Incubation of MDA-MB-436 was also at 37° C but with no gas exchange. All cells were harvested as cells reached 70-80% confluency utilizing Trypsin-EDTA (0.25%) and were split 1:10 for cells with a doubling time close to 24 h or 1:5 for cells with doubling times greater than 24 h. Cells with doubling times below 24 h had media replaced every 2-3 days or 3-5 days for cells with doubling times greater than 24 h (Table 3.3). Cells were kept under 15 passages to prevent the development of novel genomic changes.

Table 3.3: Cell Line Properties; Doubling times were determined after culturing cells for 2-3 passages as this was more accurate to cell growth speed during assays.

Cell Line	Type/Subtype	Mutations	HR Status	Growth Conditions	Doubling Time (h)
HCC1937	Basal-1	BRCA1, PTEN, RB1, TP53	+	5% FBS, DMEM, 5% CO ₂	~54
MCF7	Luminal A	CDKN2A, PIK3CA	+	10% FBS, DMEM, 5% CO ₂	~24
MDA-MB-231	Mesenchymal-like	BRAF, CDKN2A, KRAS, NF2, TP53	+	10% FBS, DMEM, 5% CO ₂	~21
MDA-MB-436	Basal-1	BRCA1, RB1, TP53	-	10% FBS, L-15, 10 µg/ml insulin, 16 µg/ml glutathione	~36
MDA-MB-468	Basal-1	PTEN, RB1, SMAD4, TP53	+	5% FBS, DMEM, 5% CO ₂	~22
SKBR3	HER2	PIK3CA, TP53	+	10% FBS, DMEM, 5% CO ₂	~30

3.3.12 Cell Proliferation

The same MTT assay was utilized here as in Chapter 2 with the additions of cell lines mentioned previously. Only changes made are including additional cell lines and inhibitors listed previously in this section.

3.4 Results

The results section can be divided into three subsections: initial network creation and analysis (Fig. 3.8A-B), comparative univariate enrichment (Fig. 3.8C), and process network

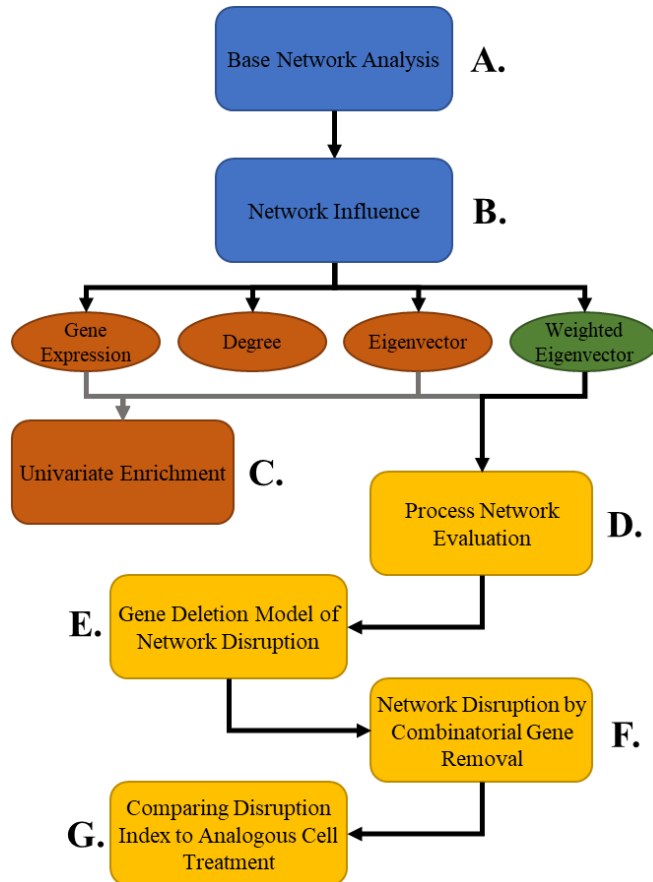


Figure 3.8: Results Section Summary

creation and evaluation (Fig. 3.8D-G). Following the parameters laid out in section 3.3.2, networks were made from each cell line (Fig. 3.8A). Basic network analysis of the entire network was used to compare the networks on a global scale. As this is not sufficient resolution to determine differences in disease response to therapeutics, multiple strategies were assessed to identify node influence within the network (Fig. 3.8B). The three variables that provide sufficient data for enrichment studies, gene expression, CE, and source-weighted CE were then separated for further analysis (Fig. 3.8C). Univariate enrichment was found to be insufficient to derive disease features consistent with clinical and experimental observations. Process

Networks were created according to section 3.3.7 (Fig. 3.8D). These were evaluated to see if they are able to describe disease features than univariate enrichment more accurately. Network disruption by node removal was compared to a LOF mutation (Fig 3.6E). Network disruption by combinatorial node removal was then used to simulate combinatorial drug treatment. This method's performance was first compared to known synergistic interactions between genomic features and a monotherapy, BRCA1 $-/-$ and PARP1 removal. Further evaluation of gene removal as a model for inhibition was accomplished using synergistic drug targets, PCNA and PARP1 removal (Fig. 3.8F). Finally, synergism predictions through our disruption model were compared to combinatorial drug treatment to validate our model (Fig. 3.8G).

3.4.1 Initial Differential Gene Expression Networks

Differential gene expression (DGE) has been utilized to interpret pathway activation and disease pathophysiology for decades.^{318–321} As tumor genomic data availability has increased so has the applications in defining signatures of cancer diseases such as the PAM50 criteria.⁹⁴ DGE often relies upon a priori knowledge of gene sets that determine either pathway or disease features.^{322,323} These gene sets include indicator genes that often show differential expression and often include transcription factors and signaling enzymes implicated in the process.^{324–326} These observations are limited to well-understood biology but prevent large sets of genes whose expression does not change from masking pathway activation. Instead, the work here has selected a subset of genes within pathways under examination by evaluating only highly dysregulated genes and genes directly interacting.

To select a gene subset for initial network creation, I utilized GO terms focusing on pathways known to be highly dysregulated in tumors: apoptosis, cell cycle, DNA damage repair, and the MAPK pathways.^{43,51,160,327–329} To focus on these pathways, I first evaluated cell line dysregulation to produce a baseline for investigation. DGE was utilized to create a subset of genes for PPI networks using the approach detailed above (Fig. 3.5). A network was created for each cell line used in this study (Fig. 3.9). These networks varied significantly in the number of nodes and edges (Table 3.4) with the most variations in number of nodes in the cell cycle and MAPK pathways. A similar amount of DDR and apoptosis-related genes were present in all cell line networks suggesting similar amounts of gene dysregulation in these processes. Density and heterogeneity do not show similarly large differences suggesting a similar level of connectivity despite the size differences. The range of clustering within networks offers different levels of interconnectivity between subnetworks within the system. In the absence of pathway specific measurements, it is unclear whether specific pathways show high interconnectivity while others show low levels or if they all generally show similarly low levels. Overall, it is clear from these results that these networks are diverse and can easily distinguish the different cell lines.

Table 3.4: Cell Line Network Summary Statistics. Density is the proportion of edges that could possibly exist compared to the amount that do. Clustering compares how connected a node's neighbors are to how connected they could possibly be. Centralization of a network is a measurement of how the average node is compared to the most central node. Heterogeneity is a measurement of the variance in the number of neighbors each node possesses throughout the whole network.

Cell Line	Nodes	Edges	Density	Clustering	Centralization	Heterogeneity
HCC1937	434	5330	0.04	0.248	0.241	0.938
MCF7	635	9383	0.032	0.285	0.29	1.094
MDA-MB 231	357	4153	0.045	0.31	0.266	0.987
MDA-MB 436	788	12555	0.028	0.223	0.257	1.038
MDA-MB 468	805	12187	0.027	0.254	0.253	1.089
SKBR3	409	5450	0.044	0.296	0.242	0.981

3.4.2 Graphical Representations of Gene Influence

Using the PPI data and the GO term limitations, I created a subset of genes to analyze. Gene enrichment through expression is a general approach to identifying which pathways are active or dysregulated in a disease state. It is also helpful to create networks to describe areas of dysregulation surrounding differentially expressed genes.^{296,301} However, the parameter that is used to assess a gene's influence on the system must be selected based on what outcomes are being measured. All approaches will have strengths and weaknesses based on what values they use to understand influence. We will assess gene expression's ability, CD, weighted and unweighted CE to designate gene influence in a system.

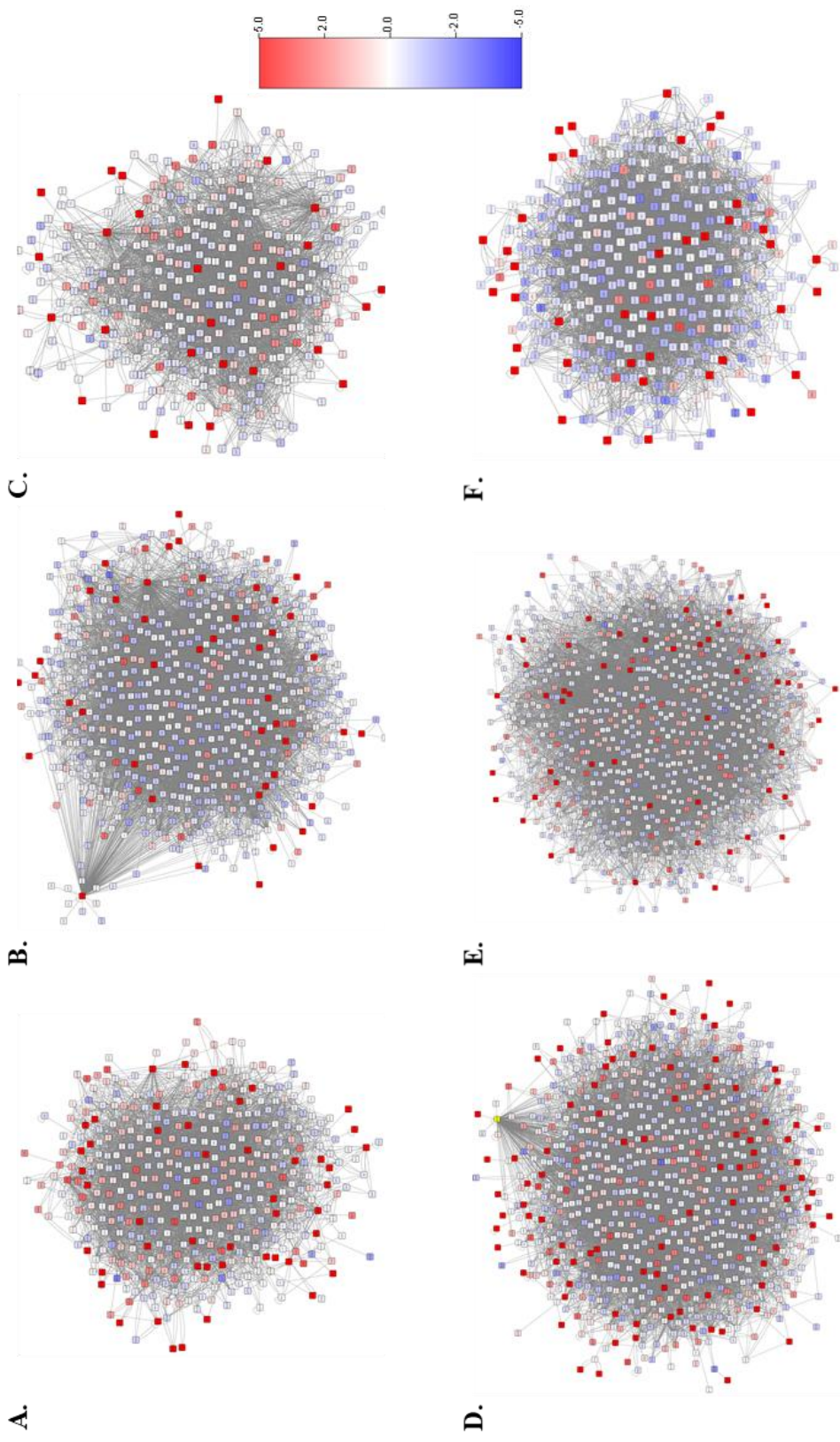


Figure 3.9: Initial Cell Line Networks; These networks were created through a $\pm 6X$ differential expression threshold. Each cell line network was then focused further on MAPK, DNA damage repair, cell cycle, and apoptosis pathway related genes. A. HCC1937; B. MCF7; C. MDA-MB-231; D. MDA-MB-436; E. MDA-MB-468; F. SKBR3;

3.4.2.1 Gene Expression

Gene expression has been the most used variable to denote the relative influence of genes in a system. This approach can be used with a PPI network to give topological markers independent of network structure identifying regions of interest. (Fig. 3.8A) A gene product's activity does not always correlate to either its own expression or to the expression of all of their interactors.³³⁰ This is because not all interactors contribute towards all of a gene product's functions. It is also true that a single interactor can be sufficient to activate a gene product. It can also be the case that the loss of one gene product allows another gene product to create a protein complex that contributes to the disease state.³³¹ For this reason, pathway analysis often utilizes the position a gene product has in the pathway to augment the significance in change of gene expression.³³² When genes are analyzed in a PPI network context, the significance of a gene's expression can be understood by an increased influence. Therefore, a gene that shows a ten-fold increase in expression that only possesses one interaction is not as disruptive as a gene that only shows a five-fold increase in expression with fifty interactors. Utilizing network features dependent on the quality of interactions ensures that the influence a gene product has within the network is not merely reliant on its own properties, similar to enrichment.

3.4.2.2 Degree Centrality

The amount any one node influences the network is known as centrality. Simple network analysis to assess a node's influence is the number of edges it possesses, known as the node degree or CD.³³³ (Fig. 3.8B) In networks of fewer than 100 nodes, CD can effectively identify one node that could modify most nodes in a network.³³⁴ CD does not provide a large number of significant nodes as the distribution of edge count is not evenly distributed. The graph only highlights a few nodes towards the center of the network and provides no additional groups to aid in analysis.

3.4.2.3 Eigenvector Centrality

In larger networks, such as those I have created, there will likely be multiple hubs and clustering around those hubs. Understanding the amount, a node contributes, both to its cluster and the overall network, becomes a more difficult question the larger the network is. Assuming that any node with more interactions is more influential ignores the possibility of a node with few

highly influential interactors having more significant influence. CE was selected as my primary centrality measurement due to its ability to prioritize nodes based on their connections to other important nodes (Fig. 3.8C). This approach emphasizes connectivity that the entire system is dependent upon. Like many other centrality measurements, CE will often correlate with CD as it utilizes the total number of edges a node has in its calculation. Network centrality can provide an alternative metric to understand a gene's influence on a system.

3.4.2.4 Source-Weighted Eigenvector Centrality

Leveraging the gene expression data through a centrality measurement creates a new metric that identifies hubs and enhances neighbors regardless of their expression level. I utilized a weighted CE analysis that scores an edge according to the source node's differential expression, including dependence on the source node's expression, but not the target node (Fig. 3.8D). There are several practical differences between this approach and simple eigenvector analysis. Firstly, a weighted CE greatly reduces the influence of under-expressed nodes and allows other hubs to emerge that take their place within the network structure. The consequence is a reduction in the edges' score that leaves the node and does not directly lower its interactors' centrality. Secondly, highly overexpressed genes enhance themselves and elevate the nodes directly connected to them, creating clusters of multiple influential genes.

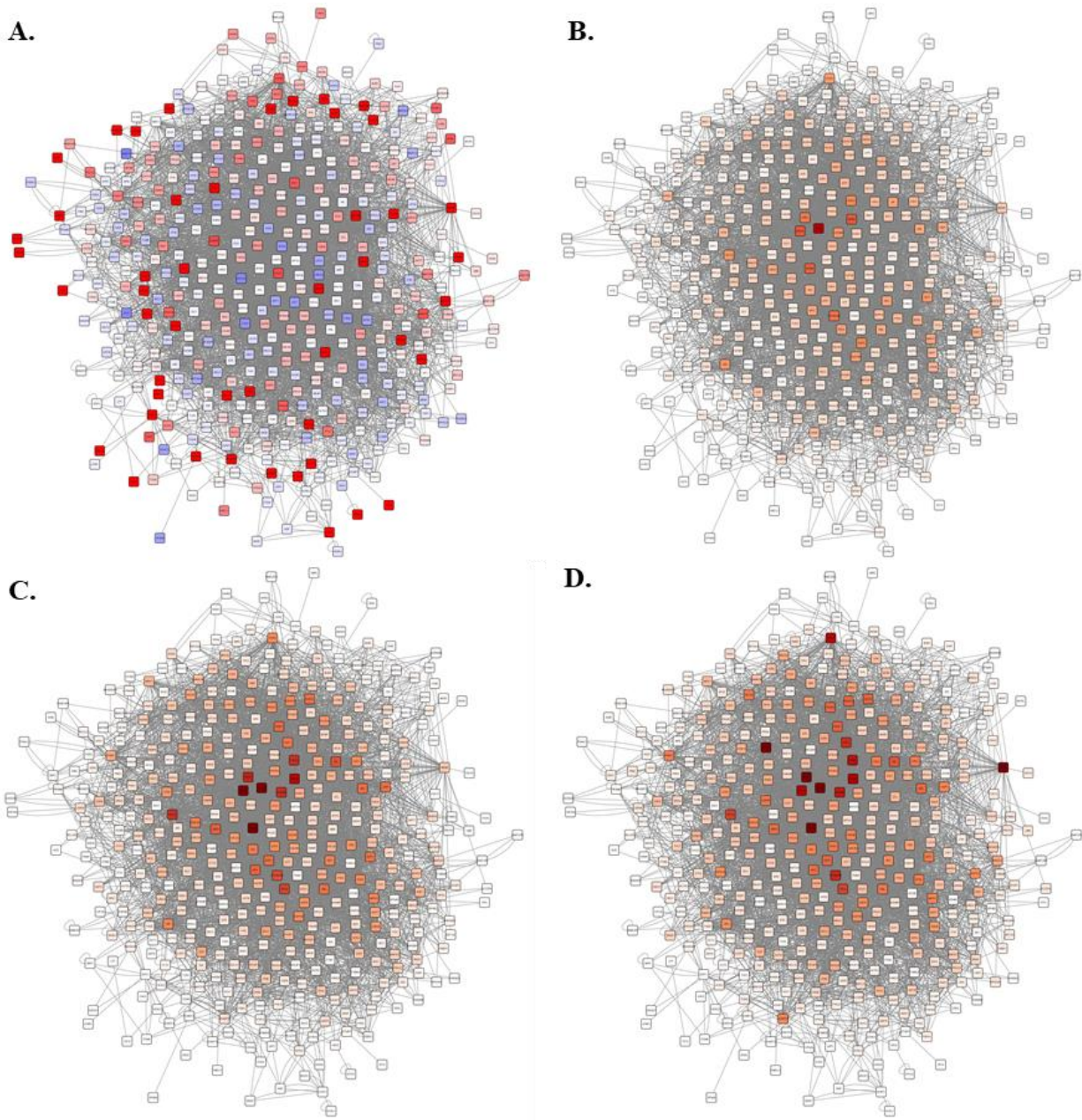


Figure 3.10: Node Attribute Analysis; The HCC1937 network was overlaid with either differential gene expression, node degree, eigenvector, or source-weighted eigenvector values. A) Differential Expression, B) Node Degree, C) Eigenvector Values, D) Weighted Eigenvector Values

3.4.2.5 Enrichment through Gene Expression Compared to Centrality

I performed pathway analyses of the subsets of genes within the networks using gene expression, CE, and source-weighted CE. (Fig. 3.9) I assess the capability of these variables to capably represent biological features of the cell line through enrichment. Some methods provide curated gene sets of indicator genes, but I avoid this technique as many gene functions can be dependent on other genomic features unique to the disease state. With this in mind, I will establish the limitations of univariate enrichment to discern biological features in these cell lines.

3.4.2.6 Gene Expression Analysis of Base Networks

When only examining gene expression, distinct signatures for each cell line are observed (Fig. 3.9A). The HCC1937 network shows extensive overexpression of genes contributing to DNA fragmentation and the execution phase of apoptosis. DNA replication is also significantly enhanced along with base-excision repair (BER), HR, and interstrand cross-linking repair (ICL). These repair pathways are often active in the S phase alongside DNA replication.^{335–337} MCF7 shows a significant increase in BER, and the execution phase of apoptosis and underexpression in DNA replication and mismatch repair (MMR). Overall, MCF7 shows far less dysregulation in these pathways.^{338–340} MDA-MB 231's sees the greatest modulation of the MAPK pathway, which matches its BRAF/KRAS mutation status.^{341,342} MDA-MB 231 also shows similar overexpression of ICL, but without the DNA replication pathway's dysregulation.^{343,344} The MDA-MB 436 network shows general dysregulation across all DNA damage repair pathways and possesses significant enrichment in genes related to the G2/M checkpoint and apoptosis's execution phase. This cell line is notably resistant to single-strand damaging agents, such as cisplatin, consistent with these results.^{344,345} MDA-MB 468's network shows the greatest enrichment of NHEJ, DNA replication, and the G2/M checkpoint. What is noticeably absent is an enrichment of MDA-MB 468's HR pathway known to be highly active.³⁴⁶ SKBR3's network shows primarily down-regulation surrounding the late steps of cell cycle proceeding cytokinesis.^{347–349} They also show a strong down-regulation of DNA fragmentation. SKBR3 is a HER2-enriched cell line that dysregulates upstream effectors and generally prioritizes cell survival mechanics preventing apoptosis.^{350–352}

Gene expression enrichment does capably highlight a number of standout pathways in each cell line. The overexpression of a number of pathways does not translate to overactivation as some pathways are fully internally regulated. HR in MDA-MB 468 is a good example of this. Also, relative gene expression values are also able to be compared across cell lines. Gene expression does not capably demonstrate possible influence on the network as a whole. This is important as many pathways show a similar level of overexpression, but this does not indicate whether these pathways are made overexpressed by other features or are the source of dysregulation. There is also the matter of MCF7 and MDA-MB 231 cell lines not showing a large number of dysregulated pathways making it difficult to differentiate pathways further. A reduced number of enrich pathways is often mitigated by curating gene sets to prevent the measurement of genes whose expression is not as dynamic. To maintain a large data set similar to what we started with requires a means of weighting gene expression to ensure influential nodes and their pathways are recognized space.

3.4.2.7 Eigenvector Centrality Analysis of Base Networks

When examining the same pathways using only the CE measurements, I observe different results (Fig. 3.9B). The HCC1937 network shows a similar focus on the apoptotic execution and DNA fragmentation phases. However, BER with NHEJ and NER are more influential in this network than HR and ICL. This result is not consistent with reported characteristics of the cell line.^{243,353} Also, the G1/S and G2/M checkpoints are emphasized in the network analysis.³⁵⁴ The MCF7 network shows a similar emphasis in the execution phase of apoptosis and BER as it did in the expression enrichment. However, I see changes in the mitochondria-related apoptosis processes^{355,356}, G1/S³⁵⁷, MMR³⁵⁸, NHEJ³⁵⁹, and NER.³⁶⁰ Hormone-related dysregulation of the G1/S pathway is consistent with a Luminal A tumor.^{361,362} These repair pathways are typically active in stressed environments that created in rapidly dividing tumor cells.³⁶³ The MDA-MB 231 network shows an extreme focus on BER and NER not indicated by the gene expression.^{344,364} While HR is less central than these two; it is still significant.³⁴⁶ Using the centrality measurement, the control of the execution phase and mitochondrial function are also emphasized.^{365,366} Lastly, MAPK is still influential and could explain the DDR pathways I see emphasized in this analysis.³⁴¹ The MDA-MB 436 network may not show the same extreme focus on a few pathways as other

cell lines. Still, it maintains a focus on the execution phase of apoptosis³⁶⁷ and BER and NER³⁶⁸, similar to the other cell lines, to control the stress of cell proliferation. The MDA-MB 468 appears similar in construction to the MDA-MB 436 network, which is unexpected due to their drug sensitivity and proliferation rate differences. The emphasis remains on the execution and mitochondria phases of apoptosis with NER and NHEJ.^{369,370} Lastly, SKBR3 is very differently represented in network analysis compared to just gene expression analysis. A decisive influence of BER and NER along with the other DDR pathways is observed.³⁷¹⁻³⁷³ There is also extensive influence in the G1/S and G2/M checkpoints^{374,375} alongside the execution and mitochondria phases of apoptosis.^{376,377}

Overall, the CE values paint a very different picture than the gene expression. Some of the observations made are consistent with features determined by gene expression. The cell lines appeared to have several trends in the DDR pathways influential, despite several studies detailing otherwise. By focusing on these pathways, I have guaranteed significant overlap in the nodes involved, which likely contributes to the trends I observed. Using only centrality will not be sufficient to differentiate cell lines. In addition, some of the observations made through simple CE did not faithfully represent the cell lines' features. Much of this occurs through a lack of emphasis rather than false emphasis. Still, the analysis requires improvements to provide an accurate model of cell activity.

3.4.2.8 Source-Weighted Eigenvector Centrality Analysis of Base Networks

The third analysis uses the source-weighted eigenvector centrality (Fig. 3.9C). The HCC1937 network distinguishes itself as being the most dysregulated network. The entirety of apoptosis shows significant influence in this network in addition to cell cycle checkpoints and arrest. The BER, MMR, NHEJ, and NER DDR pathways are the focus of this network. The MCF7 network shows few definite influences with the execution phase of apoptosis, and the BER pathway is likely to influence the processes. The MDA-MB 231 network mirrors the HCC1937 network with the only significant differences being that only the execution and mitochondria phases of apoptosis are influential. This network also has a reduced focus on the DNA replication pathway. The MDA-MB 436 network shows similar dispersion to the MCF7 network. The execution phase of apoptosis and ICL appear to be influential only as secondary pathways. No

distinguishable pathways are identifiable in the MDA-MB 468 network using this method of analysis. The SKBR3 network again shows a distinct pattern of influence with a similar DDR pathway profile as HCC1937 and MDA-MB 231. The SKBR3 network also significantly emphasizes MAPK compared to the others, focusing on the execution phase and an impressive lack of focus on DNA fragmentation.

There are several issues with using centrality enrichment alone. The MCF7, MDA-MB 436, and MDA-MB 468 networks capably show this approach's limitations with larger networks. These networks are close to double the size of the other three networks, and a simple enrichment analysis was insufficient to distinguish what processes influence the system. Upon further investigation, a significant issue in each of these networks was one node being incredibly dominant: EGFR in SKBR3, ESR1 in MCF7, and SQSTM1 in MDA-MB 436. CE is necessarily relative and determined for the entire network making the maximal central node value of 1. The remaining nodes show similar levels of centrality by comparison, which allowed the overall network centrality to appear normal. Lastly, BER seems to be a dominating force in essentially all the breast cancers. While it is a vital repair pathway, I found that many other DNA damage repair pathways share BER genes when examining the genes comprising these pathways. Much of the early detection genes of DNA damage in BER can also activate additional DNA damage responses. For this approach to be viable, accounting for the compensatory factors for pathway redundancies will need to feature either through constraining the gene subsets to limit network size or to analyze each network in total and in parts.

3.4.3 Cell Line-Specific Process Networks

Since simple enrichment was incapable of defining the system to the required resolution, I derived a metric to survey the connectivity of processes to one another. The basic hypothesis for why simple enrichment I performed failed to account for multiple features of these networks: they have several nodes in common, some nodes will dominate the entire network, and some processes have several nodes in common. Additional metrics were devised to counter these effects and allow an in-depth analysis of interactions within the key cellular processes of interest. $GA_{g,h}$ was derived to measure the number of edges between processes to assess interpathway regulation. GC_g was derived to assess how much a process regulates itself. Using these two calculations, I can

distinguish between edges and nodes shared between processes rather than seeing them as a homogenous group. GI_g is a means of focusing source-weighted CE analysis by whether nodes connect to one or more cellular processes. The analysis design allows nodes that are important to a process rather than the entire network to be still prominent. Each of these features, as mentioned above, link to standard network features of edges, self-loops or node borders, and node values themselves. Nodes and edges that serve distinct roles in a process will be evaluated separately, preventing the gross overlap and refocusing the network analyses on smaller groups of nodes in their total network context.

HCC1937 Process Network

Using these three values, I constructed descriptive process networks to replace the enrichment analysis used previously. These more detailed networks are compiled in the Appendix (X?). The HCC1937 Process Network shows a very different set of key interactions than the simple enrichment analysis (Fig. 3.11A). HCC1937 does not have a competent BER pathway to combat oxidative DNA damage.³⁷⁸ The enrichment studies presented BER as the most influential DDR pathway to cell line dysregulation. When the roles of genes within this subset are separated, this pathway is less connected to other processes and its own regulation. DNA damage repair abnormalities in HCC1937 revolve around the loss-of-function (LOF) mutation of BRCA1 and the ability of HCC1937 to maintain a functional HR pathway despite this. Previous work by others show that a combination of NER and ICL is used to compensate for the HR pathway preventing sensitivity to PARP1 inhibitors.^{379,380} It is also important to note that HR is strongly tied to the G1/S checkpoint in this cell line, as it is frequently in TNBC cell lines.^{381,382} The G1/S-HR connection is clearly on display in this network with both internal and external enhancement of these pathways. Further, an overactive MMR pathway tied to a MAPK activation is consistent with prior observations for this cell line.^{383,384} Lastly, HCC1937 is a slow-growing cell line that allows continued proliferation through dysregulation of G1/S and G2/M checkpoints to persist growth.^{385,386} This characteristic is evident in my network, and the other LOF mutations of RB1, BRCA1, and PTEN all tied to these checkpoints. Unlike KRAS and BRAF GOF mutations that increase proliferation rate to ensure proliferation, these LOF mutations reduce the likelihood of cell cycle arrest. This feature aligns with the concept that a cell cycle checkpoint can be highly dysregulated, without increasing cell proliferation rate.

MCF7 Process Network

The MCF7 network shows a completely different profile with the size of the network being beyond my ability to make observations (Fig. 3.11B). A key feature that is observed indirectly by this network is the extreme overexpression of ESR1.^{387,388} Unlike in the previous attempt using centrality alone, I can observe the downstream effects using the combination of the three defined parameters, $GA_{g,h}$, GC_g , and GI_g , A. Many of the features can also be explained by the gain-of-function (GOF) mutation to PIK3CA, which is vital MAPK and cell survival³⁸⁹, and a LOF

mutation to CDKN2A, a key cell cycle checkpoint regulator.³⁹⁰ The dysregulation in cell cycle checkpoints is linked to the CDKN2A LOF mutation. The enhanced activation of the MAPK pathway, and the connection to cell cycle indicate a reason for MCF7 rapid *in vitro* growth. The prominence of nearly all DDR pathways can be explained by ESR1 activity and is consistent with studies showing MCF7's DNA damage repair abilities to be enhanced over other breast cancer cell lines.³⁹¹⁻³⁹⁴ While the cell cycle processes do show dysregulation, self-regulation shows a reduction in capacity to activate and execute cell cycle arrest.^{395,396} Overall, this network is capably distinguished from other cell line networks by process connectivity and self-regulation dynamics.

MDA-MB 231 Process Network

The MDA-MB 231 network shows a different type of regulation than observed in HCC1937 or MCF7 (Fig. 3.11C). While there is a paucity of nodes indicating significant dysregulation and preservation of many connections between processes, MDA-MB 231 shows a cell line that has reduced flexibility to maximize its biological strategy. DNA damage repair pathways do not show significant enhancement, nor pathways that counter excessive stress. BER, NER, and NHEJ all show limited connection to other processes aside from apoptosis.^{90,397,398} The decreased emphasis on these DDR pathways leaves a combination of HR, ICL, and MMR to relieve this stress.³⁹⁹⁻⁴⁰² It is even more notable that the cell cycle process tightly regulates these pathways. HR and the cell cycle both show a diminished connection to apoptosis, preventing its activation through DNA damage stress.^{374,403,404} These biological features require tight control over cell cycle arrest and DNA replication through cell cycle dysregulation. Previous observations in MDA-MB 231s led to the use of cell cycle inhibitors to sensitize them to DNA damage. Most of the network effects tie directly to the GOF mutations in KRAS and BRAF and the LOF in CDKN2A. Overall, this approach captures that MDA-MB 231 reduces flexibility to ensure that apoptosis is not activated.

MDA-MB 436 Process Network

The MDA-MB 436 process network overcomes the network size, similarly to MCF7 (Fig. 3.11D). Unlike HCC1937, MDA-MB 436 is HR-incompetent possessing a LOF BRCA1 mutation. Despite the deficiency, HR appears to retain considerable self-regulation, similar to MDA-MB

231s. A significant difference between these two networks is that HR is strongly connected to cell cycle arrest and apoptosis rather than the G1/S checkpoint, maintaining its activity. HR possesses several key interactions with other pathways that can switch the DDR pathway that repairs the DNA damage.^{405,406} In contrast to HR, the NHEJ pathway can be enhanced by other pathways. HR is likely to give way to NHEJ as these pathways co-regulate one another to ensure only one complex forms at a damaged site.⁴⁰⁷ Similar to HCC1937, NER and ICL show increased activity to manage stress, but NHEJ is more active instead of HR in this case.^{408,409} Further, the enhanced activity of BER is supported by the MDA-MB 436 resistance to cisplatin and single-strand break.³⁶⁸ Additionally, the RB1 LOF mutation is responsible for the dysregulation of the G1/S checkpoint, and along with the TP53 LOF mutation, the connection between cell cycle arrest and apoptosis is reduced. Overall, subtle differences in different processes' connectivity indicate significant changes in system dynamics in MDA-MB 436.

MDA-MB 468 Process Network

The MDA-MB 468 network is the last large network whose resolution was enhanced through the Process Network approach (Fig. 3.11E). At first glance, it is notable that HR, ICL, BER, and MMR pathways show high levels of enhancement, self-regulation, and connectivity.⁴¹⁰⁻⁴¹² These pathways and their interconnectivity are related to the DNA damage and stress resistance characteristic of MDA-MB 468. Aside from ICL, these DDR pathways show reduced connectivity to cell cycle arrest and apoptosis.^{413,414} However, these DDR pathways and NHEJ maintain a tight connection to G1/S and G2/M processivity, maintaining their activity.^{415,416} While these checkpoints are still connected to apoptosis and cell cycle arrest, there is a reduction in their effects on DNA damage repair. The MAPK pathway shows a reduced focus on DNA damage repair potentiation and an increased effect on cell cycle activation.⁴¹⁷⁻⁴¹⁹ As observed earlier, this is due to the prominence that EGFR has in this cell line also reflected in the DNA damage repair pathways involving EGFR as a transcription factor: HR, ICL, and MMR. Overall, this network appears to be inside out, focusing on DNA damage repair that shows reduced connectivity and inter-regulation between NER and NHEJ and other DDR pathways. These cells proliferate and show significant stress resistance with a focus on cell cycle processivity and DDR pathways over

apoptosis. As emphasized before, this approach has elucidated this cell line's signature traits despite the size of the network.

SKBR3 Process Network

Finally, the SKBR3 Process Network, distinguishes from other cell lines (Fig. 3.11F). SKBR3 is the only HER2-enriched cell line and shows a reduced influence of BER and connectivity of ICL.^{375,420} NHEJ and NER both show significantly enhanced self-regulation and connectivity to cell cycle progression.⁴²¹⁻⁴²³ However, these pathways also show significant influences on the apoptosis process along with a robust connection between cell cycle arrest and apoptosis.⁴²⁴⁻⁴²⁶ These features provide a remarkable potential for apoptosis activation through normal pathways. HR and MAPK show a reduction in connectivity to apoptosis, but significant effects on cell cycle and cell cycle checkpoints.⁴²⁷⁻⁴³⁰ The prominence and dysregulation of the G1/S checkpoint processivity over that of the G2/M checkpoint is significantly different from the other breast cancer cell lines. This separation shows the dominance of upstream effectors that push for G1/S activation. Components of HR can increase the amount of G1/S related genes like transcription factors.⁴³¹⁻⁴³³ Late phase HR components also reduce cell cycle arrest processivity, as do late phase NHEJ components.^{359,365,434,435} Overall, the DDR pathways appear to possess a more direct route to apoptosis reduction in activity and G1/S functioning as a central hub of this dysregulation. Inhibition of G1/S checkpoint proteins does not reduce the efficiency of HR in HER2+ cell lines as it does in TNBC cell lines. In this network, it becomes apparent that the same connectivity does not exist.

3.4.3.1 Summary on Process Network Analysis

Overall, the primary issues observed in using source-weighted CE are resolved using the Process Network method. Individual cell lines are readily distinguished and represent phenotypic features associated with each cell line. All cell lines showed a large amount of influence from apoptosis due to increases in apoptosis exclusive genes in these networks. The high influence that apoptosis has on these networks is mitigated by TP53 LOF mutations present in most cell lines. For many cell lines, the apoptosis pathway can still proceed to cell death if other factors initiate the execution phase. However, cell lines have either disconnected apoptosis from cell cycle arrest

or multiple other processes to mitigate apoptosis activity. By identifying which connections are severed or maintained, a method to predict effective combinations will be enabled.

3.4.4 Predictions through Node Removal

A simulated target inhibition approach was devised to utilize these cell line Process Networks to predict drug responses. Current synthetic lethal networks rely upon siRNA and CRISPRi experiments to validate predictive algorithms. The genetic techniques involve reducing or eliminating a gene product. While this is not an entirely accurate representation of the impact of a small molecule inhibition on a biological system, these approaches are easily simulated. The small molecule inhibitors used in this study do not effectively reduce all functions of their targets. To assess whether removing a node from the network is an adequate measure of inhibiting the gene product, I compare these predictions to known drug-sensitive contexts.

3.4.4.1 TCGA Gene Expression Network Analysis of BRCA1 +/+ and -/- Contexts

A well-studied synthetic lethal interaction is BRCA1 LOF mutation that reduces HR efficiency with a PARP1 inhibitor.^{72,147,192} This pairing of drug and genetic deficiency has proven clinically efficacious in TNBC tumors.⁴³⁶ Expression data from RNA-seq of TCGA breast tumor samples were used to create a Process Network. The loss of BRCA1 function in these networks shows evident downregulation of HR in a gene subnetwork focused on HR (Fig. 3.12).^{437,438} This condition involves reducing the influence and expression of several regulatory proteins, including CHEK1, BRCA1 and BRCA2, which accompanies a decrease in HR complex components such as RAD51. Further, a process network for TCGA TNBC samples was created identically to the cell lines (Fig. 3.13A) to reveal a significant difference in how these tumors manage proliferation and stress. Overall, there is a reduction in apoptotic signaling and self-regulation compared to the cell lines. The TCGA samples show a similar focus on cell cycle checkpoints in regulating proliferation with priming by the MAPK pathway. The majority of influential connections to the apoptosis process are from upregulated DNA damage repair pathways, leading to its suppression.

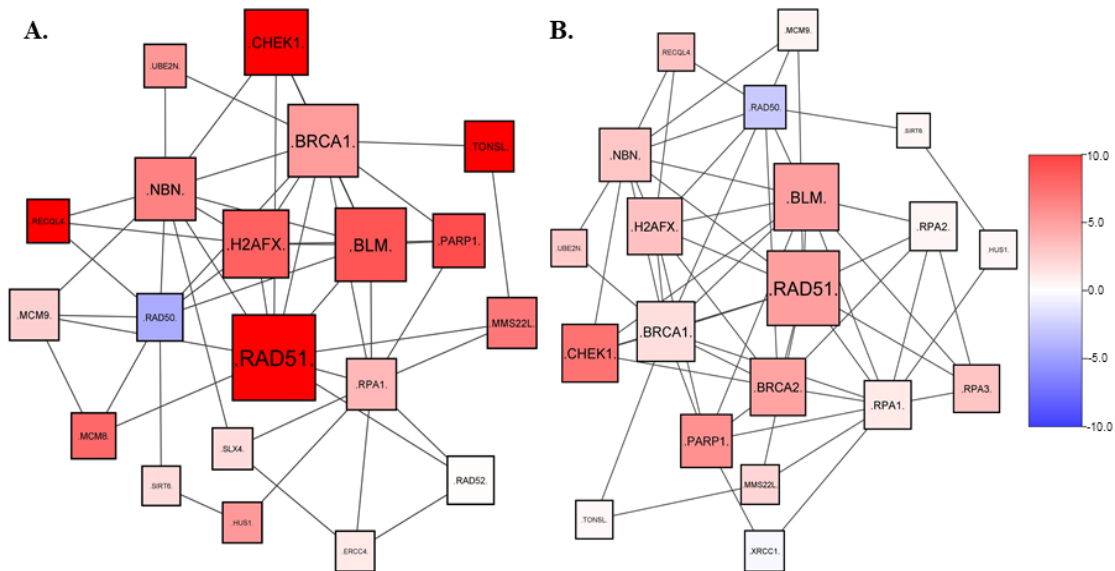


Figure 3.12: BRCA1 Loss-of-Function Mutation Effect on Homologous Recombination. Homologous recombination associated genes in TNBC tumor samples from TCGA were used to create networks. Networks were analyzed for weighted eigen centrality which corresponds to node size and with gene expression representing the color of nodes. A. BRCA1 +/+ TNBC tumor samples; B. BRCA1 -/- TNBC tumor samples

A Process Network created with only BRCA1 -/- tumor samples assessed the network's ability to reveal the changes in the HR network and tumor sensitivity (Fig. 3.13B). To understand the impact of BRCA1 LOF, a differential network was created by subtracting the original TCGA-TNBC Process Network from the BRCA1 -/- TCGA TNBC Process Network. Overall, I see significant decreases in all processes that BRCA1 directly contributes to, apoptosis, cell cycle arrest via DNA damage, the G2/M checkpoint, and HR. This deletion also reduces connectivity between these pathways and other DDR pathways, most notably NHEJ and NER.

Finally, I assessed the effects that deleting the BRCA1 node in the TCGA TNBC samples with wild-type BRCA1. This deletion's Process Network was compared to the TCGA TNBC BRCA1 +/+ samples including the BRCA1 node (Fig. 3.13C). Overall, I see similar effects, but with a lower impact and fewer modifications to connectivity. Removing BRCA1 is not able to predict the downstream effects of a loss of BRCA1's transcription factor capabilities. The ability of this approach to capably measure changes to the direct interactors of BRCA1 and BRCA1's processes is encouraging.

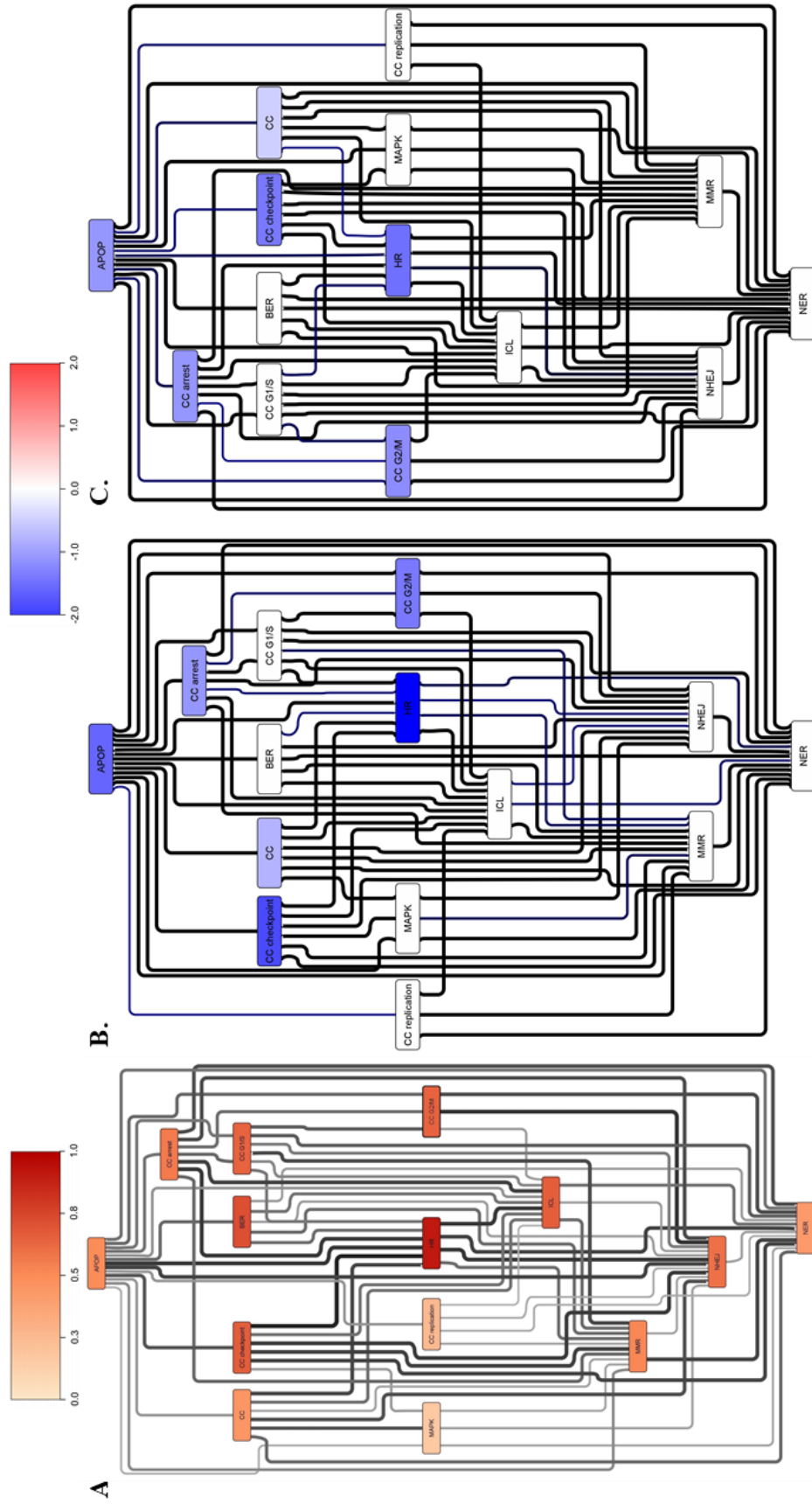


Figure 3.13: Network Disruption by Loss-of-Function Compared to Removal of Gene; Networks were created from TCGA TNBC tumor sample expression data according to the same method as the cell lines. Similar pathway analysis and centrality measurements were taken with sample groups with and without BRCA1 loss-of-function mutations. Networks were then created without BRCA1 entirely and the loss of edges and BRCA1 itself was measured. A. TCGA TNBC; B. TCGA TNBC BRCA1 -/-; C. TCGA TNBC BRCA1 removed; APOP – apoptosis; BER – base excision repair; CC – cell cycle; HR – homologous recombination; ICL – interstrand cross-linking repair; MMR – mismatch repair; NHEJ – nucleotide excision repair; NER – non-homologous end joining;

3.4.4.2 TNBC Process Network Analysis of BRCA1 -/- versus BRCA1 Simulated Deletion

To assess how synergism appears in the Process Networks, evaluating TNBC samples while simulating a loss of PARP1 was utilized in both BRCA1 +/+ and BRCA1 -/- sample sets. This case serves as a positive control to assess a likely synergistic context and a known insensitive context. The same process for calculating node removal, deletion of PARP1 reveals a decrease in the dependent processes' influence in the system, including the connections between NHEJ and NER to cell cycle checkpoints (Fig. 3.14B). ICL and BER show less modulation as they have more indirect connections to PARP1 than the other DDR pathways. The lack of impact and direct connections to apoptosis implies a lack of a lethal effect. The removal of PARP1 from BRCA1 -/- TNBC samples shows a significant reduction of cell cycle checkpoint activity, HR, and NHEJ. The connections of G1/S and G2/M checkpoints to cell cycle arrest are reduced while DDR pathways are not. This scenario would suggest that the cell cycle would be more likely to arrest when DNA damage is elevated and promote activation of apoptosis. Apoptosis also shows reduced connections to checkpoints and DDR pathways making it less likely to be deactivated. The same process of deregulation is seen in the co-removal of BRCA1 and PARP1 (Fig. 3.14C). A notable difference is that the BRCA1 -/- samples show greater dysregulation between DDR and cell cycle checkpoints. Changes seen in non-BRCA1 interactors throughout DDR and cell cycle are likely missed in the network only showing removal of BRCA1 due to the unaccounted-for expression changes from losing BRCA1 as a transcription factor. This is also assessed in MCF7 and MDA-MB 231 cell lines (Figure B.19,21)

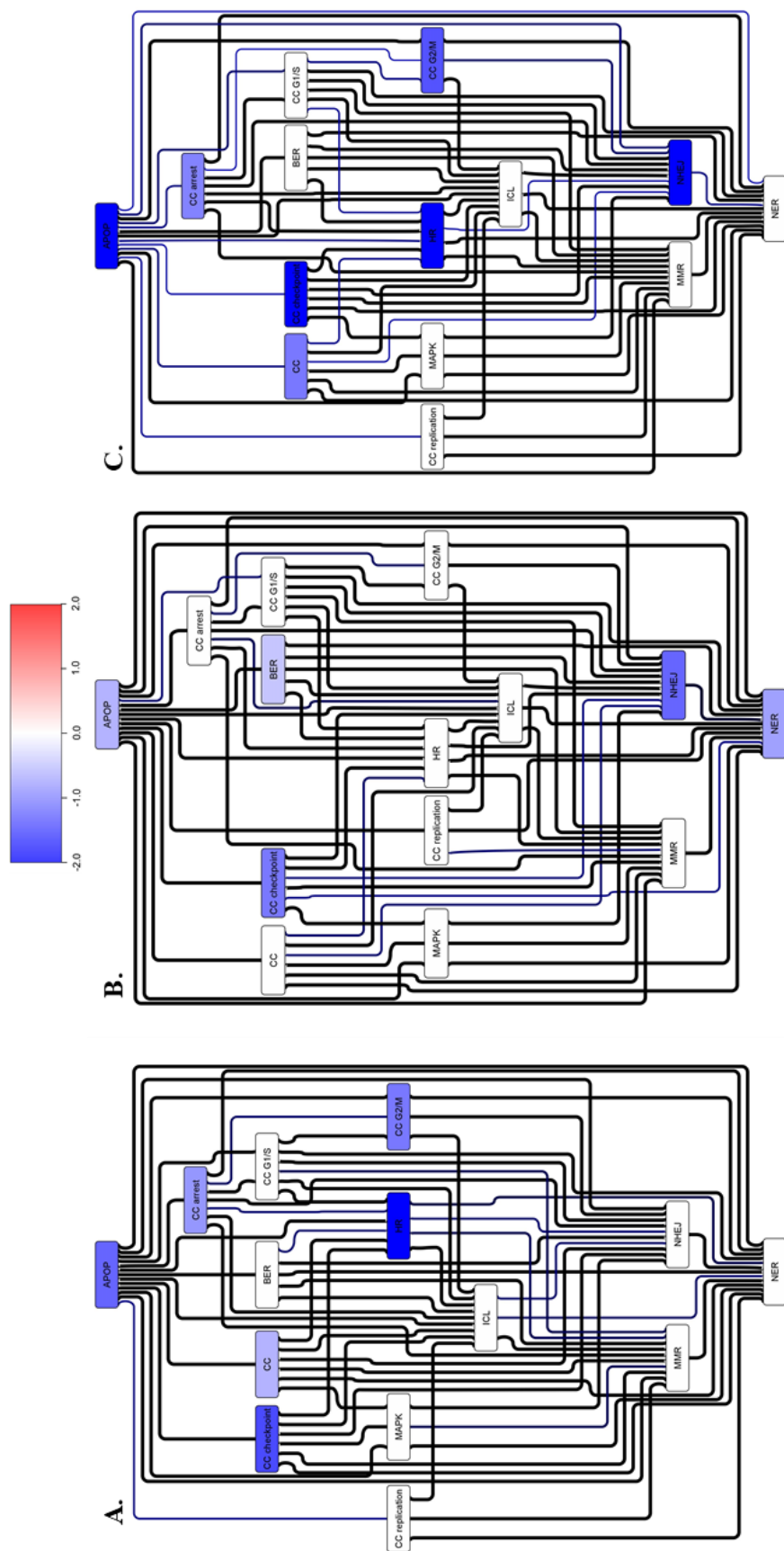


Figure 3.14: Disruption from Homologous Recombination and Non-Homologous End Joining Components in TNBC tumors; Networks were created from TNBC expression data and analyzed similarly to the base networks, but without the nodes specified. Network features were then measured as before and the relative difference in each process and their connectivity was measured. A) BRCA1; B) PARP1; C) BRCA1/PARP1; *APOP* – apoptosis; *BER* – base excision repair; *CC* – cell cycle; *HR* – homologous recombination; *ICL* – interstrand cross-linking repair; *MIR* – mismatch repair; *NER* – nucleotide excision repair; *NHEJ* – non-homologous end joining;

3.4.4.3 TNBC Process Network Analysis of BRCA1 and PARP1 Synergy through Simulated Deletion

Since I do not have reliable genetic models for each of the inhibitor pairs, it is important to assess a similar synergistic combination using the Process Network analyses. PCNA is a key HR component and the inhibitor T2AA has been reported, both earlier in this work and by other groups, to be able to target that function. Therefore, I compared the results of co-removal of PCNA and PARP1 to discern whether my differential process networks could simulate this interaction. I once again used the TCGA TNBC samples for consistency with the BRCA1 assessment. PCNA removal in the TNBC network was not as impactful as BRCA1 on HR or cell cycle phases, aside from replication (Fig. 3.15A). PCNA also had a reduced effect on apoptosis and a more substantial effect on G2/M instead of G1/S. HR connections to replication and apoptosis are reduced by the PCNA removal as well. Co-removal of PCNA and PARP1 produces the reduced connections between both HR and NHEJ to apoptosis and cell cycle arrest. Apoptosis is still well connected to cell cycle arrest, as it was with BRCA1 $-/-$ and PARP1 removal (Fig. 3.15C). This is also assessed in MCF7 and MDA-MB 231 cell lines (Figure B.20, 22).

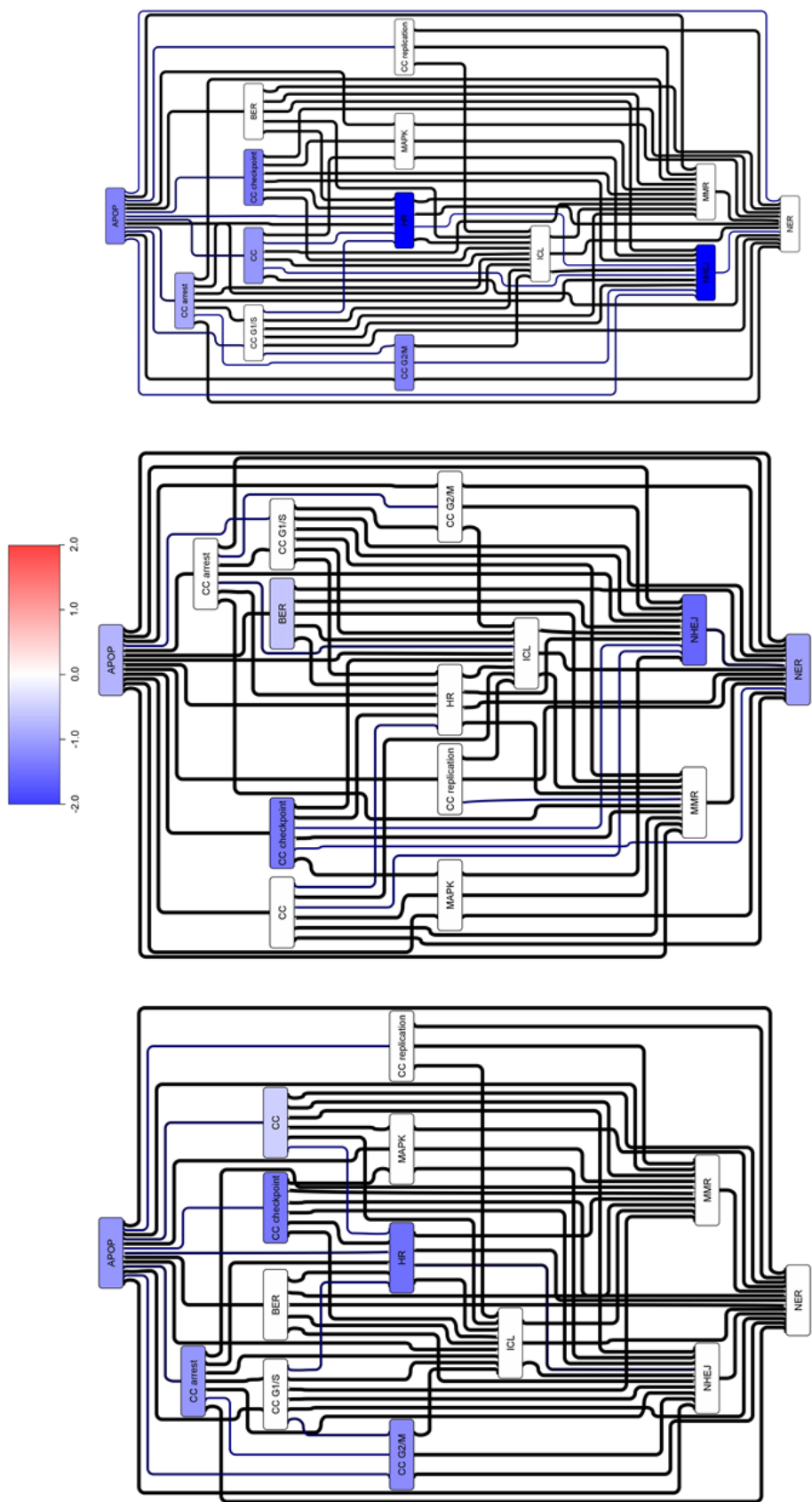


Figure 3.15: Disruption from Homologous Recombination and Non-Homologous End Joining Components in TNBC tumors; Networks were created from TNBC expression data and analyzed similarly to the base networks, but without the nodes specified. Network features were then measured as before and the relative difference in each process and their connectivity was measured. A) PCNA; B) PARP1; C) PCNA/PARP1; APOP – apoptosis; BER – base excision repair; CC – cell cycle; HR – homologous recombination; ICL – interstrand cross-linking repair; MMR – mismatch repair; NER – nucleotide excision repair; NHEJ – non-homologous end joining;

3.4.5 Synergism Predictions and Measured Outcomes

Predicting synergism over additivity or enhancement requires an understanding of network dynamics beyond a simple differential. Utilizing the Impact Matrix, I distinguish which processes and nodes are likely to contribute to or prevent cell death. A large component of this calculation considers node edges over nodes to contribute to the activation of apoptosis. For example, in cell cycle, many checkpoint proteins are understood as tumor suppressors, while other proteins involved in their regulation could be considered oncogenes.⁴³⁹⁻⁴⁴¹ It is important to assess a process not as simply whether it increases the likelihood of cell death or not. Instead, understanding the sum of the effects produced by both a single pathway and its interactions with other pathways determines the outcome. The process maps presented in earlier sections lack some of the resolution required to understand these relationships. However, to look at every individual edge and node that comprises their effect would be overwhelming. A new value, disruption index (DI), was used as a metric to measure the likelihood that changes in a network cause cell death through the loss of two nodes over either alone. As such, not all disruptions to the network will be of the same value. For example, not all connections between cell cycle and apoptosis will lead to cell death.

The Impact Matrix is designed to indicate pro-apoptotic processes and nodes positive and anti-apoptotic processes and nodes negative. Therefore, the more positive the value, the more likely there is to be cell death. The reduction in Processivity is considered to be relative to the change within the process to prevent large networks from diluting a single process's effects. However, the amount of dysregulation within the network is accounted for ensuring the greater the Influence of an affected process, the greater the Disruption Index.

In order to predict synergism, the effect of a drug combination must supersede the additive effect. The methodology used in this work prioritizes the reduction of multiple processes over that of a single process. The two genes deleted receive a higher DI if they affect different pathways from each other. Furthermore, prioritization is given to multiple regulatory connections to apoptosis over any single connection. Measuring disruption in this manner does not differentiate compensatory pathways from those that are independent of one another.

Cell proliferation assays with drug treatments are used to test the synergism predictions made by this method by comparing CI values to the DI generated by the Process Network analysis. These were conducted as detailed in section 3.3.10.

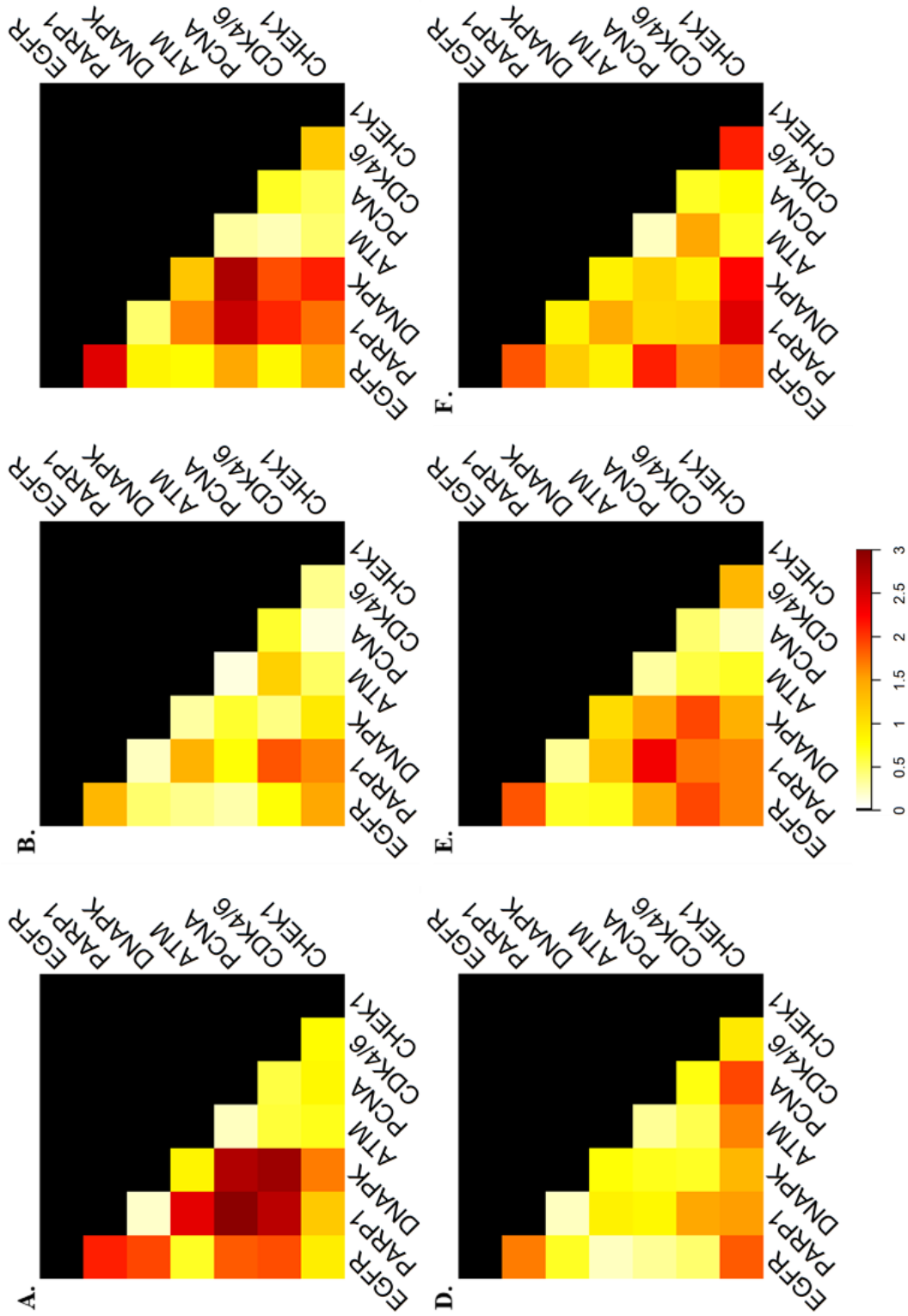


Figure 3.16: Disruption Indices for Combinatorial Gene Removal in Breast Cancer Cell Line Networks; Cell line networks were analyzed for their differential process centrality through the deletion of two genes corresponding to drug targets. Disruption indices were calculated according to our reported formula in the method section. Values above 1 indicate significant disruption to the network through the connectivity within and between processes analyzed. A. HCC1937; B. MCF7; C. MDA-MB-231; D. MDA-MB-436; E. MDA-MB-468; F. SKBR3

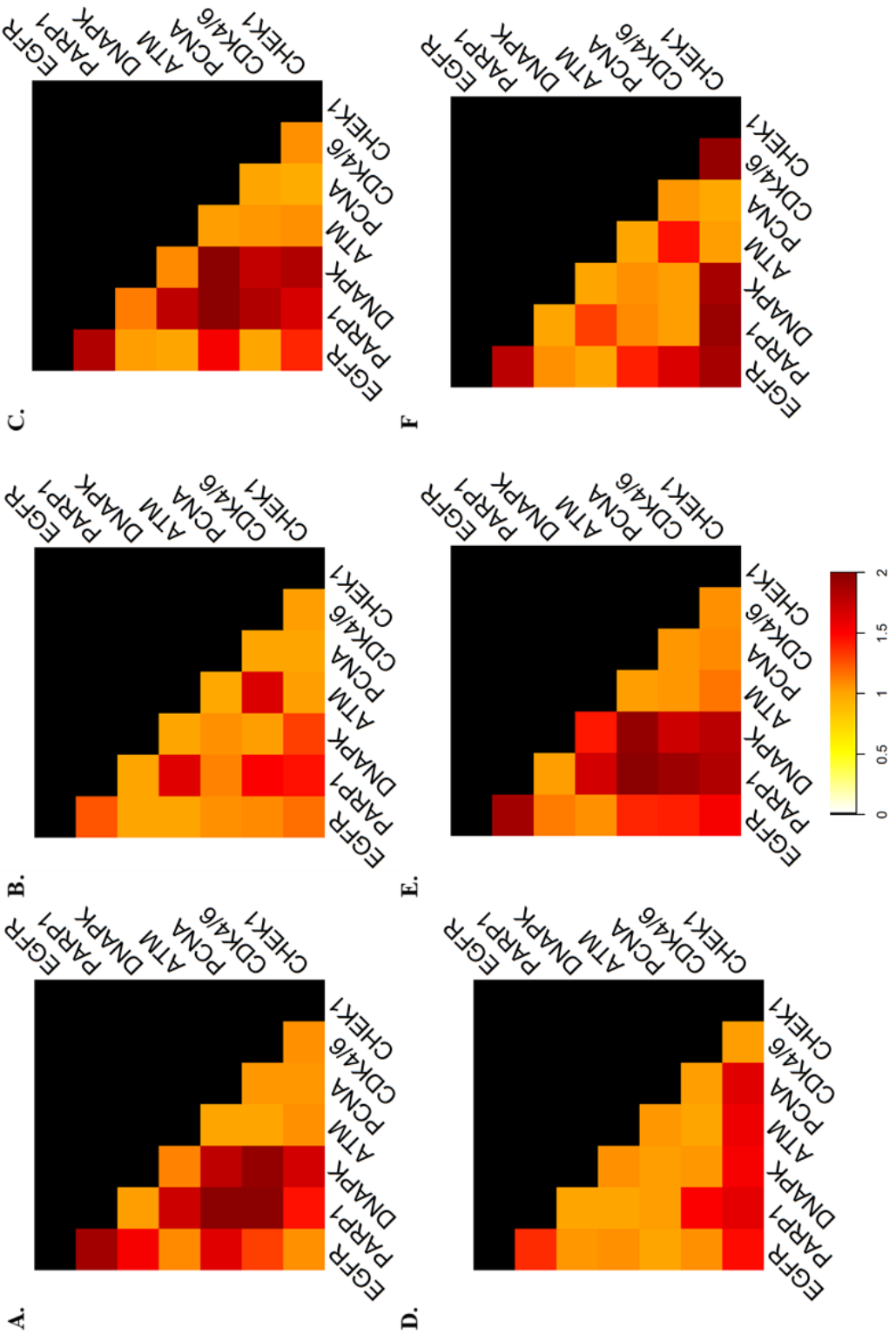


Figure 3.17: Combination Indices for Drug Combinations in Breast Cancer Cell Lines; Cells were tested in combination using a MTT assay and their combination indices (CI) determined through Chou-Talalay. The maximal 1/CI value for a concentration was above the minimal drug concentrations and below the GI_{50} concentration of a single chemotherapy. Values above 1.1 have a confidence greater than 95% to be synergistic. A. HCC1937; B. MCF7; C. MDA-MB-231; D. MDA-MB-436; E. MDA-MB-468; F. SKBR3

HCC1937 DI vs. CI Profile

Co-removals of drug targets within the HCC1937 network produced results consistent with observations in the Process Network (Fig. 3.16A). Drug targets associated with NHEJ and HR such as PARP1 and DNA-PK combinations with PCNA, EGFR, and ATM showed consistent and large DI. Also, a prediction of CHEK1 synergy with PARP1 is evident and regulates the G2/M checkpoint and Processivity of the HR pathway. Interestingly, CHEK1 deletion has a reduced impact on HR in HCC1937.^{442,443} An EGFR inhibitor was also predicted to synergize with PCNA and CDK4/6 inhibitors, which directly impact the G1/S checkpoint and DNA replication. EGFR regulates both cell cycle processes as well as their connections to apoptosis.

The CI profile complemented the HCC1937 DI profile closely (Fig. 3.17A). However, the PARP1 and CHEK1 combination showed the greatest divergence and displays the method's difficulty with downstream effects. CHEK1 does have a significant impact on HR that is not well characterized by the removal of CHEK1 in a Process Network. Interestingly, DNA-PK and CHEK1 synergism is correctly predicted. A key difference between DNA-PK and PARP1 is that in the base gene network, PARP1 interacts with CHEK1, which causes significant overlap in their interactions.

MCF7 DI vs. CI Profile

The MCF7 is a luminal A cell line showing significant differences from TNBC cell lines (Fig. 3.16B) and continues to predict synergies. Overall, the selection of combinations that focus on DDR and cell cycle are not effective. Those that are effective have significant direct connections to cell cycle. The most significant disruption is from a CDK4/6 inhibitor and a PARP1 inhibitor. Of the cell cycle processes, G1/S shows the greatest connection in regulating apoptosis. While NER is the most connected DDR pathway to cell cycle processes, NHEJ is a close second, and PARP1 is a regulator of both pathways. G1/S signaling is often tightly associated with MMR, HR, and ICL pathways' efficiency, which may come into play. The next largest DI's are associated with CHEK1 inhibition with EGFR and PARP1. CHEK1 inhibition has the most impactful effect on the G2/M checkpoint and HR regulation. EGFR and PARP1 both have strong connections to NHEJ and other DDR pathways' Processivity, as mentioned earlier. As stated above, MCF7 appears to

have a cell cycle-focused network which is understandable considering they are a hormone-dependent tumor.

The CI profile for the MCF7 cell line is qualitatively accurate, but not quantitatively (Fig. 3.17B). Using the cutoff value of 1 for both predictions of synergism for DI or 1/CI, all the predictions for both negative and positive synergism cases are accurate. The degree of synergism is not well predicted, with the combinations of ATM and CDK 4/6 or PARP1 inhibitors. ATM's position as a DNA damage sensor and an HR activator yields a significant effect on the G1/S checkpoint and HR and related pathways. For instance, there appears to be an underestimation of the ATM connection to CHEK1 and apoptosis in the network. Regardless, both combinations predict to be synergistic.

MDA-MB 231 DI vs. CI Profile

MDA-MB 231's DI profile shows many of the same hallmarks of TNBC (Fig. 3.16C). The DDR enhancement to increase the likelihood of cell survival offers a similar set of predictions as HCC1937. NHEJ and HR's co-dysregulation appear to be very disruptive in this network and simulates the known synergistic relationships between these pathways. The chief difference between MDA-MB 231 and other TNBC cell lines focuses on cell cycle and how that drives the DDR response. From these results, CHEK1 is predicted as a more likely enhancer of DDR than CDK4/6. The G2/M connection to reducing arrest potential in MDA-MB 231 is a key factor with ample CHEK1 upregulation to manage this connection. This factor allows for CHEK1 to potentiate disruption of DDR, regardless of the source of reduced efficiency. As observed before, CDK4/6 inhibitors are able to synergize with NHEJ inhibitors, but not HR inhibitors. This result follows the observation that G1/S checkpoint proteins are driving HR dependency in the cell line. Overall, this system is consistent with KRAS/BRAF GOF mutations and downstream effects due to those common mutations.

The CI profile of MDA-MB 231 closely mirrors the DI profile (Fig. 3.17C). However, the DI profile underestimates the EGFR connections in comparison to the combinatorial effects. A likely cause is the off-target effects of the EGFR inhibitor and MDA-MB 231's exceptional dependence on the MAPK pathway through the KRAS/BRAF mutations. This situation makes the DDR effects of EGFR inhibition a more significant component of the synergism than in other cell

lines. While somatic mutations directly impact the expression profiles to determine centrality, there are often more pathway-specific changes. This scenario is especially true of KRAS/BRAF mutations in MDA-MB 231 cells that affect the MAPK pathway but not the DDR pathways specific to EGFR. Overall, MDA-MB 231 predictions were confirmatory by the assays.

MDA-MB 436 DI vs. CI Profile

The MDA-MB 436 diverges sharply from other TNBC cell lines due to its BRCA1 LOF mutation. (Fig. 3.16D) The loss of an efficient HR pathway is a requirement for numerous synergistic relationships. The NHEJ inhibitors are most effective in this cell line, consistent with the observations where only synergism occurs between EGFR or CHEK1 inhibitors with DDR inhibitors. ATM and PCNA inhibitors' potential to impact DNA replication, ICL, and G1/S is likely the source of high DI with CHEK1, which would impact the G2/M checkpoint and connections. Otherwise, the accumulation of DSB's from the loss of NHEJ along with a G2/M checkpoint inhibitor is a synergistic strategy observed before. The low amount of disruption in MDA-MB 436 could also be an artifact of the generally high-level of connectivity of this network, preventing a considerable impact.

The MDA-MB 436 CI profile shows the most significant correlation with its DI profile (Fig. 3.17D). This cell line result stands out, showing the fewest synergism cases similar to the results with MCF7. The lack of an efficient HR pathway removes many of the effective combinations in the other cell lines. The heightened Influence of CHEK1 through the G2/M checkpoint and DSB repair regulation is a dominant factor in this cell line. While the DI profile does not capably display the magnitude of synergism, it does capably show the lack of synergism in most of the combinations. Overall, MDA-MB 436 presents a simple context in the focused set of pathways for testing this study's methodology.

MDAM-MB 468 DI vs. CI Profile

The MDA-MB 468 is the final TNBC cell line in the study and the DI profile is similar to the other HR-competent TNBC cell lines. (Fig. 3.16E) The combinations of HR and NHEJ inhibitors show the most potent DI. G1/S cell cycle arrest is more Influential due to its connectivity than G2/M in the MDA-MB 468 Process Network (Fig. 3.12E). This point reflects that CDK4/6

more frequently predicts a synergistic partner. However, this does not extend to HR inhibitors due to the weak connection to the HR process and the prominence of ICL. Overall, MDA-MB 468 looks very similar to other TNBC cell lines, except for its emphasis on other cell cycle components, which shifts the disruption to CDK4/6 inhibitor combinations.

The MDA-MB 468 CI profile shows separation and the most false negatives compared to other cell lines (Fig. 3.17E). These include the ATM and DNA-PK, EGFR and PARP1, and ATM and CHEK1 combinations. Two of these combinations are borderline cases where they minimally exceed the 1.1 cutoffs for synergism. It also contains one false positive in CHEK1 and CDK4/6, which shows a more significant separation. A major component of these four inaccuracies is the dominant Influence of HR and ICL, which ATM contributes to, but results in low impact on apoptosis or cell cycle arrest in the Process Network. These features reduce the prediction for disruptions to trigger apoptosis activation. G1/S and G2/M checkpoints are both well connected to apoptosis and cell cycle arrest, and numerous pathways. However, the prominence of the MAPK and survival pathways underestimate in this approach. A broader set of processes may improve the ability to predict the impact of these scenarios.

SKBR3 DI vs. CI Profile

SKBR3 is the sole HER2+ cell line and shows a unique DI profile to match (Fig. 3.16F). NHEJ and HR combinations are predicted to be only moderately effective compared to the magnitude of predictions in the TNBC cell lines. A strong focus on CHEK1 and EGFR combinations makes this profile stand out. A much stronger emphasis on the MAPK pathway and EGFR specifically in this cell line's network is a partial explanation for this characteristic. The emphasis on CHEK1 combinations likely exists through its strong connection to apoptosis and NHEJ, which stands out as the primary DDR pathway in this network. The greatest DI confirms this relationship exists between CHEK1 and NHEJ inhibitors. The reduced impact of HR inhibitors on DI is likely reflects low inhibitory effects on self-regulation, maintaining connections to cell cycle arrest while NHEJ compensates for DDR.

The CI profile of SKBR3 closely resembles the DI profile (Fig. 3.17F). There is a lack of correlation between the CI values of synergistic combinations and DI values due to the CHEK1-NHEJ inhibitor combinations. The result is more significant synergism than predicted. G2/M and

NHEJ's prominence and Influence on apoptosis, and cell cycle arrest is remarkable. The impact of this characteristic extends to DNA replication and reduces connectivity in other pathways. The focus on G2/M and NHEJ is consistent with unique HER+ tumor effects on the G2/M checkpoint.^{444,445} G2/M checkpoint modulation has been used as a prognostic marker in HER2+ tumors and has highlighted HER2 as a targetable entity in these tumors.

3.4.6 Method Results Summary

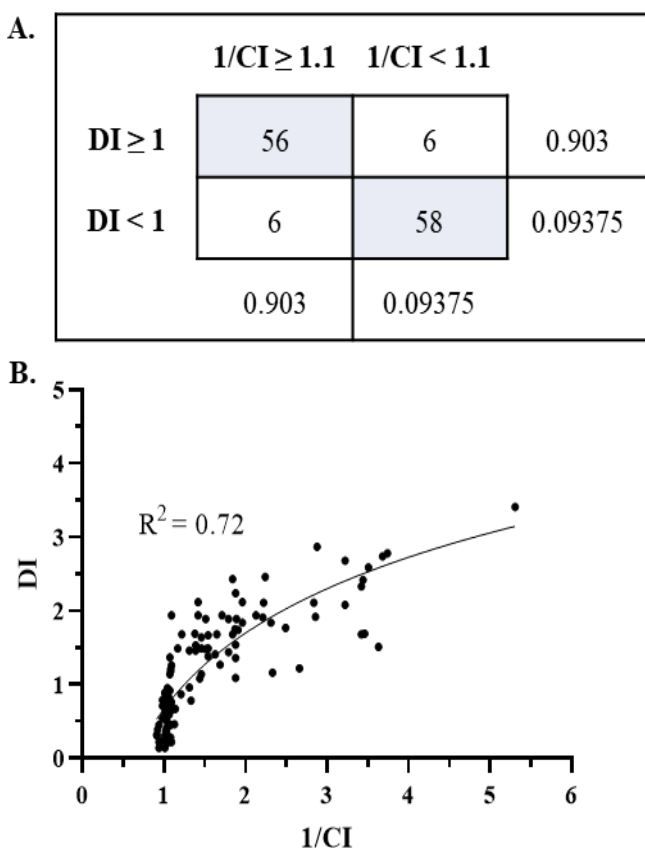


Figure 3.18: Simple Statistical Assessment of Disruption Index (DI) and Combination Index (CI). A) The ability of the DI to predict combinations that will be synergistic as seen through experimental results for CI. B) A simple correlation of DI to CI showing the ability to predict the magnitude of synergism

The methodology developed and tested in this study shows remarkable potential for predicting synergism in DDR pathways and connected processes (Fig. 3.18). A 90.3% true positive and true negative rate qualifies this method to identify likely synergistic combinations in various tumor genomes. Where this method does not excel is in predicting the degree of synergism of a combination. The R^2 value of a logarithmic trendline between DI and CI reaches 0.72, leaving considerable room for improvement. This method can be considered a qualitative analysis of synergism, but not a quantitative scoring method. One deficiency of the study is the lack of antagonistic drug combinations, which leaves its detection by this methodology unknown.

3.5 Discussion

This study establishes a novel method leveraging CE to predict drug synergism potential. A workflow design for network creation parameters includes gene expression, GO term gene sets,

and protein-protein interactions. From this network creation strategy, values describing the amount these networks representing connections between and within pathways were developed. A simple simulation of gene deletion to model network dynamics due to target inhibition was created. Finally, an effective data presentation technique was developed to leverage these data analyses. These overall workflow and metric definitions are distinctive from other network building and analysis strategies, which seek to understand differential gene expression or drug activities. By establishing a network from reliable data pooled into GO terms and interaction sets, gene expression data can be leveraged further than before. These methods, coupled with the explosion of genomic information, can discover genes with novel importance rather than relying on already known genes to determine pathway significance. This approach also ties dysregulation to known interactions to allow expedited development of drug discovery hypotheses.

3.5.1 Eigenvectors as a Biomarker Metric

CE has been used in previous studies define a broad range of systems from population evolutionary dynamics to sparse neural networks. Use of either a weighted or unweighted CE to prioritize gene selection has been utilized to replace simple enrichment. In my study, I approached a data set that includes numerous common features, by design. The goal is to simplify individual gene identifiers as significant or insignificant to a disease model. When attempting to apply this approach to my datasets focusing on individual gene groups, I was unable to distinguish datasets better than gene expression. Instead, the utility of the approach was found in identifying larger changes in network dynamics over processes that share multiple nodes. Creating a process that is able to distinguish changes in groups of nodes over individual nodes was established as a requirement to distinguish datasets. Further, CEs were useful here to study subnetwork structure within the larger parent networks to explore specific dysregulation within an individual pathway in sample sets. This use of CE creates multiple resolution levels of this analysis technique. Validation of observations is imminently possible through examining known components of the system.

3.5.2 Integrated Pathway Analysis through Inter- and Intra-connectivity

Cancer biology is a story of discrete changes in a single gene creating a dysregulated system and the novel connections that result. The work here expands the concept of dysregulation as increases or decreases of normal functions to novel connections that re-contextualize the system. This objective necessitates evaluation if pathways that are co-activated or expressed have separate co-regulation from direct pathway activity. More importantly, it is necessary to understand groups of changes as a whole instead of attempting to identify smaller datasets that indicate large changes. A consistent narrative is that a pathway's influence is notable due to the lack of "normal" processes. It implicates creating a minimal panel size that seeks to understand deeply integrated systems as a set rather than as discrete changes. In the cell lines evaluated, changes in DDR pathways were preceded by changes in cell cycle checkpoints. The means of dysregulation can change the focus of treatment towards finding gaps in the tumor biology that would allow for stressed systems to collapse. Understanding when the disease's state renders a decreased sensitivity to DNA damage due to changes in cell cycle or the MAPK pathway can allow the correct therapeutic option to be selected.

3.5.3 Gene Removal as a Model of Inhibition

Gene downregulation or even removal through siRNA, non-coding mutations, or CRISPR have become efficient means of testing the likely impact of inhibition. The removal of nodes from a network and the specificity of the genomic techniques listed are simple and direct, enabling rapid experimental design and validation through multiple means. Inhibition by a small molecule or drug is a much more complex set of interactions to be simulated through a network. Drug inhibition profiles do not entirely remove a protein or all its functions and often have additional effects. A thorough drug profile by removing the proper edges that correspond to the drug's activity would be most effective. In my networks, gene deletion proves to be effective in evaluating drug inhibition's most direct effects. The ability to further weigh the drug effect within the network by using unique features that describe a drug's specific action would require extensive mechanistic information. Understanding drug effects through differential gene expression comparing treated and untreated cells could produce that profile and indicate the amount of system disruption. This

approach could assess two drug effects and would allow the method to remain efficient and focus on the same data sets as it does now.

3.5.4 Network Disruption Measured through Pathway Dynamics

Network stress is a well-understood means of measuring changes in network adaptability and plasticity. Most network stress metrics focus on overall network connectivity or individual node connectivity. They also find the minimal network features to create connectivity between clusters or other network features. In these systems, apoptosis is the clear focus of an effective drug combination. Thus, not all types of disruption are equal, and the adaptability of these networks is not measured through my DI, but instead the likelihood of an apoptotic response. Presuming that each node acts at its maximum potential in each interaction allow network dynamics to be calculated as a whole. Each process must evaluate node deletion's net contribution within the system and also their contribution to the influence of the surrounding nodes. This condition does not allow for a single node to completely prevent a processes function. While this is not entirely accurate, there are numerous examples of homologous proteins replacing other protein's function(s). A node's ability to supplant another's role or circumvent a blocked step is not explicitly understood within this approach but is still assumed. Utilizing more definite pathway descriptions would allow for a more sensitive assessment of known systems but may constrict predictions to what is already understood.

3.6 Conclusions and Impact

This approach is the first synergism prediction strategy leveraging a protein interaction network examined using eigenvector centrality. My approach to defining the contributions of genes to a related pathway through GO terms using my equations for GO Impact, Cohesion, and Adhesion are also novel contributions to the field. While other pathway analysis techniques exist utilizing protein interactions to determine gene sets, using source-weighted eigenvectors and the relationships defining subnetworks is also novel. Utilizing these three values to create a novel Process Network to limit the impact of large networks in reducing the descriptiveness of small gene sets within a pathway. My Disruption Index (DI) value utilizing simulated gene deletion required the enhanced descriptiveness of Process Networks. The DI, while indicative of likely

synergism, is still able to be parsed into the contributions of the individual dysregulation of a pathway or gene. This is able to indicate likely mechanisms to be evaluated to understand each case of synergism. This overall process of predicting synergistic combinations is 90.4% specific and sensitive. Overall, this approach proves to be a descriptive and predictive approach in analyzing the nexus of DNA damage repair, cell cycle, apoptosis, and MAPK pathways. While more focused than other approaches that predict synergism, Process Networks and the identification of disrupted pathways provides a unique mechanistic perspective.

CHAPTER 4. FUTURE DIRECTIONS

Agents that damage DNA remain a prominent component of the tumor treatment strategies. The increased rates of proliferation in tumor cells affects stress and dependence on dysregulated cell cycle checkpoints.⁵¹ Effective DNA damage agents work by increasing DNA damage detected by the cell to those exceeding the DNA damage repair (DDR) pathways' capacity. Tumor resistance arises through further dysregulation of DDR or reduced functionality of apoptosis.^{446,447} Tumor plasticity has led to DNA damage agents' lower efficacy in recurring tumors while still possessing severe side effects. As displayed in this work, ample opportunities exist within DNA damage repair systems that could lead to innovation in oncology. The sensitization of tumors to artificially induced DNA damage and leveraging their dependence on DNA damage repair through targeted therapy remain fodder for discovery.^{448,449} My focus on drug combinations and phenotypic studies has provided a broad view of these observations' utility. What remains to be understood are what precise molecular interactions these inhibitors are targeting to bring about these results. Furthermore, any models of these interactions would require a similar understanding of the nuances of individual protein functions within protein complexes. Improving our knowledge of how various forms of inhibition can influence DDR pathways, both through biochemistry and *in silico* models, can drive this innovation.

4.1 Further Evaluation of Specific DNA Damage Repair Inhibition through PCNA

PCNA is involved in numerous pathways with functional modulation through multiple post-translational modifications (Fig. 4.1).²¹¹ Many of the protein-protein interactions required for both the modifications and pathway complexes share a similar binding motif. Therefore, multiple effects are anticipated for PCNA antagonists binding at these sites. The observations differentiating T2AA as well as our tripeptoids inhibitor are clear examples of the functional diversity of PCNA antagonism. What has not been demonstrated in this study are the exact molecular effects upon PCNA, or its interactors, that are responsible for each class of PCNA inhibitors. Since PCNA is a modular interaction platform regulated by post-translational modifications (PTM), it is vital to understand PCNA through PTMs in relevant DDR pathways. PTM assessment would involve a direct investigation of known changes related to DDR in K164

and Y211 status. With T2AA, it is already known that the mechanism of action involves an effect on K164 ubiquitination, which directly impacts TLS and HR recruitment.⁴⁵⁰ These features can be used to quickly identify likely interactors significant to each class of PCNA antagonism. However, investigating specific interactions of PCNA required by different repair pathways at specific points can further define these molecules. A focus on PCNA interactions should go beyond the work done to investigate PCNA-DNA polymerase complexes.²²⁰ Further, protein-protein interaction studies should involve the single-strand break (SSB) repair pathways that require PCNA.

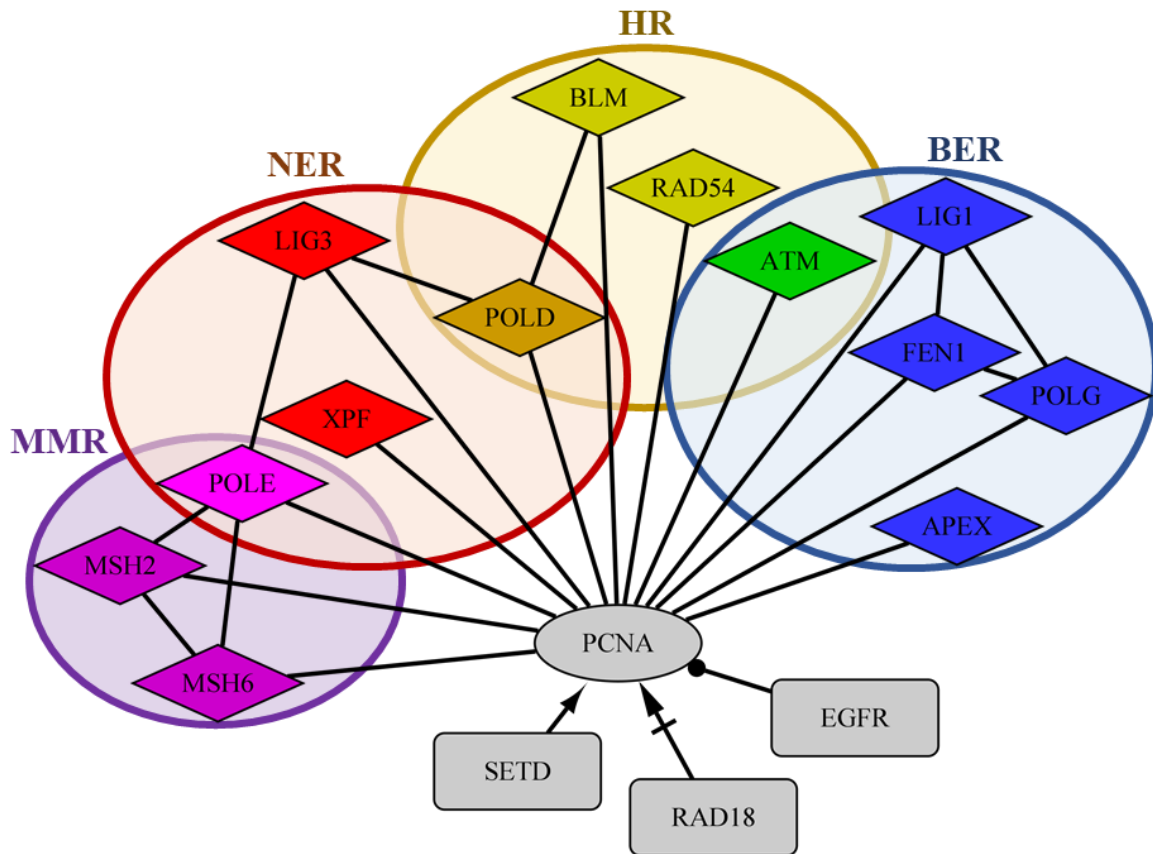


Figure 4.1: PCNA Post-Translational Modification and DNA Damage Repair Pathway Influence. PCNA is involved as a scaffold protein to form protein-DNA complexes in the four repair pathways represented: mismatch repair (MMR), nucleotide excision repair (NER), homologous recombination (HR), base excision repair (BER). Proteins that are involved in complexes with PCNA are represented by rhombuses and modifiers of PCNA are represented by rectangles. The different arrows represent different modifications with EGFR phosphorylating PCNA, RAD18 ubiquitinating PCNA, and SETD sumoylating PCNA.

4.1.1 Understanding Differential Inhibition of Homologous Recombination

The HR pathway has multiple proteins that small molecules have targeted. (Fig. 4.2) Within our studies, we have utilized our PCNA inhibitors as well as ATM inhibitor KU-55933. Rad51, Rad54, and the Bloom helicase (BLM) have all been successfully targeted to reduce HR activity.⁴⁵¹⁻⁴⁵³ ATM is necessary for end processing which allows for the formation of the Rad51 nucleofilament. Rad51 is required to initiate strand invasion to form the Holliday junction for template-derived repair. Rad54 is required to remove Rad51 to allow for stable complementation after strand invasion. BLM is then required to ensure that the Holliday junction is resolved without additional double-strand breaks (DSB) (Fig. 4.2). All these proteins physically interact with PCNA in a manner that is important to HR progression. Inhibition of HR through a selective inhibitor of PCNA protein-protein interaction (PPI) could potentially have an HR effect through any of these interactors. Our assessment of Rad51 foci formation and the PCNA inhibitors' ability to synergize with an ATM inhibitor provided insight into two types of HR inhibition. Further, testing these molecules in an HR-deficient context provides some insight into whether there are additional mechanisms to be evaluated. To fully understand the effects and types of PCNA inhibition, we should evaluate relevant PTMs of PCNA, additional foci, and additional drug combinations.

The two PTMs of PCNA relevant to HR most studied are mono-ubiquitination of K164 (ubK164) and phosphorylation of Y211 (pY211).⁴⁵⁴ There is also the less understood sumoylation of K164 (suK164), which is mutually exclusive with ubK164. ubK164 is controlled by the E3 ligase RAD18.⁴⁵⁵ Several studies have reduced RAD18 function through siRNA resulting in a reduced HR capacity.^{456,457} A direct effect on ubK164 status by a PCNA inhibitors would explain the likely set of blocked interactions. suK164 directly inhibits HR activity of PCNA as well as promotes cytoplasmic localization of PCNA.

It is possible that our inhibitors somehow, either directly or indirectly, enhance the amount of suK164. pY211 is controlled by EGFR and was initially understood as a DNA replication marker.^{458,459} pY211 prevents poly-ubiquitination of PCNA and is also required to maintain PCNA-polymerase complexes in DNA replication. The impact of pY211 on HR is not well understood. The evaluation of this PTM would also distinguish whether effects directly impact the amount of PCNA rather than a specific form of PCNA.

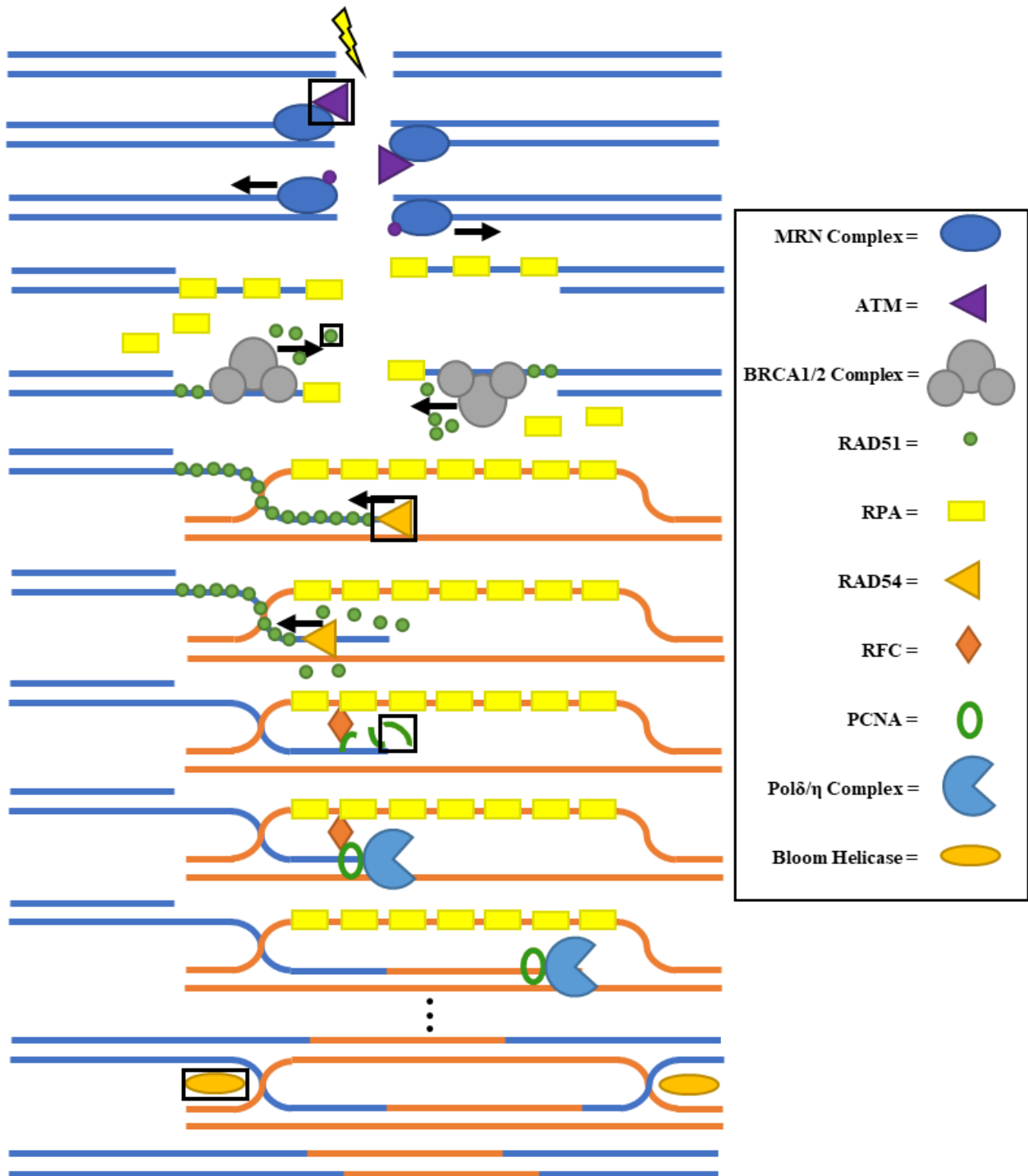


Figure 4.2: DNA Double-Strand Break Repair via Homologous Recombination with Inhibitor Targets. Black squares outline targets with selective inhibitors.

Rad51 foci were selected for evaluation as it is not directly modified by ATM and it is one of the first HR-specific marker. 53BP1 is another common marker for HR but can be modified to promote progression to non-homologous end joining (NHEJ).^{460,461} 53BP1 is also required to activate ATM's subsequent HR functions allowing ATM inhibition to render 53BP1 effects moot.^{462,463} Also, inhibition of PCNA K164 ubiquitination reduces 53BP1 foci formation, but PCNA foci formation requires 53BP1 foci dissolution.^{464,465} An evaluation of H2AX, RPA, 53BP1, RAD51, PCNA foci formation over multiple time points in a 24-hour period would define the progression through HR. Pairing this HR foci panel with Ku70/80 and PARP1 foci as controls would identify whether a reduction in HR-related foci is related to NHEJ or HR dysfunction.⁴⁶⁶

In this study, HR antagonists were not combined with NHEJ antagonists. Instead, a focus on specific effects of each PCNA inhibitor revealed separate classes. Only one HR antagonist, KU-55933, was used with a PCNA inhibitor, which prevents the formation of RAD51 foci. Evaluating only one HR antagonist combination was to focus my work on one likely mechanism of PCNA antagonism. Drug combinations of PCNA inhibitors with inhibitors of RAD51, RAD54, and BLM would establish whether they overlap with other HR steps. These combinations with the NHEJ inhibitors of PARP1 or DNA-PK could establish which HR phase is being impacted by a class of PCNA inhibitors. This could also be achieved with siRNA experiments exploring the loss of these gene products. Proteomic studies to assess notable PTMs of these proteins and downstream effectors can also interrogate the steps in between the foci development that PCNA may influence.

4.1.2 Evaluating Any PCNA Inhibition of Nucleotide Excision and Base Excision Repair

While this study focused on DSB and their direct repair, there are other means of increasing DSBs and damage-related stress. PCNA is a key component of both base excision repair (BER) (Fig. 4.3) and nucleotide excision repair (NER) (Fig. 4.4). SSBs rapidly progress to DSB through inhibition of repair pathways.^{467,468} While we possess convincing data suggesting a direct effect on HR, this does not preclude an effect on SSB repair. The selection of ATM as the HR antagonist capably differentiates the mode of HR inhibition some PCNA inhibitors exhibit. However, an ATM inhibitor was a poor choice to assess SSB repair effects of PCNA antagonists. ATM has a direct effect on BER activation which could mask PCNA inhibitory effects in SSB.⁴⁶⁹

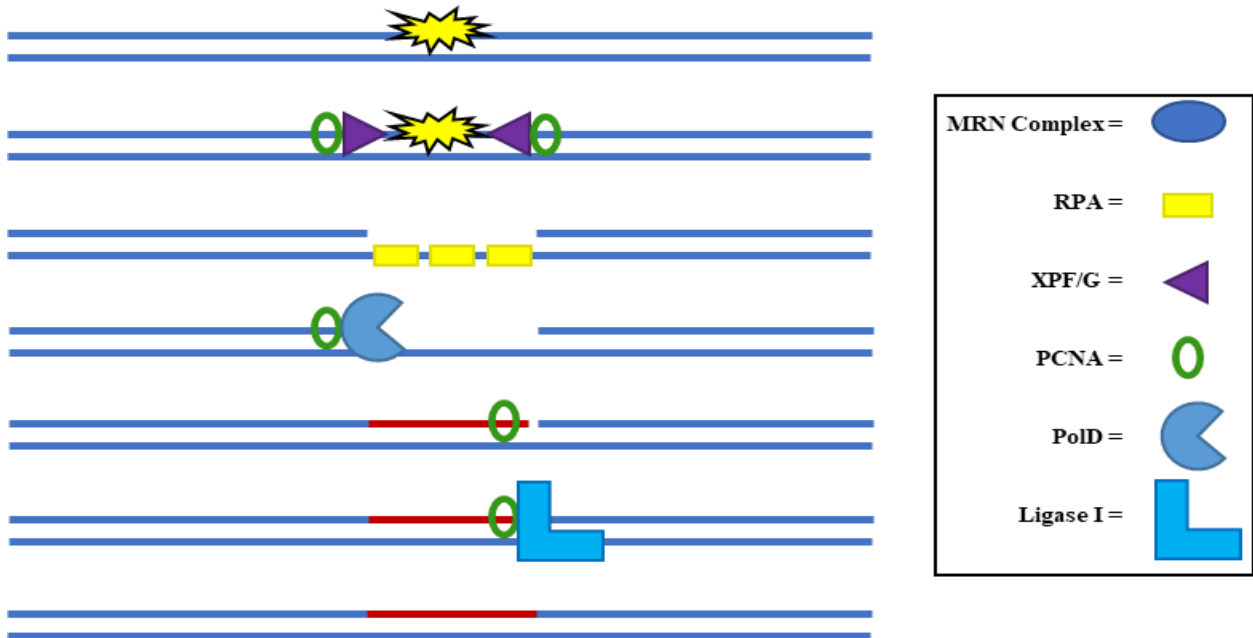


Figure 4.4: DNA Single-Strand Break Repair through Nucleotide Excision Repair

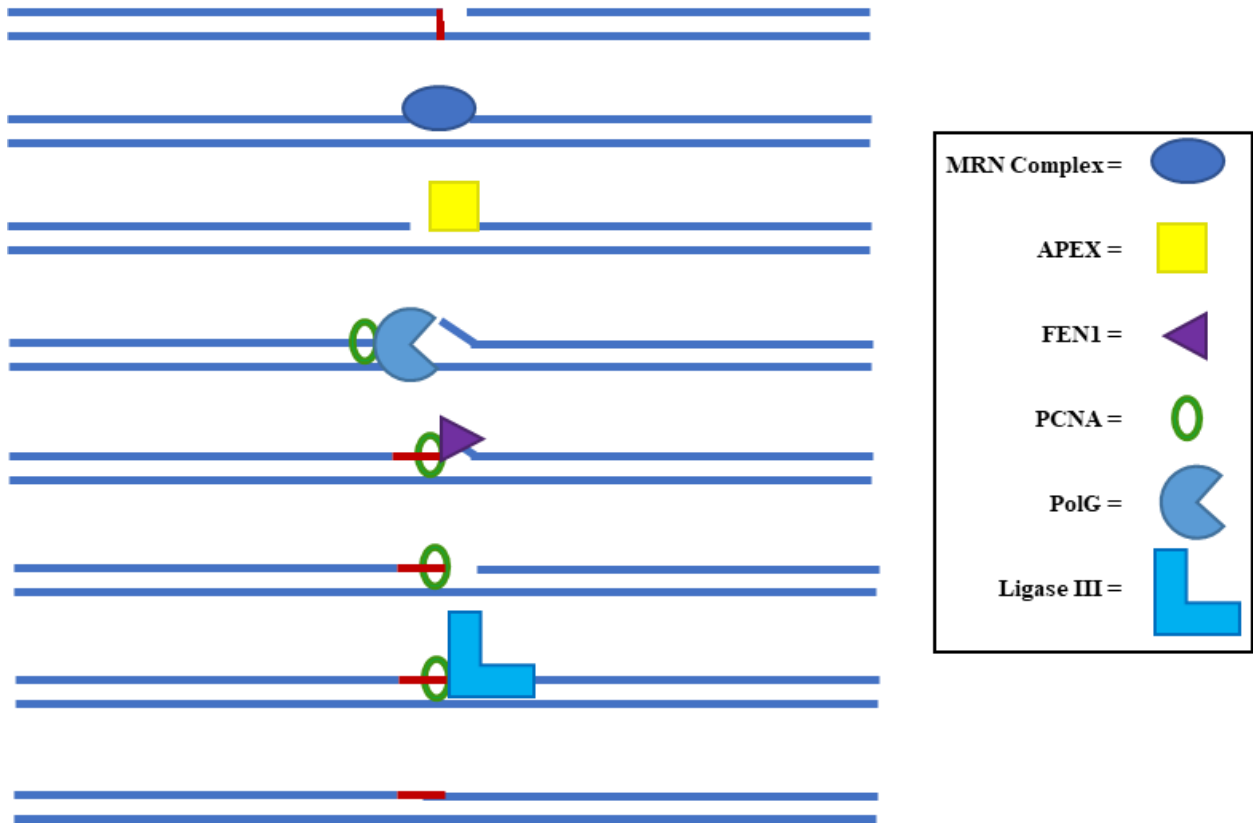


Figure 4.3: DNA Single-Strand Break Repair through Base Excision Repair

Directly measuring SSB repair of PCNA through alkaline comet assays or utilizing SSB-specific damaging agents are the first steps to be taken. If SSB damage is enhanced in the presence of PCNA inhibitors, further work focusing on interactors of PCNA in SSB repair, including APEX and XPG would be necessary.^{470,471}

4.2 Improving Process Network Mapping and Resolution

The process network maps created were able to capably separate synergistic and non-synergistic drug combinations through their disruption index (DI). While predictions of relative magnitude of synergism would be impactful, being able to describe antagonism specifically would be of greater impact. It would require additional descriptors for differentiation of changes in network dynamics. The equation developed for DI specifically highlights the disruption of the current network, as implied by the name. However, the disruption measured focuses on local features within a process and does not include a descriptor of overall network integrity and ability to accomplish a specific task. Instead, it is focused on the relative decreases in connectivity between and within processes. Still, as seen in many resistant tumors, a well-connected system is not required. Being able to define the minimal network necessary and to be able to understand likely areas of compensation would be required to evaluate resistant features.^{472,473} Including additional edge and node types would be able to describe the true connectivity of a network. As such, I recommend including both transcription factor and miRNA edges to define the regulation of the network by itself to articulate network plasticity. Further, more articulate descriptions of currently evaluated nodes and edges by likely functional significance through the formation of complexes and somatic mutations could describe the impact of gene expression.

4.2.1 Defining Node and Edge Activity as Discrete Groups through Known Complexes and Somatic Mutations

Due to the multiple functions of proteins and their interactions determining their functionality, defining proteins as discrete nodes is inaccurate. In my model, for expedience, each node was given similar influence over all nodes that they interacted with. In the case of underexpressed genes, the weighted eigenvector analysis reduces the influence genes connected to these can receive and impart. However, the loss of one interactor can enhance other interactors'

activities that are mutually exclusive, as in the case of some transcription factors.⁴⁷⁴ In this model, it is assumed that all interactions occur more or less simultaneously. To counter this feature of our model, proteins that act in concert with one another can also contribute to “compound nodes” representing a protein complex (Fig. 4.5A). Creating novel single node to represent a group of nodes is not a new concept or solution. However, the use of eigenvectors to expedite this calculation would be. Compound nodes are also often used to create sparse networks, whereas I would be doing so to make additional data points.

Another change in network structure would be to utilize the status of shared or unshared GO terms of proteins interacting with one another (Fig. 4.5B). Nodes’ GO commonality with their neighbors is data already collected to define GO Cohesion and Adhesion, allowing the model to evaluate inter-and intra-pathway regulation. GO commonality defines here how entire processes interact with one another on a large-scale. Understanding GO commonality as a local phenomenon can better define the influence of small groups of nodes instead of seeing them as the sum of disparate points. Furthermore, GO commonality can be utilized to determine which groups of genes should respond together rather than separately. The ability to gauge the capacity of the network to maintain connectivity despite disruption would allow for measurements of antagonism.

Somatic mutations are another feature that is not directly accounted for in this model. Many somatic mutations will cause downstream effects that can be observed in the gene expression profile. Loss-of-function (LOF) and gain-of-function (GOF) mutations can redefine the GO profile of a particular protein. Some somatic mutations cause changes in the protein's molecular function and others alter structural features necessary to bind to other proteins. The annotation required to define whether a somatic mutation changes just the GO profile or what edges exist could take considerable effort. However, several databases have compiled more common somatic mutations to expedite this process.^{475,476}

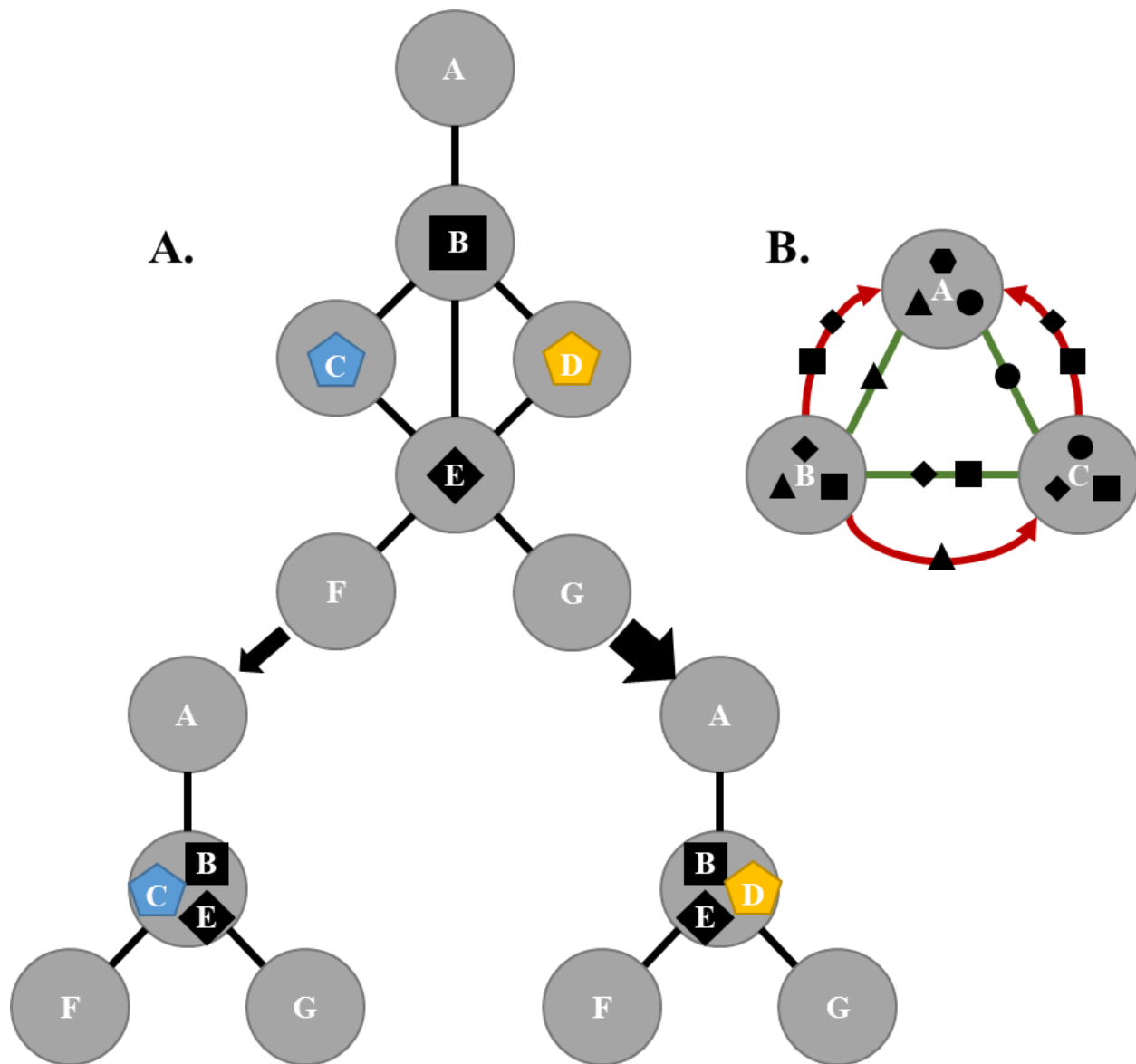


Figure 4.5: Additional Network Descriptor Model. A) Node complex model; nodes that can comprise a similar complex with interchangeable components can be modeled as a complex node. Complex nodes may possess different functions depending on the members of the complex. Overexpressed genes, designated in yellow, will be more favored over complexes including underexpressed genes, designated in blue. B) Node GO commonality can be used to described groups of nodes. Their uncommon GO terms can be used to describe the influence of nodes on other processes.

4.2.2 Introducing Transcription Factor and miRNA Networks to Create New Edges

Networks created solely on genetic data have been used to characterize disease pathology and drug responses.^{477,478} I utilized only gene expression in my networks and have also proposed

somatic mutation influences on the current node set. However, adding additional edges that are defined by a transcription factor's ability to increase or decrease the gene expression can also be used to understand influence (Fig. 4.6).⁴⁴⁷ The presence of transcription factor sets in the network can show a tumor's ability to react to certain inhibitors. Gene removal would no longer be utilized as a model for inhibition, but a fixed reduction of a target available to interact. A reduction in expression would then be able to be countered by increases in gene expression through this new model. This novel approach would require two networks to be created, one from the original data

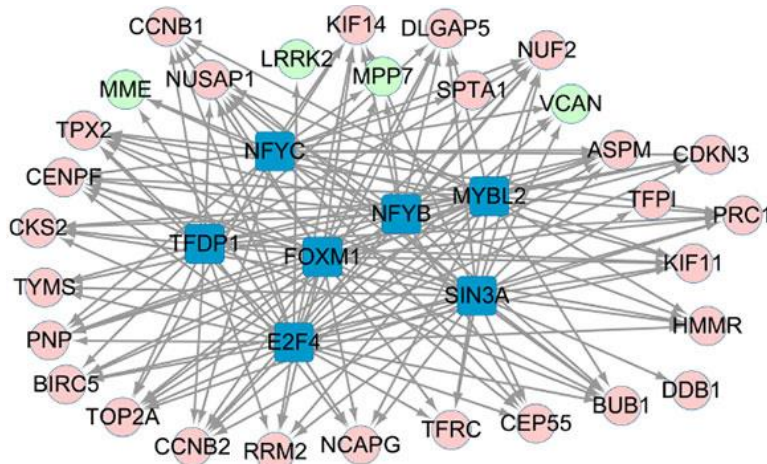


Figure 4.6: Representation of a Transcription Factor Network

and then an additional network of a simulated response through gene expression. A miRNA network could be added to these networks when the data are available. miRNA provides another key component to determining what regulation within the network may be able to compensate for changes due to inhibition. Even if a secondary network is not produced, the

presence of upregulated transcription factors and the loss of miRNA can be used to create an additional coefficient, a Resistance Index. The Resistance Index would represent the projected ability of a network to compensate for currently upregulated processes. An estimate of resistance potential would be key to predictions of antagonism and synergism and the emergence of drug resistance.

APPENDIX A. ADDITIONAL DATA CHARACTERIZING PCNA INHIBITORS OR CLASSES' MECHANISMS OF ACTION

Table A.1: PCNA Inhibitor GI₅₀ Values in Combination with DNA Damaging Agents

Treatment	<i>HCC1937</i>			<i>MDA-MB-231</i>			<i>MDA-MB-436</i>			<i>MDA-MB-468</i>		
	GI50 (μM)	SD	1/CI	GI50 (μM)	SD	1/CI	GI50 (μM)	SD	1/CI	GI50 (μM)	SD	1/CI
T2AA	>100	NA	NA	>100	NA	NA	>100	NA	NA	>100	NA	NA
AOH39	2.72	0.26	NA	2.31	0.24	NA	2.24	0.21	NA	1.89	0.24	NA
AOH1160	0.23	0.02	NA	0.18	0.03	NA	0.19	0.03	NA	0.18	0.02	NA
T2AA-NEal-NPip (TEP)	>100	NA	NA	>100	NA	NA	>100	NA	NA	>100	NA	NA
NLys-NPip-NBal (LPB)	>100	NA	NA	>100	NA	NA	>100	NA	NA	>100	NA	NA
NLys-NPip-NTyr (LPT)	>100	NA	NA	>100	NA	NA	>100	NA	NA	>100	NA	NA
Doxorubicin (Dox)	25.1	2.10	NA	53.2	4.26	NA	1.86	0.19	NA	9.23	1.26	NA
Dox+30 μM T2AA	1.72	0.17	4.58	0.61	0.09	6.2	1.21	0.14	1.25	1.2	0.16	3.58
Dox+0.2 μM*AOH39	0.9	0.08	2.71	0.28	0.04	2.94	0.18	0.03	2.33	0.6	0.08	2.52
Dox+0.01 μM*AOH1160	0.6	0.09	2.8	0.29	0.04	2.96	0.24	0.03	2.17	0.7	0.07	2.45
Dox+30 μM TEP	1.9	0.16	4.44	1.6	0.22	5.56	1.54	0.16	1.07	1	0.10	3.88
Dox+30 μM LPB	2.2	0.27	4.21	1.8	0.26	5.44	1.56	0.25	1	1.2	0.13	3.58
Dox+30 μM LPT	2.8	0.33	3.83	2.1	0.21	5.28	1.6	0.23	0.99	1.1	0.09	3.72
KU55933	33.1	3.08	NA	35.5	4.68	NA	47.1	7.38	NA	38.1	4.89	NA
KU55933+30 μM T2AA	30.5	3.83	0.94	34.5	3.48	0.9	45.8	4.32	0.9	36.3	3.53	0.91
KU55933+0.2 μM*AOH39	7.3	0.85	1.81	8.2	0.78	1.78	32.4	2.86	0.98	8.4	1.16	1.81
KU55933+0.01 μM*AOH1160	6.9	0.57	1.85	9.8	1.39	1.65	30.8	2.77	1.02	7.3	0.93	1.91
KU55933+30 μM TEP	31.3	4.62	0.92	34.8	5.34	0.89	46.1	5.78	0.89	35.1	3.84	0.94
KU55933+30 μM LPB	32.1	3.79	0.9	35.2	5.42	0.88	46.9	6.63	0.88	34.6	4.03	0.95
KU55933+30 μM LPT	32.4	5.04	0.89	30.6	4.46	0.99	44.8	6.62	0.91	35.2	5.39	0.94
NU7026	61.5	9.10	NA	55.1	8.61	NA	4.5	0.44	NA	58.7	8.01	NA
NU7026+30 μM T2AA	7.4	0.64	3.7	6.5	0.74	3.74	5.2	0.50	0.77	7.4	0.78	3.63
NU7026+0.2 μM*AOH39	6.2	0.75	2.31	7.1	0.59	2.17	1.3	0.18	1.61	3.3	0.44	2.57
NU7026+0.01 μM*AOH1160	5.9	0.56	2.33	6.9	1.02	2.19	1	0.14	1.8	2.9	0.43	2.62
NU7026+30 μM TEP	8.1	1.08	3.55	7	0.65	3.61	4.3	0.68	0.91	8.3	0.72	3.44
NU7026+30 μM LPB	8.5	1.31	3.47	7.4	0.63	3.52	4.7	0.38	0.84	9.9	1.03	3.14
NU7026+30 μM LPT	8.4	1.23	3.49	7.3	0.75	3.54	5.1	0.70	0.78	8.8	0.83	3.34
Olaparib	>100	NA	NA	6.3	0.52	NA	1.1	0.09	NA	8.4	0.75	NA
Olaparib+30 μM T2AA	4.6	0.66	5.31	0.85	0.13	3.51	0.99	0.14	0.96	1.2	0.12	3.42
Olaparib+0.2 μM*AOH39	6.8	0.58	2.57	0.92	0.12	2.09	0.23	0.02	1.85	0.91	0.12	2.27
Olaparib+0.01 μM*AOH1160	5.5	0.54	2.64	0.91	0.09	2.1	0.25	0.03	1.79	0.89	0.10	2.28
Olaparib+30 μM TEP	5.3	0.45	5.16	1	0.14	3.24	1	0.11	0.95	1.6	0.15	2.94
Olaparib+30 μM LPB	5.9	0.86	5.03	1.1	0.11	3.09	1	0.11	0.95	2.1	0.25	2.5
Olaparib+30 μM LPT	6.2	0.82	4.96	1.2	0.17	2.94	1.1	0.10	0.87	2.3	0.22	2.36

Table A.2: PCNA Inhibitor LD₅₀ Values in Combination with DNA Damaging Agents and DNA Repair Inhibitors

Treatment	<i>HCC1937</i>			<i>MDA-MB-231</i>			<i>MDA-MB-436</i>			<i>MDA-MB-468</i>		
	LD50 (μM)	SD	1/CI	LD50 (μM)	SD	1/CI	LD50 (μM)	SD	1/CI	LD50 (μM)	SD	1/CI
T2AA	>100	NA	NA	>100	NA	NA	>100	NA	NA	>100	NA	NA
AOH39	26.72	3.64	NA	22.1	3.47	NA	24.5	2.20	NA	20.9	2.57	NA
AOH1160	12.9	1.40	NA	11.4	1.72	NA	10.2	1.09	NA	10.3	1.19	NA
T2AA-NEal-NPip (TEP)	>100	NA	NA	>100	NA	NA	>100	NA	NA	>100	NA	NA
NLys-NPip-NBal (LPB)	>100	NA	NA	>100	NA	NA	>100	NA	NA	>100	NA	NA
NLys-NPip-NTyr (LPT)	>100	NA	NA	>100	NA	NA	>100	NA	NA	>100	NA	NA
Doxorubicin (Dox)	136 nM	16.4	NA	1.18	0.15	NA	1.05	0.10	NA	99.1 nM	14.3	NA
Dox+30 μM T2AA	6.72 nM	0.54	5.02	13.6 nM	2.14	6.2	181 nM	18.4	3.11	11.3 nM	1.13	3.79
Dox+0.2 μM*AOH39	4.91 nM	0.52	2.71	1.94 nM	0.22	2.99	60.2 nM	7.25	2.56	0.62 nM	0.07	3
Dox+0.01 μM*AOH1160	2.16 nM	0.21	2.87	2.05 nM	0.32	2.99	81.2 nM	10.5	2.44	0.75 nM	0.06	3
Dox+30 μM TEP	9.12 nM	0.85	4.61	17.7 nM	2.10	6.07	870 nM	98.7	1.03	1.04 nM	0.11	6.24
Dox+30 μM LPB	12.5 nM	1.99	4.14	20.8 nM	2.13	5.97	902 nM	136	1	1.23 nM	0.18	6.16
Dox+30 μM LPT	14.1 nM	2.05	3.95	26.1 nM	3.35	5.81	940 nM	110	0.96	1.17 nM	0.11	6.19
KU55933 (ATM)	>100	NA	NA	65.3	6.93	NA	>100	NA	NA	52.4	8.32	NA
KU55933+30 μM T2AA	>100	NA	NA	>100	NA	NA	>100	NA	NA	>100	NA	NA
KU55933+0.2 μM*AOH39	35.6	4.20	1.96	42.1	6.39	1.03	91.4	9.41	1.27	45.6	5.52	0.91
KU55933+0.01 μM*AOH1160	30.2	2.58	2.07	49.1	7.49	0.93	85.4	10.2	1.32	34.1	4.76	1.02
KU55933+30 μM TEP	>100	NA	NA	>100	NA	NA	>100	NA	NA	>100	NA	NA
KU55933+30 μM LPB	>100	NA	NA	>100	NA	NA	>100	NA	NA	>100	NA	NA
KU55933+30 μM LPT	>100	NA	NA	>100	NA	NA	>100	NA	NA	>100	NA	NA
NU7026 (PRKDC)	>100	NA	NA	>100	NA	NA	80.5	8.21	NA	>100	NA	NA
NU7026+30 μM T2AA	40.1	4.05	2.86	36.2	3.36	3.03	28.1	2.55	2.01	42.2	3.84	2.78
NU7026+0.2 μM*AOH39	32.2	2.69	2.03	37.4	5.54	1.93	15.1	1.53	1.92	20.2	3.16	2.31
NU7026+0.01 μM*AOH1160	28.7	2.92	2.1	35.8	5.24	1.96	11.2	1.67	2.12	16.2	2.08	2.42
NU7026+30 μM TEP	43.8	3.66	2.72	39.2	5.50	2.9	23.7	3.20	2.26	50.3	7.44	2.5
NU7026+30 μM LPB	52.5	5.57	2.43	41.5	5.80	2.8	25.1	2.13	2.17	68.7	5.63	2.03
NU7026+30 μM LPT	56.1	8.26	2.33	38	4.86	2.95	30.2	2.80	1.91	56.9	6.70	2.31
Olaparib (PARP1)	>100	NA	NA	50.1	6.71	NA	4.1	0.46	NA	43.1	6.88	NA
Olaparib+30 μM T2AA	12.6	1.04	4.7	3.22	0.44	4.67	3.6	0.36	0.98	2.44	0.22	4.84
Olaparib+0.2 μM*AOH39	25.4	2.40	2.18	4.66	0.54	2.35	0.98	0.09	1.75	2.05	0.16	2.63
Olaparib+0.01 μM*AOH1160	18.1	1.70	2.36	4.31	0.66	2.39	0.87	0.10	1.84	2.15	0.34	2.61
Olaparib+30 μM TEP	15.3	2.37	4.42	6.15	0.90	3.67	3.85	0.55	0.92	6.21	0.74	3.41
Olaparib+30 μM LPB	22.4	1.89	3.82	6.02	0.86	3.71	4.01	0.61	0.89	8.45	1.04	2.89
Olaparib+30 μM LPT	24.7	3.93	3.66	8.21	0.99	3.19	3.91	0.59	0.91	7.89	0.85	3.01

Table A.3: PCNA Inhibitor Effects on DNA Damage in Combination with DNA Damaging Agents and DNA Repair Inhibitors

Treatment	<i>HCC1937</i>			<i>MDA-MB-231</i>			<i>MDA-MB-436</i>			<i>MDA-MB-468</i>		
	% DNA Tail	SD	% No Dmg	% DNA Tail	SD	% No Dmg	% DNA Tail	SD	% No Dmg	% DNA Tail	SD	% No Dmg
Vehicle	4.6	0.48	98.1	4.5	0.39	98.1	5.1	0.50	97.5	4.2	0.60	98.6
T2AA	4.5	0.59	97.9	4.3	0.42	99.2	5.4	0.47	97.4	4.8	0.63	98.4
AOH39	8.3	0.92	73.2	7.1	0.77	82.3	7.1	0.87	82.1	7.5	0.67	79.6
AOH1160	8.2	0.67	74.1	8.4	0.76	72.9	6.9	1.01	84	7.8	1.07	77
T2AA-NEal-NPip (TEP)	4.7	0.55	97.8	4.3	0.46	99.2	5.3	0.64	99	4.9	0.47	98.3
NLys-NPip-NBal (LPB)	5	0.78	97.5	4	0.62	99.9	5.45	0.46	97.4	5.3	0.51	99.5
NLys-NPip-NTyr (LPT)	5.1	0.57	98.1	4.1	0.59	99.6	5.35	0.54	98.5	4.9	0.63	98.2
KU55933 (ATM) ~25 uM	12.6	1.92	49.6	14.5	1.98	41.6	8.7	1.29	70.7	24.6	3.07	11.4
KU55933+30 uM T2AA	13.4	1.46	46.1	14.5	1.51	41.8	7.4	0.96	80.3	24.4	2.05	11.9
KU55933+229 nM*AOH39	20.9	3.09	20.8	20.6	1.81	21.6	16.3	1.51	34.9	30.1	2.45	0.46
KU55933+19.5 nM*AOH1160	24.1	3.53	12.6	20.7	2.52	21.2	17.6	2.52	30.5	31.5	4.39	0.32
KU55933+30 uM TEP	13.6	1.75	45.2	17.4	2.06	31.1	8.2	1.01	74.4	23.5	2.72	14.2
KU55933+30 uM LPB	13.6	1.90	45.5	17.2	2.60	31.8	7.9	0.74	75.8	23.4	2.44	14.4
KU55933+30 uM LPT	14.1	1.50	43.2	17.4	2.56	31.2	8.2	1.30	74	25.1	3.64	10.4
NU7026 (PRKDC) ~30 uM	9.7	0.88	64.8	15.1	1.70	39.4	21.9	2.24	18	15.6	2.20	37.4
NU7026+30 uM T2AA	18.3	2.54	28.4	24.4	2.42	12	22.4	1.83	16.9	34.2	5.15	0.15
NU7026+229 nM*AOH39	19.4	2.19	25	24.6	3.29	11.4	30.8	4.29	0.53	31.1	3.23	0.23
NU7026+19.5 nM*AOH1160	20.5	2.05	21.9	25.4	2.86	9.6	31.2	3.03	0.47	32.2	4.08	0.71
NU7026+30 uM TEP	19.2	2.14	25.6	22.7	2.31	16.1	20.9	2.01	20.8	34.8	4.87	0.74
NU7026+30 uM LPB	17.4	2.63	31.2	23.9	3.03	13.1	21.5	2.28	19.2	35.7	5.31	0.09
NU7026+30 uM LPT	18.1	2.02	29	23.8	2.24	13.3	23.2	2.36	14.8	32.4	3.29	0.76
Olaparib (PARP1) ~5 uM	5.5	0.71	96.8	10.5	0.91	59.9	23.1	3.28	15	15.1	1.34	39.4
Olaparib+30 uM T2AA	23.3	2.48	14.6	24.8	3.72	11	24.7	2.87	11.2	38.3	5.58	0.23
Olaparib+229 nM*AOH39	22.4	2.80	16.8	27.2	3.07	5.8	32.3	3.07	0.14	40.2	3.79	0.49
Olaparib+19.5 nM*AOH1160	23.5	3.61	14.1	26.9	2.43	6.3	32.9	2.72	0.47	41.7	4.18	0.54
Olaparib+30 uM TEP	24.2	2.88	12.4	24.9	2.43	10.7	25.6	3.94	9.2	39.7	3.64	0.73
Olaparib+30 uM LPB	25.4	2.41	9.7	25.4	3.06	9.7	25.2	2.74	10	38.2	5.91	0.46
Olaparib+30 uM LPT	23.1	3.39	15.1	24.8	3.78	11.1	25.5	3.72	9.4	38.1	3.82	0.68

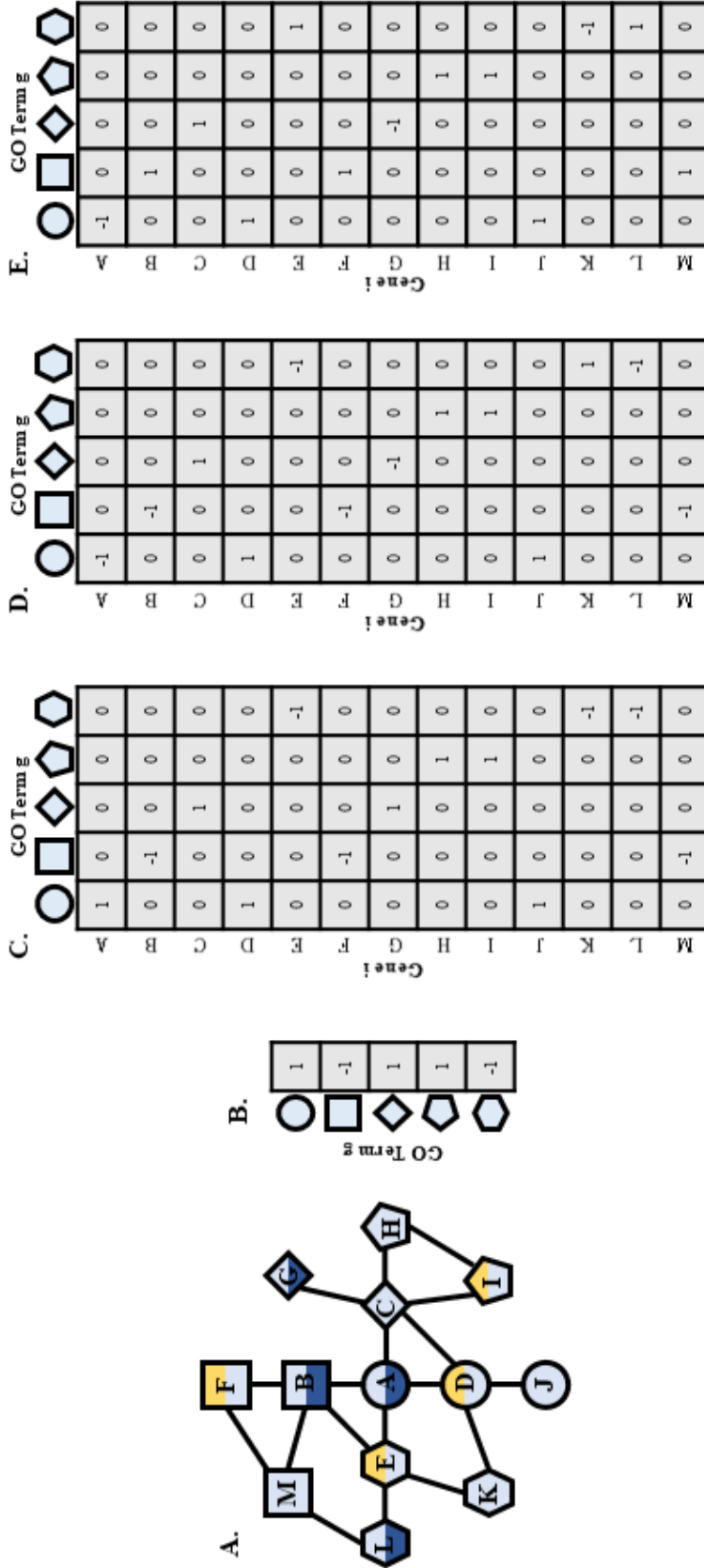
Table A.4: PCNA Inhibitor Effects on Replication

Treatment	<i>MDA-MB-231</i>						<i>MDA-MB-436</i>						<i>MDA-MB-468</i>					
	%G1	SD	%S	SD	%G2	SD	%G1	SD	%S	SD	%G2	SD	%G1	SD	%S	SD	%G2	SD
30 μ M T2AA	0.18	0.02	10.3	1.04	89.5	8.51	0.29	0.03	12.9	2.03	86.8	8.95	0.34	0.04	11.6	1.22	88.1	12.6
0.2 μ M*AOH39	0.62	0.07	1.31	0.15	98.1	8.23	0.33	0.04	1.75	0.21	87.9	8.08	0.55	0.06	1.48	0.20	84.7	13.3
0.01 μ M*AOH1160	0.33	0.03	2.65	0.29	97	13.4	0.25	0.02	1.56	0.15	84.2	7.77	0.44	0.04	1.47	0.15	83.9	12.2
30 μ M T2AA-NEal-NPip (TEP)	0.45	0.06	1.87	0.20	97.7	15.3	0.17	0.01	1.43	0.20	85.6	10.3	0.37	0.03	1.14	0.13	88.3	11.7
30 μ M NLys -NPip -NBal (LPB)	0.18	0.02	1.11	0.12	98.7	11.7	0.17	0.03	1.35	0.11	98.5	8.28	0.06	0.01	1.09	0.10	89	12.2
30 μ M NLys -NPip -NTyr (LPT)	0.16	0.02	1.41	0.13	98.4	14.6	0.39	0.04	1.27	0.19	98.3	14.1	0.11	0.01	0.65	0.10	91.2	11.2
Doxorubicin (Dox)	22	3.35	69.3	9.53	8.7	0.95	26.7	3.81	63.9	7.07	9.41	1.23	44.1	6.24	47.1	6.56	8.82	0.87
Dox+30 μ M T2AA	42.1	5.65	53.9	6.88	3.9	0.33	36.5	5.61	58.9	6.44	4.56	0.50	51.3	5.54	46.4	3.73	2.31	0.33
Dox+0.2 μ M*AOH39	56.1	6.47	42.2	4.19	1.7	0.20	68.2	7.91	29.1	3.19	2.67	0.29	73.4	10.8	24.6	3.59	1.99	0.30
Dox+0.01 μ M*AOH1160	62.3	9.37	35.2	3.36	2.5	0.31	71.3	6.85	25.4	2.43	3.31	0.49	82.9	12.5	15.1	1.57	2.01	0.23
Dox+30 μ M TEP	36.2	5.14	60.7	7.93	3.1	0.48	29.4	3.50	62.3	6.08	8.35	1.06	48.8	4.63	47.1	4.04	4.11	0.54
Dox+30 μ M LPB	35.1	2.91	61.2	8.51	3.7	0.57	27.5	3.10	64.3	9.59	8.22	1.31	50.1	7.10	46.1	6.82	3.81	0.42
Dox+30 μ M LPT	37.8	4.21	57.9	7.48	4.3	0.50	29.1	3.59	63	5.11	7.95	1.16	49.2	7.22	46.7	6.30	4.03	0.60
KU55933	0	0.00	57.8	5.23	42.2	5.55	0	0.00	59.3	6.85	40.7	3.76	0	0.00	51.4	6.19	48.6	3.98
KU55933+30 μ M T2AA	0	0.00	89.6	13.7	10.4	1.20	0	0.00	78.6	8.16	21.4	2.28	0	0.00	90	10.7	10	1.37
KU55933 +0.2 μ M*AOH39	0	0.00	55.6	5.82	44.4	6.84	0	0.00	53.1	6.39	46.9	6.28	0	0.00	55.6	8.20	44.4	4.10
KU55933 +0.01 μ M*AOH1160	0	0.00	52.1	8.25	47.9	7.07	0	0.00	51.7	5.34	48.3	6.21	0	0.00	52.1	7.90	47.9	5.96
KU55933 +30 μ M TEP	0	0.00	50.9	5.87	49.1	4.53	0	0.00	56.2	4.76	43.8	4.17	0	0.00	50.9	4.59	49.1	7.26
KU55933 +30 μ M LPB	0	0.00	53.6	4.57	46.4	7.30	0	0.00	57.1	7.43	42.9	6.69	0	0.00	53.6	6.09	46.4	5.04
KU55933 +30 μ M LPT	0	0.00	51.4	7.24	48.6	5.99	0	0.00	55.3	7.97	44.7	3.69	0	0.00	51.4	6.25	48.6	4.85
NU7026	0.36	0.03	37.9	3.22	61.7	8.06	0.22	0.03	43.1	5.99	56.7	5.80	0.61	0.09	39.1	5.36	60.2	9.16
NU7026 +30 μ M T2AA	15.2	1.53	71.9	11.1	12.9	1.26	0.55	0.05	45.3	5.40	54.2	8.50	18.1	2.15	69.5	5.80	12.4	1.09
NU7026 +0.2 μ M*AOH39	30.3	4.37	25.2	2.80	44.5	4.86	16.2	2.36	39.2	3.21	44.6	6.01	33.1	2.95	27.2	3.23	39.7	6.20
NU7026 +0.01 μ M*AOH1160	35.6	5.17	22.4	2.88	42	6.30	18.1	1.83	38.3	3.38	43.6	4.83	30.8	3.63	28.9	4.54	40.3	6.10
NU7026 +30 μ M TEP	18.7	2.90	48.1	6.52	33.2	2.68	0.28	0.04	40.1	3.34	59.6	7.21	14.3	1.89	38.1	4.41	47.6	5.38
NU7026 +30 μ M LPB	19.2	2.32	52.3	6.75	28.5	2.34	0.47	0.04	46.3	4.62	53.2	4.42	13.1	1.07	37.8	4.72	49.1	6.32
NU7026 +30 μ M LPT	18.4	2.85	49.1	6.75	32.5	4.85	0.33	0.03	44.7	4.99	54.9	7.62	11.5	1.08	35.6	3.16	52.9	6.11
Olaparib	0.27	0.02	29.4	4.70	70.3	7.04	0.31	0.03	35.1	4.68	64.5	6.96	0.61	0.07	22.8	1.84	76.5	6.47
Olaparib +30 μ M T2AA	22.3	2.67	73.4	9.72	4.3	0.45	0.78	0.10	60.3	5.73	38.9	3.14	23.4	2.35	70.8	8.16	5.8	0.80
Olaparib +0.2 μ M*AOH39	33.1	2.89	27.1	2.25	39.8	6.32	20.3	2.57	34.3	4.59	45.4	6.36	33.1	3.40	27.1	3.72	39.8	4.68
Olaparib +0.01 μ M*AOH1160	41.2	4.83	26.2	3.72	32.6	4.32	22.6	2.95	36.1	5.68	41.3	3.87	41.2	3.86	26.2	3.93	32.6	5.14
Olaparib +30 μ M TEP	15.1	2.11	40.1	5.34	44.8	4.21	0.88	0.10	34.1	4.61	65	8.33	18.6	1.94	36.1	3.38	45.3	3.69
Olaparib +30 μ M LPB	17.2	2.41	38.3	5.95	44.5	4.09	0.45	0.06	36.3	4.58	63.2	9.12	14.6	2.30	30	2.68	55.4	8.86
Olaparib +30 μ M LPT	16.8	2.12	39.7	5.82	43.5	6.01	0.12	0.02	34.9	3.51	64.9	8.23	15.4	2.13	36.5	4.98	48.1	5.70

Table A.5: PCNA Inhibitor Effects on UV Damage Tolerance within S Phase

Treatment	<i>MDA-MB-231</i>						<i>MDA-MB-436</i>						<i>MDA-MB-468</i>					
	%G1	SD	%S	SD	%G2	SD	%G1	SD	%S	SD	%G2	SD	%G1	SD	%S	SD	%G2	SD
30 μ M T2AA	0.18	0.02	10.3	0.89	89.5	11.3	0.29	0.03	12.9	1.56	86.8	13.2	0.34	0.04	11.6	1.34	88.1	7.29
0.2 μ M*AOH39	0.62	0.06	1.31	0.19	98.1	13.5	0.33	0.05	1.75	0.23	87.9	10.0	0.55	0.06	1.48	0.15	84.7	8.92
0.01 μ M*AOH1160	0.33	0.03	2.65	0.29	97	14.9	0.25	0.04	1.56	0.21	84.2	8.41	0.44	0.05	1.47	0.20	83.9	8.19
30 μ M T2AA-NEal-NPip (TEP)	0.45	0.07	1.87	0.15	97.7	10.5	0.17	0.02	1.43	0.23	85.6	12.5	0.37	0.05	1.14	0.11	88.3	11.8
30 μ M NLys-NPip-NBal (LPB)	0.18	0.02	1.11	0.13	98.7	13.2	0.17	0.02	1.35	0.15	98.5	10.4	0.06	0.01	1.09	0.12	89	12.6
30 μ M NLys-NPip-NTyr (LPT)	0.16	0.02	1.41	0.21	98.4	15.3	0.39	0.06	1.27	0.16	98.3	8.52	0.11	0.01	0.65	0.06	91.2	10.1
Doxorubicin	22	2.21	69.3	8.90	8.7	0.81	26.7	2.38	63.9	9.79	9.41	0.94	44.1	5.32	47.1	5.93	8.82	0.79
Dox+30 μ M T2AA	42.1	4.22	53.9	6.20	3.9	0.45	36.5	4.52	58.9	6.58	4.56	0.69	51.3	5.86	46.4	4.23	2.31	0.20
Dox+0.2 μ M*AOH39	56.1	5.70	42.2	4.36	1.7	0.25	68.2	10.2	29.1	3.87	2.67	0.32	73.4	6.12	24.6	2.26	1.99	0.27
Dox+0.01 μ M*AOH1160	62.3	6.69	35.2	3.46	2.5	0.33	71.3	6.99	25.4	3.07	3.31	0.53	82.9	7.99	15.1	1.87	2.01	0.31
Dox+30 μ M TEP	36.2	3.68	60.7	6.59	3.1	0.46	29.4	3.67	62.3	9.59	8.35	0.92	48.8	7.01	47.1	4.97	4.11	0.48
Dox+30 μ M LPB	35.1	4.70	61.2	8.02	3.7	0.35	27.5	2.20	64.3	7.49	8.22	0.74	50.1	4.23	46.1	5.62	3.81	0.59
Dox+30 μ M LPT	37.8	3.09	57.9	5.87	4.3	0.51	29.1	4.02	63	8.20	7.95	0.80	49.2	4.36	46.7	7.16	4.03	0.54
KU55933	0	0.00	57.8	7.93	42.2	3.87	0	0.00	59.3	6.25	40.7	5.03	0	0.00	51.4	6.21	48.6	6.78
KU55933+30 μ M T2AA	0	0.00	89.6	12.6	10.4	0.85	0	0.00	78.6	10.9	21.4	2.67	0	0.00	90	12.1	10	1.44
KU55933+0.2 μ M*AOH39	0	0.00	55.6	7.86	44.4	4.01	0	0.00	53.1	6.75	46.9	6.36	0	0.00	55.6	6.78	44.4	6.05
KU55933+0.01 μ M*AOH1160	0	0.00	52.1	6.81	47.9	4.71	0	0.00	51.7	4.47	48.3	5.48	0	0.00	52.1	8.21	47.9	6.18
KU55933+30 μ M TEP	0	0.00	50.9	7.70	49.1	6.79	0	0.00	56.2	7.93	43.8	3.93	0	0.00	50.9	7.30	49.1	4.67
KU55933+30 μ M LPB	0	0.00	53.6	6.63	46.4	4.14	0	0.00	57.1	6.58	42.9	4.80	0	0.00	53.6	5.11	46.4	4.20
KU55933+30 μ M LPT	0	0.00	51.4	5.31	48.6	5.78	0	0.00	55.3	8.57	44.7	5.81	0	0.00	51.4	6.01	48.6	5.41
NU7026	0.36	0.05	37.9	5.12	61.7	6.42	0.22	0.03	43.1	4.39	56.7	6.15	0.61	0.07	39.1	6.20	60.2	8.51
NU7026+30 μ M T2AA	15.2	2.01	71.9	10.2	12.9	1.49	0.55	0.07	45.3	3.97	54.2	4.81	18.1	2.64	69.5	6.99	12.4	1.01
NU7026+0.2 μ M*AOH39	30.3	3.30	25.2	3.38	44.5	6.69	16.2	2.37	39.2	6.00	44.6	6.94	33.1	3.60	27.2	2.75	39.7	4.66
NU7026+0.01 μ M*AOH1160	35.6	4.04	22.4	2.73	42	5.70	18.1	1.81	38.3	6.09	43.6	5.26	30.8	4.21	28.9	4.39	40.3	5.40
NU7026+30 μ M TEP	18.7	2.22	48.1	5.99	33.2	2.83	0.28	0.04	40.1	5.78	59.6	7.95	14.3	1.59	38.1	4.06	47.6	5.79
NU7026+30 μ M LPB	19.2	3.01	52.3	5.04	28.5	2.68	0.47	0.06	46.3	4.95	53.2	6.14	13.1	1.51	37.8	5.09	49.1	6.17
NU7026+30 μ M LPT	18.4	2.37	49.1	4.55	32.5	4.65	0.33	0.04	44.7	6.47	54.9	5.07	11.5	1.78	35.6	3.96	52.9	8.42
Olaparib	0.27	0.04	29.4	2.98	70.3	11.0	0.31	0.05	35.1	4.61	64.5	8.53	0.61	0.05	22.8	2.70	76.5	11.2
Olaparib+30 μ M T2AA	22.3	1.83	73.4	8.39	4.3	0.35	0.78	0.09	60.3	5.14	38.9	4.37	23.4	2.83	70.8	11.1	5.8	0.47
Olaparib+0.2 μ M*AOH39	33.1	4.02	27.1	3.68	39.8	5.50	20.3	2.93	34.3	4.46	45.4	3.99	33.1	4.83	27.1	2.33	39.8	6.00
Olaparib+0.01 μ M*AOH1160	41.2	3.78	26.2	2.70	32.6	4.26	22.6	2.78	36.1	3.13	41.3	5.78	41.2	5.41	26.2	3.70	32.6	3.08
Olaparib+30 μ M TEP	15.1	2.23	40.1	5.17	44.8	5.10	0.88	0.12	34.1	5.17	65	7.97	18.6	2.27	36.1	2.94	45.3	7.09
Olaparib+30 μ M LPB	17.2	1.48	38.3	3.88	44.5	6.60	0.45	0.04	36.3	5.01	63.2	10.0	14.6	1.17	30	4.37	55.4	7.88
Olaparib 30 μ M LPT	16.8	2.55	39.7	6.18	43.5	4.25	0.12	0.01	34.9	3.27	64.9	9.64	15.4	2.31	36.5	4.79	48.1	5.37

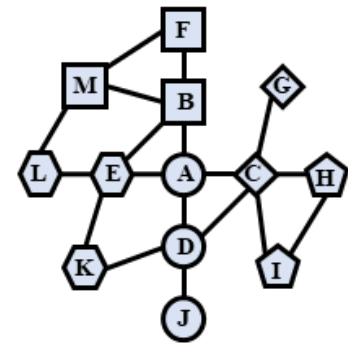
APPENDIX B: ADDITIONAL GRAPHS AND MATRICES DESCRIBING PROCESS NETWORKS



Scheme B.1: Measuring Impact of Genes on Processes; A) This network model provides the basis for these matrices. The half-yellow markings represents activation of a process and half-blue denotes the deactivation of a process. B) The GO Influence Matrix designates whether the GO term generally contributes positively or negatively to the selected phenotype. C) The Gene-GO Influence Matrix translates GO influence values over all genes in the network. D) The Gene-GO Regulation Matrix utilizes regulatory GO terms of each gene to determine whether a gene positively or negatively contributes to the process's regulation. E) The Gene-GO Impact Matrix assesses whether the overall influence and regulatory capabilities of a gene generally contributes to or subtracts from the relevant process.

Interaction Matrix

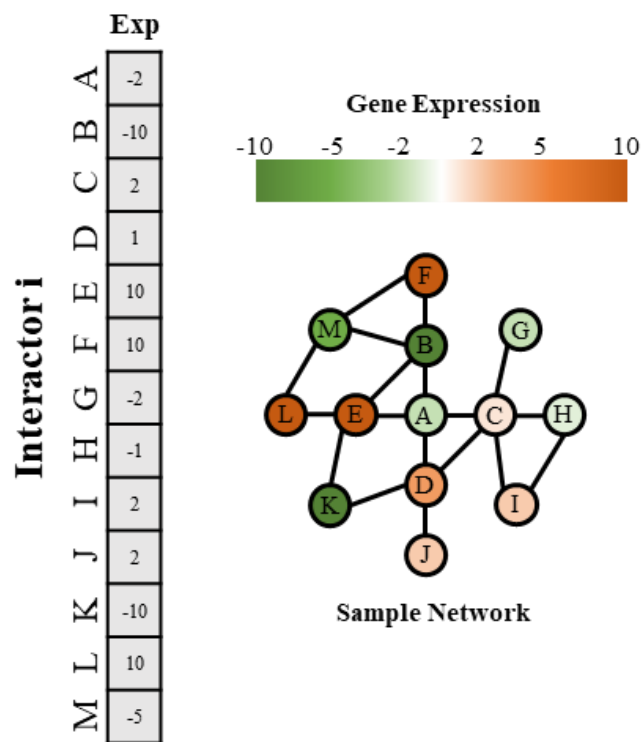
		Interactor j												
		A	B	C	D	E	F	G	H	I	J	K	L	M
Interactor i	A	-	1	1	1	1	0	0	0	0	0	0	0	0
	B	-	-	0	0	1	1	0	0	0	0	0	0	1
	C	-	-	-	1	0	0	1	1	1	0	0	0	0
	D	-	-	-	-	0	0	0	0	0	1	1	0	0
	E	-	-	-	-	-	0	0	0	0	0	1	1	0
	F	-	-	-	-	-	-	0	0	0	0	0	0	1
	G	-	-	-	-	-	-	-	0	0	0	0	0	0
	H	-	-	-	-	-	-	-	-	0	1	0	0	0
	I	-	-	-	-	-	-	-	-	-	0	0	0	0
	J	-	-	-	-	-	-	-	-	-	-	0	0	0
	K	-	-	-	-	-	-	-	-	-	-	-	0	0
	L	-	-	-	-	-	-	-	-	-	-	-	-	1
	M	-	-	-	-	-	-	-	-	-	-	-	-	-



Sample Network

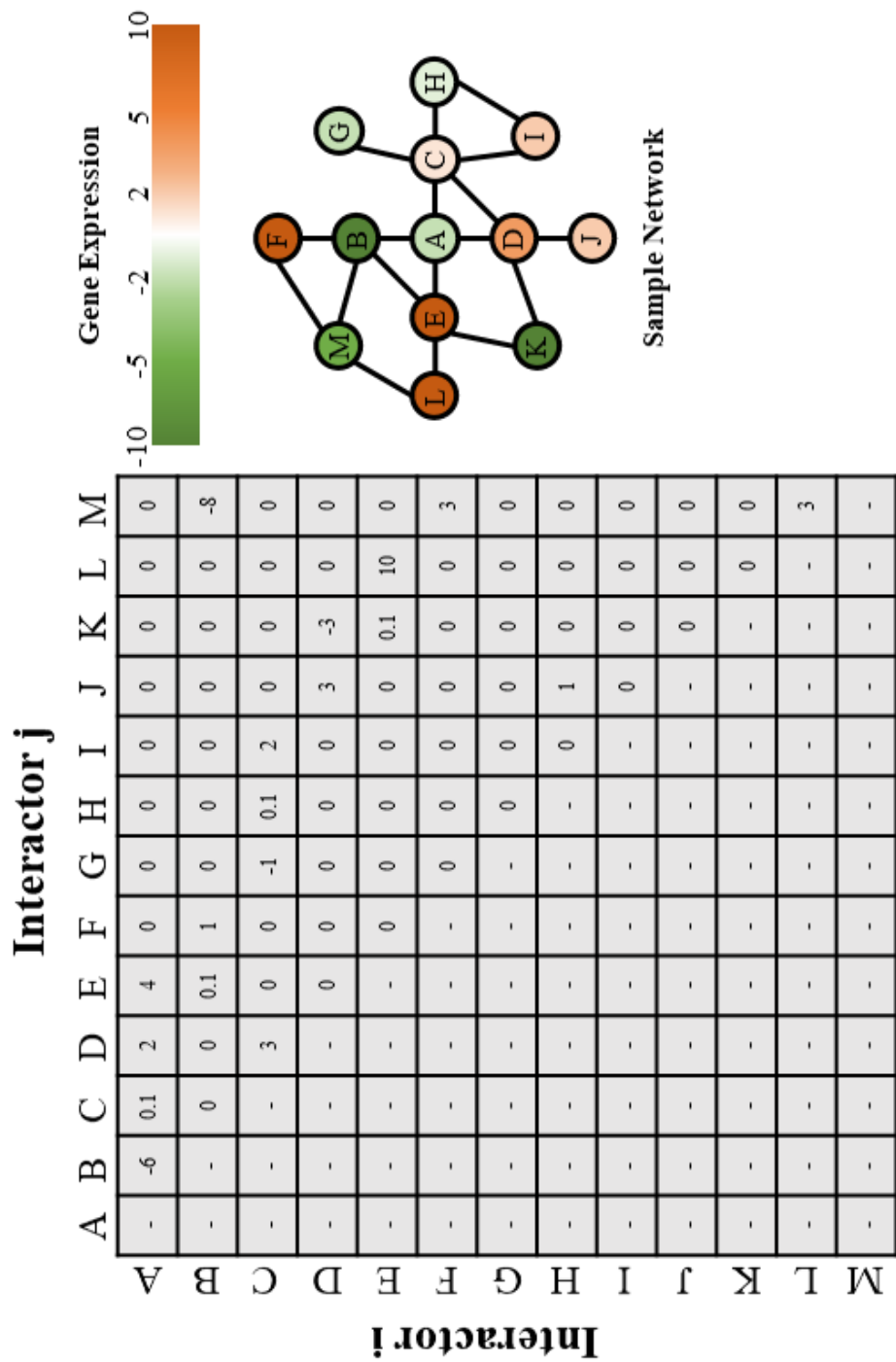
Scheme B.2: Interaction matrix with sample network. Edges are denoted by 1's where the two involved nodes intersect in the matrix

Expression Matrix



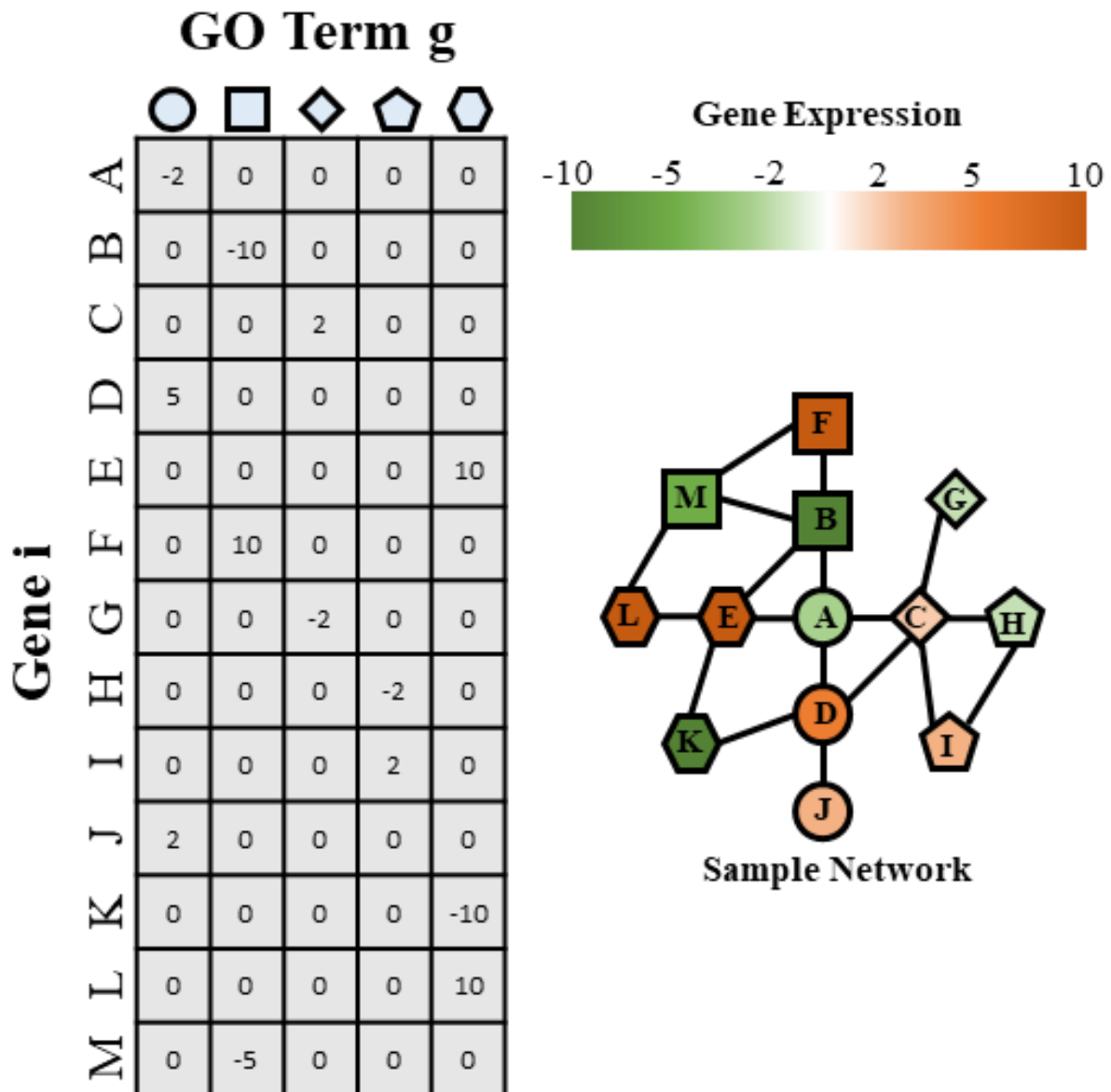
Scheme B.3: Expression matrix is made using a sample network using green and red to represent underexpression and overexpression, respectively.

Interaction Matrix – Expression



Scheme B.4: Interaction matrix with expression, this utilizes an interaction matrix, but uses an expression matrix to apply the average gene expression of the nodes involved in the interaction. These values can also utilize just the source or destination node values to create different perspectives for directed networks.

Gene-GO Matrix – Expression



Scheme B.5: GO matrix with expression designates GO terms to genes and uses their expression to create a value in the matrix

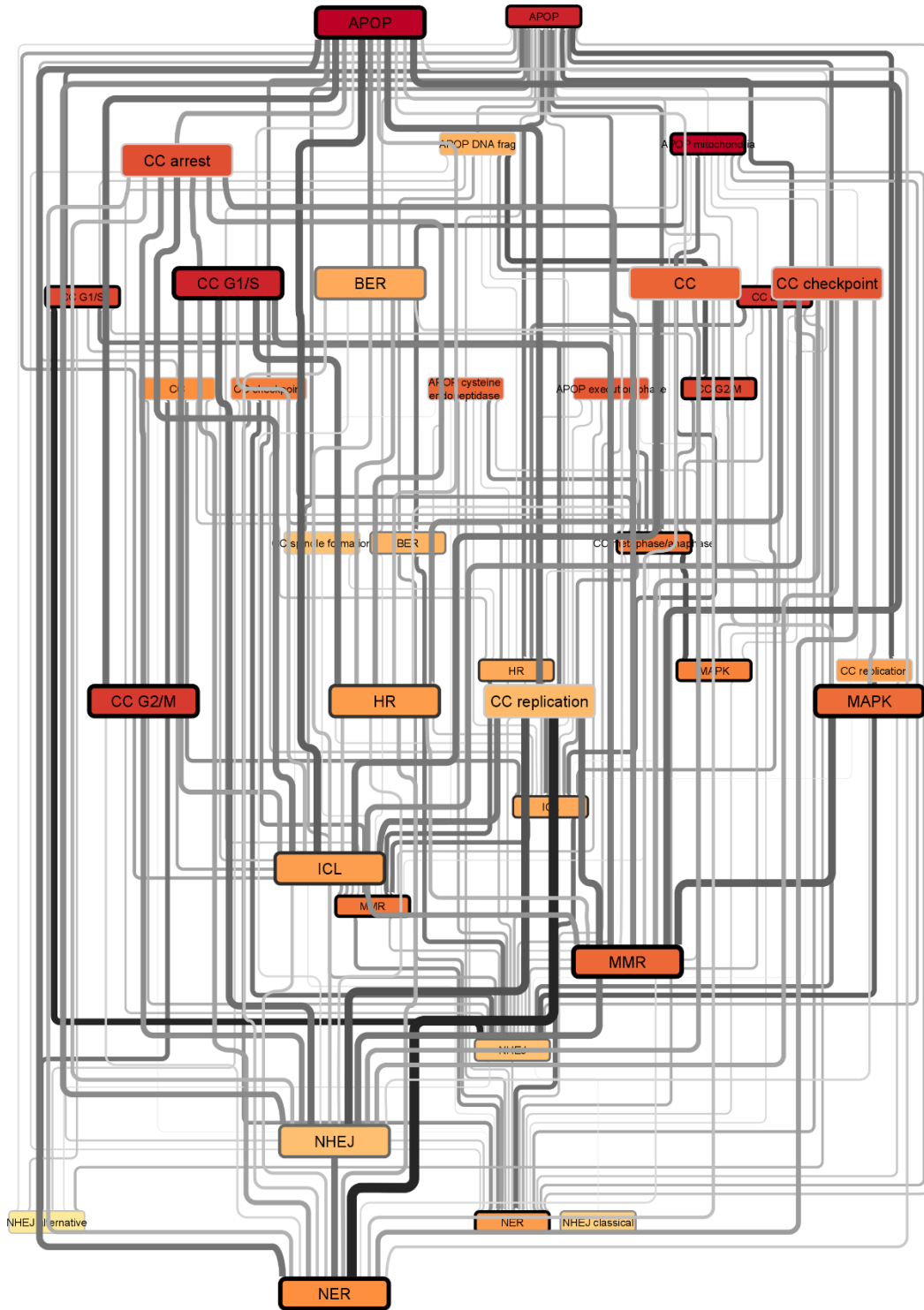


Figure B.1: HCC1937 short network shows the most condensed version of the process network

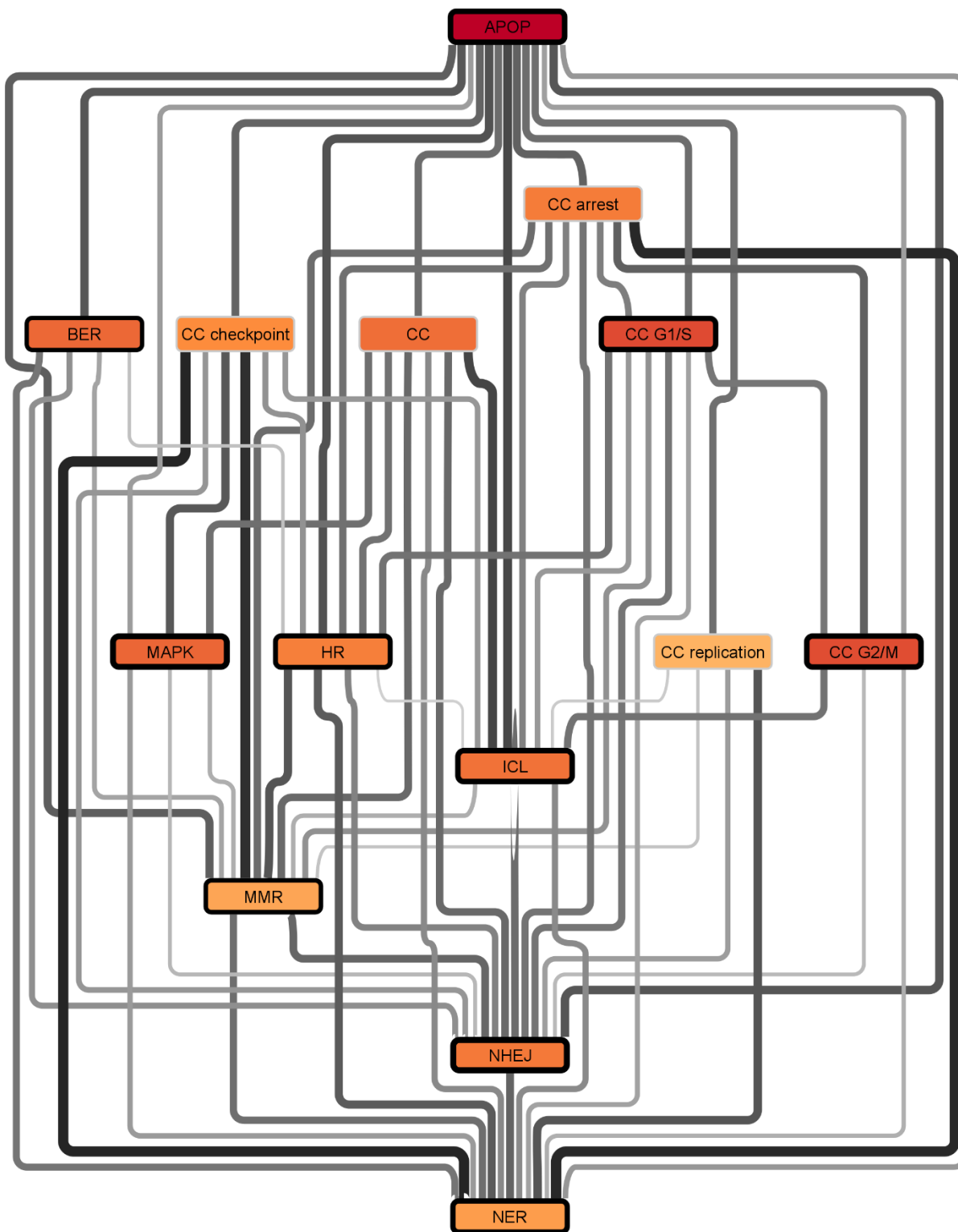


Figure B.4: MCF7 short network shows the most condensed version of the process network

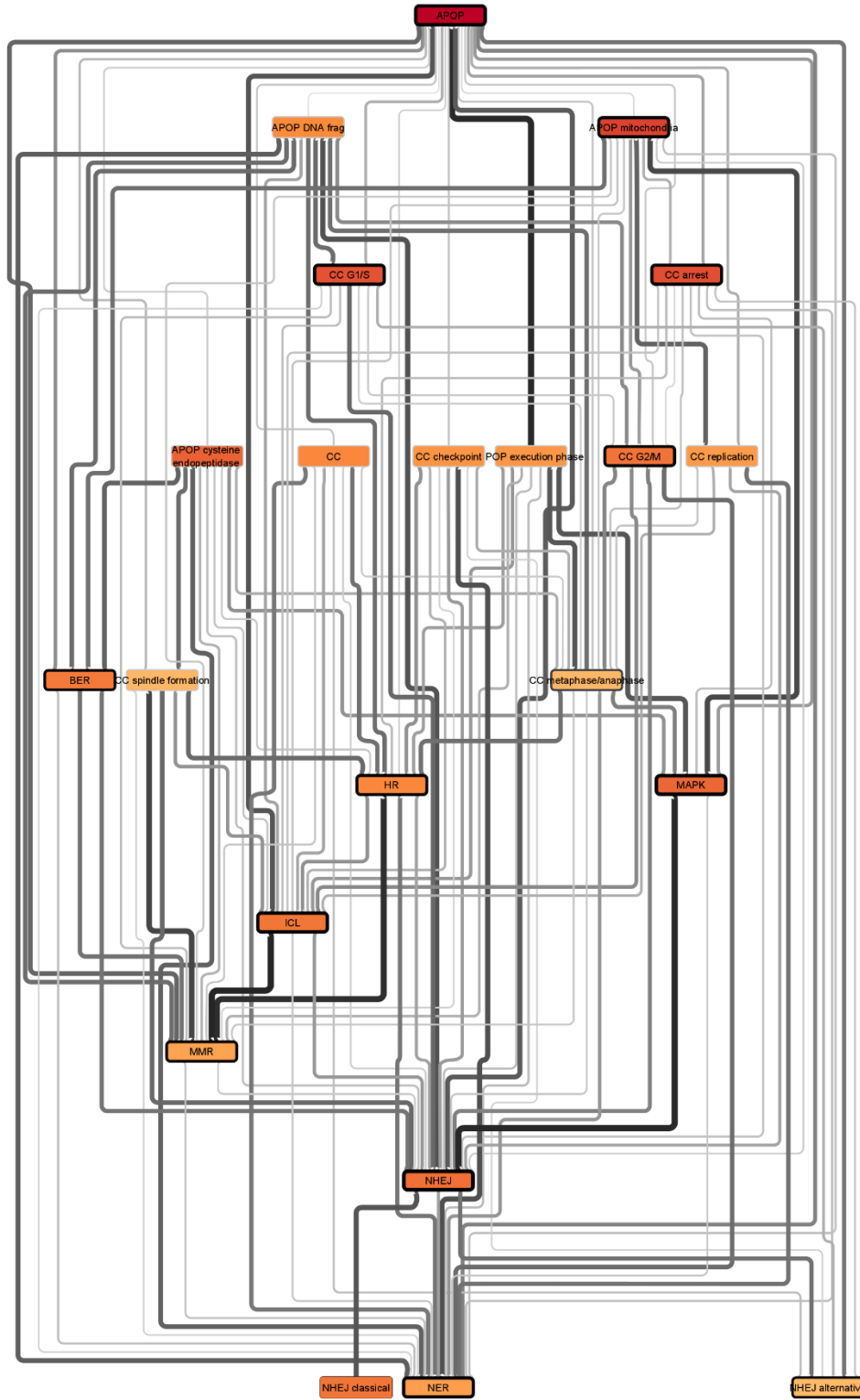


Figure B.5: MCF7 medium network shows a moderately condensed version of the process network

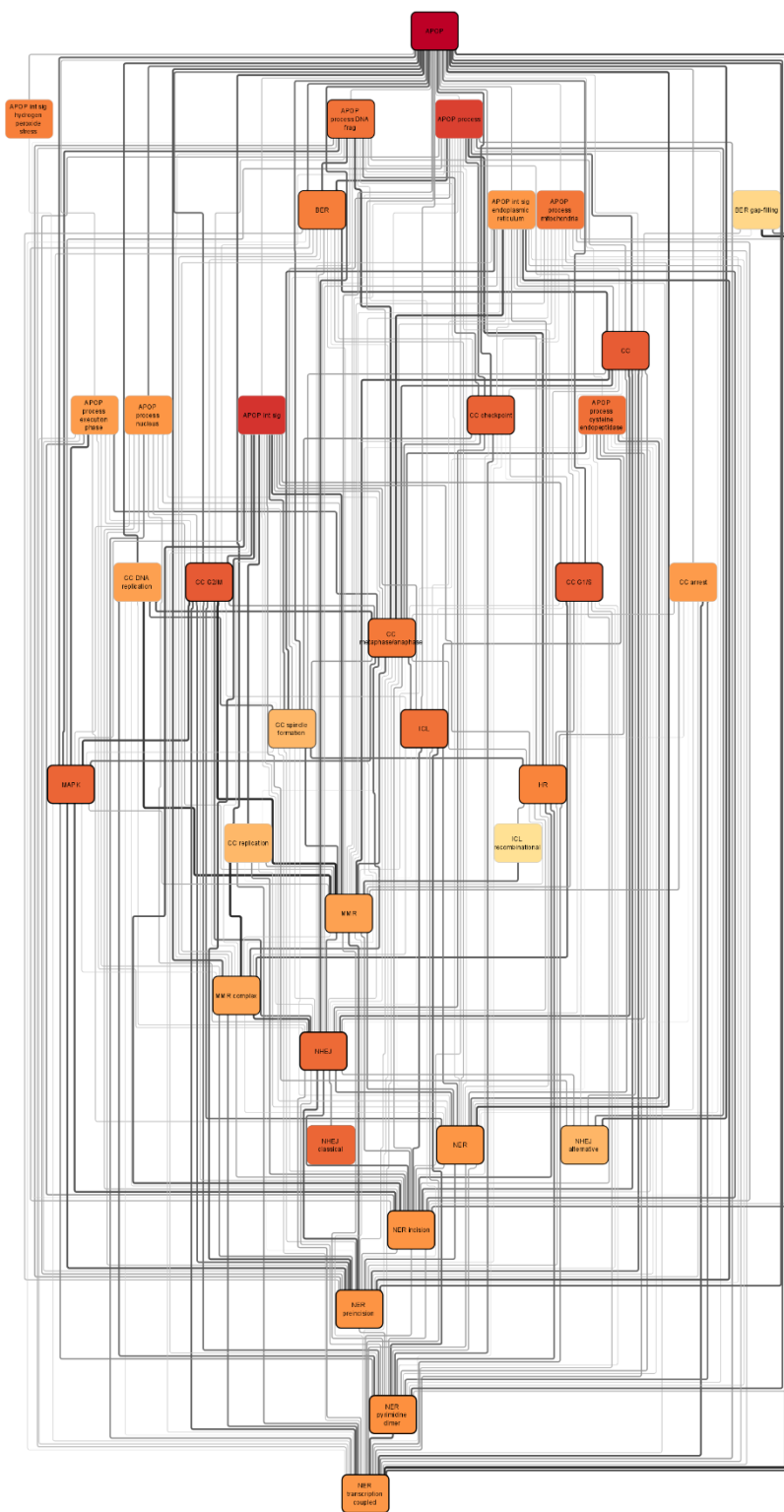


Figure B.6: MCF7 full network shows an uncondensed version of the process network

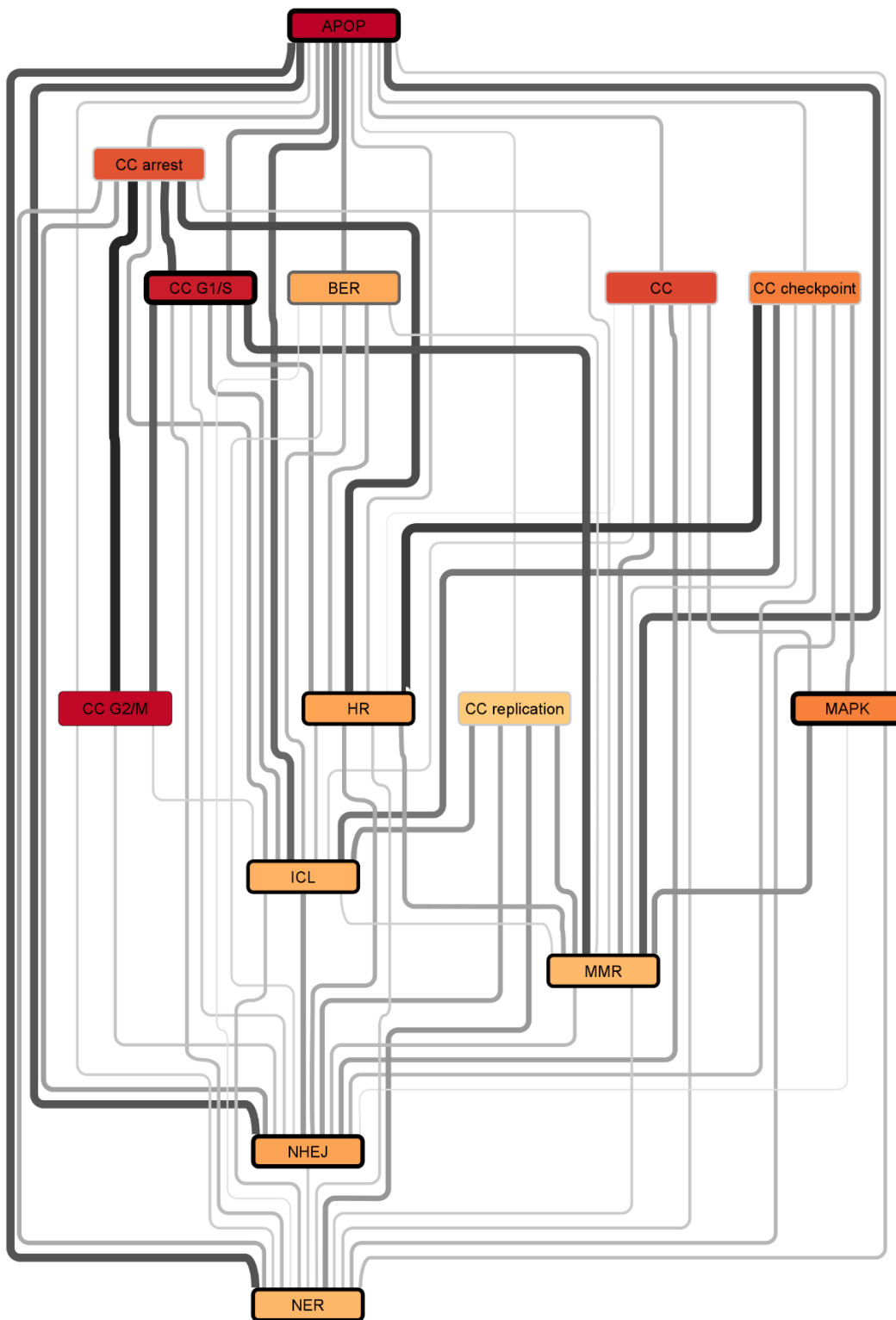


Figure B.7: MDA-MB 231 short network shows the most condensed version of the process network

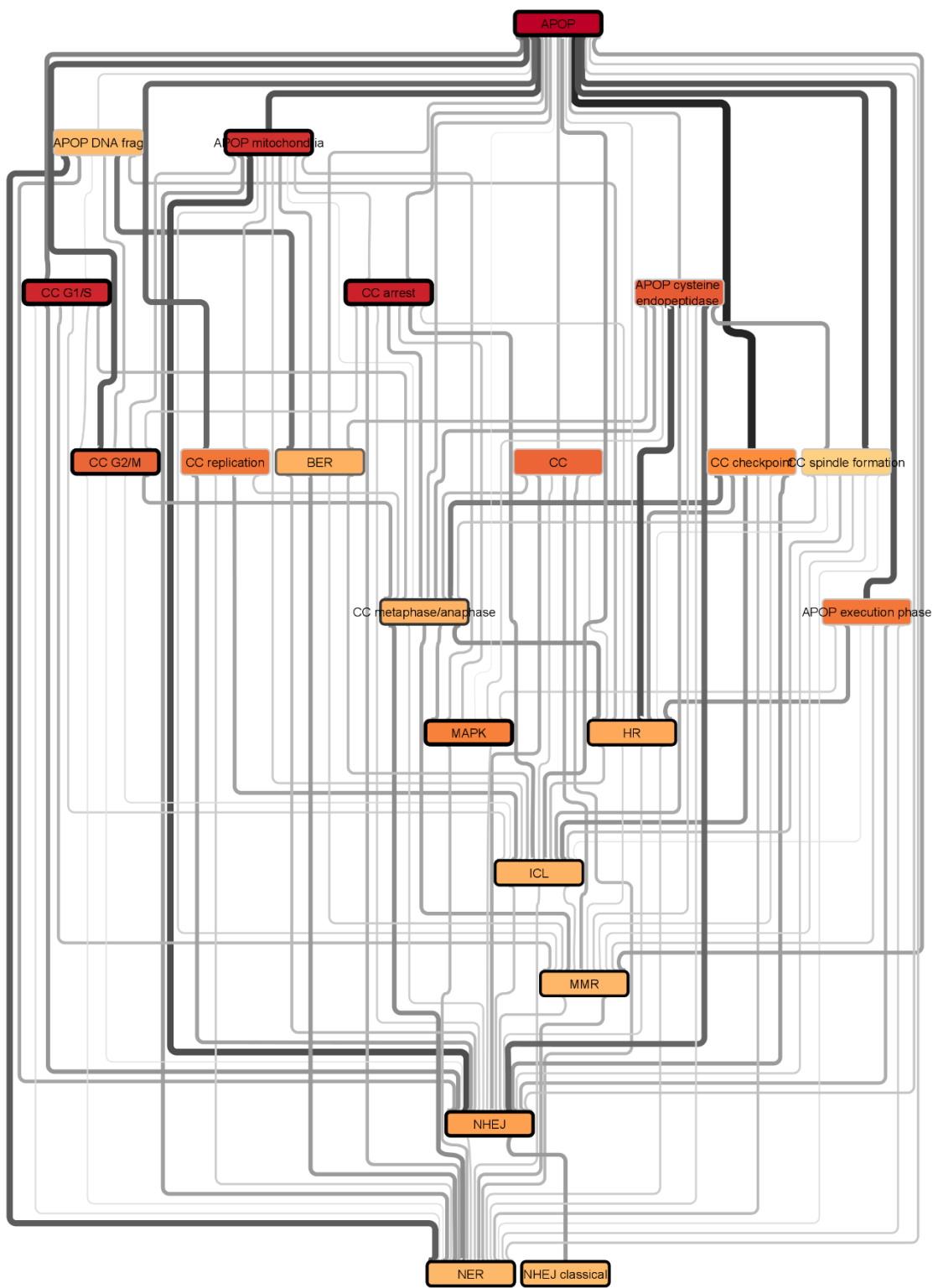


Figure B.8: MDA-MB 231 medium network shows a moderately condensed version of the process network

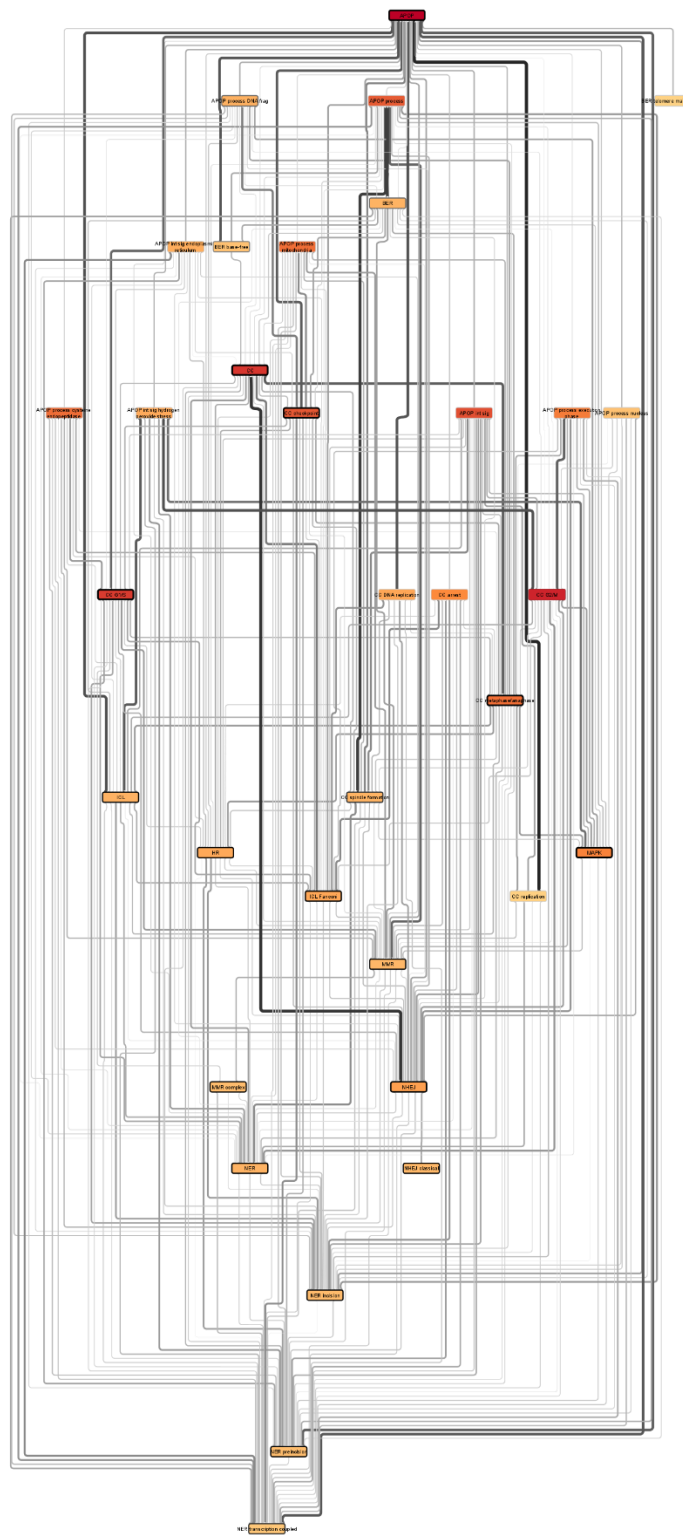


Figure B.9: MDA-MB 231 full network shows an uncondensed version of the process network

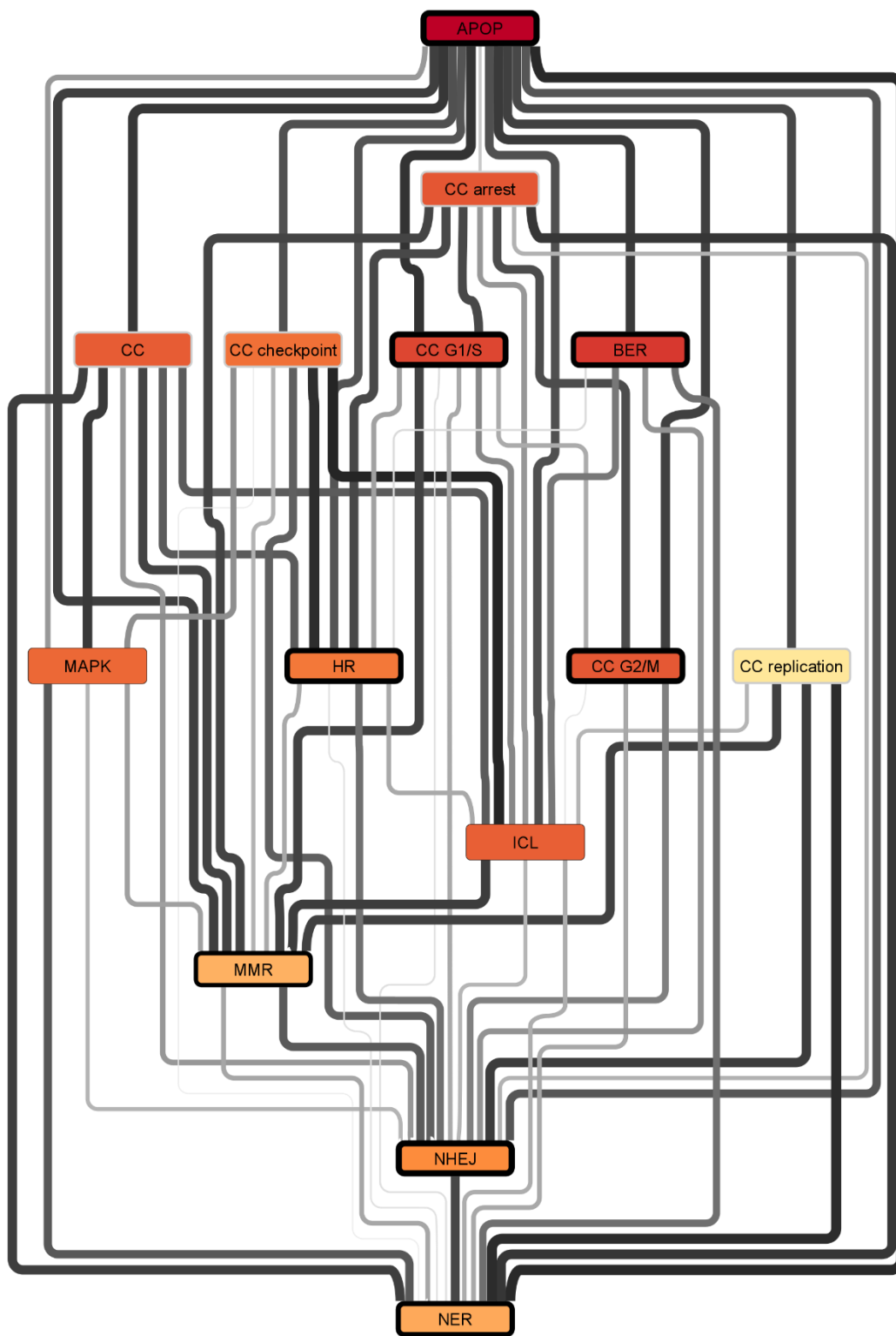


Figure B.10: MDA-MB 436 short network shows the most condensed version of the process network

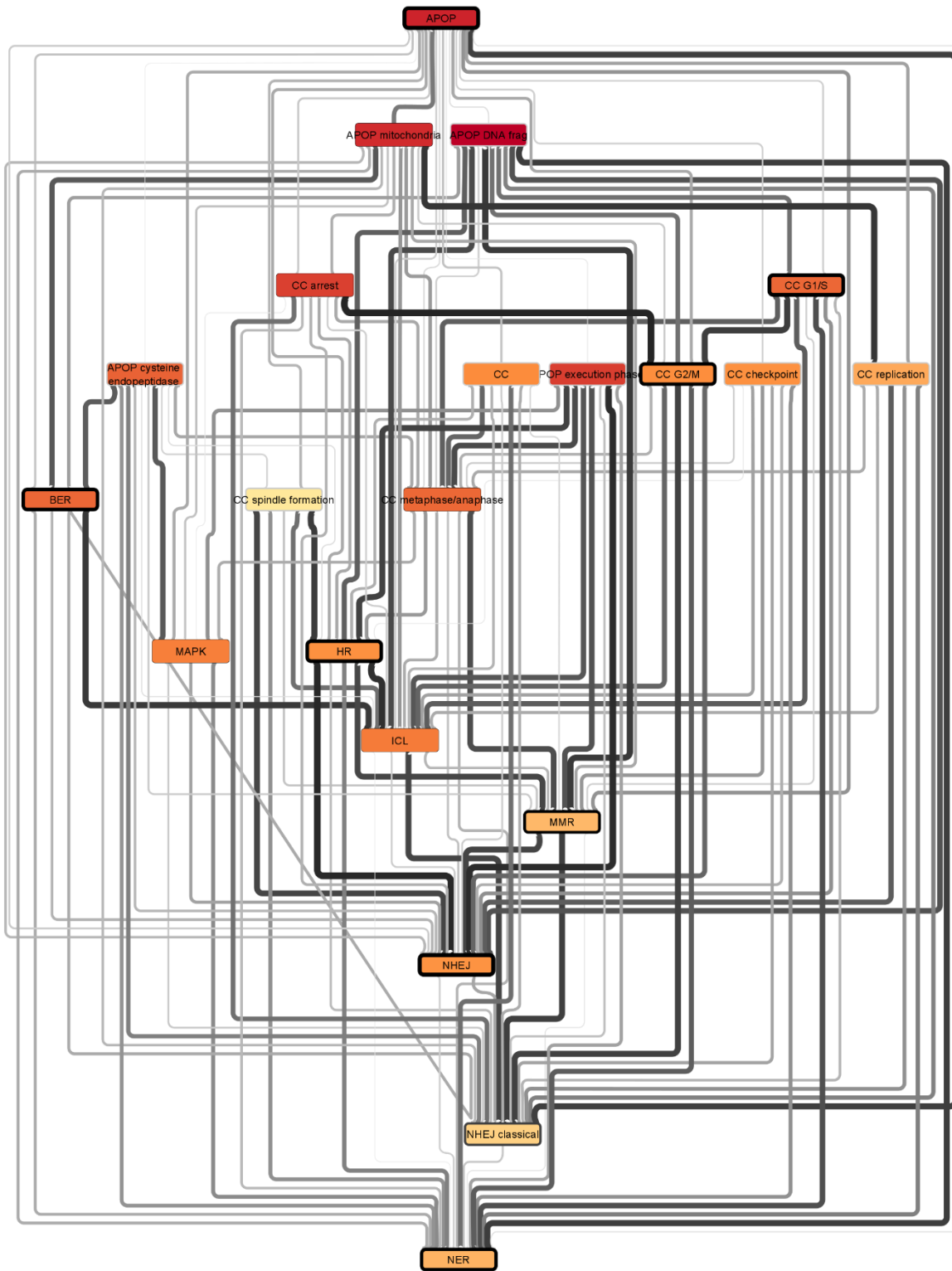


Figure B.11: MDA-MB 436 medium network shows a moderately condensed version of the process network

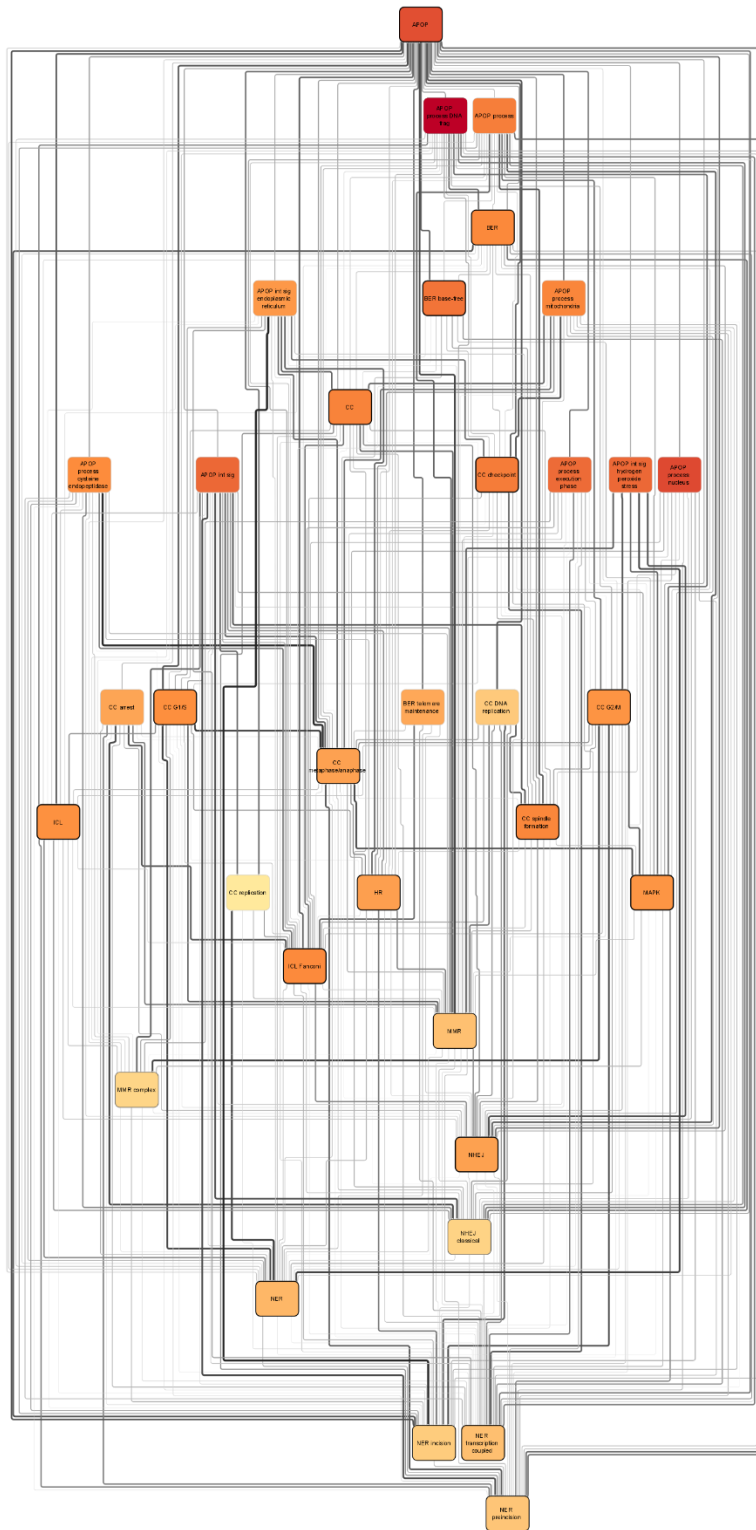


Figure B.12: MDA-MB 436 full network shows an uncondensed version of the process network

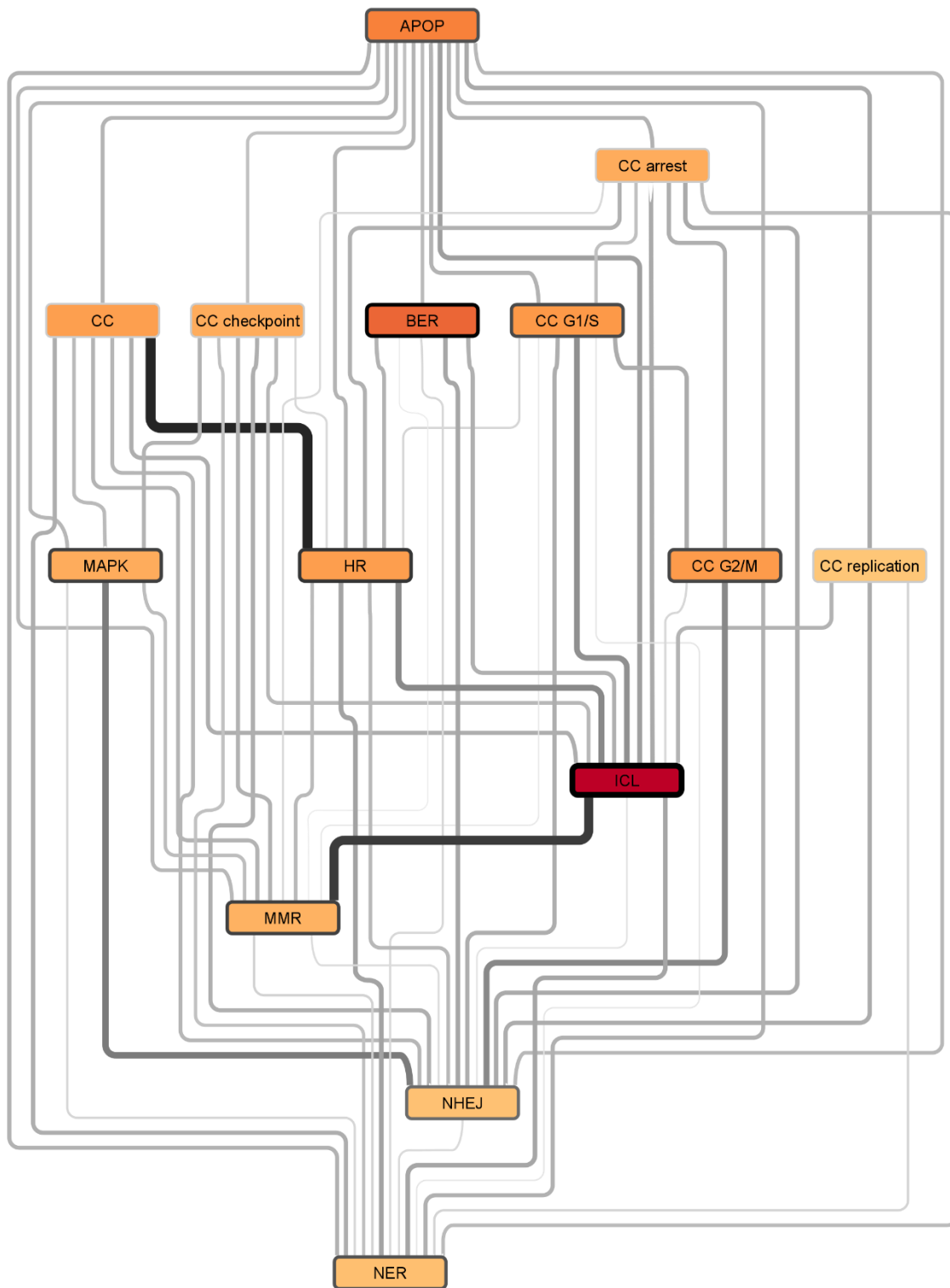


Figure B.13: MDA-MB 468 short network shows the most condensed version of the process network

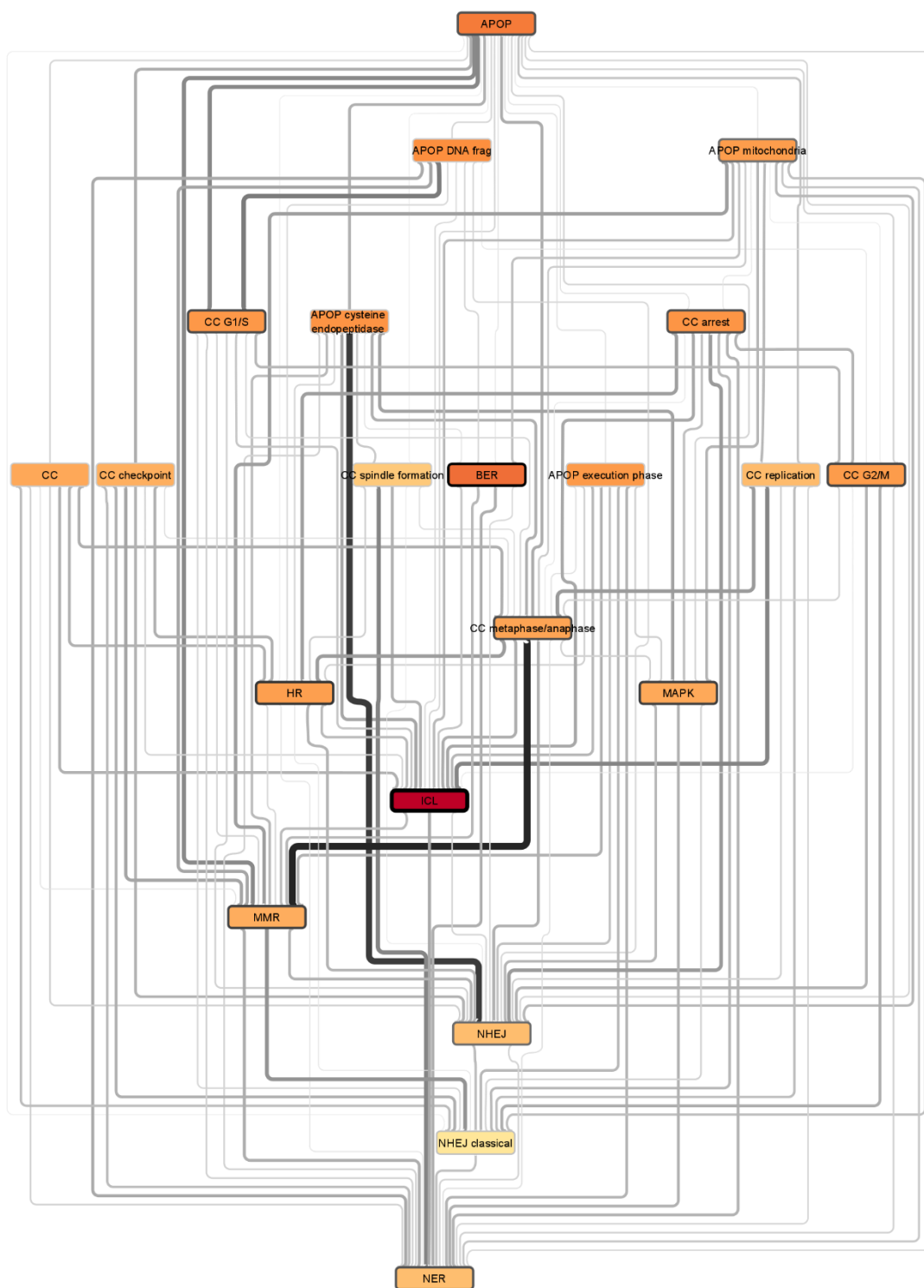


Figure B.14: MDA-MB 468 medium network shows a moderately condensed version of the process network

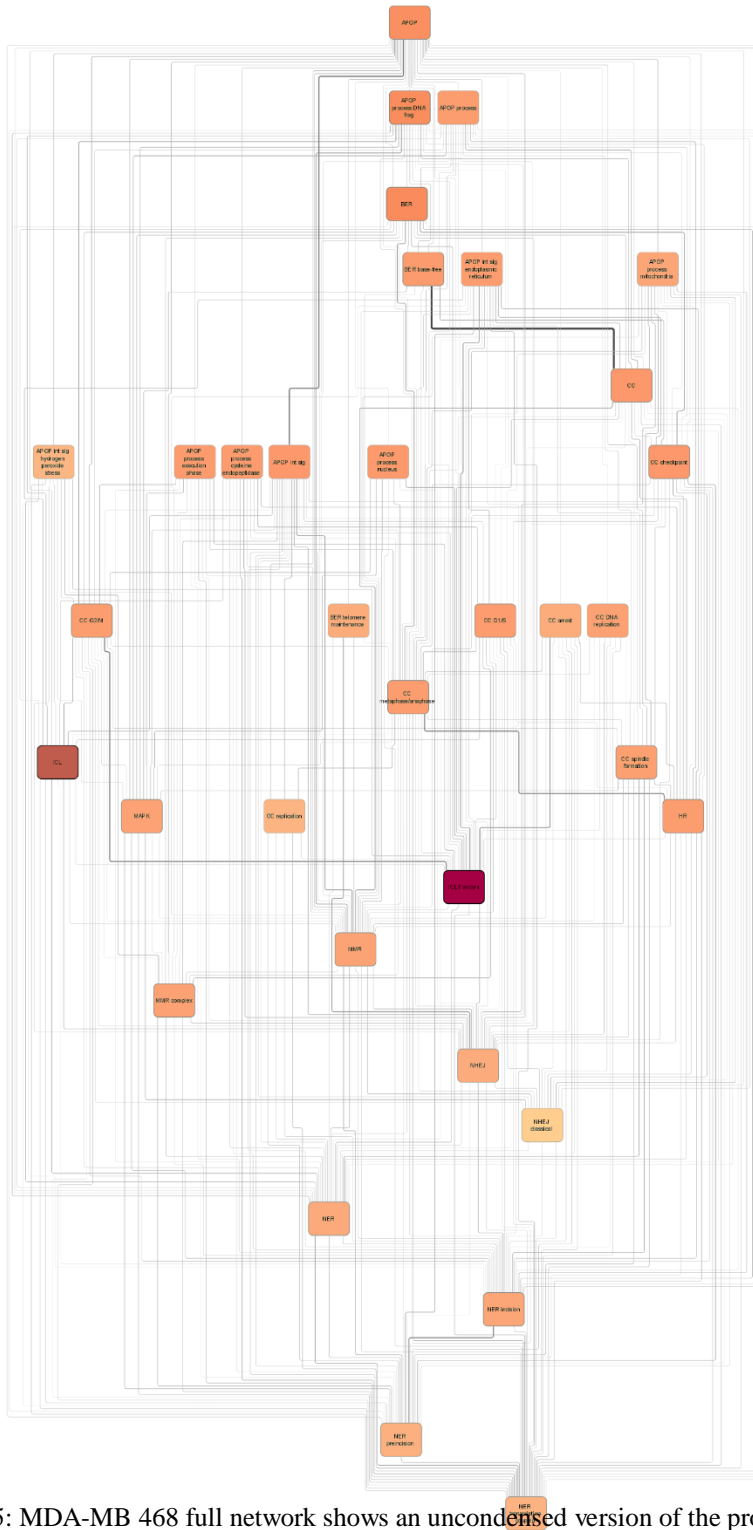


Figure B.15: MDA-MB 468 full network shows an uncondensed version of the process network

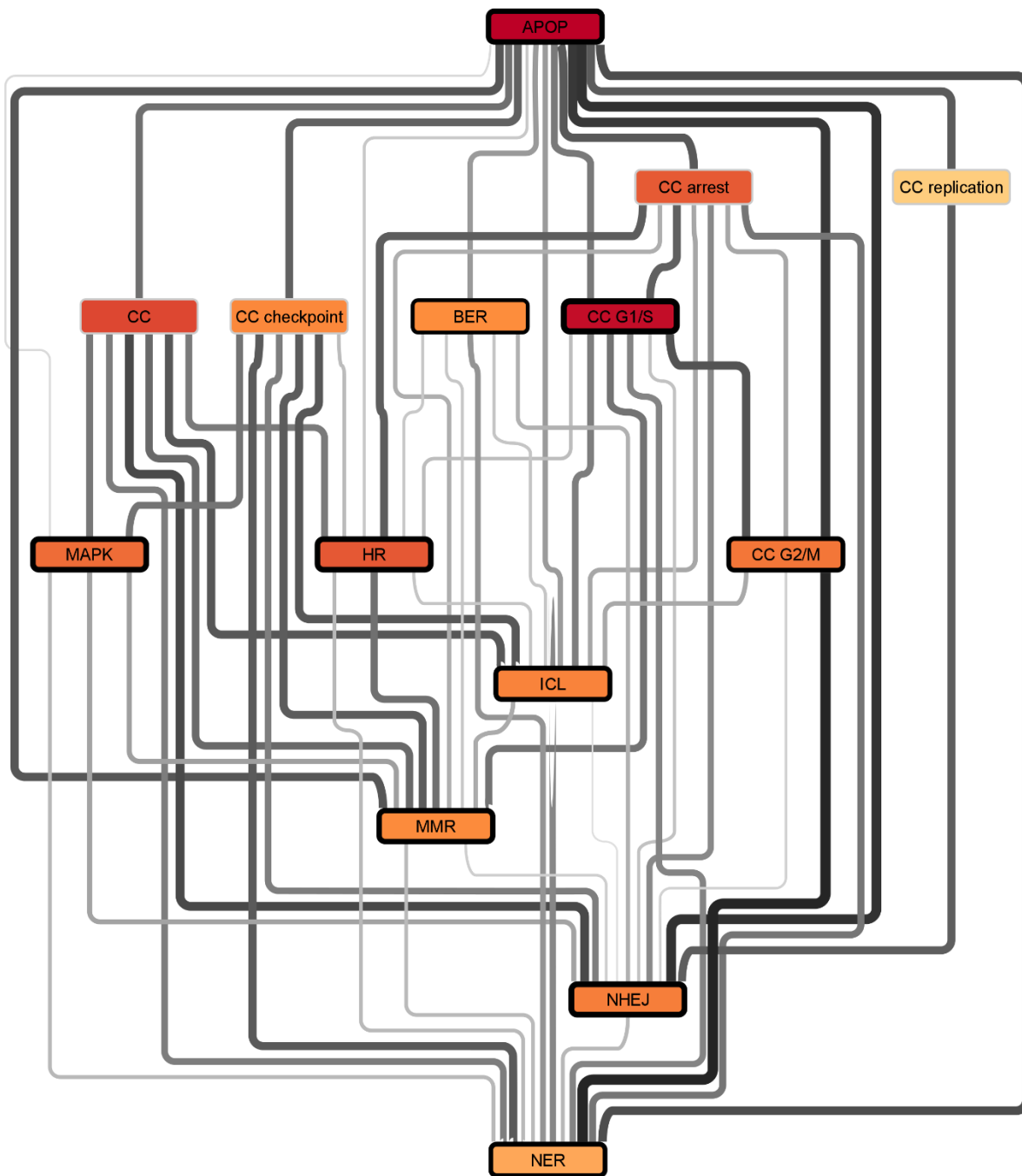


Figure B.16: SKBR3 short network shows the most condensed version of the process network

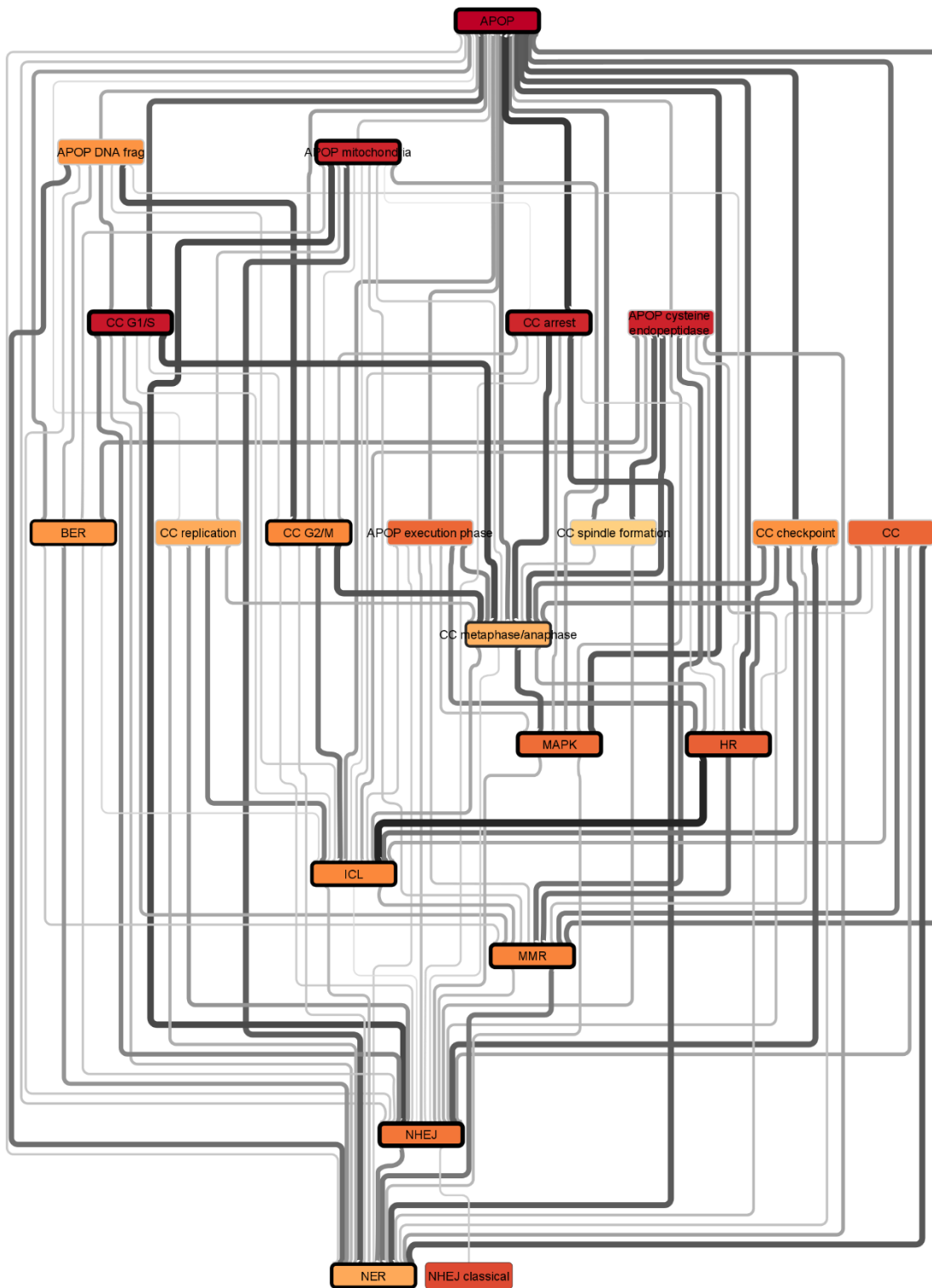


Figure B.17: SKBR3 medium network shows a moderately condensed version of the process network

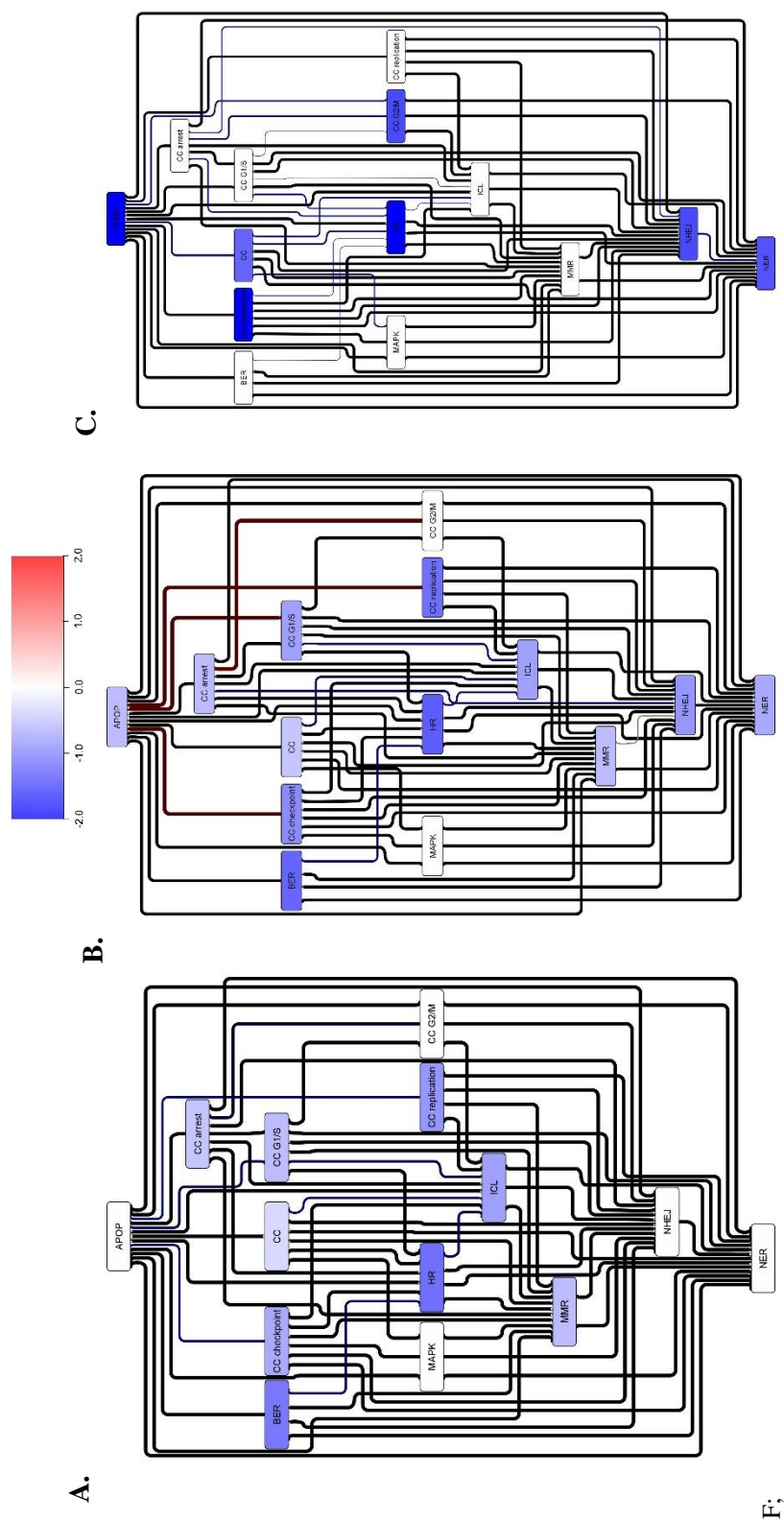


Figure B.19: Disruption from Homologous Recombination and Non-Homologous End Joining Components in MCF7; Networks were created from MCF7 expression data and analyzed similarly to the base networks, but without the nodes specified. Network features were then measured as before and the relative difference in each process and their connectivity was measured. A) BRCA1; B) PARP1; C) BRCA1/PARP1; *APOP* – apoptosis; *BER* – base excision repair; *CC* – cell cycle; *HR* – homologous recombination; *ICL* – interstrand cross-linking repair; *MMR* – mismatch repair; *NER* – nucleotide excision repair; *NHEJ* – non-homologous end joining;

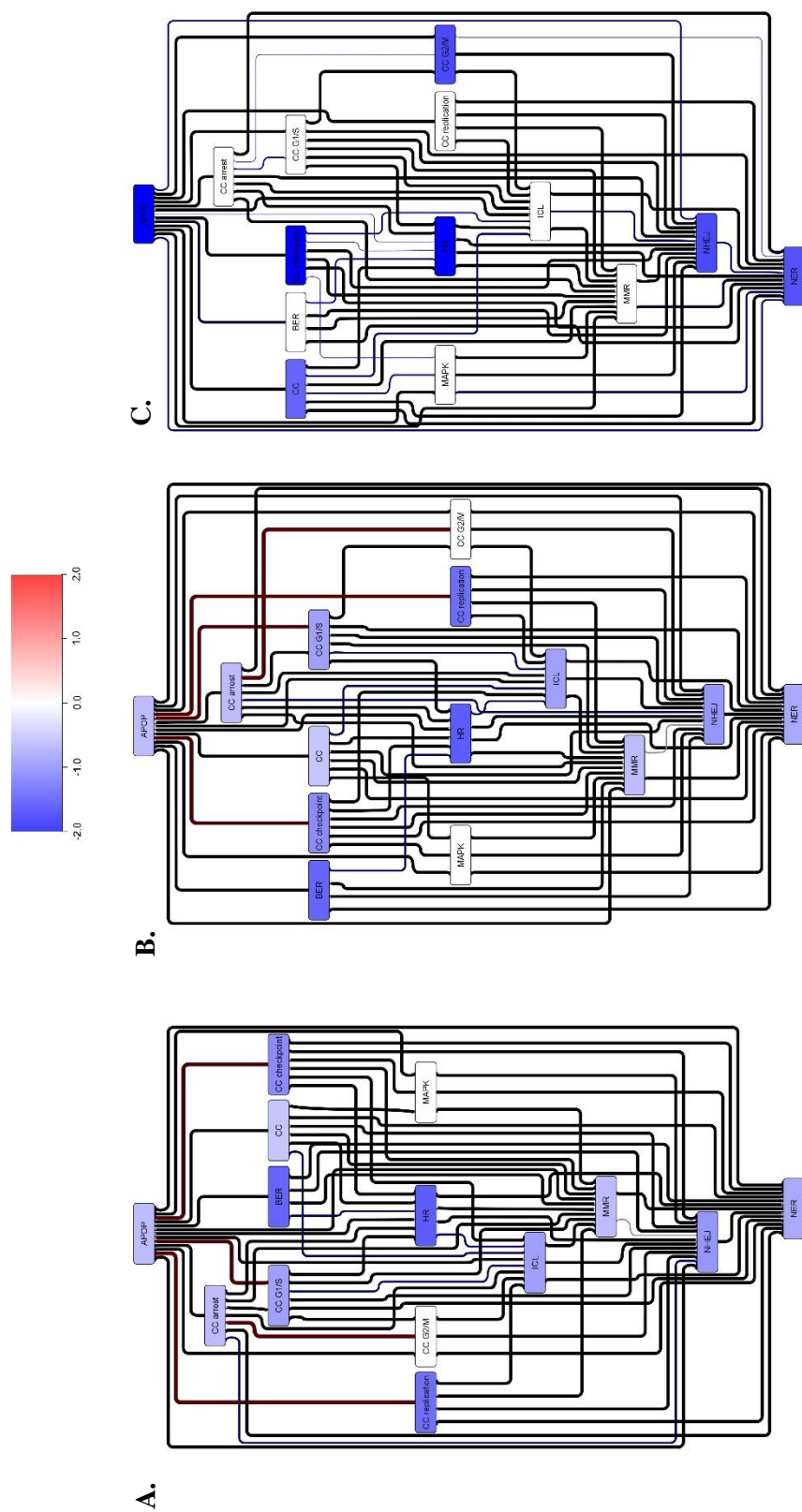


Figure B.20: Disruption from Homologous Recombination and Non-Homologous End Joining Components in MCF7; Networks were created from MCF7 expression data and analyzed similarly to the base networks, but without the nodes specified. Network features were then measured as before and the relative difference in each process and their connectivity was measured. A) PCNA; B) PARP1; C) PCNA/PARP1; *APOP* – apoptosis; *BER* – base excision repair; *CC* – cell cycle; *HR* – homologous recombination; *ICL* – interstrand cross-linking repair; *MMR* – mismatch repair; *NER* – nucleotide excision repair; *NHEJ* – non-homologous end joining;

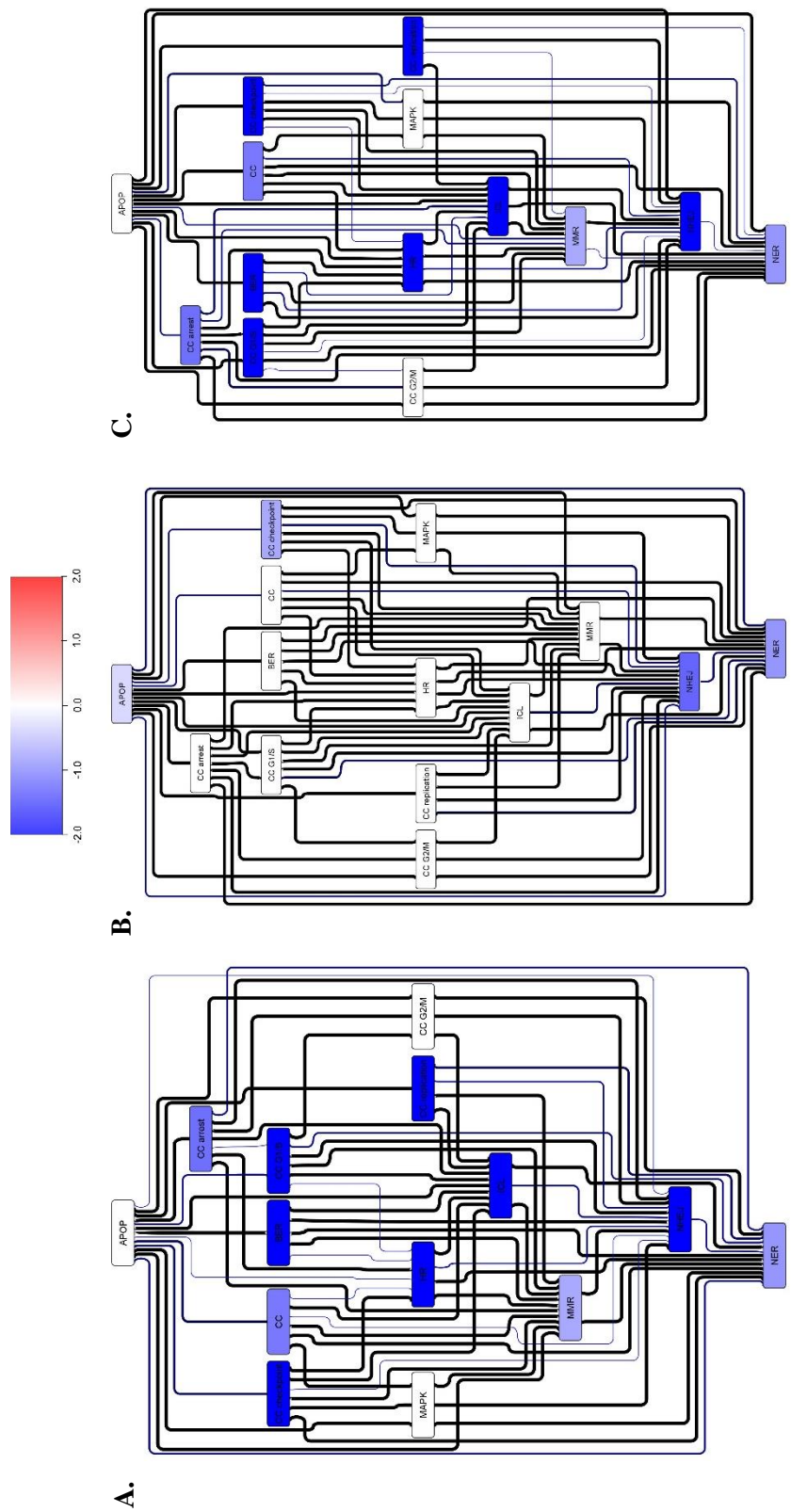


Figure B.21: Disruption from Homologous Recombination and Non-Homologous End Joining Components in MDA-MB-231; Networks were created from MDA-MB-231 expression data and analyzed similarly to the base networks, but without the nodes specified. Network features were then measured as before and the relative difference in each process and their connectivity was measured. A) BRCA1; B) PARP1; C) BRCA1/PARP1; *APOP* – apoptosis; *BER* – base excision repair; *CC* – cell cycle; *HR* – homologous recombination; *ICL* – interstrand cross-linking repair; *MMR* – mismatch repair; *NER* – nucleotide excision repair; *NHEJ* – non-homologous end joining;

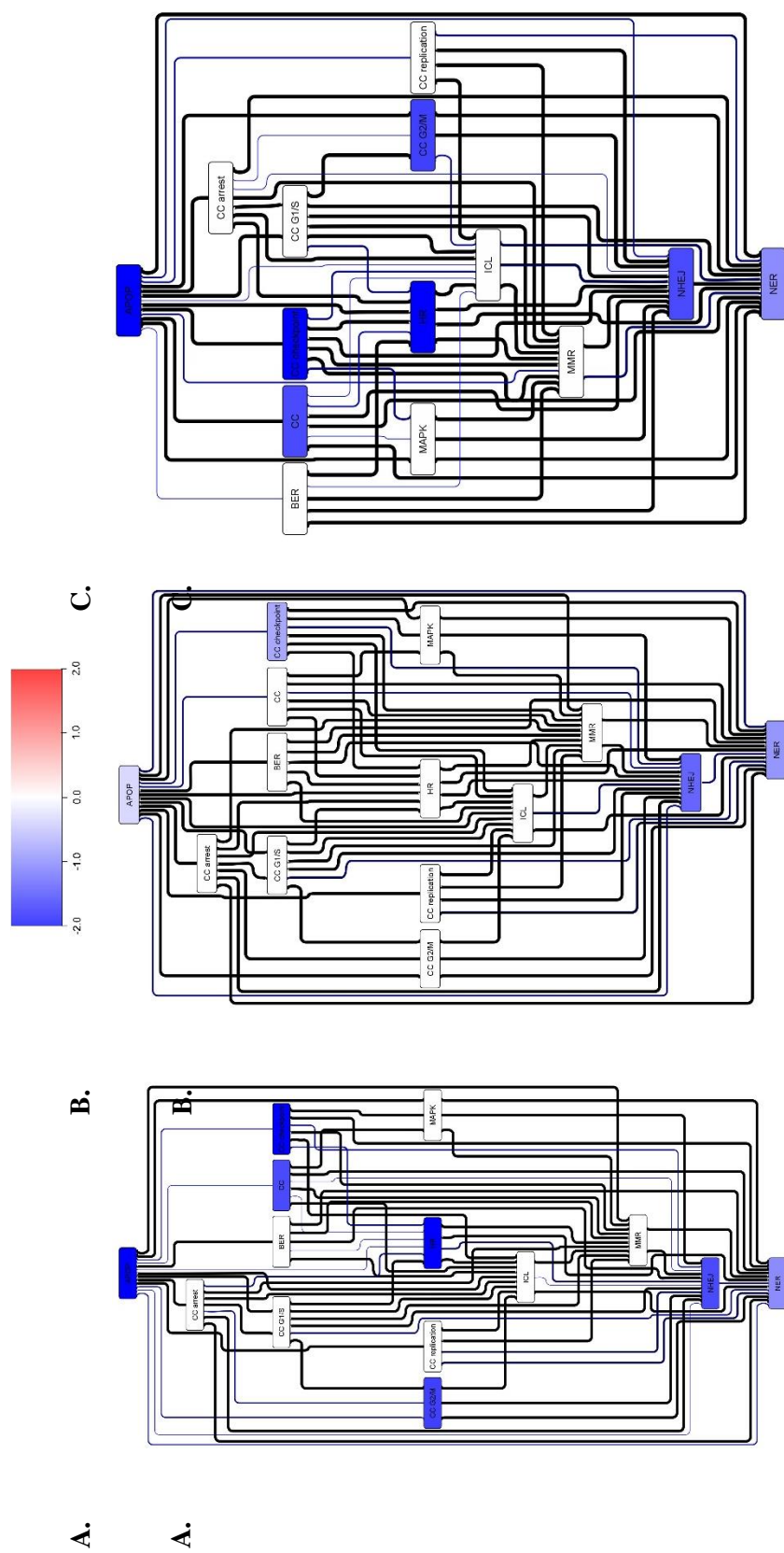


Figure B.22: Disruption from Homologous Recombination and Non-Homologous End Joining Components in MDA-MB-231; Networks were created from MDA-MB-231 expression data and analyzed similarly to the base networks, but without the nodes specified. Network features were then measured as before and the relative difference in each process and their connectivity was measured. A) PCNA; B) PARP1; C) PCNA/PARP1; *APOP* – apoptosis; *BER* – base excision repair; *CC* – cell cycle; *HR* – homologous recombination; *ICL* – interstrand cross-linking repair; *MMR* – mismatch repair; *NER* – nucleotide excision repair; *NHEJ* – non-homologous end joining;

Table B.1: Combinatorial Treatment by DNA Repair Antagonists in HCC1937, MCF7, and MDA-MB 231 Measuring GI₅₀

Primary Agent	Secondary Agent																							
	<i>Vehicle</i>			<i>Palbociclib</i>			<i>T2AA</i>			<i>KU55933</i>			<i>NU7026</i>			<i>Olaparib</i>			<i>Gefitinib</i>					
	GI ₅₀ (μM)	SD	1/CI	GI ₅₀ (μM)	SD	1/CI																		
HCC1937																								
Rabusertib (CHEK1)	2.25	0.33	1.81	0.18	1.07	1.85	0.19	1.05	1.79	0.23	1.08	0.41	0.04	3.46	0.6	0.07	2.66	1.81	0.24	1.07				
Palbociclib (CDK4/6)	88.82	8.03	NA			74.89	9.69	1.06	79.04	11.3	1.01	21.95	2.71	2.88	18.7	2.73	3.22	31.3	3.72	2.21				
T2AA (PCNA)	>100	NA	-			NA			>100	NA	0.94	20.95	2.05	3.68	10.78	1.35	5.31	40.61	5.47	2.31				
KU55933 (ATM)	33.13	3.03	-			-			NA			24.05	3.39	1.21	6.31	0.99	3.44	27.06	4.25	1.09				
NU7026 (DNA-PK)	61.52	9.18	-			-			-			NA			52.98	5.75	1.04	22.72	2.43	2.13				
Olaparib (PARP1)	5.16	0.52	-			-			-			-			NA			25.46	3.65	2.84				
Gefitinib (EGFR)	>100	NA	-			-			-			-			-			NA						
MCF7																								
Rabusertib (CHEK1)	67.76	6.19	58.93	9.00	1.03	60.23	8.68	1.01	58.93	8.66	1.03	44.89	5.80	1.31	39.58	4.90	1.46	51.07	6.51	1.17				
Palbociclib (CDK4/6)	11.05	0.93	NA			9.68	0.83	1.02	3.62	0.46	2.33	9.58	1.06	1.03	6.18	0.55	1.51	8.99	1.20	1.09				
T2AA (PCNA)	>100	NA	-			NA			>100	NA	0.94	>100	NA	1.08	94.52	9.65	1.33	>100	NA	1.08				
KU55933 (ATM)	82.64	9.42	-			-			NA			73.49	10.6	1.01	42.4	4.48	1.63	81.49	11.5	0.92				
NU7026 (DNA-PK)	2.13	0.33	-			-			-			NA			1.87	0.20	1.01	2.02	0.22	0.94				
Olaparib (PARP1)	33.23	3.43	-			-			-			-			NA			40.69	5.27	1.88				
Gefitinib (EGFR)	94.27	14.4	-			-			-			-			-			NA						
MDA-MB-231																								
Rabusertib (CHEK1)	13.07	1.19	10.71	1.23	1.08	11.93	1.29	0.98	10.71	1.36	1.08	4.54	0.60	2.22	3.91	0.61	2.49	8.03	1.16	1.39				
Palbociclib (CDK4/6)	4.96	0.65	NA			3.56	0.35	1.01	3.41	0.36	1.05	1	0.12	2.86	0.84	0.13	3.22	3.52	0.44	1.02				
T2AA (PCNA)	>100	NA	-			NA			>100	NA	0.91	18.58	1.67	3.74	20.52	2.53	3.51	60.98	7.53	1.54				
KU55933 (ATM)	35.52	5.61	-			-			NA			29.02	2.94	1.09	6.83	1.01	3.42	31.6	4.28	1.01				
NU7026 (DNA-PK)	55.14	8.17	-			-			-			NA			43.25	4.45	1.13	47.47	7.48	1.04				
Olaparib (PARP1)	4.37	0.48	-			-			-			-			NA			3.55	0.49	1.84				
Gefitinib (EGFR)	8.01	1.00	-			-			-			-			-			NA						

Table B.2: Combinatorial Treatment by DNA Repair Antagonists in MDAM-MB 436, MDA-MB 468, and SKBR3 Measuring GI₅₀

Primary Agent	Secondary Agent																							
	<i>Vehicle</i>			<i>Palbociclib</i>			<i>T2AA</i>			<i>KU55933</i>			<i>NU7026</i>			<i>Olaparib</i>			<i>Gefitinib</i>					
	GI50 (μ M)	SD	1/CI																					
MDA-MB 436																								
Rabusertib (CHEK1)	12.69	1.34		10.97	1.46	1.04	10.41	1.13	1.09	9.16	1.25	1.22	7	0.98	1.54	5.5	0.84	1.88	5.22	0.43	1.96			
Palbociclib (CDK4/6)	41.73	5.36		NA			36.34	4.62	1.03	36.74	4.91	1.02	35.57	5.19	1.05	23.46	2.98	1.51	34.47	3.98	1.08			
T2AA (PCNA)	>100	NA		-			NA			>100	NA	0.92	>100	NA	0.98	>100	NA	1.03	>100	NA	1.02			
KU55933 (ATM)	47.1	7.52		-			-			NA			39.31	3.94	1.07	41.92	5.47	1.01	39.31	3.80	1.07			
NU7026 (DNA-PK)	4.51	0.49		-			-			-			NA			3.96	0.46	1.02	3.8	0.46	1.06			
Olaparib (PARP1)	2.04	0.32		-			-			-			-			NA			1.25	0.15	1.38			
Gefitinib (EGFR)	27.64	3.80		-			-			-			-			-			NA					
MDA-MB 468																								
Rabusertib (CHEK1)	0.41	0.06		0.34	0.04	1.07	0.33	0.05	1.09	0.31	0.03	1.15	0.18	0.03	1.79	0.18	0.02	1.84	0.22	0.03	1.54			
Palbociclib (CDK4/6)	10.31	1.25		NA			8.78	0.83	1.05	8.69	1.09	1.06	4.99	0.47	1.71	4.36	0.62	1.91	6.22	0.87	1.42			
T2AA (PCNA)	>100	NA		-			NA			>100	NA	0.91	21.94	2.45	3.63	24.05	2.42	3.42	77.43	9.55	1.39			
KU55933 (ATM)	38.13	3.42		-			-			NA			22.65	2.45	1.44	18.73	1.99	1.69	31.8	3.90	1.07			
NU7026 (DNA-PK)	58.74	9.10		-			-			-			NA			51.12	5.98	1.03	45.62	4.75	1.14			
Olaparib (PARP1)	8.62	1.01		-			-			-			-			NA			3.43	0.50	1.89			
Gefitinib (EGFR)	1.63	0.15		-			-			-			-			-			NA					
SKBR3																								
Rabusertib (CHEK1)	0.05	0.01		0.02	0.00	1.96	0.05	0.00	0.98	0.04	0.00	1.03	0.02	0.00	1.88	0.02	0.00	2.24	0.02	0.00	1.87			
Palbociclib (CDK4/6)	2.13	0.29		NA			1.77	0.17	1.06	1.23	0.12	1.46	1.79	0.15	1.05	1.75	0.16	1.07	1.06	0.16	1.65			
T2AA (PCNA)	>100	NA		-			NA			>100	NA	0.96	67.27	6.45	1.46	49.67	4.66	1.88	69.49	6.00	1.42			
KU55933 (ATM)	37.08	4.90		-			-			NA			32.66	5.16	1.02	24.61	2.63	1.31	32.66	4.11	1.02			
NU7026 (DNA-PK)	29.63	4.20		-			-			-			NA			26.35	3.61	1.01	24.45	2.35	1.08			
Olaparib (PARP1)	48.21	4.03		-			-			-			-			NA			22.11	3.13	1.79			
Gefitinib (EGFR)	1.27	0.18		-			-			-			-			-			NA					

Table B.3: Disruption Measured by Disruption Index through Combinatorial Gene Removal of DNA Repair Genes from Disease Networks in HCC1937, MCF7, and MDA-MB 231

Primary Gene	Secondary Gene					
	<i>CDK4/6</i> DI	<i>PCNA</i> DI	<i>ATM</i> DI	<i>DNA-PK</i> DI	<i>PARP1</i> DI	<i>EGFR</i> DI
HCC1937						
CHEK1	0.79	0.84	0.72	1.69	1.22	0.92
CDK4/6	NA	0.59	0.61	2.87	2.68	1.91
PCNA	-	NA	0.22	2.74	3.41	1.84
ATM	-	-	NA	0.87	2.42	0.69
DNA-PK	-	-	-	NA	0.21	1.94
PARP1	-	-	-	-	NA	2.11
EGFR	-	-	-	-	-	NA
MCF7						
CHEK1	0.38	0.14	0.51	0.96	1.64	1.49
CDK4/6	NA	0.65	1.16	0.41	1.89	0.76
PCNA	-	NA	0.14	0.64	0.78	0.28
ATM	-	-	NA	0.31	1.41	0.39
DNA-PK	-	-	-	NA	0.23	0.45
PARP1	-	-	-	-	NA	1.36
EGFR	-	-	-	-	-	NA
MDA-MB-231						
CHEK1	1.21	0.54	0.45	2.11	1.77	1.53
CDK4/6	NA	0.69	0.27	1.92	2.08	0.84
PCNA	-	NA	0.32	2.78	2.59	1.49
ATM	-	-	NA	1.26	1.68	0.79
DNA-PK	-	-	-	NA	0.46	0.87
PARP1	-	-	-	-	NA	2.43
EGFR	-	-	-	-	-	NA

Table B.4: Disruption Measured by Disruption Index through Combinatorial Gene Removal of DNA Repair Genes from Disease Networks in MDA-MB 436, MDA-MB 468, and SKBR

Primary Gene	Secondary Gene					
	<i>CDK4/6</i> DI	<i>PCNA</i> DI	<i>ATM</i> DI	<i>DNA-PK</i> DI	<i>PARP1</i> DI	<i>EGFR</i> DI
MDA-MB 436						
CHEK1	0.95	1.94	1.68	1.38	1.54	1.84
CDK4/6	NA	0.74	0.56	0.68	1.48	0.45
PCNA	-	NA	0.33	0.71	0.84	0.36
ATM	-	-	NA	0.76	0.89	0.23
DNA-PK	-	-	-	NA	0.22	0.67
PARP1	-	-	-	-	NA	1.69
EGFR	-	-	-	-	-	NA
MDA-MB 468						
CHEK1	1.37	0.22	0.68	1.44	1.68	1.67
CDK4/6	NA	0.47	0.59	1.94	1.74	1.94
PCNA	-	NA	0.31	1.51	2.33	1.46
ATM	-	-	NA	1.08	1.27	0.72
DNA-PK	-	-	-	NA	0.33	0.67
PARP1	-	-	-	-	NA	1.89
EGFR	-	-	-	-	-	NA
SKBR3						
CHEK1	2.12	0.79	0.68	2.24	2.46	1.75
CDK4/6	NA	0.68	1.49	0.92	1.14	1.68
PCNA	-	NA	0.23	1.14	1.09	2.12
ATM	-	-	NA	0.89	1.46	0.89
DNA-PK	-	-	-	NA	0.88	1.18
PARP1	-	-	-	-	NA	1.89
EGFR	-	-	-	-	-	NA

REFERENCES

1. Nagai, H. & Kim, Y. H. Cancer prevention from the perspective of global cancer burden patterns. *J. Thorac. Dis.* **9**, 448–451 (2017).
2. Dagogo-Jack, I. & Shaw, A. T. Tumour heterogeneity and resistance to cancer therapies. *Nat. Rev. Clin. Oncol.* **15**, 81–94 (2018).
3. Huang, C.-Y., Ju, D.-T., Chang, C.-F., Muralidhar Reddy, P. & Velmurugan, B. K. A review on the effects of current chemotherapy drugs and natural agents in treating non–small cell lung cancer. *BioMedicine* **7**,.
4. Schirrmacher, V. From chemotherapy to biological therapy: A review of novel concepts to reduce the side effects of systemic cancer treatment (Review). *Int. J. Oncol.* **54**, 407–419 (2018).
5. Ramón y Cajal, S. *et al.* Clinical implications of intratumor heterogeneity: challenges and opportunities. *J. Mol. Med. Berl. Ger.* **98**, 161–177 (2020).
6. Sung, J.-Y. *et al.* Assessment of intratumoral heterogeneity with mutations and gene expression profiles. *PLOS ONE* **14**, e0219682 (2019).
7. Hinohara, K. & Polyak, K. Intratumoral Heterogeneity: More Than Just Mutations. *Trends Cell Biol.* **29**, 569–579 (2019).
8. Kaufman, B. *et al.* Olaparib Monotherapy in Patients With Advanced Cancer and a Germline BRCA1/2 Mutation. *J. Clin. Oncol.* **33**, 244–250 (2015).
9. Richon, V. M., Garcia-Vargas, J. & Hardwick, J. S. Development of vorinostat: Current applications and future perspectives for cancer therapy. *Cancer Lett.* **280**, 201–210 (2009).
10. André, F. *et al.* Alpelisib for PIK3CA-Mutated, Hormone Receptor–Positive Advanced Breast Cancer. *N. Engl. J. Med.* **380**, 1929–1940 (2019).
11. Ai, X. *et al.* Targeted therapies for advanced non-small cell lung cancer. *Oncotarget* **9**, 37589–37607 (2018).
12. Apicella, M., Corso, S. & Giordano, S. Targeted therapies for gastric cancer: failures and hopes from clinical trials. *Oncotarget* **8**, 57654–57669 (2017).
13. Masoud, V. & Pagès, G. Targeted therapies in breast cancer: New challenges to fight against resistance. *World J. Clin. Oncol.* **8**, 120–134 (2017).
14. Vanneman, M. & Dranoff, G. Combining immunotherapy and targeted therapies in cancer treatment. *Nat. Rev. Cancer* **12**, 237–251 (2012).

15. Ledermann, J. A. & Pujade-Lauraine, E. Olaparib as maintenance treatment for patients with platinum-sensitive relapsed ovarian cancer. *Ther. Adv. Med. Oncol.* **11**, (2019).
16. Huang, D. *et al.* Study of anlotinib combined with icotinib as the first-line treatment in non-small cell lung cancer (NSCLC) patients harboring activating EGFR mutations (ALTER-L004). *J. Clin. Oncol.* **38**, 9573–9573 (2020).
17. Pertesi, M. *et al.* Essential genes shape cancer genomes through linear limitation of homozygous deletions. *Commun. Biol.* **2**, 1–11 (2019).
18. Wang, T. *et al.* Identification and characterization of essential genes in the human genome. *Science* **350**, 1096–1101 (2015).
19. Sciences, N. A. of. In This Issue. *Proc. Natl. Acad. Sci.* **105**, 20047–20048 (2008).
20. Zhang, R., Ou, H.-Y. & Zhang, C.-T. DEG: a database of essential genes. *Nucleic Acids Res.* **32**, D271-272 (2004).
21. Kim, I. *et al.* Link clustering explains non-central and contextually essential genes in protein interaction networks. *Sci. Rep.* **9**, 11672 (2019).
22. Li, X., Li, W., Zeng, M., Zheng, R. & Li, M. Network-based methods for predicting essential genes or proteins: a survey. *Brief. Bioinform.* **21**, 566–583 (2020).
23. Mann, B. S., Johnson, J. R., Cohen, M. H., Justice, R. & Pazdur, R. FDA approval summary: vorinostat for treatment of advanced primary cutaneous T-cell lymphoma. *The Oncologist* **12**, 1247–1252 (2007).
24. Park, S.-Y. & Kim, J.-S. A short guide to histone deacetylases including recent progress on class II enzymes. *Exp. Mol. Med.* **52**, 204–212 (2020).
25. Bhaskara, S. *et al.* Hdac3 is essential for the maintenance of chromatin structure and genome stability. *Cancer Cell* **18**, 436–447 (2010).
26. Mrakovcic, M., Kleinheinz, J. & Fröhlich, L. F. p53 at the Crossroads between Different Types of HDAC Inhibitor-Mediated Cancer Cell Death. *Int. J. Mol. Sci.* **20**, (2019).
27. Hughes, M. A. *et al.* Co-operative and Hierarchical Binding of c-FLIP and Caspase-8: A Unified Model Defines How c-FLIP Isoforms Differentially Control Cell Fate. *Mol. Cell* **61**, 834–849 (2016).
28. Kerr, E. *et al.* Identification of an acetylation-dependant Ku70/FLIP complex that regulates FLIP expression and HDAC inhibitor-induced apoptosis. *Cell Death Differ.* **19**, 1317–1327 (2012).
29. Hurwitz, J. L. *et al.* Vorinostat/SAHA-induced apoptosis in malignant mesothelioma is FLIP/caspase 8-dependent and HR23B-independent. *Eur. J. Cancer Oxf. Engl. 1990* **48**, 1096–1107 (2012).

30. Choi, H.-K. *et al.* Programmed cell death 5 mediates HDAC3 decay to promote genotoxic stress response. *Nat. Commun.* **6**, 7390 (2015).
31. Singh, T., Prasad, R. & Katiyar, S. K. Inhibition of class I histone deacetylases in non-small cell lung cancer by honokiol leads to suppression of cancer cell growth and induction of cell death in vitro and in vivo. *Epigenetics* **8**, 54–65 (2013).
32. Jardim, D. L., De Melo Gagliato, D., Nikanjam, M., Barkauskas, D. A. & Kurzrock, R. Efficacy and safety of anticancer drug combinations: a meta-analysis of randomized trials with a focus on immunotherapeutics and gene-targeted compounds. *Oncoimmunology* **9**, (2020).
33. Garraway, L. A. & Lander, E. S. Lessons from the Cancer Genome. *Cell* **153**, 17–37 (2013).
34. Chen, H. *et al.* New insights on human essential genes based on integrated analysis and the construction of the HEGIAP web-based platform. *Brief. Bioinform.* **21**, 1397–1410 (2020).
35. Yau, E. H. *et al.* Genome-Wide CRISPR Screen for Essential Cell Growth Mediators in Mutant KRAS Colorectal Cancers. *Cancer Res.* **77**, 6330–6339 (2017).
36. Yilmaz, A., Peretz, M., Aharony, A., Sagi, I. & Benvenisty, N. Defining essential genes for human pluripotent stem cells by CRISPR–Cas9 screening in haploid cells. *Nat. Cell Biol.* **20**, 610–619 (2018).
37. González-Magaña, A. & Blanco, F. J. Human PCNA Structure, Function, and Interactions. *Biomolecules* **10**, (2020).
38. Prestel, A. *et al.* The PCNA interaction motifs revisited: thinking outside the PIP-box. *Cell. Mol. Life Sci.* **76**, 4923–4943 (2019).
39. Knijnenburg, T. A. *et al.* Genomic and Molecular Landscape of DNA Damage Repair Deficiency across The Cancer Genome Atlas. *Cell Rep.* **23**, 239-254.e6 (2018).
40. Weeden, C. E. & Asselin-Labat, M.-L. Mechanisms of DNA damage repair in adult stem cells and implications for cancer formation. *Biochim. Biophys. Acta BBA - Mol. Basis Dis.* **1864**, 89–101 (2018).
41. Lang, S. H. *et al.* A systematic review of the prevalence of DNA damage response gene mutations in prostate cancer. *Int. J. Oncol.* **55**, 597–616 (2019).
42. Kalucka, J. *et al.* Metabolic control of the cell cycle. *Cell Cycle* **14**, 3379–3388 (2015).
43. Icard, P., Fournel, L., Wu, Z., Alifano, M. & Lincet, H. Interconnection between Metabolism and Cell Cycle in Cancer. *Trends Biochem. Sci.* **44**, 490–501 (2019).
44. Barnum, K. J. & O’Connell, M. J. Cell Cycle Regulation by Checkpoints. *Methods Mol. Biol. Clifton NJ* **1170**, 29–40 (2014).

45. WENZEL, E. S. & SINGH, A. T. K. Cell-cycle Checkpoints and Aneuploidy on the Path to Cancer. *In Vivo* **32**, 1–5 (2018).
46. Colleoni, B. *et al.* JNKs function as CDK4-activating kinases by phosphorylating CDK4 and p21. *Oncogene* **36**, 4349–4361 (2017).
47. Hoffmann, I. The role of Cdc25 phosphatases in cell cycle checkpoints. *Protoplasma* **211**, 8–11 (2000).
48. Bower, J. J. *et al.* Patterns of cell cycle checkpoint deregulation associated with intrinsic molecular subtypes of human breast cancer cells. *Npj Breast Cancer* **3**, 1–12 (2017).
49. Tehrani, S. S. *et al.* The crosstalk between trace elements with DNA damage response, repair, and oxidative stress in cancer. *J. Cell. Biochem.* **120**, 1080–1105 (2019).
50. Barnes, R. P., Fouquerel, E. & Opresko, P. L. The impact of oxidative DNA damage and stress on telomere homeostasis. *Mech. Ageing Dev.* **177**, 37–45 (2019).
51. Turgeon, M.-O., Perry, N. J. S. & Poulogiannis, G. DNA Damage, Repair, and Cancer Metabolism. *Front. Oncol.* **8**, (2018).
52. Sun, J. *et al.* A systematic analysis of FDA-approved anticancer drugs. *BMC Syst. Biol.* **11**, (2017).
53. Yin, Q.-K. *et al.* Discovery of Isaindigotone Derivatives as Novel Bloom’s Syndrome Protein (BLM) Helicase Inhibitors That Disrupt the BLM/DNA Interactions and Regulate the Homologous Recombination Repair. *J. Med. Chem.* **62**, 3147–3162 (2019).
54. Petroni, M. *et al.* MRE11 inhibition highlights a replication stress-dependent vulnerability of MYCN-driven tumors. *Cell Death Dis.* **9**, (2018).
55. Toma, M., Sullivan-Reed, K., Śliwiński, T. & Skorski, T. RAD52 as a Potential Target for Synthetic Lethality-Based Anticancer Therapies. *Cancers* **11**, (2019).
56. Ehmsen, K. T. *et al.* Small molecule inhibitors of a human recombination-associated ATPase, RAD54. *bioRxiv* 614586 (2019) doi:10.1101/614586.
57. Hengel, S. R., Spies, M. A. & Spies, M. Small molecule inhibitors targeting DNA repair and DNA repair deficiency in research and cancer therapy. *Cell Chem. Biol.* **24**, 1101–1119 (2017).
58. Dickson, M. A. & Schwartz, G. K. Development of cell-cycle inhibitors for cancer therapy. *Curr. Oncol.* **16**, 36–43 (2009).
59. Hwang, B.-J., Adhikary, G., Eckert, R. L. & Lu, A.-L. Chk1 inhibition as a novel therapeutic strategy in melanoma. *Oncotarget* **9**, 30450–30464 (2018).

60. Kim, S. O. *et al.* Srs2 possesses a non-canonical PIP box in front of its SBM for precise recognition of SUMOylated PCNA. *J. Mol. Cell Biol.* **4**, 258–261 (2012).
61. Nicolae, C. M. *et al.* The ADP-ribosyltransferase PARP10/ARTD10 interacts with proliferating cell nuclear antigen (PCNA) and is required for DNA damage tolerance. *J. Biol. Chem.* **289**, 13627–13637 (2014).
62. Gali, H. *et al.* Role of SUMO modification of human PCNA at stalled replication fork. *Nucleic Acids Res.* **40**, 6049–6059 (2012).
63. Ulrich, H. D. & Takahashi, T. Readers of PCNA modifications. *Chromosoma* **122**, 259–274 (2013).
64. Lo, Y.-H. *et al.* Phosphorylation at tyrosine 114 of Proliferating Cell Nuclear Antigen (PCNA) is required for adipogenesis in response to high fat diet. *Biochem. Biophys. Res. Commun.* **430**, 43–48 (2013).
65. Shaheen, M., Shanmugam, I. & Hromas, R. The Role of PCNA Posttranslational Modifications in Translesion Synthesis. *J. Nucleic Acids* **2010**, (2010).
66. Slade, D. Maneuvers on PCNA Rings during DNA Replication and Repair. *Genes* **9**, (2018).
67. Ortega, J. *et al.* Phosphorylation of PCNA by EGFR inhibits mismatch repair and promotes misincorporation during DNA synthesis. *Proc. Natl. Acad. Sci. U. S. A.* **112**, 5667–5672 (2015).
68. Peng, B., Ortega, J., Gu, L., Chang, Z. & Li, G.-M. Phosphorylation of proliferating cell nuclear antigen promotes cancer progression by activating the ATM/Akt/GSK3 β /Snail signaling pathway. *J. Biol. Chem.* **294**, 7037–7045 (2019).
69. Bian, L., Meng, Y., Zhang, M. & Li, D. MRE11-RAD50-NBS1 complex alterations and DNA damage response: implications for cancer treatment. *Mol. Cancer* **18**, 169 (2019).
70. Casari, E. *et al.* Processing of DNA Double-Strand Breaks by the MRX Complex in a Chromatin Context. *Front. Mol. Biosci.* **6**, (2019).
71. Lamarche, B. J., Orazio, N. I. & Weitzman, M. D. The MRN complex in Double-Strand Break Repair and Telomere Maintenance. *FEBS Lett.* **584**, 3682–3695 (2010).
72. Ray Chaudhuri, A. & Nussenzweig, A. The multifaceted roles of PARP1 in DNA repair and chromatin remodelling. *Nat. Rev. Mol. Cell Biol.* **18**, 610–621 (2017).
73. Javle, M. & Curtin, N. J. The role of PARP in DNA repair and its therapeutic exploitation. *Br. J. Cancer* **105**, 1114–1122 (2011).
74. Roy, S. *et al.* XRCC4/XLF Interaction Is Variably Required for DNA Repair and Is Not Required for Ligase IV Stimulation. *Mol. Cell. Biol.* **35**, 3017–3028 (2015).

75. Balmus, G. *et al.* ATM orchestrates the DNA-damage response to counter toxic non-homologous end-joining at broken replication forks. *Nat. Commun.* **10**, 87 (2019).
76. Shyr, D. & Liu, Q. Next generation sequencing in cancer research and clinical application. *Biol. Proced. Online* **15**, 4 (2013).
77. Creixell, P. *et al.* Pathway and Network Analysis of Cancer Genomes. *Nat. Methods* **12**, 615–621 (2015).
78. Shyr, D. & Liu, Q. Next generation sequencing in cancer research and clinical application. *Biol. Proced. Online* **15**, 4 (2013).
79. Deng, J.-L., Xu, Y. & Wang, G. Identification of Potential Crucial Genes and Key Pathways in Breast Cancer Using Bioinformatic Analysis. *Front. Genet.* **10**, (2019).
80. Wu, J., Mamidi, T. K. K., Zhang, L. & Hicks, C. Integrating Germline and Somatic Mutation Information for the Discovery of Biomarkers in Triple-Negative Breast Cancer. *Int. J. Environ. Res. Public Health* **16**, (2019).
81. Geeleher, P. & Huang, R. S. Exploring the link between the germline and somatic genome in cancer. *Cancer Discov.* **7**, 354–355 (2017).
82. Bister, K. Discovery of oncogenes: The advent of molecular cancer research. *Proc. Natl. Acad. Sci. U. S. A.* **112**, 15259–15260 (2015).
83. Cooper, G. M. Tumor Suppressor Genes. *Cell Mol. Approach 2nd Ed.* (2000).
84. Kuijjer, M. L., Paulson, J. N., Salzman, P., Ding, W. & Quackenbush, J. Cancer subtype identification using somatic mutation data. *Br. J. Cancer* **118**, 1492–1501 (2018).
85. Iranzo, J., Martincorena, I. & Koonin, E. V. Cancer-mutation network and the number and specificity of driver mutations. *Proc. Natl. Acad. Sci.* **115**, E6010–E6019 (2018).
86. Kim, H. & Kim, Y.-M. Pan-cancer analysis of somatic mutations and transcriptomes reveals common functional gene clusters shared by multiple cancer types. *Sci. Rep.* **8**, 6041 (2018).
87. He, N., Kim, N. & Yoon, S. Somatic mutation patterns and compound response in cancers. *BMB Rep.* **46**, 97–102 (2013).
88. Rapin, N. *et al.* Comparing cancer vs normal gene expression profiles identifies new disease entities and common transcriptional programs in AML patients. *Blood* **123**, 894–904 (2014).
89. Ramaswamy, S. *et al.* Multiclass cancer diagnosis using tumor gene expression signatures. *Proc. Natl. Acad. Sci. U. S. A.* **98**, 15149–15154 (2001).
90. Shaheen, S., Fawaz, F., Shah, S. & Büsselberg, D. Differential Expression and Pathway Analysis in Drug-Resistant Triple-Negative Breast Cancer Cell Lines Using RNASeq Analysis. *Int. J. Mol. Sci.* **19**, (2018).

91. Lee, J. H., Park, Y. R., Jung, M. & Lim, S. G. Gene regulatory network analysis with drug sensitivity reveals synergistic effects of combinatory chemotherapy in gastric cancer. *Sci. Rep.* **10**, 3932 (2020).
92. Talhouk, A. & McAlpine, J. N. New classification of endometrial cancers: the development and potential applications of genomic-based classification in research and clinical care. *Gynecol. Oncol. Res. Pract.* **3**, (2016).
93. Madsen, M. J. *et al.* Reparameterization of PAM50 Expression Identifies Novel Breast Tumor Dimensions and Leads to Discovery of a Genome-Wide Significant Breast Cancer Locus at 12q15. *Cancer Epidemiol. Prev. Biomark.* **27**, 644–652 (2018).
94. Pu, M. *et al.* Research-based PAM50 signature and long-term breast cancer survival. *Breast Cancer Res. Treat.* **179**, 197–206 (2020).
95. Radosa, J. C. *et al.* Evaluation of Local and Distant Recurrence Patterns in Patients with Triple-Negative Breast Cancer According to Age. *Ann. Surg. Oncol.* **24**, 698–704 (2017).
96. He, M. Y. *et al.* Radiotherapy in triple-negative breast cancer: Current situation and upcoming strategies. *Crit. Rev. Oncol. Hematol.* **131**, 96–101 (2018).
97. O'Reilly, E. A. *et al.* The fate of chemoresistance in triple negative breast cancer (TNBC). *BBA Clin.* **3**, 257–275 (2015).
98. Leung, A. W. Y. *et al.* Combined Use of Gene Expression Modeling and siRNA Screening Identifies Genes and Pathways Which Enhance the Activity of Cisplatin When Added at No Effect Levels to Non-Small Cell Lung Cancer Cells In Vitro. *PLOS ONE* **11**, e0150675 (2016).
99. Selga, E. *et al.* Networking of differentially expressed genes in human cancer cells resistant to methotrexate. *Genome Med.* **1**, 83 (2009).
100. Chène, P. Inhibiting the p53–MDM2 interaction: an important target for cancer therapy. *Nat. Rev. Cancer* **3**, 102–109 (2003).
101. Moll, U. M. & Petrenko, O. The MDM2-p53 Interaction. *Mol. Cancer Res.* **1**, 1001–1008 (2003).
102. Grindrod, P. & Kibble, M. Review of uses of network and graph theory concepts within proteomics. *Expert Rev. Proteomics* **1**, 229–238 (2004).
103. Chisanga, D., Keerthikumar, S., Mathivanan, S. & Chilamkurti, N. Network Tools for the Analysis of Proteomic Data. *Methods Mol. Biol. Clifton NJ* **1549**, 177–197 (2017).
104. Zhao, K. & So, H.-C. Using Drug Expression Profiles and Machine Learning Approach for Drug Repurposing. *Methods Mol. Biol. Clifton NJ* **1903**, 219–237 (2019).

105. Chen, H., Zhang, H., Zhang, Z., Cao, Y. & Tang, W. Network-Based Inference Methods for Drug Repositioning. *Computational and Mathematical Methods in Medicine* vol. 2015 e130620 <https://www.hindawi.com/journals/cmmm/2015/130620/> (2015).
106. Merk, A. *et al.* Breaking Cryo-EM Resolution Barriers to Facilitate Drug Discovery. *Cell* **165**, 1698–1707 (2016).
107. Oosterheert, W. & Gros, P. Cryo-electron microscopy structure and potential enzymatic function of human six-transmembrane epithelial antigen of the prostate 1 (STEAP1). *J. Biol. Chem.* **295**, 9502–9512 (2020).
108. Agrawal, S. The Wilms' tumor (WT1) gene: Methods and protocols. *Indian J. Med. Res.* **147**, 622–624 (2018).
109. Ramsawhook, A., Ruzov, A. & Coyle, B. Wilms' Tumor Protein 1 and Enzymatic Oxidation of 5-Methylcytosine in Brain Tumors: Potential Perspectives. *Front. Cell Dev. Biol.* **6**, (2018).
110. Bojadzic, D. & Buchwald, P. Toward Small-Molecule Inhibition of Protein–Protein Interactions: General Aspects and Recent Progress in Targeting Costimulatory and Coinhibitory (Immune Checkpoint) Interactions. *Curr. Top. Med. Chem.* **18**, 674–699 (2018).
111. Arkin, M. R., Tang, Y. & Wells, J. A. Small-molecule inhibitors of protein-protein interactions: progressing towards the reality. *Chem. Biol.* **21**, 1102–1114 (2014).
112. Vicent, S. *et al.* Wilms tumor 1 (WT1) regulates KRAS-driven oncogenesis and senescence in mouse and human models. *J. Clin. Invest.* **120**, 3940–3952 (2010).
113. Wilson, R. H. C. *et al.* PCNA dependent cellular activities tolerate dramatic perturbations in PCNA client interactions. *DNA Repair* **50**, 22–35 (2017).
114. Duffy, C. M., Hilbert, B. J. & Kelch, B. A. A Disease-Causing Variant in PCNA Disrupts a Promiscuous Protein Binding Site. *J. Mol. Biol.* **428**, 1023–1040 (2016).
115. Luqmani, Y. A. Mechanisms of drug resistance in cancer chemotherapy. *Med. Princ. Pract. Int. J. Kuwait Univ. Health Sci. Cent.* **14 Suppl 1**, 35–48 (2005).
116. Alfarouk, K. O. *et al.* Resistance to cancer chemotherapy: failure in drug response from ADME to P-gp. *Cancer Cell Int.* **15**, (2015).
117. Huang, R.-X. & Zhou, P.-K. DNA damage response signaling pathways and targets for radiotherapy sensitization in cancer. *Signal Transduct. Target. Ther.* **5**, 1–27 (2020).
118. Dökümcü, K. & Farahani, R. M. Evolution of Resistance in Cancer: A Cell Cycle Perspective. *Front. Oncol.* **9**, (2019).

119. Fujii, T., Naing, A., Rolfo, C. & Hajjar, J. Biomarkers of response to immune checkpoint blockade in cancer treatment. *Crit. Rev. Oncol. Hematol.* **130**, 108–120 (2018).
120. Liu, M. *et al.* Cell-specific biomarkers and targeted biopharmaceuticals for breast cancer treatment. *Cell Prolif.* **49**, 409–420 (2016).
121. Bratman, S. V. *et al.* Personalized circulating tumor DNA analysis as a predictive biomarker in solid tumor patients treated with pembrolizumab. *Nat. Cancer* **1**, 873–881 (2020).
122. Lim, Z.-F. & Ma, P. C. Emerging insights of tumor heterogeneity and drug resistance mechanisms in lung cancer targeted therapy. *J. Hematol. Oncol. J Hematol Oncol* **12**, 134 (2019).
123. Lønning, P. E. & Knappskog, S. Mapping genetic alterations causing chemoresistance in cancer: identifying the roads by tracking the drivers. *Oncogene* **32**, 5315–5330 (2013).
124. Lavi, O. Redundancy: A Critical Obstacle to Improving Cancer Therapy. *Cancer Res.* **75**, 808–812 (2015).
125. Dand, N., Sprengel, F., Ahlers, V. & Schlitt, T. BioGranat-IG: a network analysis tool to suggest mechanisms of genetic heterogeneity from exome-sequencing data. *Bioinformatics* **29**, 733–741 (2013).
126. Gliozzo, J. *et al.* Network modeling of patients' biomolecular profiles for clinical phenotype/outcome prediction. *Sci. Rep.* **10**, 3612 (2020).
127. Wang, J. *et al.* Pathway and Network Approaches for Identification of Cancer Signature Markers from Omics Data. *J. Cancer* **6**, 54–65 (2015).
128. Richiardi, L., Barone-Adesi, F. & Pearce, N. Cancer subtypes in aetiological research. *Eur. J. Epidemiol.* **32**, 353–361 (2017).
129. Taylor, A. S., Spratt, D. E., Dhanasekaran, S. M. & Mehra, R. Contemporary Renal Tumor Categorization With Biomarker and Translational Updates: A Practical Review. *Arch. Pathol. Lab. Med.* **143**, 1477–1491 (2019).
130. Walker, A. J. *et al.* FDA Approval of Palbociclib in Combination with Fulvestrant for the Treatment of Hormone Receptor–Positive, HER2-Negative Metastatic Breast Cancer. *Clin. Cancer Res.* **22**, 4968–4972 (2016).
131. Shah, A. *et al.* FDA Approval: Ribociclib for the Treatment of Postmenopausal Women with Hormone Receptor–Positive, HER2-Negative Advanced or Metastatic Breast Cancer. *Clin. Cancer Res.* **24**, 2999–3004 (2018).
132. Caulfield, S. E., Davis, C. C. & Byers, K. F. Olaparib: A Novel Therapy for Metastatic Breast Cancer in Patients With a BRCA1/2 Mutation. *J. Adv. Pract. Oncol.* **10**, 167–174 (2019).

133. Sud, A., Kinnersley, B. & Houlston, R. S. Genome-wide association studies of cancer: current insights and future perspectives. *Nat. Rev. Cancer* **17**, 692–704 (2017).
134. Liang, B., Ding, H., Huang, L., Luo, H. & Zhu, X. GWAS in cancer: progress and challenges. *Mol. Genet. Genomics* **295**, 537–561 (2020).
135. Wang, X. Identification of common tumor signatures based on gene set enrichment analysis. *In Silico Biol.* **11**, 1–10 (2011).
136. Long, T. *et al.* Identification of differentially expressed genes and enriched pathways in lung cancer using bioinformatics analysis. *Mol. Med. Rep.* **19**, 2029–2040 (2019).
137. Kanehisa, M., Sato, Y., Kawashima, M., Furumichi, M. & Tanabe, M. KEGG as a reference resource for gene and protein annotation. *Nucleic Acids Res.* **44**, D457–D462 (2016).
138. Krämer, A., Green, J., Pollard, J. & Tugendreich, S. Causal analysis approaches in Ingenuity Pathway Analysis. *Bioinforma. Oxf. Engl.* **30**, 523–530 (2014).
139. Frost, H. R. & Amos, C. I. A multi-omics approach for identifying important pathways and genes in human cancer. *BMC Bioinformatics* **19**, (2018).
140. Ryan, M. B. *et al.* Vertical Pathway Inhibition Overcomes Adaptive Feedback Resistance to KRASG12C Inhibition. *Clin. Cancer Res.* **26**, 1633–1643 (2020).
141. Ozkan-Dagliyan, I. *et al.* Low-Dose Vertical Inhibition of the RAF-MEK-ERK Cascade Causes Apoptotic Death of KRAS Mutant Cancers. *Cell Rep.* **31**, 107764 (2020).
142. Huang, A., Garraway, L. A., Ashworth, A. & Weber, B. Synthetic lethality as an engine for cancer drug target discovery. *Nat. Rev. Drug Discov.* **19**, 23–38 (2020).
143. Lord, C. J. & Ashworth, A. BRCAness revisited. *Nat. Rev. Cancer* **16**, 110–120 (2016).
144. Dziadkowiec, K. N., Gąsiorowska, E., Nowak-Markwitz, E. & Jankowska, A. PARP inhibitors: review of mechanisms of action and BRCA1/2 mutation targeting. *Przegląd Menopauzalny Menopause Rev.* **15**, 215–219 (2016).
145. Marshall, C. H. *et al.* Differential Response to Olaparib Treatment Among Men with Metastatic Castration-resistant Prostate Cancer Harboring BRCA1 or BRCA2 Versus ATM Mutations. *Eur. Urol.* **76**, 452–458 (2019).
146. Rafiee, R. *et al.* Genome-Scale CRISPR-Cas9 Synthetic Lethal Screening of AML Cell Line Identified Functional Modulators of Etoposide Resistance Predictive of Clinical Outcome in AML Patients. *Blood* **134**, 2685–2685 (2019).
147. Dhoonmoon, A., Schleicher, E. M., Clements, K. E., Nicolae, C. M. & Moldovan, G.-L. Genome-wide CRISPR synthetic lethality screen identifies a role for the ADP-ribosyltransferase PARP14 in DNA replication dynamics controlled by ATR. *Nucleic Acids Res.* **48**, 7252–7264 (2020).

148. Liang, H., Jeyasekharan, A. & Rajan, V. Predicting Synthetic Lethal Interactions using Heterogeneous Data Sources. *bioRxiv* 660092 (2019) doi:10.1101/660092.
149. Topatana, W. *et al.* Advances in synthetic lethality for cancer therapy: cellular mechanism and clinical translation. *J. Hematol. Oncol.* **13**, 118 (2020).
150. Gerber, D. E. EGFR Inhibition in the Treatment of Non-Small Cell Lung Cancer. *Drug Dev. Res.* **69**, 359–372 (2008).
151. Li, Y., Li, X. & Dong, Z. Statistical Analysis of EGFR Structures' Performance in Virtual Screening. *J. Comput. Aided Mol. Des.* **29**, 1045–1055 (2015).
152. DrugCombDB: a comprehensive database of drug combinations toward the discovery of combinatorial therapy | *Nucleic Acids Research* | Oxford Academic. <https://academic.oup.com/nar/article/48/D1/D871/5609522>.
153. Guo, J., Liu, H. & Zheng, J. SynLethDB: synthetic lethality database toward discovery of selective and sensitive anticancer drug targets. *Nucleic Acids Res.* **44**, D1011–D1017 (2016).
154. Li, X., Mishra, S. K., Wu, M., Zhang, F. & Zheng, J. Syn-Lethality: An Integrative Knowledge Base of Synthetic Lethality towards Discovery of Selective Anticancer Therapies. *BioMed Research International* vol. 2014 e196034 <https://www.hindawi.com/journals/bmri/2014/196034/> (2014).
155. Nijman, S. M. B. Synthetic lethality: General principles, utility and detection using genetic screens in human cells. *Febs Lett.* **585**, 1–6 (2011).
156. Krause, S. A. & Gray, J. V. The functional relationships underlying a synthetic genetic network. *Commun. Integr. Biol.* **2**, 4–6 (2009).
157. Biswas, S. & Rao, C. M. Epigenetics in cancer: Fundamentals and Beyond. *Pharmacol. Ther.* **173**, 118–134 (2017).
158. DeBerardinis, R. J. & Chandel, N. S. Fundamentals of cancer metabolism. *Sci. Adv.* **2**, e1600200 (2016).
159. Peters, J., Loud, J., Dimond, E. & Jenkins, J. Cancer Genetics Fundamentals. *Cancer Nurs.* **24**, 446–461 (2001).
160. Xue, J., Liu, Y., Wan, L. & Zhu, Y. Comprehensive Analysis of Differential Gene Expression to Identify Common Gene Signatures in Multiple Cancers. *Med. Sci. Monit. Int. Med. J. Exp. Clin. Res.* **26**, e919953-1-e919953-13 (2020).
161. Mohiuddin, I. S. & Kang, M. H. DNA-PK as an Emerging Therapeutic Target in Cancer. *Front. Oncol.* **9**, (2019).
162. Berdis, A. J. Inhibiting DNA Polymerases as a Therapeutic Intervention against Cancer. *Front. Mol. Biosci.* **4**, (2017).

163. Mills, C. C., Kolb, E. & Sampson, V. B. Recent Advances of Cell-Cycle Inhibitor Therapies for Pediatric Cancer. *Cancer Res.* **77**, 6489–6498 (2017).
164. Janke, R., King, G. A., Kupiec, M. & g, J. Pivotal roles of PCNA loading and unloading in heterochromatin function. *Proc. Natl. Acad. Sci.* **115**, E2030–E2039 (2018).
165. Lowe, M., Hostager, R. & g, N. Preservation of Epigenetic Memory During DNA Replication. *J. Stem Cell Res. Ther.* **1**, (2016).
166. Boehm, E. M., Gildenberg, M. S. & Washington, M. T. The many roles of PCNA in eukaryotic DNA replication. *The Enzymes* **39**, 231–254 (2016).
167. Cheung-Ong, K., Giaever, G. & Nislow, C. DNA-Damaging Agents in Cancer Chemotherapy: Serendipity and Chemical Biology. *Chem. Biol.* **20**, 648–659 (2013).
168. Nag, S. *et al.* Targeting MDM2-p53 Interaction for Cancer Therapy: Are We There Yet? *Curr. Med. Chem.* **21**, 553–574 (2014).
169. Morrow, J. K., Lin, H.-K., Sun, S.-C. & Zhang, S. Targeting ubiquitination for cancer therapies. *Future Med. Chem.* **7**, 2333–2350 (2015).
170. Eckschlager, T., Plch, J., Stiborova, M. & Hrabeta, J. Histone Deacetylase Inhibitors as Anticancer Drugs. *Int. J. Mol. Sci.* **18**, (2017).
171. Heo, K.-S. Regulation of post-translational modification in breast cancer treatment. *BMB Rep.* **52**, 113–118 (2019).
172. Bowler, E. H. *et al.* Deep proteomic analysis of Dnmt1 mutant/hypomorphic colorectal cancer cells reveals dys-regulation of Epithelial-Mesenchymal Transition and subcellular re-localization of Beta-Catenin. *bioRxiv* 547737 (2019) doi:10.1101/547737.
173. Zhao, H. *et al.* Interaction of Proliferation Cell Nuclear Antigen (PCNA) with c-Abl in Cell Proliferation and Response to DNA Damages in Breast Cancer. *PLOS ONE* **7**, e29416 (2012).
174. Zhao, H. *et al.* Targeting Tyrosine Phosphorylation of PCNA Inhibits Prostate Cancer Growth. *Mol. Cancer Ther.* **10**, 29–36 (2011).
175. Notenboom, V. *et al.* Functional characterization of Rad18 domains for Rad6, ubiquitin, DNA binding and PCNA modification. *Nucleic Acids Res.* **35**, 5819–5830 (2007).
176. Masuda, Y. *et al.* Different types of interaction between PCNA and PIP boxes contribute to distinct cellular functions of Y-family DNA polymerases. *Nucleic Acids Res.* **43**, 7898–7910 (2015).
177. Punchihewa, C. *et al.* Identification of Small Molecule Proliferating Cell Nuclear Antigen (PCNA) Inhibitor That Disrupts Interactions with PIP-box Proteins and Inhibits DNA Replication. *J. Biol. Chem.* **287**, 14289–14300 (2012).

178. Arnoult, N. *et al.* Regulation of DNA repair pathway choice in S and G2 phases by the NHEJ inhibitor CYREN. *Nature* **549**, 548–552 (2017).
179. Zhao, X. *et al.* Cell cycle-dependent control of homologous recombination. *Acta Biochim. Biophys. Sin.* **49**, 655–668 (2017).
180. Wei, F. *et al.* Inhibition of ERK activation enhances the repair of double-stranded breaks via non-homologous end joining by increasing DNA-PKcs activation. *Biochim. Biophys. Acta BBA - Mol. Cell Res.* **1833**, 90–100 (2013).
181. Golding, S. E., Neill, S., Dent, P., Povirk, L. F. & Valerie, K. C. MAPK signaling pathways positively and negatively regulate homologous recombination repair. *Cancer Res.* **66**, 1029–1030 (2006).
182. Golding, S. E. *et al.* Extracellular signal-related kinase positively regulates ataxia telangiectasia mutated, homologous recombination repair, and the DNA damage response. *Cancer Res.* **67**, 1046–1053 (2007).
183. Li, J., Holzschu, D. L. & Sugiyama, T. PCNA is efficiently loaded on the DNA recombination intermediate to modulate polymerase δ , η , and ζ activities. *Proc. Natl. Acad. Sci.* **110**, 7672–7677 (2013).
184. Li, X., Stith, C. M., Burgers, P. M. & Heyer, W.-D. PCNA is required for initiation of recombination-associated DNA synthesis by DNA polymerase δ . *Mol. Cell* **36**, 704–713 (2009).
185. Krejci, L., Altmannova, V., Spirek, M. & Zhao, X. Homologous recombination and its regulation. *Nucleic Acids Res.* **40**, 5795–5818 (2012).
186. Mao, Z., Bozzella, M., Seluanov, A. & Gorbunova, V. DNA repair by nonhomologous end joining and homologous recombination during cell cycle in human cells. *Cell Cycle Georget. Tex* **7**, 2902–2906 (2008).
187. Kiwerska, K. & Szyfter, K. DNA repair in cancer initiation, progression, and therapy—a double-edged sword. *J. Appl. Genet.* **60**, 329–334 (2019).
188. Wei, L. *et al.* DNA damage during the G0/G1 phase triggers RNA-templated, Cockayne syndrome B-dependent homologous recombination. *Proc. Natl. Acad. Sci.* **112**, E3495–E3504 (2015).
189. Seluanov, A., Mittelman, D., Pereira-Smith, O. M., Wilson, J. H. & Gorbunova, V. DNA end joining becomes less efficient and more error-prone during cellular senescence. *Proc. Natl. Acad. Sci.* **101**, 7624–7629 (2004).
190. Rodgers, K. & McVey, M. Error-prone repair of DNA double-strand breaks. *J. Cell. Physiol.* **231**, 15–24 (2016).

191. Ledermann, J. *et al.* Olaparib Maintenance Therapy in Platinum-Sensitive Relapsed Ovarian Cancer. *N. Engl. J. Med.* **366**, 1382–1392 (2012).
192. Murai, J. *et al.* Differential trapping of PARP1 and PARP2 by clinical PARP inhibitors. *Cancer Res.* **72**, 5588–5599 (2012).
193. Hopkins, T. A. *et al.* PARP1 Trapping by PARP Inhibitors Drives Cytotoxicity in Both Cancer Cells and Healthy Bone Marrow. *Mol. Cancer Res.* **17**, 409–419 (2019).
194. Byrum, A. K., Vindigni, A. & Mosammaparast, N. Defining and Modulating ‘BRCAness’. *Trends Cell Biol.* **29**, 740–751 (2019).
195. Turner, N., Tutt, A. & Ashworth, A. Hallmarks of ‘BRCAness’ in sporadic cancers. *Nat. Rev. Cancer* **4**, 814–819 (2004).
196. Zeman, M. K. & Cimprich, K. A. Causes and Consequences of Replication Stress. *Nat. Cell Biol.* **16**, 2–9 (2014).
197. Gaillard, H., García-Muse, T. & Aguilera, A. Replication stress and cancer. *Nat. Rev. Cancer* **15**, 276–289 (2015).
198. Alexander, J. L. & Orr-Weaver, T. L. Replication fork instability and the consequences of fork collisions from rereplication. *Genes Dev.* **30**, 2241–2252 (2016).
199. Srivastava, M. *et al.* Replisome Dynamics and Their Functional Relevance upon DNA Damage through the PCNA Interactome. *Cell Rep.* **25**, 3869–3883.e4 (2018).
200. De March, M. *et al.* Structural basis of human PCNA sliding on DNA. *Nat. Commun.* **8**, 13935 (2017).
201. Douki, T., Koschimbahr, A. von & Cadet, J. Insight in DNA Repair of UV-induced Pyrimidine Dimers by Chromatographic Methods. *Photochem. Photobiol.* **93**, 207–215 (2017).
202. Leung, W., Baxley, R. M., Moldovan, G.-L. & Bielinsky, A.-K. Mechanisms of DNA Damage Tolerance: Post-Translational Regulation of PCNA. *Genes* **10**, (2018).
203. Yang, W. An Overview of Y-Family DNA Polymerases and a Case Study of Human DNA Polymerase η . *Biochemistry* **53**, 2793–2803 (2014).
204. Kunz, B. A., Straffon, A. F. L. & Vonarx, E. J. DNA damage-induced mutation: tolerance via translesion synthesis. *Mutat. Res. Mol. Mech. Mutagen.* **451**, 169–185 (2000).
205. Lehmann, A. R. Replication of damaged DNA by translesion synthesis in human cells. *FEBS Lett.* **579**, 873–876 (2005).
206. Pedley, A. M., Lill, M. A. & Davisson, V. J. Flexibility of PCNA-Protein Interface Accommodates Differential Binding Partners. *PLOS ONE* **9**, e102481 (2014).

207. Zheleva, D. I. *et al.* A Quantitative Study of the in Vitro Binding of the C-Terminal Domain of p21 to PCNA: Affinity, Stoichiometry, and Thermodynamics. *Biochemistry* **39**, 7388–7397 (2000).
208. Bartolowits, M. D. *et al.* Discovery of Inhibitors for Proliferating Cell Nuclear Antigen Using a Computational-Based Linked-Multiple-Fragment Screen. *ACS Omega* **4**, 15181–15196 (2019).
209. Kontopidis, G. *et al.* Structural and biochemical studies of human proliferating cell nuclear antigen complexes provide a rationale for cyclin association and inhibitor design. *Proc. Natl. Acad. Sci.* **102**, 1871–1876 (2005).
210. Pedley, A. M., Lill, M. A. & Davisson, V. J. Flexibility of PCNA-Protein Interface Accommodates Differential Binding Partners. *PLoS ONE* **9**, (2014).
211. González-Magaña, A. & Blanco, F. J. Human PCNA Structure, Function, and Interactions. *Biomolecules* **10**, (2020).
212. Ando, T. *et al.* Involvement of the Interaction between p21 and Proliferating Cell Nuclear Antigen for the Maintenance of G2/M Arrest after DNA Damage. *J. Biol. Chem.* **276**, 42971–42977 (2001).
213. Wegener, K. L. *et al.* Rational Design of a 310 -Helical PIP-Box Mimetic Targeting PCNA, the Human Sliding Clamp. *Chem. Weinh. Bergstr. Ger.* **24**, 11325–11331 (2018).
214. Taghdisi, S. M. *et al.* Co-delivery of doxorubicin and α -PCNA aptamer using AS1411-modified pH-responsive nanoparticles for cancer synergistic therapy. *J. Drug Deliv. Sci. Technol.* **58**, 101816 (2020).
215. Gilljam, K. M., Müller, R., Liabakk, N. B. & Otterlei, M. Nucleotide excision repair is associated with the replisome and its efficiency depends on a direct interaction between XPA and PCNA. *PloS One* **7**, e49199 (2012).
216. Müller, R. *et al.* Targeting Proliferating Cell Nuclear Antigen and Its Protein Interactions Induces Apoptosis in Multiple Myeloma Cells. *PLoS ONE* **8**, (2013).
217. Warbrick, E. A functional analysis of PCNA-binding peptides derived from protein sequence, interaction screening and rational design. *Oncogene* **25**, 2850–2859 (2006).
218. Press_Release_APIM_Therapeutics_August_31.pdf.
219. Ortega, J. *et al.* Phosphorylation of PCNA by EGFR inhibits mismatch repair and promotes misincorporation during DNA synthesis. *Proc. Natl. Acad. Sci. U. S. A.* **112**, 5667–5672 (2015).

220. Inoue, A. *et al.* A Small Molecule Inhibitor of Monoubiquitinated Proliferating Cell Nuclear Antigen (PCNA) Inhibits Repair of Interstrand DNA Cross-link, Enhances DNA Double Strand Break, and Sensitizes Cancer Cells to Cisplatin. *J. Biol. Chem.* **289**, 7109–7120 (2014).
221. PCNA-interacting peptides reduce Akt phosphorylation and TLR-mediated cytokine secretion suggesting a role of PCNA in cellular signaling. *Cell. Signal.* **27**, 1478–1487 (2015).
222. Tan, Z. *et al.* Small-molecule targeting of proliferating cell nuclear antigen chromatin association inhibits tumor cell growth. *Mol. Pharmacol.* **81**, 811–819 (2012).
223. Yao, N. Y. & O'Donnell, M. The RFC Clamp Loader: Structure and Function. *Subcell. Biochem.* **62**, 259–279 (2012).
224. Lu, S. & Dong, Z. Additive effects of a small molecular PCNA inhibitor PCNA-IIS and DNA damaging agents on growth inhibition and DNA damage in prostate and lung cancer cells. *PLOS ONE* **14**, e0223894 (2019).
225. Malkas, L. H. *et al.* A cancer-associated PCNA expressed in breast cancer has implications as a potential biomarker. *Proc. Natl. Acad. Sci. U. S. A.* **103**, 19472–19477 (2006).
226. Smith, S. J. *et al.* A Peptide Mimicking a Region in Proliferating Cell Nuclear Antigen Specific to Key Protein Interactions Is Cytotoxic to Breast Cancer. *Mol. Pharmacol.* **87**, 263–276 (2015).
227. Gu, L. *et al.* The Anticancer Activity of a First-in-class Small-molecule Targeting PCNA. *Clin. Cancer Res. Off. J. Am. Assoc. Cancer Res.* **24**, 6053–6065 (2018).
228. Gulbis, J. M., Kelman, Z., Hurwitz, J., O'Donnell, M. & Kuriyan, J. Structure of the C-Terminal Region of p21WAF1/CIP1 Complexed with Human PCNA. *Cell* **87**, 297–306 (1996).
229. Bruning, J. B. & Shamoo, Y. Structural and Thermodynamic Analysis of Human PCNA with Peptides Derived from DNA Polymerase- δ p66 Subunit and Flap Endonuclease-1. *Structure* **12**, 2209–2219 (2004).
230. Young, S. C. A Systematic Review of Antiamyloidogenic and Metal-Chelating Peptoids: Two Structural Motifs for the Treatment of Alzheimer's Disease. *Mol. J. Synth. Chem. Nat. Prod. Chem.* **23**, (2018).
231. Meibohm, B. Pharmacokinetics and Pharmacodynamics of Peptide and Protein Therapeutics. in *Pharmaceutical Biotechnology: Fundamentals and Applications* (eds. Crommelin, D. J. A., Sindelar, R. D. & Meibohm, B.) 101–132 (Springer, 2013). doi:10.1007/978-1-4614-6486-0_5.
232. Andreev, K., Martynowycz, M. W. & Gidalevitz, D. Peptoid drug discovery and optimization via surface X-ray scattering. *Biopolymers* **110**, e23274 (2019).

233. Simon, R. J. *et al.* Peptoids: a modular approach to drug discovery. *Proc. Natl. Acad. Sci.* **89**, 9367–9371 (1992).
234. Chou, T.-C. Drug Combination Studies and Their Synergy Quantification Using the Chou-Talalay Method. *Cancer Res.* **70**, 440–446 (2010).
235. Franken, N. A. P., Rodermond, H. M., Stap, J., Haveman, J. & van Bree, C. Clonogenic assay of cells in vitro. *Nat. Protoc.* **1**, 2315–2319 (2006).
236. Olive, P. L. & Banáth, J. P. The comet assay: a method to measure DNA damage in individual cells. *Nat. Protoc.* **1**, 23–29 (2006).
237. Automated Comet Assay Imaging and Dual-Mask Analysis to Determine DNA Damage on an Individual Comet Basis | July 7, 2016. <https://www.biotek.com/resources/application-notes/automated-comet-assay-imaging-and-dual-mask-analysis-to-determine-dna-damage-on-an-individual-comet-basis/>.
238. Cruz, C. *et al.* RAD51 foci as a functional biomarker of homologous recombination repair and PARP inhibitor resistance in germline BRCA-mutated breast cancer. *Ann. Oncol.* **29**, 1203–1210 (2018).
239. Jossé, R. *et al.* ATR Inhibitors VE-821 and VX-970 Sensitize Cancer Cells to Topoisomerase I Inhibitors by Disabling DNA Replication Initiation and Fork Elongation Responses. *Cancer Res.* **74**, 6968–6979 (2014).
240. van Veelen, L. R. *et al.* Ionizing radiation-induced foci formation of mammalian Rad51 and Rad54 depends on the Rad51 paralogs, but not on Rad52. *Mutat. Res.* **574**, 34–49 (2005).
241. Mason, J. M. *et al.* RAD54 family translocases counter genotoxic effects of RAD51 in human tumor cells. *Nucleic Acids Res.* **43**, 3180–3196 (2015).
242. Sunada, S., Nakanishi, A. & Miki, Y. Crosstalk of DNA double-strand break repair pathways in poly(ADP-ribose) polymerase inhibitor treatment of breast cancer susceptibility gene 1/2-mutated cancer. *Cancer Sci.* **109**, 893–899 (2018).
243. Fridlich, R., Annamalai, D., Roy, R., Bernheim, G. & Powell, S. N. BRCA1 and BRCA2 protect against oxidative DNA damage converted into double-strand breaks during DNA replication. *DNA Repair* **30**, 11–20 (2015).
244. Tian, F. *et al.* BRCA1 promotes the ubiquitination of PCNA and recruitment of translesion polymerases in response to replication blockade. *Proc. Natl. Acad. Sci. U. S. A.* **110**, 13558–13563 (2013).
245. Burgess, R. C. *et al.* The PCNA interaction protein box sequence in Rad54 is an integral part of its ATPase domain and is required for efficient DNA repair and recombination. *PLoS One* **8**, e82630 (2013).

246. Warbrick, E., Lane, D. P., Glover, D. M. & Cox, L. S. A small peptide inhibitor of DNA replication defines the site of interaction between the cyclin-dependent kinase inhibitor p21WAF1 and proliferating cell nuclear antigen. *Curr. Biol.* **5**, 275–282 (1995).
247. Ben-Shahar, T. R. *et al.* Two Fundamentally Distinct PCNA Interaction Peptides Contribute to Chromatin Assembly Factor 1 Function. *Mol. Cell. Biol.* **29**, 6353–6365 (2009).
248. Rechkoblit, O. *et al.* trans-Lesion synthesis past bulky benzo[a]pyrene diol epoxide N2-dG and N6-dA lesions catalyzed by DNA bypass polymerases. *J. Biol. Chem.* **277**, 30488–30494 (2002).
249. Roy, U. & Schärer, O. D. Involvement of Translesion Synthesis DNA Polymerases in DNA Interstrand Crosslink Repair. *DNA Repair* **44**, 33–41 (2016).
250. Quinet, A. *et al.* Translesion synthesis mechanisms depend on the nature of DNA damage in UV-irradiated human cells. *Nucleic Acids Res.* **44**, 5717–5731 (2016).
251. Burgess, R. C. *et al.* The PCNA Interaction Protein Box Sequence in Rad54 Is an Integral Part of Its ATPase Domain and Is Required for Efficient DNA Repair and Recombination. *PLOS ONE* **8**, e82630 (2013).
252. M, A. *et al.* Small molecule inhibitors of PCNA/PIP-box interaction suppress translesion DNA synthesis. *Bioorg. Med. Chem.* **21**, 1972–1977 (2013).
253. Dagenais, G. R. *et al.* Variations in common diseases, hospital admissions, and deaths in middle-aged adults in 21 countries from five continents (PURE): a prospective cohort study. *The Lancet* **395**, 785–794 (2020).
254. Yusuf, S. *et al.* Modifiable risk factors, cardiovascular disease, and mortality in 155 722 individuals from 21 high-income, middle-income, and low-income countries (PURE): a prospective cohort study. *The Lancet* **395**, 795–808 (2020).
255. Prasetyanti, P. R. & Medema, J. P. Intra-tumor heterogeneity from a cancer stem cell perspective. *Mol. Cancer* **16**, 41 (2017).
256. Hinohara, K. & Polyak, K. Intratumoral Heterogeneity: More Than Just Mutations. *Trends Cell Biol.* **29**, 569–579 (2019).
257. McGranahan, N. & Swanton, C. Clonal Heterogeneity and Tumor Evolution: Past, Present, and the Future. *Cell* **168**, 613–628 (2017).
258. ASTOLFI, L. *et al.* Correlation of adverse effects of cisplatin administration in patients affected by solid tumours: A retrospective evaluation. *Oncol. Rep.* **29**, 1285–1292 (2013).
259. Thorn, C. F. *et al.* Doxorubicin pathways: pharmacodynamics and adverse effects. *Pharmacogenet. Genomics* **21**, 440–446 (2011).

260. Turgeon, M.-O., Perry, N. J. S. & Poulogiannis, G. DNA Damage, Repair, and Cancer Metabolism. *Front. Oncol.* **8**, (2018).
261. Torgovnick, A. & Schumacher, B. DNA repair mechanisms in cancer development and therapy. *Front. Genet.* **6**, (2015).
262. Furgason, J. M. & Bahassi, E. M. Targeting DNA repair mechanisms in cancer. *Pharmacol. Ther.* **137**, 298–308 (2013).
263. Rocha, C. R. R., Silva, M. M., Quinet, A., Cabral-Neto, J. B. & Menck, C. F. M. DNA repair pathways and cisplatin resistance: an intimate relationship. *Clinics* **73**, (2018).
264. Salehan, M. R. & Morse, H. R. DNA damage repair and tolerance: a role in chemotherapeutic drug resistance. *Br. J. Biomed. Sci.* **70**, 31–40 (2013).
265. Gerber, D. E. Targeted Therapies: A New Generation of Cancer Treatments. *Am. Fam. Physician* **77**, 311–319 (2008).
266. Qi, X. *et al.* Wilms' tumor 1 (WT1) expression and prognosis in solid cancer patients: a systematic review and meta-analysis. *Sci. Rep.* **5**, 8924 (2015).
267. Papin, J. A. *et al.* Comparison of network-based pathway analysis methods. *Trends Biotechnol.* **22**, 400–405 (2004).
268. Khatri, P., Sirota, M. & Butte, A. J. Ten Years of Pathway Analysis: Current Approaches and Outstanding Challenges. *PLOS Comput. Biol.* **8**, e1002375 (2012).
269. Albert, R. Scale-free networks in cell biology. *J. Cell Sci.* **118**, 4947–4957 (2005).
270. Bolaños, J. P., Almeida, A. & Moncada, S. Glycolysis: a bioenergetic or a survival pathway? *Trends Biochem. Sci.* **35**, 145–149 (2010).
271. Luo, W. & Brouwer, C. Pathview: an R/Bioconductor package for pathway-based data integration and visualization. *Bioinforma. Oxf. Engl.* **29**, 1830–1831 (2013).
272. Qiu, X., Xiao, Y., Gordon, A. & Yakovlev, A. Assessing stability of gene selection in microarray data analysis. *BMC Bioinformatics* **7**, 50 (2006).
273. Ni, P. *et al.* Constructing Disease Similarity Networks Based on Disease Module Theory. *IEEE/ACM Trans. Comput. Biol. Bioinform.* **17**, 906–915 (2020).
274. Ahmed, K. T. *et al.* Network-based drug sensitivity prediction. *BMC Med. Genomics* **13**, 193 (2020).
275. van Dam, S., Vösa, U., van der Graaf, A., Franke, L. & de Magalhães, J. P. Gene co-expression analysis for functional classification and gene-disease predictions. *Brief. Bioinform.* **19**, 575–592 (2018).

276. Zhang, H., Li, Y. & Lai, M. The microRNA network and tumor metastasis. *Oncogene* **29**, 937–948 (2010).
277. Hébert, S. S. & De Strooper, B. Alterations of the microRNA network cause neurodegenerative disease. *Trends Neurosci.* **32**, 199–206 (2009).
278. García del Valle, E. P. *et al.* Disease networks and their contribution to disease understanding: A review of their evolution, techniques and data sources. *J. Biomed. Inform.* **94**, 103206 (2019).
279. El-Hachem, N. *et al.* Integrative Cancer Pharmacogenomics to Infer Large-Scale Drug Taxonomy. *Cancer Res.* **77**, 3057–3069 (2017).
280. Azmi, A. S. Adopting network pharmacology for cancer drug discovery. *Curr. Drug Discov. Technol.* **10**, 95–105 (2013).
281. Noguchi, T. *et al.* Gefitinib initiates sterile inflammation by promoting IL-1 β and HMGB1 release via two distinct mechanisms. *Cell Death Dis.* **12**, 1–17 (2021).
282. Tanaka, T. *et al.* Gefitinib Radiosensitizes Non–Small Cell Lung Cancer Cells by Suppressing Cellular DNA Repair Capacity. *Clin. Cancer Res.* **14**, 1266–1273 (2008).
283. Shao, J. *et al.* Gefitinib Synergizes with Irinotecan to Suppress Hepatocellular Carcinoma via Antagonizing Rad51-Mediated DNA-Repair. *PLOS ONE* **11**, e0146968 (2016).
284. Serafin, M. B., Hörner, R., Serafin, M. B. & Hörner, R. Drug repositioning, a new alternative in infectious diseases. *Braz. J. Infect. Dis.* **22**, 252–256 (2018).
285. Goh, K.-I. *et al.* The human disease network. *Proc. Natl. Acad. Sci.* **104**, 8685–8690 (2007).
286. Caberlotto, L. *et al.* Cross-disease analysis of Alzheimer’s disease and type-2 Diabetes highlights the role of autophagy in the pathophysiology of two highly comorbid diseases. *Sci. Rep.* **9**, 3965 (2019).
287. Caviness, J. N. Pathophysiology of Parkinson’s disease behavior – a view from the network. *Parkinsonism Relat. Disord.* **20**, S39–S43 (2014).
288. Bauer-Mehren, A. *et al.* Gene-Disease Network Analysis Reveals Functional Modules in Mendelian, Complex and Environmental Diseases. *PLOS ONE* **6**, e20284 (2011).
289. O’Neil, N. J., Bailey, M. L. & Hieter, P. Synthetic lethality and cancer. *Nat. Rev. Genet.* **18**, 613–623 (2017).
290. Huang, A., Garraway, L. A., Ashworth, A. & Weber, B. Synthetic lethality as an engine for cancer drug target discovery. *Nat. Rev. Drug Discov.* **19**, 23–38 (2020).

291. Randall, M., Burgess, K., Buckingham, L. & Usha, L. Exceptional Response to Olaparib in a Patient With Recurrent Ovarian Cancer and an Entire BRCA1 Germline Gene Deletion. *J. Natl. Compr. Cancer Netw. JNCCN* **18**, 223–228 (2020).
292. Matthews Hew, T. & Zuberi, L. PARP Inhibitor Olaparib Use in a BRCA1-Positive Patient With Metastatic Triple-Negative Breast Cancer, Without the Initial Use of Platinum-Based Chemotherapy, Showing Significant Rapid Near Resolution of Large Liver Metastasis While Patient Experienced Gout-Like Symptoms. *J. Investig. Med. High Impact Case Rep.* **7**, (2019).
293. Astsaturov, I. *et al.* Synthetic Lethal Screen of an EGFR-Centered Network to Improve Targeted Therapies. *Sci. Signal.* **3**, ra67–ra67 (2010).
294. Dixon, S. J. *et al.* Significant conservation of synthetic lethal genetic interaction networks between distantly related eukaryotes. *Proc. Natl. Acad. Sci.* **105**, 16653–16658 (2008).
295. Srivas, R. *et al.* A Network of Conserved Synthetic Lethal Interactions for Exploration of Precision Cancer Therapy. *Mol. Cell* **63**, 514–525 (2016).
296. Chiu, Y.-C. *et al.* Predicting drug response of tumors from integrated genomic profiles by deep neural networks. *BMC Med. Genomics* **12**, 18 (2019).
297. Matsubara, T., Nacher, J. C., Ochiai, T., Hayashida, M. & Akutsu, T. Convolutional Neural Network Approach to Lung Cancer Classification Integrating Protein Interaction Network and Gene Expression Profiles. in *2018 IEEE 18th International Conference on Bioinformatics and Bioengineering (BIBE)* 151–154 (2018). doi:10.1109/BIBE.2018.00036.
298. Guda, P., Chittur, S. V. & Guda, C. Comparative Analysis of Protein-Protein Interactions in Cancer-Associated Genes. *Genomics Proteomics Bioinformatics* **7**, 25–36 (2009).
299. Sun, J. *et al.* A multi-dimensional evidence-based candidate gene prioritization approach for complex diseases—schizophrenia as a case. *Bioinformatics* **25**, 2595–6602 (2009).
300. Li, Z. *et al.* The OncoPPi network of cancer-focused protein–protein interactions to inform biological insights and therapeutic strategies. *Nat. Commun.* **8**, 1–14 (2017).
301. Nuncia-Cantarero, M. *et al.* Functional transcriptomic annotation and protein–protein interaction network analysis identify NEK2, BIRC5, and TOP2A as potential targets in obese patients with luminal A breast cancer. *Breast Cancer Res. Treat.* **168**, 613–623 (2018).
302. Hustedt, N. & Durocher, D. The control of DNA repair by the cell cycle. *Nat. Cell Biol.* **19**, 1–9 (2017).
303. Mazouzi, A., Velimezi, G. & Loizou, J. I. DNA replication stress: Causes, resolution and disease. *Exp. Cell Res.* **329**, 85–93 (2014).
304. Fujii, N. Potential Strategies to Target Protein-Protein Interactions in the DNA Damage Response and Repair Pathways. *J. Med. Chem.* **60**, 9932–9959 (2017).

305. Ghandi, M. *et al.* Next-generation characterization of the Cancer Cell Line Encyclopedia. *Nature* **569**, 503–508 (2019).
306. Barretina, J. *et al.* The Cancer Cell Line Encyclopedia enables predictive modelling of anticancer drug sensitivity. *Nature* **483**, 603–607 (2012).
307. Alanis-Lobato, G., Andrade-Navarro, M. A. & Schaefer, M. H. HIPPIE v2.0: enhancing meaningfulness and reliability of protein–protein interaction networks. *Nucleic Acids Res.* **45**, D408–D414 (2017).
308. Oughtred, R. *et al.* The BioGRID interaction database: 2019 update. *Nucleic Acids Res.* **47**, D529–D541 (2019).
309. Guo, Y. *et al.* Large Scale Comparison of Gene Expression Levels by Microarrays and RNAseq Using TCGA Data. *PLOS ONE* **8**, e71462 (2013).
310. Silva, T. C. *et al.* TCGA Workflow: Analyze cancer genomics and epigenomics data using Bioconductor packages. *F1000Research* **5**, (2016).
311. Koutrouli, M., Karatzas, E., Paez-Espino, D. & Pavlopoulos, G. A. A Guide to Conquer the Biological Network Era Using Graph Theory. *Front. Bioeng. Biotechnol.* **8**, (2020).
312. Li, Y. & Yang, D.-Q. The ATM Inhibitor KU-55933 Suppresses Cell Proliferation and Induces Apoptosis by Blocking Akt In Cancer Cells with Overactivated Akt. *Mol. Cancer Ther.* **9**, 113–125 (2010).
313. Willmore, E. *et al.* A novel DNA-dependent protein kinase inhibitor, NU7026, potentiates the cytotoxicity of topoisomerase II poisons used in the treatment of leukemia. *Blood* **103**, 4659–4665 (2004).
314. Brehmer, D. *et al.* Cellular Targets of Gefitinib. *Cancer Res.* **65**, 379–382 (2005).
315. Kaufman, B. *et al.* Olaparib Monotherapy in Patients With Advanced Cancer and a Germline BRCA1/2 Mutation. *J. Clin. Oncol.* **33**, 244–250 (2015).
316. Turner, N. C. *et al.* Palbociclib in Hormone-Receptor-Positive Advanced Breast Cancer. *N. Engl. J. Med.* **373**, 209–219 (2015).
317. Sanabria, A. L. A. *et al.* 1944P - Pharmacological screening with Chk1 inhibitors identifies synergistic agents to overcome resistance to platinum in basal breast and ovarian cancer. *Ann. Oncol.* **30**, v783 (2019).
318. Liang, P. & Pardee, A. B. Analysing differential gene expression in cancer. *Nat. Rev. Cancer* **3**, 869–876 (2003).
319. Leek, J. T., Mosen, E., Dabney, A. R. & Storey, J. D. EDGE: extraction and analysis of differential gene expression. *Bioinformatics* **22**, 507–508 (2006).

320. Tang, Z. *et al.* GEPIA: a web server for cancer and normal gene expression profiling and interactive analyses. *Nucleic Acids Res.* **45**, W98–W102 (2017).
321. Abbas, S. Z., Qadir, M. I. & Muhammad, S. A. Systems-level differential gene expression analysis reveals new genetic variants of oral cancer. *Sci. Rep.* **10**, 14667 (2020).
322. Davis, K. U. & Sheats, M. K. Differential gene expression and Ingenuity Pathway Analysis of bronchoalveolar lavage cells from horses with mild/moderate neutrophilic or mastocytic inflammation on BAL cytology. *Vet. Immunol. Immunopathol.* **234**, 110195 (2021).
323. Ge, S. X., Son, E. W. & Yao, R. iDEP: an integrated web application for differential expression and pathway analysis of RNA-Seq data. *BMC Bioinformatics* **19**, 534 (2018).
324. Wang, T., Li, B., Nelson, C. E. & Nabavi, S. Comparative analysis of differential gene expression analysis tools for single-cell RNA sequencing data. *BMC Bioinformatics* **20**, 40 (2019).
325. Babal, Y. K., Kandemir, B. & Kurnaz, I. A. Gene Regulatory Network of ETS Domain Transcription Factors in Different Stages of Glioma. *J. Pers. Med.* **11**, 138 (2021).
326. Grove, A. Regulation of Metabolic Pathways by MarR Family Transcription Factors. *Comput. Struct. Biotechnol. J.* **15**, 366–371 (2017).
327. Burke, P. J. Mitochondria, Bioenergetics and Apoptosis in Cancer. *Trends Cancer* **3**, 857–870 (2017).
328. Carneiro, B. A. & El-Deiry, W. S. Targeting apoptosis in cancer therapy. *Nat. Rev. Clin. Oncol.* **17**, 395–417 (2020).
329. Cao, R. *et al.* TM4SF1 regulates apoptosis, cell cycle and ROS metabolism via the PPAR γ -SIRT1 feedback loop in human bladder cancer cells. *Cancer Lett.* **414**, 278–293 (2018).
330. Mahadevappa, R. *et al.* DNA Replication Licensing Protein MCM10 Promotes Tumor Progression and Is a Novel Prognostic Biomarker and Potential Therapeutic Target in Breast Cancer. *Cancers* **10**, (2018).
331. Tang, C. *et al.* Abnormal expression of FOSB correlates with tumor progression and poor survival in patients with gastric cancer. *Int. J. Oncol.* **49**, 1489–1496 (2016).
332. Du, J. *et al.* KEGG-PATH: Kyoto encyclopedia of genes and genomes-based pathway analysis using a path analysis model. *Mol. Biosyst.* **10**, 2441–2447 (2014).
333. Diestel, R. *Graph Theory*. (Springer-Verlag Berlin Heidelberg, 2017).
334. Groß, A. *et al.* Representing dynamic biological networks with multi-scale probabilistic models. *Commun. Biol.* **2**, 1–12 (2019).

335. Li, X. & Heyer, W.-D. Homologous recombination in DNA repair and DNA damage tolerance. *Cell Res.* **18**, 99–113 (2008).
336. Hashimoto, S., Anai, H. & Hanada, K. Mechanisms of interstrand DNA crosslink repair and human disorders. *Genes Environ.* **38**, 9 (2016).
337. Bjørås, K. Ø. *et al.* Monitoring of the spatial and temporal dynamics of BER/SSBR pathway proteins, including MYH, UNG2, MPG, NTH1 and NEIL1-3, during DNA replication. *Nucleic Acids Res.* **45**, 8291–8301 (2017).
338. Fusco, N. *et al.* Mismatch Repair Protein Loss as a Prognostic and Predictive Biomarker in Breast Cancers Regardless of Microsatellite Instability. *JNCI Cancer Spectr.* **2**, (2018).
339. Cheng, A. S. *et al.* Mismatch repair protein loss in breast cancer: clinicopathological associations in a large British Columbia cohort. *Breast Cancer Res. Treat.* **179**, 3–10 (2020).
340. Lee, K. J. *et al.* Defective base excision repair in the response to DNA damaging agents in triple negative breast cancer. *PLOS ONE* **14**, e0223725 (2019).
341. Jiang, L. *et al.* C-Phycocyanin exerts anti-cancer effects via the MAPK signaling pathway in MDA-MB-231 cells. *Cancer Cell Int.* **18**, 12 (2018).
342. Hsieh, M.-J., Chen, K.-S., Chiou, H.-L. & Hsieh, Y.-S. Carbonic anhydrase XII promotes invasion and migration ability of MDA-MB-231 breast cancer cells through the p38 MAPK signaling pathway. *Eur. J. Cell Biol.* **89**, 598–606 (2010).
343. Mazzio, E. A., Lewis, C. A., Elhag, R. & Soliman, K. F. Effects of Sepantronium Bromide (YM-155) on the Whole Transcriptome of MDA-MB-231 Cells: Highlight on Impaired ATR/ATM Fanconi Anemia DNA Damage Response. *Cancer Genomics Proteomics* **15**, 249–264 (2018).
344. Kothandapani, A. *et al.* Novel Role of Base Excision Repair in Mediating Cisplatin Cytotoxicity*. *J. Biol. Chem.* **286**, 14564–14574 (2011).
345. Domínguez-Gómez, G. *et al.* Nicotinamide sensitizes human breast cancer cells to the cytotoxic effects of radiation and cisplatin. *Oncol. Rep.* **33**, 721–728 (2015).
346. Mao, Z., Jiang, Y., Liu, X., Seluanov, A. & Gorbunova, V. DNA Repair by Homologous Recombination, But Not by Nonhomologous End Joining, Is Elevated in Breast Cancer Cells. *Neoplasia* **11**, 683-IN3 (2009).
347. Newell, M., Baker, K., Postovit, L. M. & Field, C. J. A Critical Review on the Effect of Docosahexaenoic Acid (DHA) on Cancer Cell Cycle Progression. *Int. J. Mol. Sci.* **18**, 1784 (2017).
348. Blajeski, A. L., Phan, V. A., Kottke, T. J. & Kaufmann, S. H. G₁ and G₂ cell-cycle arrest following microtubule depolymerization in human breast cancer cells. *J. Clin. Invest.* **110**, 91–99 (2002).

349. Yan, Y. *et al.* A novel function of HER2/Neu in the activation of G2/M checkpoint in response to γ -irradiation. *Oncogene* **34**, 2215–2226 (2015).
350. Moongkarndi, P. *et al.* Antiproliferation, antioxidation and induction of apoptosis by *Garcinia mangostana* (mangosteen) on SKBR3 human breast cancer cell line. *J. Ethnopharmacol.* **90**, 161–166 (2004).
351. Roknić, S. *et al.* In vitro Cytotoxicity of Three 4,9-Diazapyrenium Hydrogensulfate Derivatives on Different Human Tumor Cell Lines. *Chemotherapy* **46**, 143–149 (2000).
352. Silveira-Lacerda, E. de P. *et al.* The Ruthenium Complex cis - (Dichloro)tetraammineruthenium(III) Chloride Presents Selective Cytotoxicity Against Murine B Cell Lymphoma (A-20), Murine Ascitic Sarcoma 180 (S-180), Human Breast Adenocarcinoma (SK-BR-3), and Human T Cell Leukemia (Jurkat) Tumor Cell Lines. *Biol. Trace Elem. Res.* **135**, 98–111 (2010).
353. Nyaga, S. G. *et al.* Reduced repair of 8-hydroxyguanine in the human breast cancer cell line, HCC1937. *BMC Cancer* **6**, 297 (2006).
354. Ree, A. H., Bratland, A., Solberg Landsverk, K. & Fodstad, O. Ionizing radiation inhibits the PLK cell cycle gene in a G2 checkpoint-dependent manner. *Anticancer Res.* **24**, 555–562 (2004).
355. Cassago, A. *et al.* Mitochondrial localization and structure-based phosphate activation mechanism of Glutaminase C with implications for cancer metabolism. *Proc. Natl. Acad. Sci.* **109**, 1092–1097 (2012).
356. Pedram, A., Razandi, M., Wallace, D. C. & Levin, E. R. Functional Estrogen Receptors in the Mitochondria of Breast Cancer Cells. *Mol. Biol. Cell* **17**, 2125–2137 (2006).
357. Azevedo-Barbosa, H. *et al.* Phenylpropanoid-based sulfonamide promotes cyclin D1 and cyclin E down-regulation and induces cell cycle arrest at G1/S transition in estrogen positive MCF-7 cell line. *Toxicol. In Vitro* **59**, 150–160 (2019).
358. Kaplan, E. & Gündüz, U. Expression analysis of TOP2A, MSH2 and MLH1 genes in MCF7 cells at different levels of etoposide resistance. *Biomed. Pharmacother.* **66**, 29–35 (2012).
359. You, B.-J., Wu, Y.-C., Lee, C.-L. & Lee, H.-Z. Non-homologous end joining pathway is the major route of protection against 4 β -hydroxywithanolide E-induced DNA damage in MCF-7 cells. *Food Chem. Toxicol.* **65**, 205–212 (2014).
360. Liu, J. *et al.* Protein phosphatase PP4 is involved in NHEJ-mediated repair of DNA double-strand breaks. *Cell Cycle* **11**, 2643–2649 (2012).
361. Tenga, M. J. & Lazar, I. M. A Proteomic Snapshot of Breast Cancer Cell Cycle: The G1/S Transition Point. *Proteomics* **13**, 48–60 (2013).

362. Thu, K., Soria-Bretones, I., Mak, T. & Cescon, D. Targeting the cell cycle in breast cancer: towards the next phase. *Cell Cycle* **17**, 1871–1885 (2018).
363. Kang, D.-H. Oxidative Stress, DNA Damage, and Breast Cancer. *AACN Adv. Crit. Care* **13**, 540–549 (2002).
364. Gao, X. *et al.* Berberine attenuates XRCC1-mediated base excision repair and sensitizes breast cancer cells to the chemotherapeutic drugs. *J. Cell. Mol. Med.* **23**, 6797–6804 (2019).
365. Murad, H. *et al.* Induction of G1-phase cell cycle arrest and apoptosis pathway in MDA-MB-231 human breast cancer cells by sulfated polysaccharide extracted from *Laurencia papillosa*. *Cancer Cell Int.* **16**, 39 (2016).
366. Takahashi, K. & Loo, G. Disruption of mitochondria during tocotrienol-induced apoptosis in MDA-MB-231 human breast cancer cells. *Biochem. Pharmacol.* **67**, 315–324 (2004).
367. Abdollahi, P., Ebrahimi, M., Motamed, N. & Samani, F. S. Silibinin affects tumor cell growth because of reduction of stemness properties and induction of apoptosis in 2D and 3D models of MDA-MB-468. *Anticancer. Drugs* **26**, 487–497 (2015).
368. Gurkan-Alp, A. S., Alp, M., Karabay, A. Z., Koc, A. & Buyukbingol, E. Synthesis of Some Benzimidazole-derived Molecules and their Effects on PARP-1 Activity and MDA-MB-231, MDA-MB-436, MDA-MB-468 Breast Cancer Cell Viability. *Anti-Cancer Agents Med. Chem.- Anti-Cancer Agents* **20**, 1728–1738 (2020).
369. Oliveras-Ferraros, C. *et al.* Growth and molecular interactions of the anti-EGFR antibody Cetuximab and the DNA cross-linking agent cisplatin in gefitinib-resistant MDA-MB-468 cells: New prospects in the treatment of triple-negative/basal-like breast cancer. *Int. J. Oncol.* **33**, 1165–1176 (2008).
370. Billecke, C. A. *et al.* Lack of functional pRb results in attenuated recovery of mRNA synthesis and increased apoptosis following UV radiation in human breast cancer cells. *Oncogene* **21**, 4481–4489 (2002).
371. Song, L. *et al.* miR-18a Impairs DNA Damage Response through Downregulation of Ataxia Telangiectasia Mutated (ATM) Kinase. *PLOS ONE* **6**, e25454 (2011).
372. Pietras, R. J. *et al.* Monoclonal Antibody to HER-2/neuReceptor Modulates Repair of Radiation-induced DNA Damage and Enhances Radiosensitivity of Human Breast Cancer Cells Overexpressing This Oncogene. *Cancer Res.* **59**, 1347–1355 (1999).
373. Boone, J. J. M., Bhosle, J., Tilby, M. J., Hartley, J. A. & Hochhauser, D. Involvement of the HER2 pathway in repair of DNA damage produced by chemotherapeutic agents. *Mol. Cancer Ther.* **8**, 3015–3023 (2009).
374. You, S. H., Kim, J.-S. & Kim, Y.-S. Apoptosis and Cell Cycle Arrest in Two Human Breast Cancer Cell Lines by Dieckol Isolated from *Ecklonia cava*. *J. Breast Dis.* **6**, 39–45 (2018).

375. Kim, H.-J. *et al.* Anti-tumor activity of the ATR inhibitor AZD6738 in HER2 positive breast cancer cells. *Int. J. Cancer* **140**, 109–119 (2017).
376. Wang, G. *et al.* Celecoxib induced apoptosis against different breast cancer cell lines by down-regulated NF- κ B pathway. *Biochem. Biophys. Res. Commun.* **490**, 969–976 (2017).
377. Kim, M. S., Ahn, Y. T., Lee, C. W., Kim, H. & An, W. G. Astaxanthin Modulates Apoptotic Molecules to Induce Death of SKBR3 Breast Cancer Cells. *Mar. Drugs* **18**, 266 (2020).
378. Kim, D. V., Makarova, A. V., Miftakhova, R. R. & Zharkov, D. O. Base Excision DNA Repair Deficient Cells: From Disease Models to Genotoxicity Sensors. *Curr. Pharm. Des.* **25**, 298–312 (2019).
379. Chen, T. *et al.* The expression of APE1 in triple-negative breast cancer and its effect on drug sensitivity of olaparib. *Tumor Biol.* **39**, 1010428317713390 (2017).
380. Krokidis, M. G. *et al.* Purine 5',8-cyclo-2'-deoxynucleoside lesions: formation by radical stress and repair in human breast epithelial cancer cells. *Free Radic. Res.* **51**, 470–482 (2017).
381. Carey, J. P. & Keyomarsi, K. Abstract B27: CDK inhibition impairs homologous recombination and induces PARP inhibitor sensitivity via loss of c-myc expression in TNBC. *Mol. Cancer Res.* **13**, B27–B27 (2015).
382. Zhang, J., Ma, Z., Treszezamsky, A. & Powell, S. N. MDC1 interacts with Rad51 and facilitates homologous recombination. *Nat. Struct. Mol. Biol.* **12**, 902–909 (2005).
383. Li, Z., Pearlman, A. H. & Hsieh, P. DNA mismatch repair and the DNA damage response. *DNA Repair* **38**, 94–101 (2016).
384. Wagner, M. W. *et al.* Role of c-Abl Kinase in DNA Mismatch Repair-dependent G2 Cell Cycle Checkpoint Arrest Responses*. *J. Biol. Chem.* **283**, 21382–21393 (2008).
385. Yarden, R. I., Pardo-Reoyo, S., Sgagias, M., Cowan, K. H. & Brody, L. C. BRCA1 regulates the G2/M checkpoint by activating Chk1 kinase upon DNA damage. *Nat. Genet.* **30**, 285–289 (2002).
386. Tassone, P. *et al.* Loss of BRCA1 function increases the antitumor activity of cisplatin against human breast cancer xenografts in vivo. *Cancer Biol. Ther.* **8**, 648–653 (2009).
387. Stevens, T. A. & Meech, R. BARX2 and estrogen receptor- α (ESR1) coordinately regulate the production of alternatively spliced ESR1 isoforms and control breast cancer cell growth and invasion. *Oncogene* **25**, 5426–5435 (2006).
388. Chang, C. J. *et al.* Modulation of HER2 expression by ferulic acid on human breast cancer MCF7 cells. *Eur. J. Clin. Invest.* **36**, 588–596 (2006).

389. Liu, S., Tang, Y., Yan, M. & Jiang, W. PIK3CA mutation sensitizes breast cancer cells to synergistic therapy of PI3K inhibition and AMPK activation. *Invest. New Drugs* **36**, 763–772 (2018).
390. Jones, R. *et al.* A CDKN2A Mutation in Familial Melanoma that Abrogates Binding of p16INK4a to CDK4 but not CDK6. *Cancer Res.* **67**, 9134–9141 (2007).
391. Udden, N., Wang, Q. & Alluri, P. G. ESR1 Mutation Status as a Biomarker for Radiation Response in ER-Positive Breast Cancer. *Int. J. Radiat. Oncol. Biol. Phys.* **108**, e35–e36 (2020).
392. Francisco, D. C. *et al.* Induction and processing of complex DNA damage in human breast cancer cells MCF-7 and nonmalignant MCF-10A cells. *Free Radic. Biol. Med.* **44**, 558–569 (2008).
393. Zhao, M., Howard, E. W., Guo, Z., Parris, A. B. & Yang, X. p53 pathway determines the cellular response to alcohol-induced DNA damage in MCF-7 breast cancer cells. *PLOS ONE* **12**, e0175121 (2017).
394. Sinha, B. K., Tokar, E. J. & Bushel, P. R. Elucidation of Mechanisms of Topotecan-Induced Cell Death in Human Breast MCF-7 Cancer Cells by Gene Expression Analysis. *Front. Genet.* **11**, (2020).
395. Hasanzadeh, D., Mahdavi, M., Dehghan, G. & Charoudeh, H. N. Farnesiferol C induces cell cycle arrest and apoptosis mediated by oxidative stress in MCF-7 cell line. *Toxicol. Rep.* **4**, 420–426 (2017).
396. Wang, Y. *et al.* Functionalized graphene oxide triggers cell cycle checkpoint control through both the ATM and the ATR signaling pathways. *Carbon* **129**, 495–503 (2018).
397. Sawant, A. *et al.* Differential role of base excision repair proteins in mediating cisplatin cytotoxicity. *DNA Repair* **51**, 46–59 (2017).
398. Lee, K. J. *et al.* Exploiting DNA repair defects in triple negative breast cancer to improve cell killing. *Ther. Adv. Med. Oncol.* **12**, 1758835920958354 (2020).
399. Mio, C. *et al.* BET proteins regulate homologous recombination-mediated DNA repair: BRCAness and implications for cancer therapy. *Int. J. Cancer* **144**, 755–766 (2019).
400. Pan, T., Mao, T., Yang, H., Wang, H. & Wang, Y. Silencing of TGIF sensitizes MDA-MB-231 human breast cancer cells to cisplatin-induced apoptosis. *Exp. Ther. Med.* **15**, 2978–2984 (2018).
401. Elaimy, A. L. *et al.* The VEGF receptor neuropilin 2 promotes homologous recombination by stimulating YAP/TAZ-mediated Rad51 expression. *Proc. Natl. Acad. Sci.* **116**, 14174–14180 (2019).

402. Sun, X. *et al.* Glycolytic inhibition by 3-bromopyruvate increases the cytotoxic effects of chloroethylnitrosoureas to human glioma cells and the DNA interstrand cross-links formation. *Toxicology* **435**, 152413 (2020).
403. Pozo-Guisado, E., Alvarez-Barrientos, A., Mulero-Navarro, S., Santiago-Josefat, B. & Fernandez-Salguero, P. M. The antiproliferative activity of resveratrol results in apoptosis in MCF-7 but not in MDA-MB-231 human breast cancer cells: cell-specific alteration of the cell cycle. *Biochem. Pharmacol.* **64**, 1375–1386 (2002).
404. Maroufi, N. F. *et al.* The apatinib inhibits breast cancer cell line MDA-MB-231 in vitro by inducing apoptosis, cell cycle arrest, and regulating nuclear factor- κ B (NF- κ B) and mitogen-activated protein kinase (MAPK) signaling pathways. *Breast Cancer* **27**, 613–620 (2020).
405. Ceccaldi, R. *et al.* Homologous-recombination-deficient tumours are dependent on Pol θ -mediated repair. *Nature* **518**, 258–262 (2015).
406. Stefansson, O. A., Villanueva, A., Vidal, A., Martí, L. & Esteller, M. BRCA1 epigenetic inactivation predicts sensitivity to platinum-based chemotherapy in breast and ovarian cancer. *Epigenetics* **7**, 1225–1229 (2012).
407. Peng, G. *et al.* Genome-wide transcriptome profiling of homologous recombination DNA repair. *Nat. Commun.* **5**, 3361 (2014).
408. Kais, Z. *et al.* FANCD2 Maintains Fork Stability in BRCA1/2-Deficient Tumors and Promotes Alternative End-Joining DNA Repair. *Cell Rep.* **15**, 2488–2499 (2016).
409. Ávila-Arroyo, S., Nuñez, G. S., García-Fernández, L. F. & Galmarini, C. M. Synergistic Effect of Trabectedin and Olaparib Combination Regimen in Breast Cancer Cell Lines. *J. Breast Cancer* **18**, 329–338 (2015).
410. Mambo, E., Nyaga, S. G., Bohr, V. A. & Evans, M. K. Defective Repair of 8-Hydroxyguanine in Mitochondria of MCF-7 and MDA-MB-468 Human Breast Cancer Cell Lines. *Cancer Res.* **62**, 1349–1355 (2002).
411. Oliveras-Ferraros, C. *et al.* Growth and molecular interactions of the anti-EGFR antibody Cetuximab and the DNA cross-linking agent cisplatin in gefitinib-resistant MDA-MB-468 cells: New prospects in the treatment of triple-negative/basal-like breast cancer. *Int. J. Oncol.* **33**, 1165–1176 (2008).
412. Li, P.-X. *et al.* Placental Transforming Growth Factor- β Is a Downstream Mediator of the Growth Arrest and Apoptotic Response of Tumor Cells to DNA Damage and p53 Overexpression*. *J. Biol. Chem.* **275**, 20127–20135 (2000).
413. Balabhadrapathruni, S., Thomas, T. J., Yurkow, E. J., Amenta, P. S. & Thomas, T. Effects of genistein and structurally related phytoestrogens on cell cycle kinetics and apoptosis in MDA-MB-468 human breast cancer cells. *Oncol. Rep.* **7**, 3–15 (2000).

414. Messeha, S. S., Zarmouh, N. O., Asiri, A. & Soliman, K. F. A. Rosmarinic acid-induced apoptosis and cell cycle arrest in triple-negative breast cancer cells. *Eur. J. Pharmacol.* **885**, 173419 (2020).
415. Yang, Q.-S. *et al.* ShRNA-mediated Ku80 Gene Silencing Inhibits Cell Proliferation and Sensitizes to γ -radiation and Mitomycin C-induced Apoptosis in Esophageal Squamous Cell Carcinoma Lines. *J. Radiat. Res. (Tokyo)* **advpub**, 0804030028–0804030028 (2008).
416. Ueda, A. *et al.* Therapeutic potential of PLK1 inhibition in triple-negative breast cancer. *Lab. Invest.* **99**, 1275–1286 (2019).
417. Winograd-Katz, S. E. & Levitzki, A. Cisplatin induces PKB/Akt activation and p38 MAPK phosphorylation of the EGF receptor. *Oncogene* **25**, 7381–7390 (2006).
418. Squires, M. S. *et al.* Relevance of mitogen activated protein kinase (MAPK) and phosphatidylinositol-3-kinase/protein kinase B (PI3K/PKB) pathways to induction of apoptosis by curcumin in breast cells. *Biochem. Pharmacol.* **65**, 361–376 (2003).
419. Normanno, N. *et al.* The MEK/MAPK pathway is involved in the resistance of breast cancer cells to the EGFR tyrosine kinase inhibitor gefitinib. *J. Cell. Physiol.* **207**, 420–427 (2006).
420. Heijden, M. S. van der, Brody, J. R. & Kern, S. E. Functional Screen of the Fanconi Anemia Pathway in Cancer Cells by Fancd2 Immunoblot. *Cancer Biol. Ther.* **3**, 534–537 (2004).
421. Sawhney, P. U. Characterizing the relationship between the DNA repair proteins in the Classical NHEJ and the ALT NHEJ pathways and investigating the role of homeobox genes in abnormal DNA repair in breast cancer. (2012).
422. Yu, T. *et al.* Radiosensitizing effect of lapatinib in human epidermal growth factor receptor 2-positive breast cancer cells. *Oncotarget* **7**, 79089–79100 (2016).
423. Tobin, L. A. *et al.* Abstract 5495: ALT NHEJ is a therapeutic target in hormone therapy resistant ER/PR/HER+ and ER/PR/HER- breast cancers. *Cancer Res.* **71**, 5495–5495 (2011).
424. Greenshields, A. L., Fernando, W. & Hoskin, D. W. The anti-malarial drug artesunate causes cell cycle arrest and apoptosis of triple-negative MDA-MB-468 and HER2-enriched SK-BR-3 breast cancer cells. *Exp. Mol. Pathol.* **107**, 10–22 (2019).
425. Huang, H.-W. *et al.* Simularin Selectively Kills Breast Cancer Cells Showing G2/M Arrest, Apoptosis, and Oxidative DNA Damage. *Molecules* **23**, 849 (2018).
426. Choi, E. J. & Kim, G.-H. Apigenin causes G2/M arrest associated with the modulation of p21Cip1 and Cdc2 and activates p53-dependent apoptosis pathway in human breast cancer SK-BR-3 cells. *J. Nutr. Biochem.* **20**, 285–290 (2009).
427. Xu, C. *et al.* Let-7a regulates mammosphere formation capacity through Ras/NF- κ B and Ras/MAPK/ERK pathway in breast cancer stem cells. *Cell Cycle* **14**, 1686–1697 (2015).

428. Yang, Y. *et al.* Osthole Synergizes With HER2 Inhibitor, Trastuzumab in HER2-Overexpressed N87 Gastric Cancer by Inducing Apoptosis and Inhibition of AKT-MAPK Pathway. *Front. Pharmacol.* **9**, (2018).
429. Lee, Y. *et al.* The purine scaffold Hsp90 inhibitor PU-H71 sensitizes cancer cells to heavy ion radiation by inhibiting DNA repair by homologous recombination and non-homologous end joining. *Radiother. Oncol.* **121**, 162–168 (2016).
430. Nowsheen, S., Cooper, T., Bonner, J. A., LoBuglio, A. F. & Yang, E. S. HER2 Overexpression Renders Human Breast Cancers Sensitive to PARP Inhibition Independently of Any Defect in Homologous Recombination DNA Repair. *Cancer Res.* **72**, 4796–4806 (2012).
431. Grinstein, E., Jundt, F., Weinert, I., Wernet, P. & Royer, H.-D. Sp1 as G1 cell cycle phase specific transcription factor in epithelial cells. *Oncogene* **21**, 1485–1492 (2002).
432. Beishline, K. *et al.* Sp1 Facilitates DNA Double-Strand Break Repair through a Nontranscriptional Mechanism. *Mol. Cell. Biol.* **32**, 3790–3799 (2012).
433. Wei, M. *et al.* Stat6 cooperates with Sp1 in controlling breast cancer cell proliferation by modulating the expression of p21Cip1/WAF1 and p27Kip1. *Cell. Oncol.* **36**, 79–93 (2013).
434. Tavana, O., Puebla-Osorio, N., Sang, M. & Zhu, C. Absence of p53-dependent apoptosis combined with nonhomologous end-joining deficiency leads to a severe diabetic phenotype in mice. *Diabetes* **59**, 135–142 (2010).
435. Dumay, A. *et al.* Bax and Bid, two proapoptotic Bcl-2 family members, inhibit homologous recombination, independently of apoptosis regulation. *Oncogene* **25**, 3196–3205 (2006).
436. Eikesdal, H. P. *et al.* Olaparib monotherapy as primary treatment in unselected triple negative breast cancer. *Ann. Oncol. Off. J. Eur. Soc. Med. Oncol.* **32**, 240–249 (2021).
437. Benezra, M. *et al.* BRCA1 Augments Transcription by the NF- κ B Transcription Factor by Binding to the Rel Domain of the p65/RelA Subunit*. *J. Biol. Chem.* **278**, 26333–26341 (2003).
438. Rosen, E. M., Fan, S. & Ma, Y. BRCA1 regulation of transcription. *Cancer Lett.* **236**, 175–185 (2006).
439. Ho, A. & Dowdy, S. F. Regulation of G1 cell-cycle progression by oncogenes and tumor suppressor genes. *Curr. Opin. Genet. Dev.* **12**, 47–52 (2002).
440. Giono, L. E. & Manfredi, J. J. The p53 tumor suppressor participates in multiple cell cycle checkpoints. *J. Cell. Physiol.* **209**, 13–20 (2006).
441. Velez, A. M. A. & Howard, M. S. Tumor-suppressor Genes, Cell Cycle Regulatory Checkpoints, and the Skin. *North Am. J. Med. Sci.* **7**, 176–188 (2015).

442. Foray, N. *et al.* A subset of ATM- and ATR-dependent phosphorylation events requires the BRCA1 protein. *EMBO J.* **22**, 2860–2871 (2003).
443. Yarden, R. I. *et al.* BRCA1-Dependent Chk1 Phosphorylation Triggers Partial Chromatin Disassociation of Phosphorylated Chk1 and Facilitates S-Phase Cell Cycle Arrest. *Int. J. Biochem. Cell Biol.* **44**, 1761–1769 (2012).
444. Le, X. F. *et al.* Anti-HER2 antibody and heregulin suppress growth of HER2-overexpressing human breast cancer cells through different mechanisms. *Clin. Cancer Res. Off. J. Am. Assoc. Cancer Res.* **6**, 260–270 (2000).
445. Yan, Y. *et al.* A novel function of HER2/Neu in the activation of G2/M checkpoint in response to γ -irradiation. *Oncogene* **34**, 2215–2226 (2015).
446. Xu, Y. & Villalona-Calero, M. A. Irinotecan: mechanisms of tumor resistance and novel strategies for modulating its activity. *Ann. Oncol.* **13**, 1841–1851 (2002).
447. Wang, M. *et al.* Candidate genes and pathogenesis investigation for sepsis-related acute respiratory distress syndrome based on gene expression profile. *Biol. Res.* **49**, 1–9 (2016).
448. Wang, Z., Wang, F., Tang, T. & Guo, C. The role of PARP1 in the DNA damage response and its application in tumor therapy. *Front. Med.* **6**, 156–164 (2012).
449. Srinivasan, A. & Gold, B. Small-molecule inhibitors of DNA damage-repair pathways: an approach to overcome tumor resistance to alkylating anticancer drugs. *Future Med. Chem.* **4**, 1093–1111 (2012).
450. Choe, K. N. & Moldovan, G.-L. Forging ahead through darkness: PCNA, still the principal conductor at the replication fork. *Mol. Cell* **65**, 380–392 (2017).
451. Makino, E. *et al.* Targeting Rad51 as a strategy for the treatment of melanoma cells resistant to MAPK pathway inhibition. *Cell Death Dis.* **11**, 1–14 (2020).
452. Deakyne, J. S. *et al.* Analysis of the activities of RAD54, a SWI2/SNF2 protein, using a specific small-molecule inhibitor. *J. Biol. Chem.* **288**, 31567–31580 (2013).
453. Nguyen, G. H. *et al.* A small molecule inhibitor of the BLM helicase modulates chromosome stability in human cells. *Chem. Biol.* **20**, 55–62 (2013).
454. Jiang, Q. *et al.* Dissecting PCNA function with a systematically designed mutation library in yeast. *bioRxiv* 352286 (2018) doi:10.1101/352286.
455. Ulrich, H. D. & Takahashi, T. Readers of PCNA modifications. *Chromosoma* **122**, 259–274 (2013).
456. Geng, L., Huntoon, C. J. & Karnitz, L. M. RAD18-mediated ubiquitination of PCNA activates the Fanconi anemia DNA repair network. *J. Cell Biol.* **191**, 249–257 (2010).

457. Han, J. *et al.* SIVA1 directs the E3 ubiquitin ligase RAD18 for PCNA monoubiquitination. *J. Cell Biol.* **205**, 811–827 (2014).
458. Yu, Y.-L. *et al.* Targeting the EGFR/PCNA signaling suppresses tumor growth of triple-negative breast cancer cells with cell-penetrating PCNA peptides. *PloS One* **8**, e61362 (2013).
459. Ortega, J. *et al.* Phosphorylation of PCNA by EGFR inhibits mismatch repair and promotes misincorporation during DNA synthesis. *Proc. Natl. Acad. Sci. U. S. A.* **112**, 5667–5672 (2015).
460. Isono, M. *et al.* BRCA1 Directs the Repair Pathway to Homologous Recombination by Promoting 53BP1 Dephosphorylation. *Cell Rep.* **18**, 520–532 (2017).
461. Rybanska-Spaeder, I. *et al.* 53BP1 Is Limiting for NHEJ Repair in ATM-deficient Model Systems That Are Subjected to Oncogenic Stress or Radiation. *Mol. Cancer Res.* **11**, 1223–1234 (2013).
462. Lee, J.-H., Goodarzi, A. A., Jeggo, P. A. & Paull, T. T. 53BP1 promotes ATM activity through direct interactions with the MRN complex. *EMBO J.* **29**, 574–585 (2010).
463. Mochan, T. A., Venere, M., DiTullio, R. A. & Halazonetis, T. D. 53BP1, an activator of ATM in response to DNA damage. *DNA Repair* **3**, 945–952 (2004).
464. Thakar, T. *et al.* Ubiquitinated-PCNA protects replication forks from DNA2-mediated degradation by regulating Okazaki fragment maturation and chromatin assembly. *Nat. Commun.* **11**, 2147 (2020).
465. Fox, J. T., Lee, K. & Myung, K. Dynamic regulation of PCNA ubiquitylation/deubiquitylation. *FEBS Lett.* **585**, 2780–2785 (2011).
466. Reynolds, P. *et al.* The dynamics of Ku70/80 and DNA-PKcs at DSBs induced by ionizing radiation is dependent on the complexity of damage. *Nucleic Acids Res.* **40**, 10821–10831 (2012).
467. Mehta, A. & Haber, J. E. Sources of DNA Double-Strand Breaks and Models of Recombinational DNA Repair. *Cold Spring Harb. Perspect. Biol.* **6**, (2014).
468. Jeggo, P. A. & Löbrich, M. DNA double-strand breaks: their cellular and clinical impact? *Oncogene* **26**, 7717–7719 (2007).
469. Sible, E., Fiorica, G., Rahman, S., Attaway, M. & Vuong, B. Q. Elucidating the role of ATM in BER and MMR during B cell CSR. *J. Immunol.* **204**, 151.1-151.1 (2020).
470. Kabziński, J. *et al.* Impact of APEX Ile64val Gene Polymorphisms of DNA Repair Ber System on Modulation of the Risk of Colorectal Cancer in the Polish Population. *Pol. Przegl. Chir.* **87**, 121–123 (2015).

471. Graf, N., Ang, W. H., Zhu, G., Myint, M. & Lippard, S. J. Role of endonucleases XPF and XPG in nucleotide excision repair of platinated DNA and cisplatin/oxaliplatin cytotoxicity. *Chembiochem Eur. J. Chem. Biol.* **12**, 1115–1123 (2011).
472. Essaghir, A. & Demoulin, J.-B. A Minimal Connected Network of Transcription Factors Regulated in Human Tumors and Its Application to the Quest for Universal Cancer Biomarkers. *PLoS ONE* **7**, (2012).
473. Prabhakarandian, B. *et al.* Synthetic Tumor Networks for Screening Drug Delivery Systems. *J. Control. Release Off. J. Control. Release Soc.* **201**, 49–55 (2015).
474. Milde-Langosch, K., Kappes, H., Riethdorf, S., Löning, T. & Bamberger, A.-M. FosB is Highly Expressed in Normal Mammary Epithelia, but Down-Regulated in Poorly Differentiated Breast Carcinomas. *Breast Cancer Res. Treat.* **77**, 265–275 (2003).
475. Althubaiti, S. *et al.* Ontology-based prediction of cancer driver genes. *Sci. Rep.* **9**, 17405 (2019).
476. García-Nieto, P. E., Morrison, A. J. & Fraser, H. B. The somatic mutation landscape of the human body. *Genome Biol.* **20**, 298 (2019).
477. Karamouzis, M. V. & Papavassiliou, A. G. Transcription Factor Networks as Targets for Therapeutic Intervention of Cancer: The Breast Cancer Paradigm. *Mol. Med.* **17**, 1133–1136 (2011).
478. Dragomir, M., Mafra, A. C. P., Dias, S. M. G., Vasilescu, C. & Calin, G. A. Using microRNA Networks to Understand Cancer. *Int. J. Mol. Sci.* **19**, (2018).

VITA

Jonathon Michael Gast was born to parents Anthony and Dawn on December 30th, 1992 in Cincinnati, Ohio. He attended Cottonwood Elementary School and Whitaker Elementary School before attending Finneytown Highschool in 2007. Upon graduation from high school in 2011, Jonathon attended the University of Cincinnati and earned Bachelor of Science degrees in Cellular and Molecular Biology and Biochemistry. During his undergraduate studies, Jonathon studied the effects of MCR4 on obesity through rodent studies under the tutelage of Dr. Joram Mul in the lab of Dr. Sylvana Obicci. Jonathon also studied HIV cross-over events, occult-HBV identification, and sequenced a section of the GBV-C genome and aligned the other components under the tutelage and in the lab of Dr. Jason Blackard where he earned a UC SURF Fellowship. Following his graduation from the University of Cincinnati in 2014, Jonathon joined the Department of Medicinal Chemistry and Molecular Pharmacology at Purdue University. He joined the lab of Dr. Vincent Jo Davisson in the spring of 2015 and began to work on the mechanism of action of PCNA antagonists. In the summer of 2015, he began to work on informatics and network theory approaches to identifying potential drug combinations. In August 2014 he received the Andrew's Fellowship, in December 2017 he received the PhRMA Informatic Pre-Doctoral Fellowship, and in May 2018 he received the Lilly Endowment Graduate Fellowship. Jonathon completed his graduate studies in April 2021 and graduated with his Ph.D. in May of that year.